High Order 2D Finite Element Methods with Extra Smoothness

by

Charles Parker, II

B. S., University of Maryland; College Park, MD, 2017

A dissertation submitted in partial fulfillment of the requirements for the degree of Doctor of Philosophy in the Division of Applied Mathematics at Brown University

PROVIDENCE, RHODE ISLAND

May 2022

© Copyright 2022 by Charles Parker, II

This dissertation by Charles Parker, II is accepted in its present form

by the Division of Applied Mathematics as satisfying the

dissertation requirement for the degree of Doctor of Philosophy.

Date________________ ____________________________________

Mark Ainsworth, Ph.D., Advisor

Recommended to the Graduate Council

Date________________ ____________________________________

Endre Süli, Ph.D., Reader

Date________________ ____________________________________

George Karniadakis, Ph.D., Reader

Approved by the Graduate Council

Date________________ ____________________________________

Andrew G. Campbell, Dean of the Graduate School

Vita

Education

University of Maryland, College Park, MD, USA
B.S., Mathematics, *Summa Cum Laude* with High Honors, May 2017
B.S., Computer Science, *Summa Cum Laude*, May 2017

Honors

Joukowsky Presidential Fellowship, 2017-2022

Publications

1. M. Ainsworth and **C. Parker**, *Mass conserving mixed hp-FEM approximations to Stokes flow. Part III: Implementation and preconditioning*, SIAM J. Numer. Anal., to appear.

2. M. Ainsworth and **C. Parker**, *Mass conserving mixed hp-FEM approximations to Stokes flow. Part II: Optimal convergence*, SIAM J. Numer. Anal., 59 (2021), pp. 1245–1272.

3. M. Ainsworth and **C. Parker**, *Mass conserving mixed hp-FEM approximations to Stokes flow. Part I: Uniform stability*, SIAM J. Numer. Anal., 59 (2021), pp. 1218–1244.

4. M. Ainsworth and **C. Parker**, *Preconditioning high order H^2 conforming finite elements on triangles*, Numer. Math., 148 (2021), pp. 223–254.

5. M. Ainsworth and **C. Parker**, *H^2 stable polynomial liftings on triangles*, SIAM J. Numer. Anal., 58 (2020), pp. 1867–1892.

Presentations

1. *Preconditioning Mixed High Order Finite Elements for Incompressible Flow*, AMS Fall Central Sectional Meeting, October 2021

2. *High Order H^2 Conforming Finite Element Methods on Triangles*, ICOSAHOM 2020, July 2021

3. *Preconditioning Mixed High Order Finite Elements for Incompressible Flow*, SIAM CSE21, March 2021

4. *High Order H^2 Conforming Finite Element Methods on Triangles*, ICoNSoM 2019, June 2019

Teaching Experience

Brown University

- Teaching Assistant, Applied Partial Differential Equations I, Fall 2018 & Spring 2019

University of Maryland

- Teaching Assistant, Advanced Data Structures, Fall 2015 – Summer 2017
- Teaching Assistant, Computer Architecture, Spring 2016 – Spring 2017
- Teaching Assistant, Introduction to Computer Systems, Fall 2014 & Spring 2015

Acknowledgments

I first would like to thank my advisor Professor Mark Ainsworth for all of his advice and guidance over the past five years. The countless hours we spent in weekly meetings are a testament to his dedication and respect for his students. I also would like to thank Professors Endre Süli and George Karniadakis for their time serving on my committee. Lastly, I would like to express my deepest gratitude to my parents for their neverending love and support.

Contents

List of Tables

List of Figures

Chapter One

Introduction

Finite element methods (FEMs) are used to discretize partial differential equations (PDEs) in a wide array of applications, including fluid flow [48, 55], solid mechanics [29, 31], electromagnetism [41, 43], optimal control [22, 112], and magnetohydrodynamics [52, 94]]. A FEM typically consists of two components: a mesh of the domain and spaces of piecewise polynomials defined on the mesh. The terms “low order” and “high order” delineate the use of low and high degree polynomials, respectively. While low order FEMs are often preferred for their simplicity and ease of implementation, high order FEMs offer numerous advantages over their lower order counterparts. Some of these advantages include exponential convergence rates for many problems [20] (including singular perturbation problems [81]), better resolution of small-scale features [67], less numerical dissipation and dispersion [3, 10], quantifiable robustness for parameter-dependent problems [18, 19, 20, 107], and better computational efficiency in large scale supercomputing applications [87, 116].

Despite the success of high order methods, the development of stable high order FEMs for many physical systems (e.g., incompressible flow, linear elasticity, and electromagnetism) remains a challenging problem, even in two space dimensions. Stability is crucial for obtaining optimal convergence rates of the FEMs, inhibiting nonphysical artifacts in the numerical solution, and developing efficient solvers for the algebraic problems resulting from discretization.

Some applications, including 2D incompressible fluid flow [55], elastic models of thin plates and shells [72], and nonlinear phase field models for materials [36], involve fourth order elliptic operators. For these problems, conforming FEMs are the most straightforward way of achieving a stable discretization and entail the use of finite elements with C^1-continuity between elements [24, 38], the first of which goes back over half a century, Argyris et. al. [11]. The Argyris elements have "extra smoothness" in the sense that they are globally C^1 and C^2 at element vertices, whereas only global C^1 continuity is required for conformity. Despite the long history of such methods, more elaborate schemes, such as discontinuous Galerkin or mixed finite elements, both of which require lower continuity, are often used in practice. One issue with conforming methods is that the condition number of the stiffness matrix grows rapidly in both the mesh size h and the polynomial degree p. For example, a straightforward textbook implementation of the lowest order Argyris elements in conjunction with a direct solver [21, pp.374-7] results in prohibitively large condition numbers after just 2-3 refinements of a relatively coarse initial mesh.

Although a variety of preconditioners are available for pure h-version methods (see, e.g., [35, 92, 118, 119]), there are no preconditioners currently available for the p- or hp-version FEMs with C^1 elements. Chapters 2 and 3 address this gap in the literature. Chapter 2 establishes an H^2-stable polynomial extension theorem that is crucial in the analysis of the iterative sub-structuring preconditioner for high order Argyris elements given and analyzed in Chapter 3. The preconditioner in Chapter 3 is similar in spirit to the classical preconditioners for second order elliptic problems of Bramble et al. [33] for the h-version and Babuška et al. [13] for the p-version. The asymptotic growth of the conditioner number of the preconditioned system is $\mathcal{O}(1+\log^3 p)$, independent of the mesh size h, and is comparable to the $\mathcal{O}(1+\log^2 p)$

growth of the preconditioner for C^0 elements in [13].

The final three chapters Chapters 4 to 6 turn attention to the 2D Stokes equations, which describe the velocity and pressure of slow-moving, viscous flow and often appear in mantle convection [80, 97, 120] and glaciology [75, 115]. FEMs that solve for the fluid velocity and pressure simultaneously necessitate the use of mixed methods. In this case, two finite element spaces are needed: $\boldsymbol{V}$ for the fluid velocity and Q for the fluid pressure. However, stability cannot be guaranteed by simply choosing $\boldsymbol{V}$ and Q to be conforming finite element spaces; instead stability is dictated by the *inf-sup constant*:

$$\beta := \inf_{q \in Q} \sup_{\boldsymbol{v} \in \boldsymbol{V}} \frac{(\operatorname{div} \boldsymbol{v}, q)}{\|\boldsymbol{v}\|_{\boldsymbol{H}^1} \|q\|_{L^2}}.$$

If there exists $\beta_0 > 0$ such that $\beta \geq \beta_0$ independently of the mesh size h and/or polynomial degree p, then the method is uniformly stable in h and/or p, respectively. Constructing stable pairings $\boldsymbol{V} \times Q$ is a nontrivial task.

One tool that has enjoyed success in the design of stable pairing is the so-called Stokes complex [50, 66]. Roughly speaking, one starts with a finite element space Σ, typically used in H^2 problems, and constructs $\boldsymbol{V}$ and Q so that $\mathbf{curl}\, \Sigma \subset \boldsymbol{V}$ and $\operatorname{div} \boldsymbol{V} = Q$. Then, the pair $\boldsymbol{V} \times Q$ is often uniformly stable in the mesh size h. In Chapter 4, we take Σ to be a slight modification of the high order Argyris space used in Chapter 3 and construct the spaces $\boldsymbol{V}$ and Q to have extra smoothness at element vertices as in [50]. It was previously shown [50] that $\boldsymbol{V} \times Q$ is uniformly stable in the mesh size h. We prove that, in fact, $\boldsymbol{V} \times Q$ is uniformly stable in h *and* p. This result is the first uniform-in-p stability result for triangular elements. Chapter 5 establishes optimal approximation theory results for the spaces in Chapter 4, including results for the space used in Chapter 3. This thesis concludes with Chapter 6, which discusses the implementation of the method in Chapter 4, including the construction and analysis of an efficient block diagonal preconditioner.

Chapter Two

H^2-Stable Polynomial Liftings on Triangles

2.1 Introduction

Polynomial extension, or lifting, operators extend piecewise polynomial data specified on the boundary ∂K to give a polynomial defined over the whole element K that matches the specified data on the boundary. The existence of stable lifting operators plays a critical role in the analysis of high order and spectral methods for the numerical approximation of PDEs. For instance, in the numerical approximation of second order elliptic PDEs the existence of an extension operator mapping polynomial boundary data from $H^{1/2}(\partial K)$ to a polynomial in $H^1(K)$, which is uniformly bounded in terms of the polynomial degree, is vital to both approximation theory and the analysis of domain decomposition methods for high order finite element approximations of such problems.

In particular, Babuška and Suri [16] constructed such a polynomial extension operator and used it to obtain convergence rates for the *hp* finite element method (FEM) with inhomogeneous boundary data in two dimensions. Subsequently, the basic polynomial extension result in [16] was generalized by Babuška et. al [13] and used to obtain condition number estimates for a substructuring preconditioner for the *p*-version finite element method in two dimensions. The extension theorem from [13] also plays a role in the analysis of domain decomposition preconditioners for the *hp*-version of the finite element method in two dimensions [2, 59] and in developing a priori error estimates for non-uniform order piecewise polynomial approximation [42]. Polynomial extension operators for three dimensional elements were developed by

Ben Belgacem [23] and Rafael Muñoz-Sola [84] on cubes and tetrahedra, respectively, and used to obtain a priori error estimates for the hp-version FEM of second order problems. These basic polynomial extension results play a key role in obtaining optimal error rates for second order elliptic problems; c.f. [58, 61, 62, 63, 64] and the references therein.

Liftings of polynomial traces also play an important role in the analysis of spectral methods; Maday [77] and Bernardi and Maday [27] studied polynomial extensions on triangles and squares in weighted Sobolev spaces and in interpolation spaces to obtain optimal error estimates for spectral approximation. Moreover, Bernardi et al. [25, 26] analyzed the operator norm of the liftings in various spaces with applications to optimal polynomial inverse inequalities. The analysis of high order mixed finite element approximation also requires polynomial liftings in vector-valued spaces: a right inverse of the trace operator on $\boldsymbol{H}(\mathrm{div})$ in the case of triangles which preserves polynomials was given in [10]; extension operators that respect the de Rham complex in three dimensions were developed in [44, 45, 46]. Minimal polynomial extensions with respect to the $L^2(K)$ norm play a key role in the analysis of a substructuring preconditioner for the mass matrix in two [6] and three [7] dimensions.

Nevertheless, while there is an extensive literature devoted to developing polynomial extension operators in the context of $H^1(K)$, relatively little is available when it comes to polynomial extensions from the boundary into the space $H^2(K)$. Such extension operators play a key role in the analysis and preconditioning of the p-version finite element approximation of fourth order elliptic problems (see e.g. Chapter 3 for their use in the analysis of a substructuring preconditioner for C^1-conforming p-version approximation and Chapter 5 for their use in approximation theory) and mixed hp FEMs for Stokes flow (Chapters 4 and 5).

The nature of the extension problem in $H^2(K)$ is somewhat different from the corresponding problem in the $H^1(K)$ setting. First, one seeks an extension that preserves both the function values on the boundary (and, a fortiori, the tangential derivatives) and, in addition, a prescribed normal derivative on the boundary. This means that the boundary data consists of two pieces of information: the standard trace f and the normal derivative g. Second, while the boundary data in $H^{1/2}(\partial K)$ can be specified arbitrarily in the $H^1(K)$ setting, this is not the case in the $H^2(K)$ setting where the two pieces of data f and g must satisfy appropriate compatibility conditions in order for there to exist an extension, polynomial or otherwise. Moreover, additional compatibility conditions are needed in order for there to exist a *polynomial* extension [25]. These issues are amplified and stated in detail in Section 2.2 along with a discussion of the appropriate choice of norm for the corresponding trace spaces.

This chapter is concerned with the construction of a polynomial extension with the following properties: Given piecewise polynomial boundary data f and g satisfying the appropriate compatibility conditions, find an extension U that is a polynomial, whose function value and normal derivative on the boundary agree with f and g, and such that the $H^2(K)$ norm depends continuously on the norm of the data f and g with constant independent of the polynomial degree. Lederer and Schöberl

[73] consider a related problem that arises in the analysis of hp mixed finite element approximation of the Stokes problem: Given a polynomial vector field $\boldsymbol{v}$ defined over the entire triangle, a lifting $\mathcal{E}(\boldsymbol{v})$ is constructed which is continuous from $\boldsymbol{H}^1(K)$ to $H^2(K)$ whose tangential derivatives match the tangential components of $\boldsymbol{v}$ on the boundary. The normal derivative, although shown to be a good approximation in $L^2(\partial K)$, differs from the normal component of $\boldsymbol{v}$ in general. The analysis of conforming and other schemes requires an extension which agrees with both the specified trace and normal derivative. We believe that the current work is the first to develop such $H^2(K)$ stable polynomial liftings.

2.2 Review of Traces of $H^2(\Omega)$ and Statement of Main Result

Let Ω be a simply connected polygon with boundary $\Gamma = \partial\Omega$. For ease of notation we assume $\Omega = \hat{T}$ is a triangle as shown in Figure 2.1. Although traces in $H^1(\hat{T})$ are well-understood, the corresponding results for functions in $H^2(\hat{T})$ are less widely appreciated. In the current section, we will review some basic properties concerning traces in $H^2(\hat{T})$ and develop some results which will be needed in the sequel.

If $u \in H^2(\hat{T})$, then $\nabla u \in \boldsymbol{H}^1(\hat{T})$ and $\nabla u|_\Gamma \in \boldsymbol{H}^{1/2}(\Gamma)$. We use the notation H^s to denote the usual Sobolev spaces [1] and $\boldsymbol{H}^s$ to denote spaces of vector fields or tensors. In particular, if $\hat{\boldsymbol{n}}$ and $\hat{\boldsymbol{t}}$ denote the outward unit normal and tangent vectors

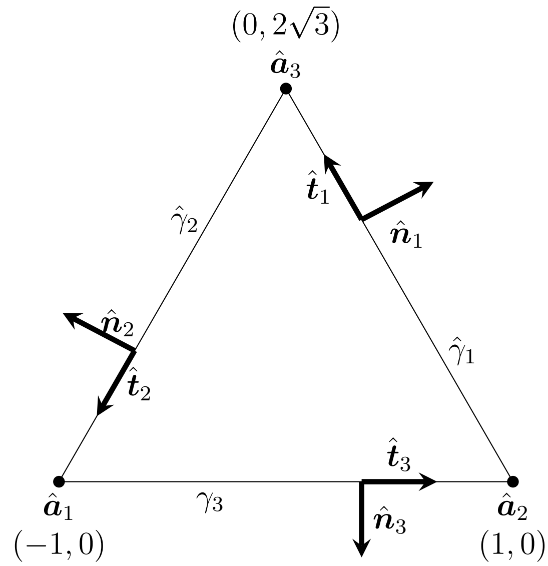

Figure 2.1: Schema for the reference triangle $\hat{T}$

on Γ, then $\partial_n u = \hat{\boldsymbol{n}} \cdot \nabla u$ and $\partial_t u = \hat{\boldsymbol{t}} \cdot \nabla u$ each belong to $L^2(\Gamma)$ [86, §2.4 Theorem 4.11], but the jump in the unit normal at a vertex rules out higher regularity in general. Thus, $u \in H^1(\Gamma)$ and $\partial_n u \in L^2(\Gamma)$.

For $f \in H^1(\Gamma)$ and $g \in L^2(\Gamma)$, define $\boldsymbol{\sigma}$ by the rule

$$\boldsymbol{\sigma}(f, g) := (\partial_t f)\hat{\boldsymbol{n}} - g\hat{\boldsymbol{t}}. \tag{2.2.1}$$

Hence, for $u \in H^2(\hat{T})$, we have $\boldsymbol{\sigma}(u, \partial_n u) = (\partial_t u)\hat{\boldsymbol{n}} - (\partial_n u)\hat{\boldsymbol{t}}$ so that[1]

$$\boldsymbol{\sigma}(u, \partial_n u)^\perp = (\partial_t u)\hat{\boldsymbol{n}}^\perp - (\partial_n u)\hat{\boldsymbol{t}}^\perp = (\partial_t u)\hat{\boldsymbol{t}} + (\partial_n u)\hat{\boldsymbol{n}} = \nabla u.$$

[1]We denote $(\sigma_1, \sigma_2)^\perp = (\sigma_2, -\sigma_1)$ and $\nabla^\perp u = (\nabla u)^\perp$.

Hence, $\boldsymbol{\sigma}(u,\partial_n u) \in \boldsymbol{H}^{1/2}(\Gamma)$ for $u \in H^2(\hat{T})$, and in addition,

$$\|\boldsymbol{\sigma}(u,\partial_n u)\|_{\boldsymbol{H}^{1/2}(\Gamma)} = \|(\nabla u)^{\perp}\|_{\boldsymbol{H}^{1/2}(\Gamma)} \leq C\|\nabla u\|_{\boldsymbol{H}^1(\Omega)} \leq C\|u\|_{H^2(\Omega)}.$$

Consequently, the operator

$$H^2(\hat{T}) \ni u \mapsto \boldsymbol{\sigma}(u,\partial_n u) \in \boldsymbol{H}^{1/2}(\Gamma)$$

can be regarded as a trace operator on $H^2(\hat{T})$ which is linear and continuous.

Suppose that $f \in H^1(\Gamma)$ and $g \in L^2(\Gamma)$ are given. When does there exist $u \in H^2(\hat{T})$ such that (f,g) is the trace of u, i.e. $u|_\Gamma = f$ and $\partial_n u|_\Gamma = g$? Observe that a necessary condition for the existence of u is that the data (f,g) satisfy the *compatibility condition* $\boldsymbol{\sigma}(f,g) = (\partial_t f)\hat{\boldsymbol{n}} - g\hat{\boldsymbol{t}} \in \boldsymbol{H}^{1/2}(\Gamma)$. In order to more fully grasp the implications of this condition, we make use of the following norm equivalence on $H^{1/2}(\Gamma)$. Let $v \in H^{1/2}(\Gamma)$ and let v_1, v_2, v_3 denote the restriction of v to the edges $\hat{\gamma}_1$, $\hat{\gamma}_2$, $\hat{\gamma}_3$ shown in Figure 2.1 parameterized by $s \in (-1,1)$ in the tangential direction. It may be shown [56, Theorem 1.5.2.3] that the norm on $H^{1/2}(\Gamma)$ is equivalent to

$$\begin{aligned}
&\|v_1\|^2_{H^{1/2}((-1,1))} + \|v_2\|^2_{H^{1/2}((-1,1))} + \|v_3\|^2_{H^{1/2}((-1,1))} \\
&\quad + \|(1+\xi)^{-1/2}(v_1(\xi) - v_3(-\xi))\|^2_{L^2((-1,1))} + \|(1+\xi)^{-1/2}(v_2(\xi) - v_1(-\xi))\|^2_{L^2((-1,1))} \\
&\quad + \|(1+\xi)^{-1/2}(v_3(\xi) - v_2(-\xi))\|^2_{L^2((-1,1))}.
\end{aligned}$$

A similar norm equivalence is valid on $\boldsymbol{H}^{1/2}(\Gamma)$. Indeed, since $\boldsymbol{\sigma}(f,g) = (\partial_t f)\hat{\boldsymbol{n}} - g\hat{\boldsymbol{t}}$

with $\hat{\boldsymbol{n}}, \hat{\boldsymbol{t}}$ orthonormal on each edge, the equivalence can be rewritten in the form (using similar notation to above)

$$\begin{aligned}
\|\boldsymbol{\sigma}(f,g)\|^2_{\boldsymbol{H}^{1/2}(\Gamma)} \approx \|\partial_t f_1\|^2_{H^{1/2}((-1,1))} + \|\partial_t f_2\|^2_{H^{1/2}((-1,1))} + \|\partial_t f_3\|^2_{H^{1/2}((-1,1))} \\
+ \|g_1\|^2_{H^{1/2}((-1,1))} + \|g_2\|^2_{H^{1/2}((-1,1))} + \|g_3\|^2_{H^{1/2}((-1,1))} \\
+ \|(1+\xi)^{-1/2}(\boldsymbol{\sigma}_1(f,g)(\xi) - \boldsymbol{\sigma}_3(f,g)(-\xi))\|_{\boldsymbol{L}^2((-1,1))} \\
+ \|(1+\xi)^{-1/2}(\boldsymbol{\sigma}_2(f,g)(\xi) - \boldsymbol{\sigma}_1(f,g)(-\xi))\|^2_{\boldsymbol{L}^2((-1,1))} \\
+ \|(1+\xi)^{-1/2}(\boldsymbol{\sigma}_3(f,g)(\xi) - \boldsymbol{\sigma}_2(f,g)(-\xi))\|^2_{\boldsymbol{L}^2((-1,1))}.
\end{aligned}$$

Hence, $\boldsymbol{\sigma}(f,g) \in \boldsymbol{H}^{1/2}(\Gamma)$ implies $f \in H^{3/2}(\hat{\gamma})$ and $g \in H^{1/2}(\hat{\gamma})$ for $\hat{\gamma} \in \{\hat{\gamma}_1, \hat{\gamma}_2, \hat{\gamma}_3\}$. In addition, the data on adjacent edges must be compatible at the shared vertex in the sense that terms of the following form must be bounded

$$\|(1+\xi)^{-1/2}(\boldsymbol{\sigma}_2(f,g)(\xi) - \boldsymbol{\sigma}_1(f,g)(-\xi))\|_{\boldsymbol{L}^2((-1,1))} < \infty. \tag{2.2.2}$$

This condition implies a non-trivial coupling between the data on edges $\hat{\gamma}_1$ and $\hat{\gamma}_2$ at the shared vertex $\hat{\boldsymbol{a}}_3$. For the reference triangle $\hat{T}$, these conditions read

$$f_2(-1) = f_1(1) \tag{2.2.3a}$$

$$\boldsymbol{\sigma}_2^{\perp}(f,g)(-1) = \boldsymbol{\sigma}_1^{\perp}(f,g)(1) \tag{2.2.3b}$$

The boundary Γ is one-dimensional, so $H^1(\Gamma)$ continuously embeds in $C(\Gamma)$, giving the first condition. Equality in the second condition is understood to mean that (2.2.2) is valid. Equally well, for a vertex located at a corner with internal angle θ

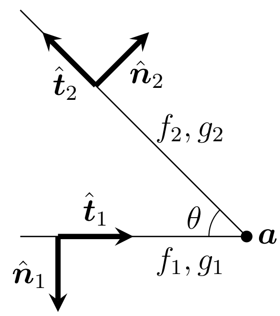

Figure 2.2: Schema for general compatibility conditions at the vertex $\boldsymbol{a}$.

as shown in Figure 2.2, the compatibility conditions read

$$f_2(\boldsymbol{a}) = f_1(\boldsymbol{a}) \tag{2.2.4a}$$

$$\partial_t f_2(\boldsymbol{a}) = -\partial_t f_1(\boldsymbol{a}) \cos\theta - g_1(\boldsymbol{a}) \sin\theta \tag{2.2.4b}$$

$$g_2(\boldsymbol{a}) = \partial_t f_1(\boldsymbol{a}) \sin\theta - g_1(\boldsymbol{a}) \cos\theta \tag{2.2.4c}$$

The condition $\boldsymbol{\sigma}(f, g) \in \boldsymbol{H}^{1/2}(\Gamma)$ is *necessary* for the existence of a function $u \in H^2(\hat{T})$ such that u has trace (f, g). The question of whether this condition is *sufficient* is considered in [25, 54] upon which the following discussion is based.

Consider the linear functional defined by the rule

$$\boldsymbol{H}^1(\hat{T}) \ni \boldsymbol{v} \mapsto L(\boldsymbol{v}) = \int_\Gamma \boldsymbol{v} \cdot \partial_t \boldsymbol{\sigma}(f, g)\ dt,$$

where here, and in what follows, the integral is understood in the sense of duality pairings. Since each component σ_α of $\boldsymbol{\sigma} = \boldsymbol{\sigma}(f, g)$ belongs to $H^{1/2}(\Gamma)$, there exists

$\sigma_\alpha^* \in H^1(\hat{T})$ such that $\sigma_\alpha^* = \sigma_\alpha$ on Γ with $\|\sigma_\alpha^*\|_{H^1(\hat{T})} \leq C\|\sigma_\alpha\|_{H^{1/2}(\Gamma)}$. Hence,

$$\begin{aligned}|L(\boldsymbol{v})| &= \left|\int_\Gamma \boldsymbol{v}\cdot\partial_t\boldsymbol{\sigma}dt\right| \leq \sum_\alpha \left|\int_\Gamma v_\alpha(\hat{\boldsymbol{t}}\cdot\nabla)\sigma_\alpha^* dt\right| = \sum_\alpha \left|\int_\Gamma v_\alpha \nabla^\perp\sigma_\alpha^*\cdot\hat{\boldsymbol{n}}\ dt\right| \\ &= \sum_\alpha \left|\int_T \nabla v_\alpha\cdot\nabla^\perp\sigma_\alpha^* dx\right| \leq \|\boldsymbol{v}\|_{\boldsymbol{H}^1(\hat{T})}\|\boldsymbol{\sigma}^*\|_{\boldsymbol{H}^1(\hat{T})} \leq C\|\boldsymbol{v}\|_{\boldsymbol{H}^1(\hat{T})}\|\boldsymbol{\sigma}\|_{\boldsymbol{H}^{1/2}(\Gamma)},\end{aligned}$$

where we used that $\nabla^\perp\sigma_\alpha^* \in \boldsymbol{H}(\mathrm{div};\hat{T})$ and applied [55, §1, Corollary 2.1]. Thus L is continuous and linear on $\boldsymbol{H}^1(\hat{T})$. Moreover,

$$L(\boldsymbol{e}_\alpha) = \int_\Gamma \hat{\boldsymbol{t}}\cdot\nabla\sigma_\alpha dt = 0$$

since $\sigma_\alpha \in H^{1/2}(\Gamma)$ and

$$\begin{aligned}L(\boldsymbol{x}^\perp) &= \int_\Gamma (x_2\partial_t\sigma_1 - x_1\partial_t\sigma_2)dt = \int_\Gamma \{\partial_t(x_2\sigma_1 - x_1\sigma_2) - \sigma_1\partial_t x_2 + \sigma_2\partial_t x_1\}dt \\ &= \int_\Gamma \boldsymbol{\sigma}\cdot\hat{\boldsymbol{n}}dt = \int_\Gamma \partial_t f dt = 0\end{aligned}$$

since $f \in H^{1/2}(\Gamma)$. Consequently, $L(\boldsymbol{v}) = 0$ for all $\boldsymbol{v} \in \boldsymbol{RM}$, where $\boldsymbol{RM}$ denotes the space of rigid body motions. Alternatively, if we introduce the strain tensor $\boldsymbol{\epsilon}(\cdot)$ given by $\epsilon_{\alpha\beta}(\boldsymbol{w}) = \frac{1}{2}(\partial_\alpha w_\beta + \partial_\beta w_\alpha)$, then $\boldsymbol{RM} = \ker\boldsymbol{\epsilon}(\cdot)$. Now, for $\boldsymbol{v} \in \boldsymbol{H}^1(\hat{T})$ and $\boldsymbol{r} \in \boldsymbol{RM}$:

$$\begin{aligned}|L(\boldsymbol{v})| = \inf_{\boldsymbol{r}\in\boldsymbol{RM}} |L(\boldsymbol{v}-\boldsymbol{r})| &\leq C \inf_{\boldsymbol{r}\in\boldsymbol{RM}} \|\boldsymbol{v}-\boldsymbol{r}\|_{\boldsymbol{H}^1(\hat{T})}\|\boldsymbol{\sigma}\|_{\boldsymbol{H}^{1/2}(\Gamma)} \\ &= C\|\boldsymbol{v}\|_{\boldsymbol{H}^1(\hat{T})/\boldsymbol{RM}}\|\boldsymbol{\sigma}\|_{\boldsymbol{H}^{1/2}(\Gamma)},\end{aligned}$$

and hence L is continuous and linear on the quotient space $\boldsymbol{H}^1(\hat{T})/\boldsymbol{RM}$. Consequently, thanks to the Riesz Representation Theorem, there exists $\boldsymbol{w} \in \boldsymbol{H}^1(\hat{T})/\boldsymbol{RM}$ such that

$$L(\boldsymbol{v}) = \int_{\hat{T}} \epsilon(\boldsymbol{w}) : \epsilon(\boldsymbol{v})\ dx \qquad \forall \boldsymbol{v} \in \boldsymbol{H}^1(\hat{T})/\boldsymbol{RM} \quad \text{with} \quad \|\epsilon(\boldsymbol{w})\|_{\boldsymbol{L}^2(\hat{T})} \leq C\|\boldsymbol{\sigma}\|_{\boldsymbol{H}^{1/2}(\Gamma)}. \tag{2.2.5}$$

In turn, thanks to [54, Theorem 2], there exists $u \in H^2(\hat{T})$ such that

$$\epsilon(\boldsymbol{w}) = \begin{bmatrix} u_{yy} & -u_{xy} \\ -u_{xy} & u_{xx} \end{bmatrix}.$$

As shown by [54, Theorem 3], we have $u = f$ and $\partial_n u = g$ on Γ. A routine application of the Petree-Tartar lemma[2] yields

$$\|u\|_{H^2(\hat{T})} \leq C \left(|u|_{H^2(\hat{T})} + \|u\|_{L^2(\Gamma)} + \|\partial_n u\|_{L^2(\Gamma)} \right),$$

and hence, by (2.2.5),

$$\begin{aligned} \|u\|_{H^2(\hat{T})} &\leq C \left(\|\boldsymbol{\epsilon}(\boldsymbol{w})\|_{\boldsymbol{L}^2(\hat{T})} + \|f\|_{L^2(\Gamma)} + \|\boldsymbol{\sigma}(f,g)\|_{\boldsymbol{H}^{1/2}(\Gamma)} \right) \\ &\leq C \left(\|f\|_{L^2(\Gamma)} + \|\boldsymbol{\sigma}(f,g)\|_{\boldsymbol{H}^{1/2}(\Gamma)} \right). \end{aligned}$$

The preceding discussion readily generalizes to an arbitrary polygonal domain Ω,

[2] Using the notation of [49, A.38] choose $X = H^2(\hat{T})$, $Y = \boldsymbol{L}^2(\hat{T}) \times \mathbb{R} \times \mathbb{R}$, $Z = H^1(\hat{T})$, and $Au = (D^2 u, \int_\Gamma u dt, \int_\Gamma \partial_n u dt)$. By the trace theorem, A is continuous, and the embedding $H^2(\hat{T})$ into $H^1(\hat{T})$ is compact (see e.g. [56, Theorem 1.4.3.2]).

which leads to the follow characterization of the trace of $H^2(\Omega)$ [25, Corollary 5.8]:

Theorem 2.2.1 ($H^2(\Omega)$ traces and extensions)**.** *Let*

$$\mathrm{Tr}H^2(\Omega) := \{(f,g) \in H^1(\Gamma) \times L^2(\Gamma) : \exists u \in H^2(\Omega) \text{ with } u|_\Gamma = f,\ \partial_n u = g\}$$

equipped with the natural norm

$$\|(f,g)\|_{\mathrm{Tr}H^2(\Omega)} = \inf_{\substack{u\in H^2(\Omega)\\ u|_\Gamma = f\\ \partial_n u|_\Gamma = g}} \|u\|_{H^2(\Omega)}.$$

Then, $\|f\|_{L^2(\Gamma)} + \|\boldsymbol{\sigma}(f,g)\|_{\boldsymbol{H}^{1/2}(\Gamma)}$ *is an equivalent norm on* $\mathrm{Tr}H^2(\Omega)$*. In particular, the following two statements hold:*

(i) For $u \in H^2(\Omega)$*, there holds*

$$\|u\|_{L^2(\Gamma)} + \|\boldsymbol{\sigma}(u, \partial_n u)\|_{\boldsymbol{H}^{1/2}(\Gamma)} \leq C\|u\|_{H^2(\Omega)}. \tag{2.2.6}$$

(ii) Let $f \in H^1(\Gamma)$*,* $g \in L^2(\Gamma)$*, and* $\boldsymbol{\sigma}(f,g) \in \boldsymbol{H}^{1/2}(\Gamma)$*. Then,* $(f,g) \in \mathrm{Tr}H^2(\Omega)$*, and there exists* $u \in H^2(\Omega)$ *such that* $u|_\Gamma = f$*,* $\partial_n u|_\Gamma = g$ *with*

$$\|u\|_{H^2(\Omega)} \leq C\left(\|f\|_{L^2(\Gamma)} + \|\boldsymbol{\sigma}(f,g)\|_{\boldsymbol{H}^{1/2}(\Gamma)}\right). \tag{2.2.7}$$

The question which we wish to consider in the current work is under what conditions does there exist a *polynomial* extension $U \in \mathcal{P}_p(\hat{T})$ of (f,g) satisfying (2.2.7)?

Of course, given that $f = U$ and $g = \partial_n U$ on Γ, it is necessary that the data f and g are piecewise polynomials of degree at most p and $p-1$, respectively, on Γ. In addition, the compatibility conditions (2.2.4) must also be respected. However, in the case of polynomial data, there is an additional condition which arises by considering the second order tangential derivatives on adjacent edges; in the scenario depicted in Figure 2.2, the condition reads

$$\partial_t g_2(\boldsymbol{a}) = \partial_{tt} f_2(\boldsymbol{a}) \cot\theta - \partial_{tt} f_1(\boldsymbol{a}) \cot\theta - \partial_t g_1(\boldsymbol{a}). \tag{2.2.8}$$

In terms of $\boldsymbol{\sigma}$, (2.2.8) reads

$$\partial_t \boldsymbol{\sigma}_2^{\perp}(f,g)(\boldsymbol{a}) \cdot \hat{\boldsymbol{t}}_1 = \partial_t \boldsymbol{\sigma}_1^{\perp}(f,g)(\boldsymbol{a}) \cdot \hat{\boldsymbol{t}}_2. \tag{2.2.9}$$

We now summarize the compatibility conditions needed in the case of polynomial boundary data on Γ, for data f and g parameterized with respect to arc length in the tangential direction: for $i = 1, 2, 3$

$$\begin{aligned} f_{i+1}(0) &= f_i(2), & \partial_t f_{i+1}(0) &= -\frac{1}{2}\partial_t f_i(2) - \frac{\sqrt{3}}{2} g_i(2), \\ g_{i+1}(0) &= \frac{\sqrt{3}}{2}\partial_t f_i(2) - \frac{1}{2} g_i(2), & \partial_t g_{i+1}(0) &= \frac{\sqrt{3}}{3}\left(\partial_{tt} f_{i+1}(0) - \partial_{tt} f_i(2)\right) - \partial_t g_i(2). \end{aligned} \tag{2.2.10}$$

where the indices are taken modulo 3.

The main result of this chapter is the following *polynomial extension theorem*:

Theorem 2.2.2. *Suppose f and g are defined on Γ such that $f_i = f|_{\hat{\gamma}_i} \in \mathcal{P}_p(\hat{\gamma}_i)$, $g_i = g|_{\hat{\gamma}_i} \in \mathcal{P}_{p-1}(\hat{\gamma}_i)$, $p \geq 1$. Then, there exists $U \in \mathcal{P}_p(\hat{T})$ with*

$$U|_\Gamma = f \quad \textit{and} \quad \partial_n U|_\Gamma = g$$

if and only if f and g satisfy the compatibility conditions (2.2.10)*. Moreover, U can be chosen such that*

$$\|U\|_{H^2(\hat{T})} \leq C \left(\|f\|_{L^2(\Gamma)} + \|\boldsymbol{\sigma}(f, g)\|_{\boldsymbol{H}^{1/2}(\Gamma)} \right), \tag{2.2.11}$$

with C independent of f, g, and p.

The proof is given in Section 2.6. Then, we have the following analogue of Theo-

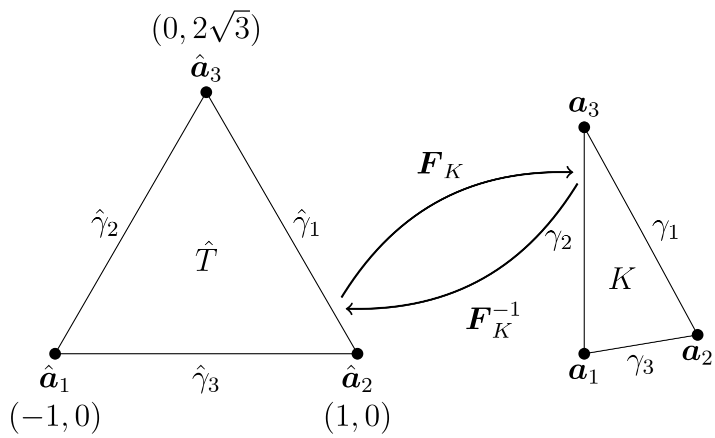

Figure 2.3: Notation used for a general triangle K and affine mapping $\boldsymbol{F}_K$

rem 2.2.2 for a general triangle K:

Corollary 2.2.3. *Suppose f and g are defined on ∂K such that $f_i = f|_{\gamma_i} \in \mathcal{P}_p(\gamma_i)$,*

$g_i = g|_{\gamma_i} \in \mathcal{P}_{p-1}(\gamma_i)$, $p \geq 1$. Then, there exists a $U \in \mathcal{P}_p(K)$ satisfying

$$U|_{\partial K} = f \quad \textit{and} \quad \partial_n U|_{\partial K} = g$$

if and only if f and g satisfy the compatibility conditions (2.2.4) *and* (2.2.8) *at each vertex of K. Moreover, U can be chosen such that*

$$\|U\|_{H^2(K)} \leq C \left(\|f\|_{L^2(\partial K)} + \|\boldsymbol{\sigma}(f,g)\|_{\boldsymbol{H}^{1/2}(\partial K)} \right), \tag{2.2.12}$$

and C independent of f, g, and p.

Proof. We begin by defining the corresponding data on the triangle $\hat{T}$ as follows: Define $\hat{f}, \hat{g} : \partial \hat{T} \to \mathbb{R}$ by

$$\hat{f}_i(t) := f_i \left(\frac{|\gamma_i|}{2} t \right), \quad \hat{g}_i(t) := \hat{\boldsymbol{n}}_{\hat{\gamma}_i} \cdot D\boldsymbol{F}_K^T \boldsymbol{\sigma}_i^{\perp}(f,g) \left(\frac{|\gamma_i|}{2} t \right) \tag{2.2.13}$$

for $i = 1, 2, 3$, using the notation in Figure 2.3. A simple calculation reveals that

$$\hat{\boldsymbol{\sigma}}_i^{\perp}(\hat{f}, \hat{g})(t) := \partial_t \hat{f}_i(t) \hat{\boldsymbol{t}}_{\hat{\gamma}_i} + \hat{g}_i(t) \hat{\boldsymbol{n}}_{\hat{\gamma}_i} = D\boldsymbol{F}_K^T \boldsymbol{\sigma}_i^{\perp}(f,g) \left(\frac{|\gamma_i|}{2} t \right), \tag{2.2.14}$$

which shows that $\hat{f}$ is the standard pull-back while $\hat{g}$ is the normal component of the Piola transformation and, as such, preserves the normal component of $\boldsymbol{\sigma}_i$. We then appeal to Theorem 2.2.2 to create a polynomial extension of $\hat{f}$ and $\hat{g}$ on $\hat{T}$. To this end, it suffices to check the compatibility conditions (2.2.3) and (2.2.9). Clearly $\hat{f}_{i+1}(0) = \hat{f}_i(2)$ is equivalent to (2.2.3a). Differentiating (2.2.14) in the tangential direction and using that

$$\hat{\boldsymbol{t}}_{\hat{\gamma}_j} = \frac{|\gamma_j|}{2} D\boldsymbol{F}_K^{-1}\hat{\boldsymbol{t}}_{\gamma_j},$$

we have

$$\partial_t \hat{\boldsymbol{\sigma}}_i^{\perp}(\hat{f},\hat{g})\cdot\hat{\boldsymbol{t}}_{\hat{\gamma}_j} = \frac{|\gamma_i||\gamma_j|}{4}\partial_t\boldsymbol{\sigma}_i^{\perp}(f,g)\left(\frac{|\gamma_i|}{2}t\right)\cdot\hat{\boldsymbol{t}}_{\gamma_j},$$

Thus (2.2.3b) and (2.2.9) hold if and only if $\hat{f}$ and $\hat{g}$ satisfy (2.2.10). Now, let $\hat{U}$ be given by Theorem 2.2.2 and take $U = \hat{U}\circ\boldsymbol{F}_K^{-1}$. Property (2.2.13) means that the trace of U is given by (f,g). From (2.2.11), we have

$$\|U\circ\boldsymbol{F}_K\|_{H^2(\hat{T})} = \|\hat{U}\|_{H^2(\hat{T})} \le C\left(\|\hat{f}\|_{L^2(\partial\hat{T})} + \|\hat{\boldsymbol{\sigma}}(\hat{f},\hat{g})\|_{\boldsymbol{H}^{1/2}(\partial\hat{T})}\right).$$

Now, using (2.2.6), we have

$$\|\hat{f}\|_{L^2(\partial\hat{T})} + \|\hat{\boldsymbol{\sigma}}(\hat{f},\hat{g})\|_{\boldsymbol{H}^{1/2}(\partial\hat{T})} \le C \inf_{\substack{\hat{w}\in H^2(\hat{T})\\ \hat{w}|_{\partial\hat{T}}=\hat{f}\\ \partial_n\hat{w}|_{\partial\hat{T}}=\hat{g}}} \|\hat{w}\|_{H^2(\hat{T})}.$$

Furthermore,

$$\inf_{\substack{\hat{w}\in H^2(\hat{T})\\ \hat{w}|_{\partial\hat{T}}=\hat{f}\\ \partial_n\hat{w}|_{\partial\hat{T}}=\hat{g}}} \|\hat{w}\|_{H^2(\hat{T})} = \inf_{\substack{w\in H^2(K)\\ w|_{\partial K}=f\\ \partial_n w|_{\partial K}=g}} \|w\circ\boldsymbol{F}_K^{-1}\|_{H^2(\hat{T})} \le C \inf_{\substack{w\in H^2(K)\\ w|_{\partial K}=f\\ \partial_n w|_{\partial K}=g}} \|w\|_{H^2(K)}.$$

Again, using (2.2.6), we have

$$\|U\|_{H^2(K)} \approx \|U \circ \boldsymbol{F}_K\|_{H^2(\hat{T})} \leq C\left(\|f\|_{L^2(\partial K)} + \|\boldsymbol{\sigma}(f,g)\|_{\boldsymbol{H}^{1/2}(\partial K)}\right).$$

$\square$

2.3 Hardy Inequalities

Let $I = (0,1)$. We use the standard Sobolev spaces $H^s(I)$, $s \in [0,\infty)$, with $H^0(I) = L^2(I)$. In particular, the fractional order spaces $H^{1/2}(I)$, $H^{1/2}_{00}(I)$, $H^{3/2}(I)$, and $H^{3/2}_{00}(I)$ are equipped with the following norms:

$$\begin{aligned}
\|u\|^2_{H^{1/2}(I)} &:= \|u\|^2_{L^2(I)} + \int_0^1 \int_0^1 \left|\frac{u(x)-u(y)}{x-y}\right|^2 \, dx \, dy,\\
\|u\|^2_{H^{1/2}_{00}(I)} &:= \|u\|^2_{H^{1/2}(I)} + 2\int_0^1 \frac{u^2(x)}{x} \, dx + 2\int_0^1 \frac{u^2(x)}{1-x} \, dx,\\
\|u\|^2_{H^{3/2}(I)} &:= \|u\|^2_{L^2(I)} + \|u'\|^2_{H^{1/2}(I)}\\
\|u\|^2_{H^{3/2}_{00}(I)} &:= \|u\|^2_{L^2(I)} + \|u'\|^2_{H^{1/2}_{00}(I)}.
\end{aligned}$$

The corresponding spaces $H^s(\gamma)$ and $\boldsymbol{H}^s(\gamma)$ are defined on an element edge $\gamma \in \{\gamma_1, \gamma_2, \gamma_3\}$ in a similar fashion.

Various forms of Hardy's inequality will be required. To this end, define the onesided space $H^1_L(I) = \{u \in H^1(I) : u(0) = 0\}$ and the interpolation space $H^{1/2}_L(I)$ equipped with the norm

$$\|u\|^2_{H^{1/2}_L(I)} := \|u\|^2_{H^{1/2}(I)} + \int_0^1 \frac{u^2(t)}{t}\, dt.$$

Define the operators $A^{k,l}_L$ and $B^{k,l}_R$ by the rules

$$A^{k,l}_L(f)(x) := \frac{1}{x^k}\int_0^x t^l f(t)\, dt, \qquad k, l \in \mathbb{N}_0 \tag{2.3.1}$$

$$B^{k,l}_R(f)(x) := x^l \int_x^1 \frac{1}{t^k} f(t)\, dt, \qquad k, l \in \mathbb{N}_0. \tag{2.3.2}$$

The following Hardy type inequalities are derived in Section 2.7.

Lemma 2.3.1. *Let $A^{k,l}_L$ and $B^{k,l}_R$ be defined as above. Then, for $k \geq 0$,*

(i) for $n \in \{0, 1, \ldots,\}$ and $f \in H^n(I)$,

$$\frac{d^m}{dx^m}\left[A^{k+1,k}_L f\right] = A^{k+1+m,k+m}_L f^{(m)}, \qquad m \in \{0, 1, \ldots, n\}. \tag{2.3.3}$$

(ii) for $n \in \{0, 1, \ldots,\}$ and $f \in H^n(I)$,

$$\left\|A^{k+1,k}_L f\right\|_{H^s(I)} \leq \frac{1}{k + \frac{1}{2}}\|f\|_{H^s(I)}, \qquad 0 \leq s \leq n \tag{2.3.4}$$

(iii) for $n \in \{0, 1, \ldots, \}$ *and* $f \in H^n(I)$,

$$\|A_L^{k,k} f\|_{L^2(I)} \leq \|f\|_{L^2(I)} \text{ and } \|A_L^{k,k} f\|_{H^s(I)} \leq \left(\frac{k}{k+1/2} + 1\right) \|f\|_{H^{s-1}(I)},\ 1 \leq s \leq n. \tag{2.3.5}$$

(iv) for $f \in L^2(I)$,

$$\left\|B_R^{k+1,k} f\right\|_{L^2(I)} \leq \frac{1}{k+\frac{1}{2}} \|f\|_{L^2(I)}. \tag{2.3.6}$$

(v) for $n \in \{1, 2\}$ *and* $f \in H^n(I) \cap H_L^1(I)$,

$$\left\|B_R^{k+1,k} f\right\|_{H^m(I)} \leq 6\|f\|_{H^m(I)}, \qquad m \in \{0, \ldots, n\}. \tag{2.3.7}$$

and

$$\left\|B_R^{k+1,k} f\right\|_{H^{1/2}(I)} \leq 2\sqrt{3}\, \|f\|_{H_L^{1/2}(I)} \tag{2.3.8}$$

(vi) for $f \in L^2(I)$,

$$\left\|B_R^{k,k} f\right\|_{L^2(I)} \leq \|f\|_{L^2(I)} \quad \text{and} \quad \left\|B_R^{k,k} f\right\|_{H^1(I)} \leq 3\|f\|_{L^2(I)}, \tag{2.3.9}$$

and there exists a constant C *independent of* k *such that for* $f \in H^1(I)$ *(pro-*

vided $f(0) = 0$ in the case $k = 1$)

$$\left\| B_R^{k,k} f \right\|_{H^2(I)} \leq C(k+1)\|f\|_{H^1(I)}. \tag{2.3.10}$$

(vii) for $f \in H^1(I)$ and $g \in H_L^1(I)$,

$$\begin{aligned} \left\| B_R^{k,k} f \right\|_{H^{3/2}(I)} &\leq C\sqrt{k+1}\|f\|_{H^{1/2}(I)}, \quad k \neq 1 \\ \left\| B_R^{k,k} g \right\|_{H^{3/2}(I)} &\leq C\sqrt{k+1}\,\|g\|_{H_L^{1/2}(I)}, \quad k \geq 0. \end{aligned} \tag{2.3.11}$$

The following two results are easy consequences of Lemma 2.3.1.

Lemma 2.3.2. *There exists a constant $C > 0$ such that*

$$\int_0^1 \frac{1}{t^3} u^2(t)\; dt + \int_0^1 \frac{1}{(1-t)^3} u^2(t)\; dt, \leq C\|u'\|^2_{H_{00}^{1/2}(I)} \qquad \forall u \in H_{00}^{3/2}(I) \tag{2.3.12}$$

Proof. Using (2.3.4), we have

$$\begin{aligned} \int_0^1 \frac{1}{t^3} u^2(t)\; dt &= \int_0^1 \left| \frac{1}{t} \cdot \frac{1}{t^{1/2}} \int_0^t u'(s)\; ds \right|^2\; dt \leq \int_0^1 \left| \frac{1}{t} \int_0^t \frac{1}{s^{1/2}} u'(s)\; ds \right|^2\; dt \\ &= \left\| A_L^{1,0}(\xi^{-1/2} u'(\xi)) \right\|^2_{L^2(I)} \leq 4 \left\| \xi^{-1/2} u'(\xi) \right\|^2_{L^2(I)} \leq C\|u'\|^2_{H_{00}^{1/2}(I)}. \end{aligned}$$

The result then follows by applying this estimate to the function $t \mapsto u(1-t)$ and summing. $\square$

Lemma 2.3.3. *Let $n \in \{1, 2, \ldots, \}$. There exists a constant $C > 0$ such that*

$$\left\|\xi^{-1} f(\xi)\right\|_{H^s(I)} \leq C\|f\|_{H^{s+1}(I)}, \qquad 0 \leq s \leq n-1, \qquad \forall f \in H^n(I) \cap H_0^1(I).$$

Proof. The estimate follows from (2.3.4) at once on noting that

$$t^{-1} f(t) = t^{-1} \int_0^t f'(s)\, ds = A_L^{1,0}(f')(t).$$

□

2.4 Polynomial Extensions from a Single Edge

Thanks to Corollary 2.2.3, it suffices to prove Theorem 2.2.2 on any triangle. In particular, we will work with the right triangle $\hat{T}$ shown in Figure 2.4 for the remainder of this chapter, which results in simpler formulae appearing in our proofs.

We recall following elementary single edge extension operators from [64, eq. (2.1)] and [73, eq. (5.22)]:

$$\begin{aligned}
\mathcal{E}(f)(x, y) &:= \int_0^1 f(x + sy)\, ds = \frac{1}{y} \int_x^{x+y} f(t)\, dt \\
\mathcal{E}^{\boldsymbol{n}}(f)(x, y) &:= y \int_0^1 a(s) f(x + sy)\, ds,
\end{aligned}$$

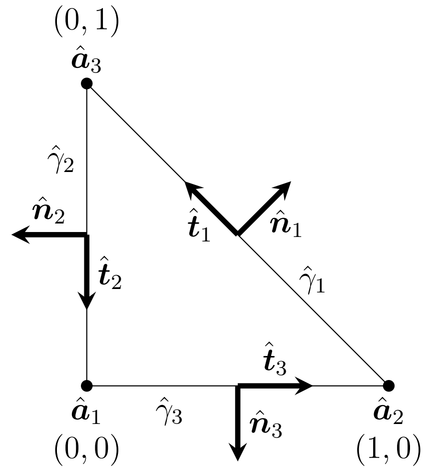

Figure 2.4: Schema for the right angle triangle $\hat{T}$ used in Section 2.4

where $a(s) = -6s(1-s)$. The following lemma follows immediately from [64] and [73, §5.3]:

Lemma 2.4.1. *There exists a constant $C > 0$ such that*

$$\begin{aligned} \|\mathcal{E}(f)\|_{L^2(\hat{T})} &\leq 2 \left\| \xi^{1/2} f(\xi) \right\|_{L^2(\hat{\gamma}_3)} && \forall f \in L^2(\hat{\gamma}_3), \\ \|\mathcal{E}(f)\|_{H^2(\hat{T})} &\leq C \|f\|_{H^{3/2}(\hat{\gamma}_3)} && \forall f \in H^{3/2}(\hat{\gamma}_3), \\ \|\mathcal{E}^{\boldsymbol{n}}(f)\|_{H^2(\hat{T})} &\leq C \|f\|_{H^{1/2}(\hat{\gamma}_3)} && \forall f \in H^{1/2}(\hat{\gamma}_3). \end{aligned} \tag{2.4.1}$$

Moreover, if $f \in \mathcal{P}_p(\hat{\gamma}_3)$, then $\mathcal{E}(f) \in \mathcal{P}_p(\hat{T})$ and $\mathcal{E}^{\boldsymbol{n}}(f) \in \mathcal{P}_{p+1}(\hat{T})$.

The following result, proved in detail in [64], is the 2D analogue of the results in [84]:

Theorem 2.4.2. *The operators given by*

$$\begin{aligned}
\mathcal{R}_{1,L}(f)(x,y) &:= x\mathcal{E}\left(\frac{f(\xi)}{\xi}\right)(x,y),\\
\mathcal{R}_{1,R}(f)(x,y) &:= (1-x-y)\mathcal{E}\left(\frac{f(\xi)}{1-\xi}\right)(x,y),\\
\mathcal{R}_{1}(f)(x,y) &:= x(1-x-y)\mathcal{E}\left(\frac{f(\xi)}{\xi(1-\xi)}\right)(x,y),
\end{aligned}$$

for $(x,y) \in T$*, are continuous* $H^{1/2}_{00}(\hat{\gamma}_3) \to H^1(\hat{T})$ *and map* $\mathcal{P}_p(\hat{\gamma}_3) \cap H^{1/2}_{00}(\hat{\gamma}_3)$ *into* $\mathcal{P}_p(\hat{T})$*.*

The following analogue will be useful in the $H^2(\hat{T})$ case:

Theorem 2.4.3. *Let* $f \in H^{3/2}_{00}(\hat{\gamma}_3)$ *and let*

$$\mathcal{R}_2(f)(x,y) = x^2(1-x-y)^2\mathcal{E}\left(\frac{f(\xi)}{\xi^2(1-\xi)^2}\right)(x,y).$$

Then, $\mathcal{R}_2(f) \in H^2(\hat{T})$ *and there exists a constant* C *independent of* f *and* p *such that*

$$\|\mathcal{R}_2(f)\|_{H^2(\hat{T})} \leq C\|f\|_{H^{3/2}_{00}(\hat{\gamma}_3)}. \tag{2.4.2}$$

Moreover, if $f \in \mathcal{P}_p(\hat{\gamma}_3)$*, then* $\mathcal{R}_2(f) \in \mathcal{P}_p(\hat{T})$ *and the trace of* $\mathcal{R}_2(f)$ *vanishes on* $\partial\hat{T} \setminus \hat{\gamma}_3$*.*

Before proving Theorem 2.4.3,we first collect some technical lemmas which concern terms that appear in various computations in the proof of Theorem 2.4.3.

Lemma 2.4.4. *There exists a constant $C > 0$ such that*

$$\int_0^1 \int_0^{1-x} \left| \frac{f(x+y) - f(x)}{y} \right|^2 \, dy \, dx \leq C \|f\|^2_{H^{1/2}(\hat{\gamma}_3)} \qquad \forall f \in H^{1/2}(\hat{\gamma}_3), \tag{2.4.3}$$

$$\int_0^1 \int_0^{1-x} \left| \frac{f(x+y)}{x+y} \right|^2 \, dy \, dx \leq C \|f\|^2_{H^{1/2}_{00}(\hat{\gamma}_3)} \qquad \forall f \in H^{1/2}_{00}(\hat{\gamma}_3). \tag{2.4.4}$$

Proof. For (2.4.3), we have

$$\begin{aligned} \int_0^1 \int_0^{1-x} \left| \frac{f(x+y) - f(x)}{y} \right|^2 \, dy \, dx &\overset{z=x+y}{=} \int_0^1 \int_x^1 \left| \frac{f(z) - f(x)}{z-x} \right|^2 \, dz \, dx \\ &\leq C \|f\|^2_{H^{1/2}(\hat{\gamma}_3)}. \end{aligned}$$

Similarly, for (2.4.4),

$$\begin{aligned} \int_0^1 \int_0^{1-x} \left| \frac{f(x+y)}{x+y} \right|^2 \, dy \, dx \overset{z=x+y}{=} \int_0^1 \int_x^1 \left| \frac{f(z)}{z} \right|^2 \, dz \, dx &= \int_0^1 \left| \frac{f(z)}{z} \right|^2 \int_0^z \, dx \, dz \\ &= \int_0^1 \frac{|f(z)|^2}{z} \, dz \leq C \|f\|^2_{H^{1/2}_{00}(\hat{\gamma}_3)}. \end{aligned}$$

$\square$

Lemma 2.4.5. *There exists a constant $C > 0$ such that*

$$\int_0^1 \int_0^{1-y} \left| \frac{f(x+y)}{(x+y)^2} \right|^2 \, dx \, dy + \|g\|^2_{L^2(\hat{T})} \leq C \|f\|^2_{H^{3/2}_{00}(\hat{\gamma}_3)} \qquad \forall f \in H^{3/2}_{00}(\hat{\gamma}_3), \tag{2.4.5}$$

where

$$g(x, y) := y^{-2} \int_x^{x+y} \left| A^{1,0}_L(f')(x+y) - A^{1,0}_L(f')(t) \right| \, dt. \tag{2.4.6}$$

Proof. We estimate each of the terms separately. For the first term,

$$\int_0^1 \int_0^{1-y} \left| \frac{f(x+y)}{(x+y)^2} \right|^2 dx\, dy \overset{z=x+y}{=} \int_0^1 \int_x^1 \left| \frac{f(z)}{z^2} \right|^2 dz\, dx = \int_0^1 \left| \frac{f(z)}{z^2} \right|^2 \int_0^z dx\, dz$$
$$= \int_0^1 \frac{1}{z^3} |f(z)|^2\, dz \le C \|f\|_{H_{00}^{3/2}(\hat{\gamma}_3)}$$

by (2.3.12). For the second term, we have

$$\begin{aligned}
\|g\|^2_{L^2(\hat{T})} &\le \int_0^1 \int_0^{1-x} \frac{1}{y^3} \int_x^{x+y} \left| A_L^{1,0}(f')(x+y) - A_L^{1,0}(f')(t) \right|^2 dt\, dy\, dx \\
&\overset{z=x+y}{=} \int_0^1 \int_x^1 \frac{1}{(z-x)^3} \int_x^z \left| A_L^{1,0}(f')(z) - A_L^{1,0}(f')(t) \right|^2 dt\, dz\, dx \\
&= \int_0^1 \int_0^z \int_0^t \frac{|A_L^{1,0}(f')(z) - A_L^{1,0}(f')(t)|^2}{(z-x)^3}\, dx\, dt\, dz \\
&= \frac{1}{2} \int_0^1 \int_0^z \left| A_L^{1,0}(f')(z) - A_L^{1,0}(f')(t) \right|^2 \left(\frac{1}{(z-t)^2} - \frac{1}{z^2} \right) dt\, dz \\
&\le \int_0^1 \int_0^1 \left| \frac{A_L^{1,0}(f')(z) - A_L^{1,0}(f')(t)}{z-t} \right|^2 dt\, dz \\
&\le C \|A_L^{1,0}(f')\|_{H^{1/2}(\hat{\gamma}_3)} \\
&\le C \|f\|_{H_{00}^{3/2}(\hat{\gamma}_3)} \quad \text{by (2.3.4).}
\end{aligned}$$

$\square$

Now we show that $\mathcal{R}_{1,L}$ is bounded from $H_{00}^{3/2}(\hat{\gamma}_3)$ to $H^2(\hat{T})$.

Lemma 2.4.6. *There exists a constant $C > 0$ such that*

$$\|\mathcal{R}_{1,L}(f)\|_{H^2(\hat{T})} \le C \|f\|_{H_{00}^{3/2}(\hat{\gamma}_3)} \qquad \forall f \in H_{00}^{3/2}(\hat{\gamma}_3).$$

Proof. We only need to bound the second derivatives. As in [84], we compare with derivatives of $\mathcal{E}$.

∂_{xx} **estimate**:

$$\partial_{xx}\mathcal{R}_{1,L}(f)(x,y) - \partial_{xx}\mathcal{E}(f)(x,y) = \frac{1}{y}\left(\frac{f(x+y)}{x+y} - \frac{f(x)}{x}\right) - \frac{f'(x+y)}{x+y} + \frac{f(x+y)}{(x+y)^2}$$
$$=: E_1 - E_2 + E_3.$$

For E_1, we have

$$\begin{aligned}
\|E_1\|^2_{L^2(\hat{T})} &= \int_0^1 \int_0^{1-x} \left|\frac{1}{y}\left(\frac{1}{x+y}\int_0^{x+y} f'(s)\ ds - \frac{1}{x}\int_0^x f'(s)\ ds\right)\right|^2\ dy\ dx \\
&= \int_0^1 \int_0^{1-x} \left|\frac{1}{y}\left(A_L^{1,0}(f')(x+y) - A_L^{1,0}(f')(x)\right)\right|^2\ dy\ dx \\
&\overset{z=x+y}{=} \int_0^1 \int_x^1 \left|\frac{A_L^{1,0}(f')(z) - A_L^{1,0}(f')(x)}{z-x}\right|^2\ dz\ dx \\
&\le C\|A_L^{1,0}(f')\|^2_{H^{1/2}(\hat{\gamma}_3)} \\
&\le C\|f'\|^2_{H^{1/2}_{00}(\hat{\gamma}_3)}.
\end{aligned}$$

Applying (2.4.4) to f' for E_2 and (2.4.5) for E_3, we have $\|\partial_{xx}\mathcal{R}_{1,L}(f)\|_{L^2(\hat{T})} \le C\|f\|_{H^{3/2}_{00}(\hat{\gamma}_3)}$.

∂_{xy} **estimate**:

$$
\begin{aligned}
&\partial_{xy}\mathcal{R}_{1,L}(f)(x,y) - \partial_{xy}\mathcal{E}(f)(x,y) \\
&\quad = \left[-\frac{1}{y^2}\int_x^{x+y}\frac{f(t)}{t}\,dt + \frac{f(x+y)}{y(x+y)}\right] + \frac{f(x+y)}{(x+y)^2} - \frac{f'(x+y)}{x+y} =: E_4 + E_3 - E_2.
\end{aligned}
$$

For E_4, we have

$$
\begin{aligned}
|E_4| &\leq \frac{1}{y^2}\int_x^{x+y}\left|\frac{1}{x+y}\int_0^{x+y} f'(s)\,ds - \frac{1}{t}\int_0^t f'(s)\,ds\right|\,dt \\
&= \frac{1}{y^2}\int_x^{x+y}\left|A_L^{1,0}(f')(x+y) - A_L^{1,0}(f')(t)\right|\,dt.
\end{aligned}
$$

Using (2.4.5) and (2.4.6) and that E_2 and E_3 are the same as above, we have the estimate for $\partial_{xy}\mathcal{R}_{1,L}(f)$.

∂_{yy} **estimate**:

$$
\begin{aligned}
&\partial_{yy}\mathcal{R}_{1,L}(y)(f)(x,y) - \partial_{yy}\mathcal{E}(f)(x,y) \\
&\quad = \left\{-\frac{2}{y^3}\int_x^{x+y} f(t)\left(1-\frac{x}{t}\right)\,dt + \frac{f(x+y)}{y(x+y)}\right\} + \frac{f(x+y)}{(x+y)^2} - \frac{f'(x+y)}{x+y} \\
&\quad =: E_5 + E_3 - E_2.
\end{aligned}
$$

For E_5, note that

$$
E_5 = \frac{2}{y^3}\int_x^{x+y}\left[\frac{f(x+y)}{x+y} - \frac{f(t)}{t}\right](t-x)\,dt.
$$

Using that $t - x \le y$,

$$|E_5| \le \frac{2}{y^2} \int_x^{x+y} \left| \frac{f(x+y)}{x+y} - \frac{f(t)}{t} \right| \, dt = \frac{2}{y^2} \int_x^{x+y} \left| A_L^{1,0}(f')(x+y) - A_L^{1,0}(f')(t) \right| \, dt,$$

and so the estimate for $\partial_{yy}\mathcal{R}_{1,L}(f)$ follows from (2.4.5) and (2.4.6) and the estimates for E_2 and E_3. $\square$

Next, we show $\mathcal{R}_{2,L}$ is bounded from $H_{00}^{3/2}(\hat{\gamma}_3) \to H^2(\hat{T})$.

Lemma 2.4.7. *Let $f \in H_{00}^{3/2}(\hat{\gamma}_3)$ and define $R_{2,L}$ by*

$$\mathcal{R}_{2,L}(f)(x,y) := x^2 \mathcal{E}\left(\frac{f(\xi)}{\xi^2}\right)(x,y).$$

Then, there exists a constant $C > 0$ independent of f such that

$$\|\mathcal{R}_{2,L}(f)\|_{H^2(\hat{T})} \le C \|f\|_{H_{00}^{3/2}(\hat{\gamma}_3)}.$$

Proof. The L^2 estimate is the same as for $\mathcal{R}_{1,L}$:

$$|R_{2,L}(f)(x,y)| \le \frac{1}{y} \int_x^{x+y} |f(t)| \, dt = \mathcal{E}(|f|)(x,y).$$

We again proceed by comparing the derivatives to $\mathcal{R}_{1,L}$ or $\mathcal{E}$.

∂_x **estimate**: We compare the derivative to $\mathcal{R}_{1,L}$.

$$\partial_x \mathcal{R}_{2,L}(f)(x,y) - \partial_x \mathcal{R}_{1,L}(f)(x,y) = \frac{1}{y}\int_x^{x+y} \frac{f(t)}{t}\left(\frac{2x}{t} - 1\right)\, dt - \frac{x}{x+y}\frac{f(x+y)}{x+y}$$
$$=: E_1 - E_2.$$

For E_1, we have

$$|E_1| \leq \frac{1}{y}\int_x^{x+y} \left|\frac{f(t)}{t}\right|\, dt = \mathcal{R}_{1,L}(|f|)(x,y) \implies \|E_1\|_{L^2(\hat{T})} \leq C\|f\|_{L^2(\hat{T})}.$$

by Theorem 2.4.2. Moreover,

$$|E_2| \leq \left|\frac{f(x+y)}{x+y}\right| \implies \|E_2\|_{L^2(\hat{T})} \leq C\|f\|_{H^{1/2}_{00}(I)} \quad \text{by (2.4.4)}$$

Thus, $\|\partial_x \mathcal{R}_{2,L}(f)\|_{L^2(\hat{T})} \leq C\|f\|_{H^{1/2}_{00}(\hat{\gamma}_3)}$.

∂_y **estimate**: We compare the derivative to $\mathcal{R}_{1,L}$.

$$\partial_y \mathcal{R}_{2,L}(f)(x,y) - \partial_y \mathcal{R}_{1,L}(f)(x,y) = \frac{1}{y^2}\int_x^{x+y} \frac{x}{t}\left(1 - \frac{x}{t}\right) f(t)\, dt - \frac{x}{x+y} \cdot \frac{f(x+y)}{x+y}$$
$$=: E_3 - E_2.$$

For E_3, we use the same technique as before:

$$|E_3| \leq \frac{1}{y}\int_x^{x+y} \left|\frac{f(t)}{t}\right| dt = \mathcal{R}_{1,L}\left(|f|\right)(x,y) \Longrightarrow \|E_3\|_{L^2(\hat{T})} \leq C\|f\|_{H^{1/2}_{00}(\hat{\gamma}_3)}.$$

by Theorem 2.4.2. E_2 is the same as above, and so $\|\partial_y \mathcal{R}_{2,L}\|_{L^2(\hat{T})} \le C\|f\|_{H^{1/2}_{00}(\hat{\gamma}_3)}$.

∂_{xx} **estimate**: We again compare to $\mathcal{R}_{1,L}$.

$$
\begin{aligned}
&\partial_{xx}\mathcal{R}_{2,L}(x,y) - \partial_{xx}\mathcal{R}_{1,L}(f)(x,y) \\
&\qquad = \frac{2}{y}\int_x^{x+y} \frac{f(t)}{t^2}\, dt + \frac{1}{y}\left[\frac{f(x+y)}{x+y} - \frac{f(x)}{x}\right] + \left(\frac{2x}{x+y} - 3\right)\frac{f(x+y)}{(x+y)^2} \\
&\qquad\quad - \frac{x}{x+y}\cdot\frac{f'(x+y)}{x+y} \\
&\quad =: E_4 + E_5 + E_6 - E_7.
\end{aligned}
$$

For E_4,

$$
|E_4| \le \frac{2}{y}\int_x^{x+y} \frac{|f(t)|}{t^2}\, dt = 2\mathcal{E}\left(\frac{|f(\xi)|}{\xi^2}\right).
$$

Thanks to (2.4.1) and (2.3.12), there holds

$$
\|E_4\|_{L^2(\hat{T})} \le C\|\xi^{-3/2} f(\xi)\|_{L^2(\hat{\gamma}_3)} \le C\|f'\|_{H^{1/2}_{00}(\hat{\gamma}_3)}.
$$

E_5 is the same as E_1 in Lemma 2.4.6, and so $\|E_5\|_{L^2(\hat{T})} \le C\|f\|_{H^{3/2}_{00}(\hat{\gamma}_3)}$. For E_6 and E_7,

$$
|E_6| + |E_7| \le C\frac{|f(x+y)|}{(x+y)^2} + \frac{|f'(x+y)|}{x+y}.
$$

Applying (2.4.5) to the first term and (2.4.4) to f' in the second term gives $\|E_6\|_{L^2(\hat{T})} + \|E_7\|_{L^2(\hat{T})} \le C\|f\|_{H^{3/2}_{00}(\hat{\gamma}_3)}$. Thus, $\|\partial_{xx}\mathcal{R}_{2,L}(f)\|_{L^2(\hat{T})} \le C\|f\|_{H^{3/2}_{00}(\hat{\gamma}_3)}$.

∂_{xy} **estimate**: We compare to $\mathcal{E}$.

$$
\begin{aligned}
&\partial_{xy}\mathcal{R}_{2,l}(f)(x,y) - \partial_{xy}\mathcal{E}(f)(x,y) \\
&\quad = \left\{ -\frac{2x}{y^2}\int_x^{x+y} \frac{f(t)}{t^2}\,dt + \frac{2x}{y}\cdot\frac{f(x+y)}{(x+y)^2} \right\} + \left(1 + \frac{2x}{x+y}\right)\cdot\frac{f(x+y)}{(x+y)^2} \\
&\qquad - \frac{2x+y}{x+y}\cdot\frac{f'(x+y)}{x+y} \\
&\quad =: E_8 + E_9 - E_{10}
\end{aligned}
$$

For E_8, we have

$$
\begin{aligned}
E_8 &= \frac{2x}{y^2}\int_x^{x+y}\left[\frac{1}{(x+y)^2}\int_0^{x+y} f'(s)\,ds - \frac{1}{t^2}\int_0^t f'(s)\,ds\right]\,dt \\
&= \frac{x}{y^2}\int_x^{x+y}\left[\frac{tA_L^{1,0}(f')(x+y) - (x+y)A_L^{1,0}(f')(t)}{t(x+y)}\right]\,dt.
\end{aligned}
$$

Now, taking absolute values, we have

$$
\begin{aligned}
|E_8| &\leq \frac{2}{y^2}\int_x^{x+y}\left|\frac{tA_L^{1,0}(f')(x+y) - (x+y)A_L^{1,0}(f')(t)}{x+y}\right|\,dt \\
&\leq \frac{2}{y^2}\int_x^{x+y}\left|A_L^{1,0}(f')(x+y) - A_L^{1,0}(f')(t)\right|\,dt \\
&\qquad + \frac{2}{y^2}\int_x^{x+y}\frac{t-x-y}{x+y}\cdot|A_L^{1,0}(f')(x+y)|\,dt \\
&=: F_1 + F_2.
\end{aligned}
$$

From (2.4.5) and (2.4.6), we have $\|F_1\|_{L^2(\hat{T})} \leq C\|f\|_{H_{00}^{3/2}(\hat{\gamma}_3)}$. For F_2, note that

$|t-x-y| \le y$ and so

$$|F_2| \le \frac{2}{y}\int_x^{x+y} \frac{1}{x+y}|A_L^{1,0}(f')(x+y)|\,dt = \frac{|A_L^{1,0}(f')(x+y)|}{x+y}.$$

Thus, $\|F_2\|_{L^2(\hat{T})} \le C\|A_L^{1,0}(f')\|_{H_{00}^{1/2}(\hat{\gamma}_3)} \le C\|f\|_{H_{00}^{3/2}(\hat{\gamma}_3)}$ by (2.4.4) and (2.3.4). As a result, $\|\partial_{xy}\mathcal{R}_{2,L}\|_{L^2(\hat{T})} \le C\|f\|_{H_{00}^{3/2}(\hat{\gamma}_3)}$.

∂_{yy} **estimate**: We compare to $\mathcal{R}_{1,L}$.

$$\begin{aligned}
&\partial_{yy}\mathcal{R}_{2,L}(f)(x,y) - \partial_{yy}\mathcal{R}_{1,L}(f)(x,y)\\
&\quad= \left[\frac{2x}{y^3}\int_x^{x+y}\frac{f(t)}{t}\left(\frac{x}{t}-1\right) + \frac{x}{(x+y)^2}\cdot\frac{f(x+y)}{y}\right] + \frac{2x}{x+y}\cdot\frac{f(x+y)}{(x+y)^2}\\
&\qquad - \frac{x}{x+y}\cdot\frac{f'(x+y)}{x+y}\\
&\quad=: E_{11} + E_{12} - E_7.
\end{aligned}$$

For E_{11}, we have

$$|E_{11}| = \frac{2x}{y^3}\left|\int_x^{x+y}\left[\frac{f(x+y)}{(x+y)^2} - \frac{f(t)}{t^2}\right](t-x)\,dt\right| \le \frac{2x}{y^2}\int_x^{x+y}\left|\frac{f(x+y)}{(x+y)^2} - \frac{f(t)}{t^2}\right|\,dt.$$

This is the same term that appears in our estimate for E_8, and so $\|E_{11}\|_{L^2(\hat{T})} \le C\|f\|_{H_{00}^{3/2}(\hat{\gamma}_3)}$. For E_{12},

$$|E_{12}| \le \frac{|f(x+y)|}{(x+y)^2} \implies \|E_{12}\|_{L^2(\hat{T})} \le C\|f\|_{H_{00}^{3/2}(\hat{\gamma}_3)} \quad \text{by (2.4.5)}$$

E_7 is the same as above and so $\|\partial_{yy}\mathcal{R}_{2,L}\|_{L^2(\hat{T})} \le C\|f\|_{H_{00}^{3/2}(\hat{\gamma}_3)}$. □

Corresponding operators and estimates for the right hand node also hold.

Lemma 2.4.8. *Let* $f \in H^{3/2}_{00}(\hat{\gamma}_3)$*. Let*

$$\mathcal{R}_{2,R}(f)(x,y) = (1-x-y)^2 \mathcal{E}\left(\frac{f(\xi)}{(1-\xi)^2}\right)(x,y).$$

Then, there exists a constant C *such that*

$$\|\mathcal{R}_{1,R}(f)\|_{H^2(\hat{T})} + \|\mathcal{R}_{2,R}(f)\|_{H^2(\hat{T})} \leq C\|f\|_{H^{3/2}_{00}(\hat{\gamma}_3)}.$$

Proof. The result follows at once from Lemmas 2.4.6 and 2.4.7 by defining $f^*(\eta) = f(1-\eta)$ and observing that $\mathcal{R}_{1,R}(f)(x,y) = \mathcal{R}_{1,L}(f^*)(1-x-y,y)$ and $\mathcal{R}_{2,R}(f)(x,y) = \mathcal{R}_{2,L}(f^*)(1-x-y,y)$. □

We now are in a position to complete the proof of the theorem.

Proof of Theorem 2.4.3. We have the following decomposition

$$\begin{aligned}\mathcal{R}_2(f)(x,y) &= (1-x-y)^2\mathcal{R}_{2,L}(f)(x,y) + 2x(1-x-y)^2\mathcal{R}_{1,L}(f)(x,y)\\ &\quad - 2x^2(1-x-y)\mathcal{R}_{1,R}(f)(x,y) + x^2\mathcal{R}_{2,R}(f)(x,y).\end{aligned}$$

The H^2 continuity follows from Lemmas 2.4.6 to 2.4.8. If $f \in \mathcal{P}_p(\hat{\gamma}_3)$, then $f(0) = f'(0) = f(1) = f'(1) = 0$, and so $f(t) = t^2(1-t)^2 g(t)$ for some $g \in \mathcal{P}_{p-4}(\hat{\gamma}_3)$. Thus, $\mathcal{R}_2(f) \in \mathcal{P}_p(\hat{T})$. □

Remark 2.4.9. Of course, we can analogously define extension operators for the other sides of $\hat{T}$. In the sequel, we use $\mathcal{E}_i$, $\mathcal{E}_i^{\boldsymbol{n}}$, and $\mathcal{R}_{2,i}$ to denote the respective extension operators associated with $\hat{\gamma}_i$ and use the corresponding bounds without proof.

Finally, we recall result from [73] concerning the existence of a normal extension operator as follows:

Theorem 2.4.10. *For every $p \geq 1$, there exists $\mathcal{R}_i^{\boldsymbol{n}} : \mathcal{P}_{p-1}(\hat{\gamma}_i) \cap H_0^2(\hat{\gamma}_i) \to \mathcal{P}_p(\hat{T})$ and a constant C independent of p such that for all $f \in H_{00}^{1/2}(\hat{\gamma}_i)$, there holds*

$$\mathcal{R}_i^{\boldsymbol{n}}(f)|_\Gamma = 0, \quad \partial_n \mathcal{R}_i^{\boldsymbol{n}}(f)|_{\hat{\gamma}_j} = \delta_{ij} f, \quad \textit{and} \quad \|\mathcal{R}_i^{\boldsymbol{n}}(f)\|_{H^2(\hat{T})} \leq C \|f\|_{H_{00}^{1/2}(\hat{\gamma}_i)}.$$

2.5 Polynomial Extensions from Two Edges

In the next stage of the argument, we create an extension from two sides of $\hat{T}$. Then, we use the single edge extensions Theorem 2.4.3 and Theorem 2.4.10 to adjust the traces on the remaining edge and thereby obtain the desired extension operator from the entire boundary.

Note the following properties of the elementary single-edge extensions:

$$\begin{aligned} \mathcal{E}_3(f)(x,0) &= f(x), & \mathcal{E}_3(f)(0,y) &= \int_0^1 f(sy)\ ds, \\ \partial_{n_3}\mathcal{E}_3(f)(x,0) &= -\frac{1}{2}f'(x), & \partial_{n_2}\mathcal{E}_3(f)(0,y) &= -\int_0^1 f'(sy)\ ds, \\ \mathcal{E}_3^{\boldsymbol{n}}(g)(x,0) &= 0, & \mathcal{E}_3^{\boldsymbol{n}}(g)(0,y) &= y\int_0^1 a(s)g(sy)\ ds, \\ \partial_{n_3}\mathcal{E}_3^{\boldsymbol{n}}(g)(x,0) &= g(x,0), & \partial_{n_2}\mathcal{E}_3^{\boldsymbol{n}}(g)(0,y) &= -y\int_0^1 a(s)g'(sy)\ ds. \end{aligned}$$

By symmetry, we have analogous relations for $\mathcal{E}_2$ and $\mathcal{E}_2^{\boldsymbol{n}}$.

Lemma 2.5.1. *Suppose f and g are such that $f_i = f|_{\hat{\gamma}_i} \in \mathcal{P}_p(\hat{\gamma}_i)$, $g_i = g|_{\hat{\gamma}_i} \in \mathcal{P}_{p-1}(\hat{\gamma}_i)$ and f_i, g_i satisfy the compatibility conditions* (2.2.10). *Then, there exists F_2, F_3, G_2, G_3, and a constant C independent of f, g, and p such that*

(i) $U = \mathcal{E}_2(F_2) + \mathcal{E}_3(F_3) + \mathcal{E}_2^{\boldsymbol{n}}(G_2) + \mathcal{E}_3^{\boldsymbol{n}}(G_3) \in \mathcal{P}_p(\hat{T})$.

(ii) $U|_{\hat{\gamma}_i} = f_i$, $\partial_n U|_{\hat{\gamma}_i} = g_i$, $i = 2, 3$.

(iii) $\|U\|_{H^2(\hat{T})} \leq C\left(\|f\|_{L^2(\Gamma)} + \|\boldsymbol{\sigma}(f,g)\|_{\boldsymbol{H}^{1/2}(\Gamma)}\right)$.

Proof. For notational convenience, we reparametrize f_2 such that $f_2(0) = f(\hat{\boldsymbol{a}}_1)$ and

$f_2(1) = f(\hat{\boldsymbol{a}}_3)$. The desired functions F_i and G_i satisfy a system of integral equations:

$$
\begin{aligned}
f_2(x) &= F_2(x) + \int_0^1 F_3(sx)\ ds + x\int_0^1 a(s)G_3(sx)\ ds,\\
f_3(x) &= F_3(x) + \int_0^1 F_2(sx)\ ds + x\int_0^1 a(s)G_2(sx)\ ds,\\
g_2(x) &= -\frac{1}{2}F_2'(x) - \int_0^1 F_2'(sx)\ ds + G_2(x) - x\int_0^1 a(s)G_3'(sx)\ ds,\\
g_3(x) &= -\frac{1}{2}F_3'(x) - \int_0^1 F_2'(sx)\ ds + G_3(x) - x\int_0^1 a(s)G_2'(sx)\ ds.
\end{aligned}
$$

Let $\Phi_1 = F_2 + F_3$, $\Phi_2 = F_2 - F_3$, $\Psi_1 = G_2 + G_3$, $\Psi_2 = G_2 - G_3$, $h_1 = f_2 + f_3$, $h_2 = f_2 - f_3$, $l_1 = g_2 + g_3$, $l_2 = g_2 - g_3$. Then, the system decouples to become

$$
\begin{aligned}
h_1(x) &= \Phi_1(x) + \int_0^1 \Phi_1(sx)\ ds + x\int_0^1 a(s)\Psi_1(sx)\ ds,\\
l_1(x) &= -\frac{1}{2}\Phi_1'(x) - \int_0^1 \Phi_1'(sx)\ ds + \Psi_1(x) - x\int_0^1 a(s)\Psi_1'(sx)\ ds,
\end{aligned}
\tag{2.5.1}
$$

and

$$
\begin{aligned}
h_2(x) &= \Phi_2(x) - \int_0^1 \Phi_2(sx)\ ds - x\int_0^1 a(s)\Psi_2(sx)\ ds,\\
l_2(x) &= -\frac{1}{2}\Phi_2'(x) + \int_0^1 \Phi_2'(sx)\ ds + \Psi_2(x) + x\int_0^1 a(s)\Psi_2'(sx)\ ds.
\end{aligned}
\tag{2.5.2}
$$

Note that the compatibility conditions (2.2.10) under this new parametrization read as

$$
h_1'(0) + l_1(0) = 0, \qquad h_2(0) = l_2'(0) = 0, \qquad h_2'(0) = l_2(0). \tag{2.5.3}
$$

First system: It is straight forward to check that a solution to (2.5.1) is given by

$$\Phi_1(t) = \frac{4}{5}h_1(t) + \frac{54}{5t^4}\int_0^t s^3 h_1(s)\ ds - \frac{9}{t^3}\int_0^t s^2 h_1(s)\ ds - \frac{36}{5t^4}\int_0^t s^4 l_1(s)\ ds$$
$$+ \frac{9}{t^3}\int_0^t s^3 l_1(s)\ ds - \frac{2}{t^2}\int_0^t s^2 l_1(s)\ ds - \frac{t}{5}\int_t^1 \frac{h_1'(s) + l_1(s)}{s}\ ds$$

and

$$\Psi_1(t) = \frac{1}{2}h_1'(t) + \frac{1}{2t^4}\int_0^t s^3 h_1'(s)\ ds - \frac{9}{5t^5}\int_0^t s^4 h_1'(s)\ ds + l_1(t) + \frac{3}{2t^4}\int_0^t s^3 l_1(s)\ ds$$
$$- \frac{3}{10}\int_t^1 \frac{h_1'(s) + l_1(s)}{s}\ ds$$

For instance, one may verify that the above are solutions to (2.5.1), by expressing h_1 and l_1 as a sum of monomials, directly substituting and equating coefficients. Applying (2.3.4) to (2.3.11) term-by-term and using (2.5.3), we have the estimate

$$\|\Phi_1\|_{H^{3/2}(I)} + \|\Psi_1\|_{H^{1/2}(I)} \leq C\left(\|h_1\|_{H^{3/2}(I)} + \|l_1\|_{H^{1/2}(I)} + \|h_1' + l_1\|_{H_L^{1/2}(I)}\right).$$

Since $h_1'(t) + l_1(t) = tq(t)$ where $q \in \mathcal{P}_{p-2}(I)$, it follows that $\Phi_1 \in \mathcal{P}_p(I)$ and $\Psi_1 \in \mathcal{P}_{p-1}(I)$.

Second system: In a similar vein, a solution to (2.5.2) is given by

$$\Phi_2(t) = 4h_2(t) - \frac{1}{t^3}\int_0^t s^2 h(s)\ ds + \frac{3}{5t^3}\int_0^t s^3 l_2(s)\ ds - 2\int_t^1 \frac{h_2(s)}{s}\ ds$$
$$+ 3t\int_t^1 \frac{h_2'(s) - l_2(s)}{s}\ ds + \frac{18t^2}{5}\int_t^1 \frac{l_2(s)}{s^2}\ ds$$

and

$$\Psi_2(t) = \frac{h_2'(t)}{2} - \frac{1}{3}\cdot\frac{h_2(t)}{t} - \frac{1}{6t^4}\int_0^t s^3 h_2'(s)\ ds + l_2(t) - \frac{3}{10t^4}\int_0^t s^3 l_2(s)\ ds$$
$$- \frac{3}{2}\int_t^1 \frac{h_2'(s) - l_2(s)}{s}\ ds - \frac{24t}{5}\int_t^1 \frac{l_2(s)}{s^2}\ ds.$$

By (2.3.4) to (2.3.11) and Lemma 2.3.3 and using (2.5.3), we have the estimate

$$\|\Phi_2\|_{H^{3/2}(I)} + \|\Psi_2\|_{H^{1/2}(I)} \le C\left(\|h_2\|_{H^{3/2}(I)} + \|l_2\|_{H^{1/2}(I)} + \|h_2' - l_2\|_{H_L^{1/2}(I)}\right).$$

Note that $h(t) = tq_1(t)$ where $q_1 \in \mathcal{P}_{p-1}(I)$, $h_2'(t) + l_2(t) = tq_2(t)$ where $q_2 \in \mathcal{P}_{p-2}(I)$, and that $l_2(t) = l(0) + t^2 q_3(t)$, where $q_3 \in \mathcal{P}_{p-3}(I)$. Consequently, $\Phi_2 \in \mathcal{P}_p(I)$ and $\Psi_2 \in \mathcal{P}_{p-1}(I)$.

By Lemma 2.4.1, we have found F_i and G_i that satisfy (i) and (ii). Substituting in for h_i and l_i, we get

$$\sum_{i=2,3}\left\{\|F_i\|^2_{H^{3/2}(I)}+\|G_i\|^2_{H^{1/2}(I)}\right\}\le C\Bigg[\sum_{i=2,3}\left\{\|f_i\|^2_{H^{3/2}(I)}+\|g_i\|^2_{H^{1/2}(I)}\right\}$$
$$+\int_0^1\frac{|f_2'(t)+g_3(t)|^2+|f_3'(t)+g_2(t)|^2}{t}\,dt\Bigg]$$
$$\le C\left(\|f\|^2_{L^2(\Gamma)}+\|\boldsymbol{\sigma}(f,g)\|^2_{\boldsymbol{H}^{1/2}(\Gamma)}\right),$$

and (iii) follows by using Lemma 2.4.1. □

2.6 Proof of Theorem 2.2.2

Assume first that $U\in\mathcal{P}_p(\hat{T})$. From the discussion in Section 2.2, conditions (2.2.10) are satisfied. Now assume that f and g are given and satisfy the compatibility conditions (2.2.10). By Lemma 2.5.1, we can find a $U_1\in\mathcal{P}_p(\hat{T})$ such that $U_1|_{\hat{\gamma}_i}=f_i$, $\partial_n U_1|_{\hat{\gamma}_i}=g_i$, $i=2,3$, and

$$\|U_1\|_{H^2(\hat{T})}\le C\left(\|f\|_{L^2(\Gamma)}+\|\boldsymbol{\sigma}(f,g)\|_{\boldsymbol{H}^{1/2}(\Gamma)}\right).$$

We now adjust the functional values of U_1 on $\hat{\gamma}_1$ to match f_1. Denote $h_1:=U_1|_{\hat{\gamma}_1}$ and $l_1:=\partial_n U_1|_{\hat{\gamma}_1}$. U_1 is a polynomial, so it also satisfies the compatibility conditions.

Thus,

$$f_1(0) = h_1(0), \quad f_1'(0) = h_1'(0), \quad f_1(\sqrt{2}) = h_1(\sqrt{2}), \quad \text{and} \quad f_1'(\sqrt{2}) = h_1'(\sqrt{2}),$$

and so, $f_1 - h_1 \in H_{00}^{3/2}(I)$. Prompted by Theorem 2.4.3, we set

$$U_2 := U_1 + \mathcal{R}_{2,1}(f_1 - h_1),$$

where $\mathcal{R}_{2,1}$ is defined in Remark 2.4.9. Then, thanks to the properties of $\mathcal{R}_{2,1}$ and U_1, we have

$$U_2|_{\hat{\gamma}_i} = f_i, \quad i = 1, 2, 3, \quad \partial_n U_2|_{\hat{\gamma}_j} = g_j, \quad j = 2, 3, \tag{2.6.1}$$

and $\|U_2\|_{H^2(\hat{T})} \leq C\left(\|f\|_{L^2(\Gamma)} + \|\boldsymbol{\sigma}(f,g)\|_{\boldsymbol{H}^{1/2}(\Gamma)} + \|f_1 - h_1\|_{H_{00}^{3/2}(\hat{\gamma}_1)}\right)$. To estimate the third term, we have

$$\begin{aligned}\|f_1 - h_1\|^2_{H_{00}^{3/2}(\hat{\gamma}_1)} \approx \|f_1 - h_1\|^2_{H^{3/2}(\hat{\gamma}_1)} &+ \int_0^{\sqrt{2}} \frac{|f_1'(t) - h_1'(t)|^2}{t}\, dt \\ &+ \int_0^{\sqrt{2}} \frac{|f_1'(t) - h_1'(t)|^2}{\sqrt{2} - t}\, dt.\end{aligned}$$

The compatibility conditions (2.2.10) imply that $(f,g) \in \mathrm{Tr} H^2(\hat{T})$. Thus, we can use Theorem 2.2.1 to find $w \in H^2(\hat{T})$ whose trace is (f,g) and which satisfies $\|w\|_{H^2(\hat{T})} \leq$

$C\left(\|f\|_{L^2(\Gamma)} + \|\boldsymbol{\sigma}(f,g)\|_{\boldsymbol{H}^{1/2}(\Gamma)}\right)$. Then, we have

$$\begin{aligned}
&\|w - U_1\|^2_{L^2(\Gamma)} + \|\boldsymbol{\sigma}(w - U_1, \partial_n(w - U_1))\|^2_{\boldsymbol{H}^{1/2}(\Gamma)} \\
&\quad \approx \|f_1 - h_1\|^2_{H^{3/2}(\hat{\gamma}_1)} + \|g_1 - l_1\|^2_{H^{1/2}(\hat{\gamma}_1)} \\
&\qquad + \int_0^{\sqrt{2}} \frac{|(f_1'(t) - h_1'(t))\boldsymbol{n}_1 - (g_1(t) - l_1(t))\boldsymbol{t}_1|^2}{t}\,dt \\
&\qquad + \int_0^{\sqrt{2}} \frac{|(f_1'(t) - h_1'(t))\boldsymbol{n}_1 - (g_1(t) - l_1(t))\boldsymbol{t}_1|^2}{\sqrt{2} - t}\,dt
\end{aligned}$$

Observe that $f_1'(t) - h_1'(t) = \boldsymbol{n}_1 \cdot [(f_1'(t) - h_1'(t))\boldsymbol{n}_1 - (g_1(t) - l_1(t))\boldsymbol{t}_1]$, and so

$$\begin{aligned}
\|f_1 - h_1\|_{H^{3/2}_{00}(\hat{\gamma}_1)} &\le C\left(\|w - U_1\|_{L^2(\Gamma)} + \|\boldsymbol{\sigma}(w - U_1, \partial_n(w - U_1))\|_{\boldsymbol{H}^{1/2}(\Gamma)}\right) \\
&\le C\left(\|w\|_{H^2(\hat{T})} + \|U_1\|_{H^2(\hat{T})}\right) \\
&\le C\left(\|f\|_{L^2(\Gamma)} + \|\boldsymbol{\sigma}(f,g)\|_{\boldsymbol{H}^{1/2}(\Gamma)}\right).
\end{aligned}$$

This gives $\|U_2\|_{H^2(\hat{T})} \le C\left(\|f\|_{L^2(\Gamma)} + \|\boldsymbol{\sigma}(f,g)\|_{\boldsymbol{H}^{1/2}(\Gamma)}\right)$.

Now we need to adjust the normal trace of U_2 on $\hat{\gamma}_1$ to agree with g_1. Denote $\tilde{l}_1 = \partial_n U_2|_{\hat{\gamma}_1}$. Note that $g_1 - \tilde{l}_1$ has a repeated zero at $t = 0$ and $t = \sqrt{2}$. Indeed, U_2 is a polynomial and so it satisfies the compatibility conditions (2.2.10):

$$g_1(0) = \tilde{l}_1(0), \quad g_2'(0) = \tilde{l}_1(0), \quad g_1(\sqrt{2}) = \tilde{l}_1(\sqrt{2}), \quad \text{and} \quad g_1'(\sqrt{2}) = \tilde{l}_2'(\sqrt{2}),$$

where we used (2.6.1). Now define

$$U := U_2 + \mathcal{R}_1^{\boldsymbol{n}}\left(g_1 - \tilde{l}_1\right).$$

By Theorem 2.4.10, we only need to bound $\|g_1 - \tilde{l}_1\|_{H_{00}^{1/2}(\hat{\gamma}_1)}$. Arguing as before,

$$\begin{aligned}\left\|g_1 - \tilde{l}_1\right\|^2_{H_{00}^{1/2}(\hat{\gamma}_1)} &\approx \left\|g_1 - \tilde{l}_1\right\|^2_{H^{1/2}(\hat{\gamma}_1)} + \int_0^{\sqrt{2}} \frac{\left|g_1(t) - \tilde{l}_1(t)\right|^2}{t} + \int_0^{\sqrt{2}} \frac{\left|g_1(t) - \tilde{l}_1(t)\right|^2}{\sqrt{2} - t} \\ &\approx \|w - U_2\|^2_{L^2(\Gamma)} + \|\boldsymbol{\sigma}(w - U_2, \partial_n(w - U_2))\|^2_{\boldsymbol{H}^{1/2}(\Gamma)} \\ &\leq C\left(\|f\|^2_{L^2(\Gamma)} + \|\boldsymbol{\sigma}(f, g)\|^2_{\boldsymbol{H}^{1/2}(\Gamma)}\right).\end{aligned}$$

By the properties of the various component extension operators used, we have $U \in \mathcal{P}_p(\hat{T})$. $\square$

2.7 Proof of Lemma 2.3.1

Let $k \geq 0$. We prove (2.3.3) by induction. The case $m = 0$ is clear, so assume the formula holds for an arbitrary m and $f \in H^{m+1}(I)$. Then,

$$\frac{d^{m+1}}{dx^{m+1}} A_L^{k+1,k} f = \frac{d}{dx} A_L^{k+1+m,k+m} f^{(m)} = -\frac{k+1+m}{x^{k+1+m+1}} \int_0^x t^{k+m} f^{(m)}(t)\ dt + \frac{f^{(m)}(x)}{x}.$$

One integration by parts gives

$$-\frac{k+1+m}{x^{k+1+m+1}}\int_0^x t^{k+m} f^{(m)}(t)\ dt + \frac{f^{(m)}(x)}{x} = \frac{1}{x^{k+1+m+1}}\int_0^x t^{k+m+1} f^{(m+1)}(t)\ dt$$
$$= A_L^{k+1+m+1,k+m+1} f^{(m+1)},$$

which proves (2.3.3). Now we prove (2.3.4). By interpolation, it suffices to show the result for integer s. Using Theorem 6.20 [53] with $K(x,t) = t^k x^{-(k+1)}\chi_{t<x}$ and $p = 2$ gives

$$\|A_L^{k+1,k} f\|_{L^2(I)} \leq C\|f\|_{L^2(I)} \quad \text{with} \quad C = \int_0^1 t^{k-1/2}\ dt = \frac{1}{k+\frac{1}{2}}.$$

Now, using (2.3.3), we have

$$\left\|\frac{d^s}{dx^s} A_L^{k+1,k} f\right\|_{L^2(I)} = \left\|A_L^{k+1+s,k+s} f^{(s)}\right\|_{L^2(I)} \leq \frac{1}{s+k+\frac{1}{2}}\left\|f^{(s)}\right\|_{L^2(I)}.$$

Thus, we have (2.3.4). Now we prove (2.3.5). For the L^2 norm, we have

$$\left|A_L^{k,k} f(x)\right| \leq \int_0^x |f(t)|\ dt \implies \|A_L^{k,k} f\|_{L^2(I)} \leq \|f\|_{L^2(I)} \quad \text{by Cauchy-Schwarz.}$$

Then, taking one derivative gives

$$\frac{d}{dx}\left[A_L^{k,k} f(x)\right] = f(x) - \frac{k}{x^{k+1}}\int_0^x t^k f(t)\ dt = f(x) - kA_L^{k+1,k} f(x).$$

Again applying (2.3.4), we have

$$\left\| \frac{d}{dx} \left[A_L^{k,k} f(x) \right] \right\|_{H^s(I)} \leq \left(1 + \frac{k}{k+\frac{1}{2}} \right) \|f\|_{H^s(I)},$$

which finishes (2.3.5). (2.3.6) comes from taking $K(\cdot,\cdot)$ as above and applying Theorem 6.20 [53] again:

$$\left\| B_R^{k+1,k} f \right\|_{L^2(I)} \leq \frac{1}{k+\frac{1}{2}} \|f\|_{L^2(I)}.$$

We now prove (2.3.7). In the case $k = 0$, we have

$$B_R^{1,0} f(x) = \int_x^1 \frac{1}{t} f(t)\ dt \quad \text{and} \quad \frac{d}{dx} B_R^{1,0} f(x) = -\frac{f(x)}{x} = -A_L^{1,0} f'(x).$$

Using (2.3.4), we have $\left\| B_R^{1,0} f \right\|_m \leq 2\|f\|_m$ for $0 \leq m \leq n$. For general $k \geq 1$, we have

$$\begin{aligned} B_R^{k+1,k} f(x) &= x^k \int_x^1 \frac{1}{t^{k+1}} f(t)\ dt \\ \frac{d}{dx} B_R^{k+1,k} f(x) &= k x^{k-1} \int_x^1 \frac{1}{t^{k+1}} f(t)\ dt - \frac{f(x)}{x} = k B_R^{k,k-1} A_L^{1,0} f'(x) - A_L^{1,0} f'(x). \end{aligned}$$

Thus, using the L^2 norm estimate and (2.3.4), we have $\|B_R^{k+1,k} f(x)\|_{H^1(I)} \leq 6\|f\|_{H^1(I)}$. For the second derivative, we have

$$\left\| \frac{d}{dx} B_R^{k+1,k} f(x) \right\|_{H^1(I)} \leq k \left\| B_R^{k,k-1} A_L^{1,0} f' \right\|_{H^1(I)} + \left\| A_L^{1,0} f' \right\|_{H^1(I)}.$$

Using the H^1 estimate we just proved, we have since $k \geq 1$

$$\left\| \frac{d}{dx} B_R^{k+1,k} f(x) \right\|_{H^1(I)} \leq \left(\frac{k}{k-\frac{1}{2}} + 1 \right) \left\| A_L^{1,0} f' \right\|_{H^1(I)} \leq 6 \left\| f' \right\|_{H^1(I)} \leq 6 \left\| f \right\|_{H^2(I)},$$

which completes (2.3.7). By interpolation, we get (2.3.8). Now we prove (2.3.9). Let $k \geq 0$. For the L^2 estimate, note that

$$\left| B_R^{k,k} f \right| \leq x^k \int_x^1 \frac{1}{t^k} |f(t)| \, dt \leq \int_x^1 |f(t)| \, dt,$$

Using Cauchy-Schwarz, we have $\left\| B_R^{k,k} f \right\|_{L^2(I)} \leq \|f\|_{L^2(I)}$. Then, taking one derivative gives

$$\frac{d}{dx} B_R^{k,k} f(x) = k B_R^{k,k-1} f(x) - f(x). \tag{2.7.1}$$

Here and what follows, $B_R^{k,l}$ with negative k or l is understood to be the zero operator. First, applying (2.3.6), we have

$$\left\| \frac{d}{dx} B_R^{k,k} f(x) \right\|_{L^2(I)} \leq \left(\frac{k}{k-\frac{1}{2}} + 1 \right) \|f\|_{L^2(I)} \leq 3 \|f\|_{L^2(I)},$$

which completes (2.3.9). Now we prove (2.3.10). Since we assumed $f(0) = 0$ in the case $k = 1$, we can apply (2.3.7) to estimate the second derivative. In the case $k \neq 1$, taking one more derivative and performing one integration by parts gives

$$\begin{aligned}\frac{d^2}{dx^2}B_R^{k,k}f(x) &= k\left[(k-1)x^{k-2}\int_x^1 \frac{1}{t^k}f(t)\ dt - \frac{f(x)}{x}\right] - f'(x)\\ &= kB_R^{k-1,k-2}(f') - kx^{k-2}f(1) - f'(x)\end{aligned}$$

Recalling the embedding $\|f\|_{L^\infty(I)} \le C\|f\|_{H^1(I)}$ and using (2.3.6), we have

$$\left\|\frac{d^2}{dx^2}B_R^{k,k}f\right\|_{L^2(I)} \le C(k+1)\|f\|_{H^1(I)},$$

which completes (2.3.10). (2.3.11) follows from interpolation. $\square$

2.8 Conclusions

This chapter established the existence of an H^2-stable polynomial lifting of compatible piecewise polynomial boundary data. The extension operator in Corollary 2.2.3 plays a key role in various results throughout this thesis. In Chapter 3, Corollary 2.2.3 is used in the analysis of an iterative substructuring preconditioner for the discretization of fourth order elliptic problem by H^2-conforming finite elements and in the construction of special rapidly decaying vertex functions in Section 3.7. Corollary 2.2.3 also appears in the proof of Lemma 4.3.6 which is an extension theorem involving vector-valued functions on triangles and in Chapter 5 in the construction of interpolants with optimal approximation properties. Future directions include the generalization of Corollary 2.2.3 to tetrahedra and to H^k spaces with $k > 2$.

Chapter Three

Preconditioning High Order H^2-Conforming Finite Elements on Triangles

3.1 Introduction

Fourth order partial differential equations arise in a variety of applications ranging from incompressible fluid flow [55] and elastic models of thin plates and shells [72] to nonlinear phase field models for materials [36]. A conforming finite element approximation of such problems entails the use of elements with C^1-continuity between elements [24, 38], the first of which goes back over half a century, Argyris et. al. [11].

The natural stability of conforming schemes means that the convergence and approximation properties of such elements is on a sound footing. In the context of the h-version finite element setting a classical finite element error analysis can be carried out [38]. The space of C^1 piecewise degree p polynomials was characterized in [83], and optimal convergence rates in the polynomial degree p are derived in [106] in the case of finite Sobolev regularity, while exponential convergence rates for the hp-version are derived in [57]. In particular, the p-version and hp-version offer superior convergence rates over the h-version. The theoretical results for high order H^2-conforming elements are also borne out in practice; the numerical results reported in Section 3.6 are typical of what one observes using such methods.

One might expect to find that, in view of the range of applications, the natural stability and a sound theoretical support of C^1-elements, conforming schemes are widely used in practice. On the contrary, C^1-elements are a rarity and often passed by in favour of more elaborate schemes such as discontinuous Galerkin or mixed finite elements which require lower continuity. The relative scarcity of C^1-finite element schemes in practice stems in part from the rapid growth of the condition number of the associated stiffness matrix which, in the case of the h-version, grows at a rate $\mathcal{O}(h^{-4})$ compared with $\mathcal{O}(h^{-2})$ for second order problems. For instance, a straightforward textbook implementation of the lowest order Argyris elements in conjunction with a direct solver is found [21, pp.374-7] to result in prohibitively large condition numbers after just 2-3 refinements of a relatively coarse initial mesh. The situation when it comes to the p-version is even worse with exponential growth in the polynomial degree p being observed if a Lagrange basis is used with respect to the set of canonical degrees of freedom (dofs).

Preconditioning schemes are available for C^1-elements in the context of the h-version. Widlund and Zhang [117, 118, 119] constructed additive Schwarz preconditioners for the lowest order Bell, Argyris, and Hermitian elements and showed that the condition number of the resulting system grows at most as $1 + \log^2(H/h)$ for some two level methods [119] and is uniformly bounded for some multilevel methods [118]. Subsequently, Bramble and Zhang [35] developed a multigrid algorithm for h-version conforming approximations. On the numerical linear algebra side, Pestana et. al. [92] tested a variety of block preconditioners for the lowest order quadrilateral Hermite elements with some success.

Although good preconditioners are available for the h-version, the situation regarding the p-version with C^1-elements is bleak with no effective preconditioners currently available. The present work aims to address this problem. We give an iterative sub-structuring preconditioner similar in spirit to the classical preconditioners for second order elliptic problems of Bramble et al. [33] for the h-version and Babuška et al. [13] for the p-version.

While our preconditioner shares similarities with domain decomposition preconditioners for the p-version FEM approximation of second order elliptic problems [2, 13, 59], there are some important differences in the choice of basic decomposition and in the assumptions under which the scheme is shown to be effective. The presence of an interior space is standard and corresponds to a partial orthogonalization or static condensation of the interior degrees of freedom on each element. Likewise, a low order global coarse space is needed to ensure that the condition number estimate is independent of the number of elements. It is shown that the C^1 coarse space contributes a factor $\mathcal{O}(1 + \log p)$ to the growth to the condition number of the preconditioned system. The presence of C^2 degrees of freedom presents a new difficulty not seen in the analysis of second order problems. The following (sharp) inequality bounds the pointwise values of the second derivatives of a polynomial:

$$\|D^2 v\|_{L^\infty(K)} \leq C p^2 |v|_{H^2(K)} \qquad \forall v \in \mathcal{P}_p(K). \tag{3.1.1}$$

If standard (Argyris) basis functions were used for the second order nodal functions, then estimate (3.1.1) would result in $\mathcal{O}(p^2)$ factor appearing in the growth of the condition number. A judicious choice of the corresponding basis functions to have energy which decays as $\mathcal{O}(p^{-2})$ compensates for the $\mathcal{O}(p^2)$ growth in (3.1.1) with the result that the C^2 splitting contributes no p growth in the condition number.

Finally, the edge dofs are decoupled from each other, which will be shown to contribute a $\mathcal{O}(1+\log^2 p)$ factor resulting in an overall growth of $\mathcal{O}(1+\log^3 p)$. The analysis permits the use of inexact interior solves which lends itself to a more efficient implementation while maintaining the same $\mathcal{O}(1+\log^3 p)$ asymptotic growth of the preconditioned system. Finally, we demonstrate the effectiveness of the preconditioner on three model problems.

This chapter is organized as follows. We describe the model problem and setup in Section 3.2; our new preconditioner and main theorem is in Section 3.3; the analysis of the preconditioner on a single element is in Section 3.4; implementation aspects, including the construction of the vertex basis functions, are discussed in Section 3.5; we apply the preconditioner to three model problems in Section 3.6; and some technical results are recorded in Section 3.7.

3.2 Model Problem

Let Ω be a polygonal two-dimensional domain and X be a closed subspace of $H^2(\Omega)$ such that $H_0^2(\Omega) \subset X$ and $a(u,v) = (D^2 u, D^2 v)_\Omega$ defines an inner product on X. We consider the following problem.

$$u \in X : \qquad B(u,v) = L(v) \qquad \forall v \in X, \tag{3.2.1}$$

where $L \in X^*$ and $B : X \times X \to \mathbb{R}$ is symmetric, bilinear, continuous, and elliptic on X. That is, there exists positive constants α and M such that

$$|B(u,v)| \leq M|u|_{H^2(\Omega)}|v|_{H^2(\Omega)} \qquad \forall u,v \in X, \tag{3.2.2a}$$

$$B(u,u) \geq \alpha|u|^2_{H^2(\Omega)} \qquad \forall u \in X. \tag{3.2.2b}$$

In particular, hypothesis (3.2.2) allows for variable coefficients. Examples in the case where $B(\cdot,\cdot)$ has constant coefficients will be found in Section 3.6.

Let $\mathcal{T}$ be a regular triangulation of Ω satisfying the usual finite element assumptions [38, p.38]. We assume that each element $K \in \mathcal{T}$ is the image of the reference element $\hat{T} = \{(x,y) : 0 \leq x, y, x+y \leq 1\}$ under a bijective affine map $\boldsymbol{F}_K : \hat{T} \to K$, and there exists a non-negative constant κ such that for all $K \in \mathcal{T}$ there holds

$$h_K \leq \kappa\rho_K, \tag{3.2.3}$$

where h_K is the diameter of K and ρ_K is the diameter of the largest inscribed circle in K. Let $h = \max_{K\in\mathcal{T}} h_K$. For the remainder of this thesis, all constants C may depend on κ, even if this dependence is not explicitly stated.

Let $\mathcal{V}$ and $\mathcal{E}$ denote the sets of element vertices and edges, respectively, in $\mathcal{T}$. Given an element K, let $\mathcal{V}_K$ and $\mathcal{E}_K$ denote the vertices and edges of K. Each edge $\gamma \in \mathcal{E}$ is oriented by choosing a normal vector $\hat{\boldsymbol{n}}_\gamma$ arbitrarily. For edges on the domain boundary, $\hat{\boldsymbol{n}}_\gamma$ is chosen to be the outward normal $\hat{\boldsymbol{n}}$. We also let $\mathcal{T}_{\boldsymbol{a}}$ and $\mathcal{T}_\gamma$ be the neighborhood of $\boldsymbol{a} \in \mathcal{V}$ and $\gamma \in \mathcal{E}$, respectively; that is,

$$\mathcal{T}_{\boldsymbol{a}} = \{K \in \mathcal{T} : \boldsymbol{a} \in \partial K\} \quad \text{and} \quad \mathcal{T}_{\gamma} = \{K \in \mathcal{T} : \gamma \subset \partial K\}.$$

The p-version finite element approximation of (3.2.1) is

$$u_p \in \Sigma_X : \qquad B(u_p, v) = L(v) \qquad \forall v \in \Sigma_X, \tag{3.2.4}$$

where $\Sigma := \{v \in H^2(\Omega) : v|_K \in \mathcal{P}_p(K)\ \forall K \in \mathcal{T},\ v \text{ is } C^2 \text{ at element nodes}\}$ and $\Sigma_X := \Sigma \cap X$. We remind the reader that, as in the previous chapter, $\mathcal{P}_p(K)$ denotes the set of polynomials of total degree at most p on the triangle K.

3.3 Preconditioner and Statement of Main Result

By introducing a basis for the space Σ_X, such as the one described below, problem (3.2.4) may be reformulated as a matrix equation. The condition number of the stiffness matrix typically grows rapidly with the polynomial degree p and the number of elements. Our objective here is to develop a preconditioner which ameliorates the ill-conditioning. The preconditioner will be based on a decomposition of the global finite element space into local subspaces augmented with a global lower order vertex space as follows. For each $K \in \mathcal{T}$, define the interior space on a single element

$$\Sigma_I^{(K)} := \{v \in \Sigma : v|_K \in H_0^2(K) \text{ and } \operatorname{supp} v \in K\}.$$

with the corresponding global interior space given by

$$\Sigma_I = \bigoplus_{K \in \mathcal{T}} \Sigma_I^{(K)},$$

Let $\Sigma_I^{\perp}$ denote the orthogonal complement of the (closed) subspace Σ_I in Σ with respect to the bilinear form $a(\cdot, \cdot)$, i.e.

$$\Sigma = \Sigma_I \oplus \Sigma_I^{\perp} \qquad \text{and} \qquad \Sigma_I \perp \Sigma_I^{\perp},$$

and let $\tilde{\Sigma}_B := \Sigma_I^{\perp} \cap X$. In other words, $v \in \Sigma_I^{\perp}$ if and only if $a(v, w) = 0$ for all $w \in \Sigma_I$.

We further decompose $\tilde{\Sigma}_B$ into subspaces associated with C^1, C^2, and edge dofs as follows. For each $\boldsymbol{a} \in \mathcal{V}$, we assign a six element set as follows:

$$\Upsilon_{\boldsymbol{a}} = \{\mathbf{0}, \hat{\boldsymbol{\mu}}, \hat{\boldsymbol{\nu}}, (\hat{\boldsymbol{\eta}}_1, \hat{\boldsymbol{\eta}}_2), (\hat{\boldsymbol{\rho}}_1, \hat{\boldsymbol{\rho}}_2), (\hat{\boldsymbol{\omega}}_1, \hat{\boldsymbol{\omega}}_2)\}.$$

Given $\alpha \in \Upsilon_{\boldsymbol{a}}$ and a function $v \in \Sigma$, we define $\partial_\alpha v(\boldsymbol{a})$ by the rule

$$\partial_\alpha v(\boldsymbol{a}) := \begin{cases} v(\boldsymbol{a}) & \text{if } \alpha = \mathbf{0}, \\ Dv(\boldsymbol{a}) \cdot \alpha & \text{if } \alpha \in \{\hat{\boldsymbol{\mu}}, \hat{\boldsymbol{\nu}}\}, \\ \alpha_1^T D^2 v(\boldsymbol{a}) \cdot \alpha_2 & \text{if } \alpha = (\alpha_1, \alpha_2) \in \{(\hat{\boldsymbol{\eta}}_1, \hat{\boldsymbol{\eta}}_2), (\hat{\boldsymbol{\rho}}_1, \hat{\boldsymbol{\rho}}_2), (\hat{\boldsymbol{\omega}}_1, \hat{\boldsymbol{\omega}}_2)\}. \end{cases}$$

We also define $|\alpha| \in \{0, 1, 2\}$ to be the order of derivative corresponding to $\partial_\alpha v(\boldsymbol{a})$. We assume that the sets $\Upsilon_{\boldsymbol{a}}$ are chosen so that:

(i) The degrees of freedom $\{v \mapsto \partial_\alpha v(\boldsymbol{a}) : \forall \alpha \in \Upsilon_{\boldsymbol{a}}\ \forall \boldsymbol{a} \in \mathcal{V}\}$ are linearly independent for $v \in \Sigma$.

(ii) There exist subsets $\Lambda_{\boldsymbol{a}} \subseteq \Upsilon_{\boldsymbol{a}}$ such that for $v \in \Sigma_X$, $\partial_\alpha v(\boldsymbol{a}) = 0$ for all $\alpha \in \Upsilon_{\boldsymbol{a}} \setminus \Lambda_{\boldsymbol{a}}$, and if $\partial_\alpha v(\boldsymbol{a}) = 0$ for all $\alpha \in \Lambda_{\boldsymbol{a}}$, then $D^\beta v(\boldsymbol{a}) = 0$ for all $|\beta| \leq 2$.

Let $\tilde{\Phi}^\alpha_{\boldsymbol{a}} \in \Sigma_I^\perp$, $\alpha \in \Upsilon_{\boldsymbol{a}}$, denote a Lagrange basis function associated with the degree of freedom $v \mapsto \partial_\alpha v(\boldsymbol{a})$ at vertex $\boldsymbol{a} \in \mathcal{V}$; that is, for $\boldsymbol{b} \in \mathcal{V}$ and $\beta \in \Upsilon_{\boldsymbol{a}}$,

$$\partial_\beta \tilde{\Phi}^\alpha_{\boldsymbol{a}}(\boldsymbol{b}) = \delta_{\alpha\beta}\delta_{\boldsymbol{ab}} \quad \text{and} \quad \operatorname{supp} \tilde{\Phi}^\alpha_{\boldsymbol{a}} \subseteq \mathcal{T}_{\boldsymbol{a}}.$$

These conditions do not uniquely determine the vertex basis functions. A specific construction will be detailed later since, as we shall see, the choice of these basis functions is crucial for the effectiveness of the resulting preconditioner.

The *zeroth* and *first order* vertex degrees of freedom are aggregated to form a single low order *global coarse* space as follows:

$$\tilde{\Sigma}_c := \operatorname{span}\left\{\tilde{\Phi}_{\boldsymbol{a}}^{\alpha} : \ \alpha \in \Lambda_{\boldsymbol{a}} \setminus \Lambda_{\boldsymbol{a}}^2, \ \boldsymbol{a} \in \mathcal{V}\right\}.$$

Conversely, the *second order* vertex degrees of freedom are decoupled into *a collection of one–dimensional* subspaces associated with each vertex $\boldsymbol{a} \in \mathcal{V}$ and each second derivative separately:

$$\tilde{\Sigma}_{\boldsymbol{a},\alpha} := \operatorname{span}\left\{\tilde{\Phi}_{\boldsymbol{a}}^{\alpha}\right\} \quad \text{for} \quad \alpha \in \Lambda_{\boldsymbol{a}}^2,$$

where $\Lambda_{\boldsymbol{a}}^2 := \{\alpha \in \Lambda_{\boldsymbol{a}} : |\alpha| = 2\}$ and $\Upsilon_{\boldsymbol{a}}^2$ is defined analogously. Lastly, we have the *edge* functions, associated with the trace and normal derivative along each edge $\gamma \in \mathcal{E}$; that is,

$$\tilde{\Sigma}_\gamma := \left\{v \in \tilde{\Sigma}_B : \operatorname{supp} v \subset \mathcal{T}_\gamma \text{ and } D^\beta v(\boldsymbol{a}) = 0 \ \forall |\beta| \leq 2, \ \forall \boldsymbol{a} \in \mathcal{V}\right\},$$

These subspaces yield a decomposition of the global space as follows:

$$\Sigma_X = \Sigma_I \oplus \tilde{\Sigma}_c \oplus \bigoplus_{\substack{\boldsymbol{a}\in\mathcal{V} \\ \alpha\in\Lambda_{\boldsymbol{a}}^2}} \tilde{\Sigma}_{\boldsymbol{a},\alpha} \oplus \bigoplus_{\gamma\in\mathcal{E}} \tilde{\Sigma}_\gamma. \tag{3.3.1}$$

Equation (3.3.1) means that every $u \in \Sigma_X$ may be written as a sum of contributions from each of the subspaces appearing on the right hand side:

$$u = u_I + u_c + \sum_{\substack{\boldsymbol{a}\in\mathcal{V} \\ \alpha\in\Lambda^2_{\boldsymbol{a}}}} u_{\boldsymbol{a},\alpha} + \sum_{\gamma\in\mathcal{E}} u_\gamma \tag{3.3.2}$$

where $u_I \in \Sigma_I$, $u_c \in \tilde{\Sigma}_c$, etc. Moreover, these functions are uniquely determined by condition (3.3.2). The space Σ_I is equipped with the scalar product $a(\cdot,\cdot)$ and each subspace of $\tilde{\Sigma}_B$ is equipped with the scalar product $B(\cdot,\cdot)$.

In turn, the decomposition gives rise to an Additive Schwarz Method (ASM) preconditioner [37, 103, 111] whose action on a linear functional $r \in \Sigma_X^*$ consists of solving independent problems on each of the subspaces as defined in Algorithm 1.

Algorithm 1 ASM preconditioner $\quad \Sigma_X^* \ni r \mapsto u \in \Sigma_X$

(i) $u_I \in \Sigma_I : \qquad a(u_I, v) = r(v) \qquad \forall v \in \Sigma_I$

(ii) $\begin{cases} u_c \in \tilde{\Sigma}_c : & B(u_c, v) = r(v) & \forall v \in \tilde{\Sigma}_c \\ u_{\boldsymbol{a},\alpha} \in \tilde{\Sigma}_{\boldsymbol{a},\alpha} : & B(u_{\boldsymbol{a},\alpha}, v) = r(v) & \forall v \in \tilde{\Sigma}_{\boldsymbol{a},\alpha} \\ u_\gamma \in \tilde{\Sigma}_\gamma : & B(u_\gamma, v) = r(v) & \forall v \in \tilde{\Sigma}_\gamma \end{cases}$

(iii) $u = u_I + u_c + \sum_{\substack{\boldsymbol{a}\in\mathcal{V} \\ \alpha\in\Lambda^2_{\boldsymbol{a}}}} u_{\boldsymbol{a},\alpha} + \sum_{\gamma\in\mathcal{E}} u_\gamma$

In particular, the problem (i) posed on the interior space Σ_I can be performed on each element in isolation with the solution u_I given by the sum of the element-wise solutions. Similarly, the problems in (ii) are independent of one another and may be carried out in parallel. The coarse grid solve for $u_c \in \tilde{\Sigma}_c$ requires the solution of a coupled problem with three unknowns per vertex on all vertices but, for the

p-version scheme we have in mind, will not dominate the overall cost of applying the preconditioner.

Theorem 3.3.1. *The abstract ASM defined Algorithm 1 is equivalent to solving the following variational problem:*

$$u \in \Sigma_X : \qquad c(u,v) = r(v) \qquad \forall v \in \Sigma_X, \tag{3.3.3}$$

where $c : \Sigma_X \times \Sigma_X \to \mathbb{R}$ *denotes the SPD bilinear form given by*

$$c(u,v) := a(u_I, v_I) + B(u_c, v_c) + \sum_{\substack{\boldsymbol{a}\in\mathcal{V} \\ \alpha\in\Lambda^2_{\boldsymbol{a}}}} B(u_{\boldsymbol{a},\alpha}, v_{\boldsymbol{a},\alpha}) + \sum_{\gamma\in\mathcal{E}} B(u_\gamma, v_\gamma), \tag{3.3.4}$$

and u_I*,* u_c*,* $u_{\boldsymbol{a},\alpha}$ *and* u_γ *are uniquely defined by the splitting* (3.3.2).

Proof. Suppose that u satisfies (3.3.3). Then, for any $v \in \Sigma_I$, we have

$$a(u_I, v) = c(u,v) = r(v),$$

and so (i) in Algorithm 1 is satisfied. Analogous arguments yield (ii)-(iv). Now assume that u is constructed as in Algorithm 1. Let $v \in \Sigma_X$. Then,

$$\begin{aligned} c(u,v) &= a(u_I, v_I) + B(u_c, v_c) + \sum_{\substack{\boldsymbol{a}\in\mathcal{V} \\ \alpha\in\Lambda^2_{\boldsymbol{a}}}} B(u_{\boldsymbol{a},\alpha}, v_{\boldsymbol{a},\alpha}) + \sum_{\gamma\in\mathcal{E}} B(u_\gamma, v_\gamma) \\ &= r(v_I) + r(v_c) + \sum_{\substack{\boldsymbol{a}\in\mathcal{V} \\ \alpha\in\Lambda^2_{\boldsymbol{a}}}} r(v_{\boldsymbol{a},\alpha}) + \sum_{\gamma\in\mathcal{E}} r(v_\gamma) = r(v), \end{aligned}$$

and so (3.3.3) is satisfied. $\square$

Our main result can now be stated:

Theorem 3.3.2. *Suppose the nodal basis functions* $\{\tilde{\Phi}_{\boldsymbol{a}}^{\alpha} : \alpha \in \Upsilon_{\boldsymbol{a}},\ \boldsymbol{a} \in \mathcal{V}\}$ *satisfy the following properties:*

(i) for all $K \in \mathcal{T}$, *there holds*

$$\mathcal{P}_1(K) \subset \operatorname{span}\{\tilde{\Phi}_{\boldsymbol{a}}^{\alpha} : \alpha \in \Upsilon_{\boldsymbol{a}} \setminus \Upsilon_{\boldsymbol{a}}^2,\ \boldsymbol{a} \in \mathcal{V}_K\}. \tag{3.3.5}$$

(ii) for all $K \in \mathcal{T}$, *there exists a positive constant* C *independent of* p *such that for* $\alpha \in \Upsilon_{\boldsymbol{a}} \setminus \Upsilon_{\boldsymbol{a}}^2$, $\boldsymbol{a} \in \mathcal{V}_K$, *there holds*

$$|\tilde{\Phi}_{\boldsymbol{a}}^{\alpha}|_{H^m(K)} \leq C h_K^{1+|\alpha|-m}, \qquad m \in \{0,1,2\}. \tag{3.3.6}$$

(iii) for each $K \in \mathcal{T}$, *there exists a positive constant* C *such that for* $\alpha \in \Upsilon_{\boldsymbol{a}}^2$, $\boldsymbol{a} \in \mathcal{V}_K$, *there holds*

$$|\tilde{\Phi}_{\boldsymbol{a}}^{\alpha}|_{H^m(K)} \leq C h_K^{3-m} p^{-2}, \qquad m \in \{0,1,2\}. \tag{3.3.7}$$

Then, there exists positive constants C_1 *and* C_2 *independent of* p *and* h *such that*

$$C_1 B(u,u) \leq c(u,u) \leq C_2(1+\log^3 p) B(u,u) \qquad \forall u \in \Sigma_X. \tag{3.3.8}$$

Proof. First note that $a(\cdot,\cdot)$ and $c(\cdot,\cdot)$ can be written as a sum of elementwise contributions:

$$a(u,v)=\sum_{K\in\mathcal{T}}a_K(u,v),\qquad c(u,v)=\sum_{K\in\mathcal{T}}c_K(u,v),$$

where

$$\begin{aligned}a_K(u,v)&=(D^2u,D^2v)_K,\\ c_K(u,v)&=a_K(u_I,v_I)+B_K(u_c,v_c)+\sum_{\substack{\boldsymbol{a}\in\mathcal{V}_K\\ \alpha\in\Lambda^2_{\boldsymbol{a}}}}B_K(u_{\boldsymbol{a},\alpha},v_{\boldsymbol{a},\alpha})+\sum_{\gamma\in\mathcal{E}_K}B_K(u_\gamma,v_\gamma),\end{aligned}$$

and $B_K(\cdot,\cdot)$ is the restriction of $B(\cdot,\cdot)$ to an element $K\in\mathcal{T}$. Define $\bar{c}(\cdot,\cdot):\Sigma_X\times\Sigma_X\to\mathbb{R}$ as the sum of the element-wise contributions of the local preconditioning form $\bar{c}_K(\cdot,\cdot)$ defined in (3.4.1):

$$\bar{c}(u,v):=\sum_{K\in\mathcal{T}}\bar{c}_K(u,v)=a(u_I,v_I)+a(u_c,v_c)+\sum_{\substack{\boldsymbol{a}\in\mathcal{V}\\ \alpha\in\Lambda^2_{\boldsymbol{a}}}}a(u_{\boldsymbol{a},\alpha},v_{\boldsymbol{a},\alpha})+\sum_{\gamma\in\mathcal{E}}a(u_\gamma,v_\gamma).$$

The equivalence

$$C_1a(u,u)\le\bar{c}(u,u)\le C_2(1+\log^3 p)a(u,u)\tag{3.3.9}$$

is then a trivial consequence of Theorem 3.4.1 by summing over $K\in\mathcal{T}$. In view of conditions (3.2.2), the following equivalences hold independent of h and p:

$$B(u,u) \approx a(u,u) \quad \text{and} \quad c(u,u) \approx \bar{c}(u,u). \tag{3.3.10}$$

(3.3.8) is an immediate consequence of (3.3.9) and (3.3.10). $\square$

Assumption (i) ensures that the coarse space contains the null space $\mathcal{P}_1(K)$ of the local bilinear form $(D^2u, D^2v)_K$ in order to achieve h-independence of the preconditioner. Assumption (ii) allows the C^1 vertex functions to be uniformly bounded in $H^2(K)$. Later, we shall see that the C^1 space contributes $\mathcal{O}(1+\log p)$ growth to the condition number. Assumption (iii) means that the basis functions $\tilde{\Phi}_{\boldsymbol{a},\alpha}$, $\alpha \in \Upsilon^2_{\boldsymbol{a}}$, $\boldsymbol{a} \in \mathcal{V}$, have energy which decays as $\mathcal{O}(p^{-2})$ which compensates for the $\mathcal{O}(p^2)$ growth in (3.1.1) with the result that the C^2 splitting contributes no p growth in the condition number. We show how to construct a basis for $\tilde{\Sigma}_B$ with vertex functions $\tilde{\Phi}^{\alpha}_{\boldsymbol{a}}$ satisfying (3.3.5) to (3.3.7) in Section 3.5. Finally, the edge dofs are decoupled from each other, which will be shown to contribute a $\mathcal{O}(1+\log^2 p)$ factor resulting in an overall growth of $\mathcal{O}(1+\log^3 p)$.

3.4 Preconditioner on a Single Element

We first develop and analyze a related preconditioner $\bar{c}_K(\cdot,\cdot)$ on a single element $K \in \mathcal{T}$ (see Figure 2.3) for the bilinear form $a_K(u,v) := (D^2u, D^2v)_{L^2(K)}$, where

$$\bar{c}_K(u,v) := a_K(u_I, v_I) + a_K(u_c, v_c) + \sum_{\substack{\boldsymbol{a}\in\mathcal{V}_K \\ \alpha\in\Upsilon^2_{\boldsymbol{a}}}} a_K(u_{\boldsymbol{a},\alpha}, v_{\boldsymbol{a},\alpha}) + \sum_{\gamma\in\mathcal{E}_K} a_K(u_\gamma, v_\gamma). \quad (3.4.1)$$

Let $\Sigma_I^{(K)}$ be defined as above and let $\tilde{\Sigma}_B^{(K)}$ denote the orthogonal complement of $\Sigma_I^{(K)}$ in $\Sigma^{(K)} = \mathcal{P}_p(K)$ with respect to $a_K(\cdot,\cdot)$; i.e.,

$$\Sigma^{(K)} = \Sigma_I^{(K)} \oplus \tilde{\Sigma}_B^{(K)} \quad \text{and} \quad a_K(u,v) = 0 \qquad \forall u \in \Sigma_I^{(K)},\ \forall v \in \tilde{\Sigma}_B^{(K)}.$$

Consequently every $u \in \Sigma^{(K)}$ can be uniquely expressed as a sum $u = u_I + \tilde{u}_B$ with $u_I \in \Sigma_I^{(K)}$, $\tilde{u}_B \in \tilde{\Sigma}_B^{(K)}$ and satisfying

$$a_K(u_I, u_I) + a_K(\tilde{u}_B, \tilde{u}_B) = a_K(u,u). \quad (3.4.2)$$

The local spaces are defined by

$$\begin{aligned}
\tilde{\Sigma}_c^{(K)} &:= \operatorname{span}\left\{\tilde{\Phi}^\alpha_{\boldsymbol{a}}|_K : \boldsymbol{a} \in \mathcal{V}_K,\ \alpha \in \Upsilon_{\boldsymbol{a}} \setminus \Upsilon^2_{\boldsymbol{a}}\right\}, \\
\tilde{\Sigma}_{\boldsymbol{a},\alpha}^{(K)} &:= \operatorname{span}\left\{\tilde{\Phi}^\alpha_{\boldsymbol{a}}|_K\right\}, \quad \boldsymbol{a} \in \mathcal{V}_K,\ \alpha \in \Upsilon^2_{\boldsymbol{a}}, \\
\tilde{\Sigma}_\gamma^{(K)} &:= \{v \in \tilde{\Sigma}_B^{(K)} : D^\beta v(\boldsymbol{a}) = 0\ \forall|\beta| \le 2,\ \forall \boldsymbol{a} \in \mathcal{V} \\
&\qquad \text{and} \quad v|_{\gamma'} = \partial_n v|_{\gamma'} = 0\ \forall\gamma' \in \mathcal{E}_K \setminus \{\gamma\}\}, \quad \gamma \in \mathcal{E}_K.
\end{aligned}$$

Theorem 3.4.1 (Single element case)**.** *There exist positive constants C_1, C_2 independent of p and h_K such that*

$$C_1 a_K(u,u) \leq \bar{c}_K(u,u) \leq C_2(1+\log^3 p)a_K(u,u) \qquad \forall u \in \Sigma^{(K)}.$$

We apply the standard framework as described in [111, §2] for the analysis of additive Schwarz methods to the single element scenario described above.

Each function $u \in \Sigma^{(K)}$ has a unique decomposition of the form

$$u = u_I + u_c + \sum_{\substack{\boldsymbol{a}\in\mathcal{V}_K \\ \alpha\in\Upsilon^2_{\boldsymbol{a}}}} u_{\boldsymbol{a},\alpha} + \sum_{\gamma\in\mathcal{E}_K} u_\gamma, \tag{3.4.3}$$

with $u_I \in \Sigma_I^{(K)}$, $u_c \in \tilde{\Sigma}_c^{(K)}$, $u_{n_i,\alpha} \in \tilde{\Sigma}_{n_i,\alpha}^{(K)}$ $|\alpha| = 2$, $u_{\gamma_i} \in \tilde{\Sigma}_{\gamma_i}^{(K)}$, and a simple application of (3.4.2) and the Cauchy-Schwarz inequality gives

$$a_K(u,u) \leq 11\bar{c}_K(u,u). \tag{3.4.4}$$

The converse inequality is less straightforward:

Theorem 3.4.2 (Stable Decomposition on Single Element)**.** *Suppose that the basis functions satisfy conditions (i)-(iii) of Theorem 3.3.2. Then, there exists a constant C independent of p and h_K such that*

$$\bar{c}_K(u,u) \leq C(1+\log^3 p)a_K(u,u), \qquad \forall u \in \Sigma^{(K)}. \tag{3.4.5}$$

Proof. We begin by proving the result in the special case $h_K = 1$. Let $u \in \mathcal{P}_p(K)$. It suffices to bound each of the terms in $\bar{c}_K(u, u)$ separately. The contribution from the interior component is readily bounded using (3.4.2) to obtain

$$a_K(u_I, u_I) \leq a_K(u, u). \tag{3.4.6}$$

In fact, since $u_I \in H_0^2(K)$, Poincaré's inequality gives $\|u_I\|_{H^2(K)} \leq C|u_I|_{H^2(K)} \leq C|u|_{H^2(K)}$. Now define $u_B = u - u_I$. Then, there holds

$$\|u_B\|_{H^2(K)} \leq \|u\|_{H^2(K)} + \|u_I\|_{H^2(K)} \leq C\|u\|_{H^2(K)}. \tag{3.4.7}$$

The coarse grid component is bounded by first using Cauchy-Schwarz and (3.3.6) to yield

$$\|u_c\|_{H^2(K)} \leq \sum_{\substack{\boldsymbol{a} \in \mathcal{V} \\ \alpha \in \Upsilon_{\boldsymbol{a}} \setminus \Upsilon_{\boldsymbol{a}}^2}} |\partial_\alpha u(\boldsymbol{a})| \cdot \|\tilde{\Phi}_{\boldsymbol{a}}^\alpha\|_{H^2(K)} \leq C\|u\|_{W^{1,\infty}(\partial K)}.$$

By [13, Corollary 6.3], there holds

$$\|v\|_{L^\infty(\partial K)} \leq C(1 + \log^{1/2} p)\|v\|_{H^1(K)} \qquad \forall v \in \mathcal{P}_p(K),$$

and so taking $v = \partial_\alpha u$, $\alpha \in \Upsilon_{\boldsymbol{a}} : |\alpha| = 1$, gives

$$\|\partial_\alpha u\|_{L^\infty(\partial K)} \leq C(1 + \log^{1/2} p)\|\partial_\alpha u\|_{H^1(K)} \leq C(1 + \log^{1/2} p)\|u\|_{H^2(K)}.$$

Hence, thanks to the continuity of the embedding $H^2(K) \hookrightarrow L^\infty(K)$, we obtain $\|u\|_{W^{1,\infty}(\partial K)} \leq C(1 + \log^{1/2} p)\|u\|_{H^2(K)}$, and the coarse grid component may be bounded as follows:

$$\|u_c\|_{H^2(K)} \leq C(1 + \log^{1/2} p)\|u\|_{H^2(K)}. \tag{3.4.8}$$

Turning to the contributions from the C^2 basis functions, we apply [6, Lemma 6.1]:

$$\max_{\boldsymbol{a}\in\mathcal{V}_K} |v(\boldsymbol{a})| \leq Cp^2\|v\|_{L^2(K)} \qquad \forall v \in \mathcal{P}_p(K)$$

to $v = \partial_\alpha u$, $\alpha \in \Upsilon^2_{\boldsymbol{a}}$, and use property (3.3.7) of the second order basis functions to obtain

$$\|u_{\boldsymbol{a},\alpha}\|_{H^2(K)} \leq C|\partial_\alpha u(\boldsymbol{a})| \cdot \|\tilde{\Phi}^\alpha_{\boldsymbol{a}}\|_{H^2(K)} \leq C|u|_{H^2(K)} \qquad \forall \alpha \in \Upsilon^2_{\boldsymbol{a}},\ \forall \boldsymbol{a} \in \mathcal{V}_K. \tag{3.4.9}$$

Define $u^\# = u_B - u_c - \sum_{i=1}^3 \sum_{|\alpha|=2} u_{n_i,\alpha}$. Then, by the triangle inequality, (3.4.6), (3.4.8) and (3.4.9) we have

$$\|u^\#\|_{H^2(K)} \leq C(1 + \log^{1/2} p)\|u\|_{H^2(K)}. \tag{3.4.10}$$

For an edge $\gamma \in \partial K$, define $f_\gamma, g_\gamma : \partial K \to \mathbb{R}$ by the rules

$$f_\gamma := \begin{cases} u^\# & \text{on } \gamma, \\ 0 & \text{else}, \end{cases} \quad \text{and} \quad g_\gamma := \begin{cases} \partial_n u^\# & \text{on } \gamma, \\ 0 & \text{else}. \end{cases}$$

Corollary 3.7.2 shows that there exists an extension of the boundary data (f_γ, g_γ), denoted by $\bar{u}_\gamma \in \tilde{\Sigma}_\gamma^{(K)} \oplus \Sigma_I^{(K)}$, satisfying

$$\begin{aligned} \|\bar{u}_\gamma\|_{H^2(K)} &\leq C \left(\|f_\gamma\|_{L^2(\partial K)} + \|\boldsymbol{\sigma}(f_\gamma, g_\gamma)\|_{\boldsymbol{H}^{1/2}(\partial K)} \right) \\ &\leq C \left(\|u^\#\|_{H_{00}^{3/2}(\gamma)} + \|\partial_n u^\#\|_{H_{00}^{1/2}(\gamma)} \right), \end{aligned}$$

where we recall that $\boldsymbol{\sigma}(f, g) := (\partial_t f)\hat{\boldsymbol{n}} - g\hat{\boldsymbol{t}}$. Using [13, Theorem 6.5] and the trace theorem Theorem 2.2.1, we have

$$\begin{aligned} \|\bar{u}_\gamma\|_{H^2(K)} &\leq C(1 + \log p) \left(\|u^\#\|_{H^{3/2}(\gamma)} + \|\partial_n u^\#\|_{H^{1/2}(\gamma)} \right) \\ &\leq C(1 + \log p) \left(\|u^\#\|_{L^2(\partial K)} + \|\boldsymbol{\sigma}(u^\#, \partial_n u^\#)\|_{\boldsymbol{H}^{1/2}(\partial K)} \right) \\ &\leq C(1 + \log p)\|u^\#\|_{H^2(K)}, \end{aligned}$$

and so by (3.4.10), $a_K(\bar{u}_\gamma, \bar{u}_\gamma) \leq C(1 + \log^3 p)\|u\|_{H^2(K)}^2$. Since $u_\gamma - \bar{u}_\gamma \in \Sigma_I^{(K)}$, we have

$$a_K(u_\gamma, u_\gamma) \leq a_K(\bar{u}_\gamma, \bar{u}_\gamma) \leq C(1 + \log^3 p)\|u\|_{H^2(K)}^2 \tag{3.4.11}$$

by (3.4.2). Gathering (3.4.6), (3.4.8), (3.4.9) and (3.4.11), we obtain

$$\bar{c}_K(u,u) \le C(1+\log^3 p)\|u\|^2_{H^2(K)}. \tag{3.4.12}$$

It remains to show that one may replace the full norm $\|u\|_{H^2(K)}$ in the estimate (3.4.12) with the H^2 semi-norm. Let $q \in \mathcal{P}_1(K)$. The uniqueness of the splitting (3.4.3) together with (3.3.5) shows that $u - q$ may be decomposed in the form (3.4.3) with u_c replaced by $u_c - q$, and hence

$$\begin{aligned}\bar{c}_K(u-q,u-q) = a_K(u_I,u_I) + a_K(u_c-q,u_c-q) + \sum_{\substack{\boldsymbol{a}\in\mathcal{V}\\ \alpha\in\Lambda^2_{\boldsymbol{a}}}} a_K(u_{\boldsymbol{a},\alpha},u_{\boldsymbol{a},\alpha}) \\ + \sum_{\gamma\in\partial K} a_K(u_\gamma,u_\gamma).\end{aligned} \tag{3.4.13}$$

Thus, thanks to (3.4.12) we obtain

$$\bar{c}_K(u,u) = \bar{c}_K(u-q,u-q) \le C(1+\log^3 p)\|u-q\|^2_{H^2(K)}. \tag{3.4.14}$$

Taking the infimum over all $q \in \mathcal{P}_1(K)$ and using the bound [86, §Theorem 7.2]

$$\inf_{q\in\mathcal{P}_1(K)} \|u-q\|_{H^2(K)} \le C|u|_{H^2(K)},$$

we arrive at (3.4.5)

Now we consider the case $h_K \neq 1$ and let $u \in \mathcal{P}_p(K)$. Define $\hat{K} = \{\boldsymbol{x} \in \mathbb{R}^2 :$

$h_K \boldsymbol{x} \in K\}$ so that $h_{\hat{K}} = 1$, and define $\hat{\Phi}^{\alpha}_{\hat{\boldsymbol{a}}} : \hat{K} \to \mathbb{R}$ as follows:

$$\hat{\Phi}^{\alpha}_{\hat{\boldsymbol{a}}}(\hat{\boldsymbol{x}}) = h_K^{-|\alpha|} \tilde{\Phi}^{\alpha}_{\boldsymbol{a}}(h_K \hat{\boldsymbol{x}}) \qquad \text{for } \hat{\boldsymbol{x}} \in \hat{K}.$$

The chain rule and a simple change of variable shows that $\hat{\Phi}^{\alpha}_{\hat{\boldsymbol{a}}}$ satisfies (3.3.5) to (3.3.7) with h_K replaced by $h_{\hat{K}} = 1$. Let $\hat{u} : \hat{K} \to \mathbb{R}$, the pullback of u onto $\hat{K}$, be given by $\hat{u}(\hat{\boldsymbol{x}}) := u(h_K \hat{\boldsymbol{x}})$. By scaling, there holds

$$a_{\hat{K}}(\hat{\boldsymbol{u}}, \hat{\boldsymbol{u}}) = h_K^2 a_K(\boldsymbol{u}, \boldsymbol{u}). \tag{3.4.15}$$

Moreover, u and $\hat{u}$ have the following decomposition:

$$\begin{aligned} u(\boldsymbol{x}) &= \sum_{\substack{\boldsymbol{a} \in \mathcal{V}_K \\ \alpha \in \Upsilon_{\boldsymbol{a}}}} c_{\alpha, \boldsymbol{a}} \tilde{\Phi}^{\alpha}_{\boldsymbol{a}}(\boldsymbol{x}) + \sum_{\gamma \in \mathcal{E}_K} u_\gamma(\boldsymbol{x}) + u_I(\boldsymbol{x}) \\ \hat{u}(\hat{\boldsymbol{x}}) &= \sum_{\substack{\hat{\boldsymbol{a}} \in \mathcal{V}_{\hat{K}} \\ \alpha \in \Upsilon_{\boldsymbol{a}}}} \hat{c}_{\alpha, \hat{\boldsymbol{a}}} \hat{\Phi}^{\alpha}_{\hat{\boldsymbol{a}}}(\hat{\boldsymbol{x}}) + \sum_{\gamma \in \mathcal{E}_K} u_\gamma(h_K \hat{\boldsymbol{x}}) + u_I(h_K \hat{\boldsymbol{x}}), \end{aligned}$$

where $c_{\alpha, \boldsymbol{a}}$ is the α derivative of u at the vertex $\boldsymbol{a}$ and $\hat{c}_{\alpha, \hat{\boldsymbol{a}}}$ is defined analogously. Again, by the chain rule and scaling, there holds

$$\hat{u}_c(\hat{\boldsymbol{x}}) = u_c(h_K \hat{\boldsymbol{x}}) \qquad \text{and} \qquad \hat{u}_{\hat{\boldsymbol{a}}, \alpha}(\hat{\boldsymbol{x}}) = u_{\boldsymbol{a}, \alpha}(h_K \hat{\boldsymbol{x}}) \qquad \forall \boldsymbol{a} \in \mathcal{V}_K, \ \forall \alpha \in \Upsilon^2_{\boldsymbol{a}},$$

and so

$$\bar{c}_{\hat{K}}(\hat{u}, \hat{u}) = h_K^2 \bar{c}_K(u, u). \tag{3.4.16}$$

Applying (3.4.5) to $\hat{u}$ and using (3.4.15) and (3.4.16) gives the result in the case $h_K \neq 1$. $\square$

Theorem 3.4.1 is now an immediate consequence of (3.4.4) and Theorem 3.4.2 by the standard ASM theory (see e.g. Theorem 2.7 of [111]).

3.5 Implementation

The ASM described in Algorithm 1 entails the solution of problems posed on subspaces $\tilde{\Sigma}_B$, the $a(\cdot,\cdot)$ orthogonal complement of Σ_I in Σ_X. This implies that the basis functions for the subspaces $\tilde{\Sigma}_c$, $\tilde{\Sigma}_{\boldsymbol{a},\alpha}$, and $\tilde{\Sigma}_\gamma$ depend on the shape of the elements in the mesh and, as such, cannot readily be written in closed form. How, then, is one to implement Algorithm 1 in practice?

3.5.1 Generating a Basis for $\tilde{\Sigma}_B$

Let $\Sigma_B \subset \Sigma_X$ denote *any* subspace for which $\Sigma_B \cap \Sigma_I = \{0\}$ and $\Sigma_X = \Sigma_B \oplus \Sigma_I$, and let $\vec{\Phi}_B$ be a basis for Σ_B. Likewise, let $\vec{\Phi}_I$ denote a basis for Σ_I so that $[\vec{\Phi}_I, \vec{\Phi}_B]$

gives a basis for Σ_X. The p-version FEM problem (3.2.4) then takes the form

$$\begin{bmatrix} \boldsymbol{B}_{II} & \boldsymbol{B}_{IB} \\ \boldsymbol{B}_{BI} & \boldsymbol{B}_{BB} \end{bmatrix} \begin{bmatrix} \vec{\alpha}_I \\ \vec{\alpha}_B \end{bmatrix} = \begin{bmatrix} L(\vec{\Phi}_I) \\ L(\vec{\Phi}_B) \end{bmatrix} \tag{3.5.1}$$

where $\boldsymbol{B}_{II} = B(\vec{\Phi}_I, \vec{\Phi}_I^T)$, $\boldsymbol{B}_{IB} = B(\vec{\Phi}_I, \vec{\Phi}_B^T)$, etc. Similarly, the matrix $\boldsymbol{A}$ is defined to be

$$\boldsymbol{A} = \begin{bmatrix} \boldsymbol{A}_{II} & \boldsymbol{A}_{IB} \\ \boldsymbol{A}_{BI} & \boldsymbol{A}_{BB} \end{bmatrix}$$

where $\boldsymbol{A}_{II} = a(\vec{\Phi}_I, \vec{\Phi}_I^T)$, $\boldsymbol{A}_{IB} = a(\vec{\Phi}_I, \vec{\Phi}_B^T)$, etc. The subblock $\boldsymbol{A}_{II}$ is non-singular and we may therefore define a new set of basis functions as follows:

$$\vec{\tilde{\Phi}}_B = \vec{\Phi}_B - \boldsymbol{A}_{BI}\boldsymbol{A}_{II}^{-1}\vec{\Phi}_I. \tag{3.5.2}$$

Observe that

$$a(\vec{\tilde{\Phi}}_B, \vec{\Phi}_I^T) = a(\vec{\Phi}_B, \vec{\Phi}_I^T) - \boldsymbol{A}_{BI}\boldsymbol{A}_{II}^{-1}a(\vec{\Phi}_I, \vec{\Phi}_I^T) = \boldsymbol{A}_{BI} - \boldsymbol{A}_{BI}\boldsymbol{A}_{II}^{-1}\boldsymbol{A}_{II} = \boldsymbol{0} \tag{3.5.3}$$

which shows that the functions $\vec{\tilde{\Phi}}_B$ are contained in the space $\tilde{\Sigma}_B$. Moreover, $\text{span}\{\vec{\tilde{\Phi}}_B\} \cap \Sigma_I = \{0\}$, and it follows that $\tilde{\Sigma}_B = \text{span}\{\vec{\tilde{\Phi}}_B\}$. That is to say, $\vec{\tilde{\Phi}}_B$ is a basis for $\tilde{\Sigma}_B$ and $[\vec{\Phi}_I, \vec{\tilde{\Phi}}_B]$ is a basis for Σ_X relative to which problem (3.2.4) takes the form

$$\begin{bmatrix} \boldsymbol{B}_{II} & \tilde{\boldsymbol{B}}_{IB} \\ \tilde{\boldsymbol{B}}_{BI} & \tilde{\boldsymbol{B}}_{BB} \end{bmatrix} \begin{bmatrix} \vec{\tilde{\alpha}}_I \\ \vec{\alpha}_B \end{bmatrix} = \begin{bmatrix} L(\vec{\Phi}_I) \\ L(\vec{\tilde{\Phi}}_B) \end{bmatrix} \tag{3.5.4}$$

where the subblocks are constructed using $\vec{\Phi}_I$ and $\vec{\tilde{\Phi}}_B$ viz:

$$\begin{aligned} \tilde{\boldsymbol{B}}_{BB} &:= B(\vec{\tilde{\Phi}}_B, \vec{\tilde{\Phi}}_B) \\ &= B(\vec{\Phi}_B - \boldsymbol{A}_{BI}\boldsymbol{A}_{II}^{-1}\vec{\Phi}_I, \vec{\Phi}_B^T - \vec{\Phi}_I^T\boldsymbol{A}_{II}^{-1}\boldsymbol{A}_{IB}) \\ &= \boldsymbol{B}_{BB} - \boldsymbol{A}_{BI}\boldsymbol{A}_{II}^{-1}\boldsymbol{B}_{IB} - \boldsymbol{B}_{BI}\boldsymbol{A}_{II}^{-1}\boldsymbol{A}_{IB} + \boldsymbol{A}_{BI}\boldsymbol{A}_{II}^{-1}\boldsymbol{B}_{II}\boldsymbol{A}_{II}^{-1}\boldsymbol{A}_{IB}, \\ \tilde{\boldsymbol{B}}_{BI} &:= B(\vec{\tilde{\Phi}}_B, \vec{\Phi}_I^T) = B(\vec{\Phi}_B - \boldsymbol{A}_{BI}\boldsymbol{A}_{II}^{-1}\vec{\Phi}_I, \vec{\Phi}_I^T) = \boldsymbol{B}_{BI} - \boldsymbol{A}_{BI}\boldsymbol{A}_{II}^{-1}\boldsymbol{B}_{II}, \end{aligned} \tag{3.5.5}$$

and

$$L(\vec{\tilde{\Phi}}_B) = L(\vec{\Phi}_B) - \boldsymbol{A}_{BI}\boldsymbol{A}_{II}^{-1}L(\vec{\Phi}_I). \tag{3.5.6}$$

In other words, given the matrix $\boldsymbol{A}_{II}^{-1}\boldsymbol{A}_{IB}$, the matrix form of problem (3.2.4) relative to the decomposition $\Sigma_I \oplus \tilde{\Sigma}_B$ can readily be obtained from the standard (non-orthogonal) discrete form (3.5.1) using the foregoing formulae. More precisely, given a residual vector $\vec{r}$, the ASM given in Algorithm 1 takes the discrete form given in Algorithm 2.

Algorithm 2 Matrix form of ASM preconditioner $\quad \vec{r} \mapsto (\vec{\alpha}_I, \vec{\alpha}_B)$

(i) $\vec{\tilde{\alpha}}_I = \boldsymbol{A}_{II}^{-1}\vec{r}_I$

(ii) $$\begin{cases} \vec{\alpha}_c = \tilde{\boldsymbol{B}}_c^{-1}\left(\vec{r}_c - \boldsymbol{A}_{cI}\vec{\tilde{\alpha}}_I\right) \\ \vec{\alpha}_{\boldsymbol{a},\alpha} = \tilde{\boldsymbol{B}}_{\boldsymbol{a},\alpha}^{-1}\left(\vec{r}_{\boldsymbol{a},\alpha} - \boldsymbol{A}_{\boldsymbol{a},\alpha I}\vec{\tilde{\alpha}}_I\right) \\ \vec{\alpha}_\gamma = \tilde{\boldsymbol{B}}_\gamma^{-1}\left(\vec{r}_\gamma - \boldsymbol{A}_{\gamma I}\vec{\tilde{\alpha}}_I\right) \end{cases}$$

(iii) $$\begin{aligned} \vec{\alpha}_B &= \begin{bmatrix}\vec{\alpha}_c & (\vec{\alpha}_{\boldsymbol{a},\alpha})_{\boldsymbol{a}\in\mathcal{V},\alpha\in\Lambda^2_{\boldsymbol{a}}} & (\vec{\alpha}_\gamma)_{\gamma\in\mathcal{E}}\end{bmatrix} \\ \vec{\alpha}_I &= \vec{\tilde{\alpha}}_I - \boldsymbol{A}_{II}^{-1}\boldsymbol{A}_{IB}\vec{\alpha}_B \end{aligned}$$

---

where $\tilde{\boldsymbol{B}}_c$, $\tilde{\boldsymbol{B}}_{\boldsymbol{a},\alpha}$, and $\tilde{\boldsymbol{B}}_\gamma$ are subblocks of the diagonal of the matrix $\tilde{\boldsymbol{B}}_{BB}$ given by (3.5.5), and $\boldsymbol{A}_{cI} = a(\vec{\Phi}_c, \vec{\Phi}_I^T)$, where $\vec{\Phi}_c$ is a vector of the zeroth and first order vertex basis functions with $\boldsymbol{A}_{\boldsymbol{a},\alpha I}$ and $\boldsymbol{A}_{\gamma I}$ defined analogously.

Remark 3.5.1. In many typical applications (see Section 3.6), one finds that the bilinear form $B(\cdot,\cdot)$ has the property that

$$B(u,v) = (D^2u, D^2v)_\Omega = a(u,v) \qquad \forall u \in H^2(\Omega),\ \forall v \in H_0^2(\Omega). \tag{3.5.7}$$

If this condition holds, then the subblocks of $\boldsymbol{A}$ and $\boldsymbol{B}$ satisfy $\boldsymbol{B}_{BI} = \boldsymbol{A}_{BI}$ and $\boldsymbol{B}_{II} = \boldsymbol{A}_{II}$. Inserting these relations into (3.5.5) and simplifying gives

$$\tilde{\boldsymbol{B}}_{BB} = \boldsymbol{B}_{BB} - \boldsymbol{B}_{BI}\boldsymbol{B}_{II}^{-1}\boldsymbol{B}_{IB}, \quad \tilde{\boldsymbol{B}}_{BI} = \boldsymbol{0}, \ \text{ and } \ L(\vec{\tilde{\Phi}}_B) = L(\vec{\Phi}_B) - \boldsymbol{B}_{BI}\boldsymbol{B}_{II}^{-1}L(\vec{\Phi}_I),$$

meaning that the system of equations (3.5.4) decouples into independent problems over the interior and boundary degrees of freedom

$$\boldsymbol{B}_{II}\vec{\tilde{\alpha}}_I = L(\vec{\Phi}_I) \quad \text{and} \quad \tilde{\boldsymbol{B}}_{BB}\vec{\alpha}_B = L(\vec{\tilde{\Phi}}_B).$$

Consequently, in cases where (3.5.7) is satisfied, the solution of (3.5.4) may be computed as follows:

(i) Compute $\vec{\tilde{\alpha}}_I = \boldsymbol{B}_{II}^{-1}L(\vec{\Phi}_I)$.

(ii) Solve $\tilde{\boldsymbol{B}}_{BB}\vec{\alpha}_B = L(\vec{\tilde{\Phi}}_B)$ using an iterative method, applying step (ii) in Algorithm 2 as the preconditioner.

(iii) Compute $\vec{\alpha}_I = \vec{\tilde{\alpha}}_I - \boldsymbol{B}_{II}^{-1}\boldsymbol{B}_{IB}\vec{\alpha}_B$.

The advantage of this formulation over Algorithm 2 is that the matrix $\boldsymbol{B}_{II}^{-1}$ need only be applied once at the beginning, to statically condense out the interior degrees of freedom, and (after the iteration for the boundary degrees of freedom has converged) once again at the end, to backsolve for the interior values.

3.5.2 Computational Cost of the Preconditioner

The cost of Algorithm 2 consists of two parts: one-time setup costs, including storage, and recurring costs associated with each application of Algorithm 2. The setup cost is dominated by computing the action of the matrix $\boldsymbol{A}_{II}^{-1}$ in the change of basis formula (3.5.2) and its subsequent application in the modification of the stiffness matrix (3.5.5) and load vector (3.5.6). By taking advantage of the block diagonal structure of $\boldsymbol{A}_{II}$, we may factor $\boldsymbol{A}_{II}$ once at a cost of $\mathcal{O}(|\mathcal{T}|p^6)$ operations. We may then compute the change of basis (3.5.2) element-by-element at a total cost of $\mathcal{O}(|\mathcal{T}|p^5)$ operations. The modifications to the stiffness matrix (3.5.5) and load vector (3.5.6) may also be computed at the element level and sub-assembled at a cost of $\mathcal{O}(|\mathcal{T}|p^5)$ operations. The final setup cost is factoring the matrices $\tilde{\boldsymbol{B}}_c$ and $\tilde{\boldsymbol{B}}_\gamma$, $\gamma \in \mathcal{E}$, leading to an overall setup cost of $\mathcal{O}(|\mathcal{V}|^3 + |\mathcal{E}|p^3 + |\mathcal{T}|p^6)$ operations. The factors of $\boldsymbol{A}_{II}^{-1}$, $\tilde{\boldsymbol{B}}_c^{-1}$, and $\tilde{\boldsymbol{B}}_\gamma^{-1}$ require $\mathcal{O}(|\mathcal{T}|p^4 + |\mathcal{V}|^2 + |\mathcal{E}|p^2)$ storage, while the blocks $\boldsymbol{A}_{cI}$, $\boldsymbol{A}_{\boldsymbol{a},\alpha I}$, and $\boldsymbol{A}_{\gamma I}$ require $\mathcal{O}(|\mathcal{T}|p^3)$ storage, leading to an overall storage cost of $\mathcal{O}(|\mathcal{V}|^2 + |\mathcal{E}|p^2 + |\mathcal{T}|p^4)$.

We now turn to the recurring costs associated with each application of Algorithm 2. The interior solve in (i) and (iii) takes $\mathcal{O}(|\mathcal{T}|p^4)$ operations. The vertex and edge solves in (ii) cost $\mathcal{O}(|\mathcal{V}|^2 + |\mathcal{E}|p^2)$ operations, while the multiplication by the interior subblocks $\boldsymbol{A}_{cI}$, $\boldsymbol{A}_{\gamma I}$, etc. in (ii) and (iii) cost $\mathcal{O}(|\mathcal{T}|p^3)$ operations. Thus, the total cost of applying Algorithm 2 is $\mathcal{O}(|\mathcal{V}|^2 + |\mathcal{E}|p^2 + |\mathcal{T}|p^4)$ operations. In the setting of Remark 3.5.1, the asymptotic setup and storage costs are the same as above; however, the application cost reduces to $\mathcal{O}(|\mathcal{V}|^2 + |\mathcal{E}|p^2)$ operations since only step (ii) of Algorithm 2 is performed each iteration.

3.5.3 Vertex Basis Functions

We now want to construct vertex functions such that the modified basis functions $\vec{\tilde{\Phi}}_B$ given by (3.5.2) satisfy the conditions (3.3.5) to (3.3.7). To this end, given a function $u \in \Sigma$, there exists a unique $\tilde{u} \in \Sigma_I^\perp$ satisfying

$$a(\tilde{u}, v) = 0 \qquad \forall v \in \Sigma_I, \tag{3.5.8a}$$

$$(\tilde{u} - u)|_{\partial K} = \partial_n(\tilde{u} - u)|_{\partial K} = 0 \qquad \forall K \in \mathcal{T}. \tag{3.5.8b}$$

Let $\mathbb{E} : \Sigma \to \Sigma_I^\perp$ denote the mapping $u \mapsto \mathbb{E}u := \tilde{u}$. If $\Phi_B \in \Sigma_B$ is a basis function, then direct verification reveals that $\tilde{\Phi}_B := \mathbb{E}\Phi_B$ is given by (3.5.2). The following result relates the $H^m(K)$ norms of a function u and $\mathbb{E}u$:

Lemma 3.5.2. *Let $u \in \Sigma$. For all $K \in \mathcal{T}$, there exists a positive constant C independent of h_K and p such that*

$$\|\mathbb{E}u\|_{L^2(K)} \leq C \inf_{v \in \Sigma_K(u)} \left\{ \|v\|_{L^2(K)} + h_K^2 |v|_{H^2(K)} \right\}, \tag{3.5.9a}$$

$$|\mathbb{E}u|_{H^1(K)} \leq C \inf_{v \in \Sigma_K(u)} \left\{ |v|_{H^1(K)} + h_K |v|_{H^2(K)} \right\}, \tag{3.5.9b}$$

$$|\mathbb{E}u|_{H^2(K)} \leq C \inf_{v \in \Sigma_K(u)} |v|_{H^2(K)}, \tag{3.5.9c}$$

where $\Sigma_K(u) := \{v \in \mathcal{P}_p(K) : v|_{\partial K} = u|_{\partial K},\ \partial_n v|_{\partial K} = \partial_n u|_{\partial K}\}$.

Proof. Let $v \in \Sigma_K(u)$. Then, $\bar{u} = \mathbb{E}u - v \in \Sigma_I^{(K)}$ and, thanks to (3.5.3),

$$a_K(\bar{u}, w) = a_K(\mathbb{E}u, w) - a_K(v, w) = -a_K(v, w) \qquad \forall w \in \Sigma_I^{(K)}.$$

Choosing $w = \bar{u}$ and applying the Cauchy-Schwarz inequality gives $|\bar{u}|_{H^2(K)} \leq |v|_{H^2(K)}$. Finally, using Poincaré's inequality on $H_0^2(K)$ and a scaling argument, we have the following bound for $\bar{u}$:

$$h_K^{-2}\|\bar{u}\|_{L^2(K)} + h_K^{-1}|\bar{u}|_{H^1(K)} + |\bar{u}|_{H^2(K)} \leq C|\bar{u}|_{H^2(K)} \leq C|v|_{H^2(K)}. \tag{3.5.10}$$

Now, using (3.5.10) gives

$$\|\mathbb{E}u\|_{L^2(K)} \leq \|v\|_{L^2(K)} + \|\bar{u}\|_{L^2(K)} \leq \|v\|_{L^2(K)} + Ch_K^2|v|_{H^2(K)}$$

for all $v \in \Sigma_K(u)$, and (3.5.9a) follows. A similar argument gives (3.5.9b) and (3.5.9c).

□

3.5.3.1 C^1 Vertex Functions

The standard (fifth order) Argyris basis functions [11] are Lagrange basis functions with respect to the following set of 21 degrees of freedom on each element $K \in \mathcal{T}$:

$$D^\beta \Psi(\boldsymbol{a}) \qquad \forall |\beta| \leq 2, \ \forall \boldsymbol{a} \in \mathcal{V}_K \quad \text{and} \quad \partial_{n_\gamma}\Psi(\boldsymbol{m}_\gamma) \qquad \forall \gamma \in \mathcal{E}_K,$$

where $\boldsymbol{m}_\gamma$ is the midpoint of the edge γ. Denote the corresponding vertex basis functions by $\{\Psi_{\boldsymbol{a}}^\beta : |\beta| \le 1,\ \boldsymbol{a} \in \mathcal{V}_K\}$ and edge functions by $\{\Psi_\gamma : \gamma \in \mathcal{E}_K\}$. We introduce the following functions:

$$\Phi_{\boldsymbol{a}}^{(0,0)} := \Psi_{\boldsymbol{a}}^{(0,0)} \quad \text{and} \quad \Phi_{\boldsymbol{a}}^\beta := \Psi_{\boldsymbol{a}}^\beta + \frac{1}{2} \sum_{\substack{\gamma \in \mathcal{E}_K \\ \boldsymbol{a} \in \partial\gamma}} \hat{\boldsymbol{n}}_\gamma^\beta \Psi_\gamma, \qquad |\beta| = 1.$$

Note that from standard properties of the Argyris basis functions [117, p.12-13], we have $\mathcal{P}_1(K) \subset \operatorname{span}\{\Phi_{\boldsymbol{a}}^\beta : \boldsymbol{a} \in \mathcal{V}_K,\ |\beta| \le 1\}$ and $|\Phi_{\boldsymbol{a}}^\beta|_{H^m(K)} \le C h_K^{1+|\beta|-m}$ for $m \in \{0,1,2\}$, $|\beta| \le 1$, and $\forall \boldsymbol{a} \in \mathcal{V}$.

Let $\alpha, \beta \in \Upsilon_{\boldsymbol{a}}$ with $|\alpha| = |\beta| = 1$ be the first order directional derivative dofs at $\boldsymbol{a}$. Then, the functions

$$\begin{bmatrix} \Phi_{\boldsymbol{a}}^\alpha \\ \Phi_{\boldsymbol{a}}^\beta \end{bmatrix} := \begin{bmatrix} \alpha & \beta \end{bmatrix}^{-1} \begin{bmatrix} \Phi_{\boldsymbol{a}}^{(1,0)} \\ \Phi_{\boldsymbol{a}}^{(0,1)} \end{bmatrix}$$

satisfy

$$\partial_\rho \Phi_{\boldsymbol{a}}^\alpha(\boldsymbol{b}) = \delta_{\boldsymbol{ab}} \delta_{\alpha\rho} \quad \text{and} \quad \partial_\rho \Phi_{\boldsymbol{a}}^\alpha(\boldsymbol{b}) = \delta_{\boldsymbol{ab}} \delta_{\beta\rho} \qquad \forall \rho \in \Upsilon_{\boldsymbol{b}},\ \forall \boldsymbol{b} \in \mathcal{V}.$$

Moreover, by the properties of the Argyris basis functions, there holds

$$\mathcal{P}_1(K) \subset \operatorname{span}\{\Phi_{\boldsymbol{a}}^\alpha : \boldsymbol{a} \in \mathcal{V}_K,\ \alpha \in \Upsilon_{\boldsymbol{a}} \setminus \Upsilon_{\boldsymbol{a}}^2\}, \tag{3.5.11}$$

and

$$|\Phi_{\boldsymbol{a}}^{\alpha}|_{H^m(K)} \leq Ch_K^{1+|\alpha|-m} \qquad \forall m \in \{0,1,2\},\ \forall \alpha \in \Upsilon_{\boldsymbol{a}} \setminus \Upsilon_{\boldsymbol{a}}^2,\ \forall \boldsymbol{a} \in \mathcal{V}. \tag{3.5.12}$$

Let $\tilde{\Phi}_{\boldsymbol{a}}^{\alpha} = \mathbb{E}\Phi_{\boldsymbol{a}}^{\alpha} \in \Sigma_I^{\perp}$, $\alpha \in \Upsilon_{\boldsymbol{a}} \setminus \Upsilon_{\boldsymbol{a}}^2$, $\boldsymbol{a} \in \mathcal{V}$. In the case $\alpha \in \Lambda_{\boldsymbol{a}}$, then $\tilde{\Phi}_{\boldsymbol{a}}^{\alpha}$ coincides with (3.5.2) applied to $\Phi_{\boldsymbol{a}}^{\alpha}$.

We first verify that condition (3.3.5) holds. Let $q \in \mathcal{P}_1(K)$. By (3.5.11) we have $q = \sum_{\substack{\boldsymbol{a}\in\mathcal{V}_K \\ \alpha\in\Upsilon_{\boldsymbol{a}}\setminus\Upsilon_{\boldsymbol{a}}^2}} c_{\boldsymbol{a},\alpha}\Phi_{\boldsymbol{a}}^{\alpha}$ for suitable $c_{\boldsymbol{a},\alpha} \in \mathbb{R}$. Define $\tilde{q} := \sum_{\substack{\boldsymbol{a}\in\mathcal{V}_K \\ \alpha\in\Upsilon_{\boldsymbol{a}}\setminus\Upsilon_{\boldsymbol{a}}^2}} c_{\boldsymbol{a},\alpha}\tilde{\Phi}_{\boldsymbol{a}}^{\beta}$. Then, $q - \tilde{q} \in \Sigma_I^{(K)}$ and thanks to (3.5.8a), $a_K(q - \tilde{q}, v) \equiv 0$ for all $v \in \Sigma_I^{(K)}$. Hence, $\tilde{q} \equiv q \in \mathcal{P}_1(K)$ and (3.3.5) holds. Moreover, choosing $v = \Phi_{\boldsymbol{a}}^{\alpha}$ in Lemma 3.5.2 and using (3.5.9) gives for $m \in \{0,1,2\}$,

$$|\tilde{\Phi}_{\boldsymbol{a}}^{\alpha}|_{H^m(K)} \leq C\{|\Phi_{\boldsymbol{a}}^{\alpha}|_{H^m(K)} + h_K^{2-m}|\Phi_{\boldsymbol{a}}^{\alpha}|_{H^2(K)}\} \leq Ch_K^{1+|\alpha|-m}.$$

Hence, $\{\tilde{\Phi}_{\boldsymbol{a}}^{\alpha}, \alpha \in \Upsilon_{\boldsymbol{a}} \setminus \Upsilon_{\boldsymbol{a}}^2\}$, satisfy conditions (i-ii) of Theorem 3.3.2.

3.5.3.2 C^2 Vertex Functions

Let $\Phi_{\boldsymbol{a}}^{\alpha} \in \mathcal{P}_p(K)$, $\alpha \in \Upsilon_{\boldsymbol{a}}^2$, $\boldsymbol{a} \in \mathcal{V}$, be any polynomial with boundary values matching those of $\bar{\Phi}_{\boldsymbol{a}}^{\alpha}$ (3.7.8). Then, $\tilde{\Phi}_{\boldsymbol{a}}^{\alpha} := \mathbb{E}\Phi_{\boldsymbol{a}}^{\alpha}$ is a C^2 vertex functions in the sense that

$$D^{\beta}\tilde{\Phi}_{\boldsymbol{a}}^{\beta}(\boldsymbol{b}) = \delta_{\alpha\beta}\delta_{\boldsymbol{ab}} \qquad \forall \alpha \in \Upsilon_{\boldsymbol{a}},\ \forall \beta \in \Upsilon_{\boldsymbol{b}},\ \forall \boldsymbol{b} \in \mathcal{V}.$$

In the case $\alpha \in \Lambda_{\boldsymbol{a}}$, then $\tilde{\Phi}_{\boldsymbol{a}}^{\alpha}$ coincides with (3.5.2) applied to $\Phi_{\boldsymbol{a}}^{\alpha}$. Thanks to (3.7.9), choosing $v = \bar{\Phi}_{\boldsymbol{a}}^{\alpha}$ in (3.5.9) gives (3.3.7).

3.5.4 Preconditioner with Approximate Interior Solves

Examining Algorithm 2 reveals that the dominant cost arises from the need to compute the action of the matrix $\boldsymbol{A}_{II}^{-1}$. Of course, one can exploit the block diagonal structure of $\boldsymbol{A}_{II}$ to work on an element by element basis in parallel. However, this will still require the evaluation of the action of the element interior matrices $\boldsymbol{A}_{II}^{(K)}$ which, in turn, will differ from element to element due to the influence of the element geometry in $\boldsymbol{A}_{II}^{(K)}$. In this section, we seek to reduce the cost of this step by replacing the interior solve $\boldsymbol{A}_{II}^{(K)}$ by one involving the matrix $h_K^{-2}\hat{\boldsymbol{A}}_{II}$ which, up to a scaling by h_K, is *identical for all elements* K. This means that the matrix $\hat{\boldsymbol{A}}_{II}$ can be factored *once* and utilized by all elements $K \in \mathcal{T}$, thereby avoiding having to compute factorizations for every element.

Define the bilinear form $\breve{a}(\cdot,\cdot)$ as follows:

$$\breve{a}(u,v) := \sum_{K\in\mathcal{T}} \breve{a}_K(u,v), \quad \text{where} \quad \breve{a}_K(u,v) := h_K^{-2}(D^2(u \circ \boldsymbol{F}_K), D^2(v \circ \boldsymbol{F}_K))_{L^2(\hat{T})}$$

and $\boldsymbol{F}_K$ and $\hat{T}$ are given in Section 3.2. That is, on each element K, the action of $\breve{a}(u,v)$ is defined to be the action of $h_K^{-2}(D^2\cdot, D^2\cdot)_{\hat{T}}$ on the pull-backs of u and v onto the reference element $\hat{T}$. A change of variables and the chain rule show that there exists positive constants C_1 and C_2 independent of h and p such that

$$C_1 a_K(u,u) \le \check{a}_K(u,u) \le C_2 a_K(u,u) \qquad \forall u \in \Sigma^{(K)}. \tag{3.5.13}$$

In order to take advantage of (3.5.13), we define $\Sigma_I^{\perp}$ to be the orthogonal complement of Σ_I in X *with respect to* $\check{a}(\cdot,\cdot)$, rather than $a(\cdot,\cdot)$. Moreover, both Σ_I and $\tilde{\Sigma}_B := \Sigma_I^{\perp} \cap X$ are equipped with the inner product $\check{a}(\cdot,\cdot)$. Then, the preconditioning form $\check{c}(\cdot,\cdot)$ is defined to be

$$\check{c}(u,v) = \check{a}(u_I, v_I) + \check{a}(u_c, v_c) + \sum_{\substack{\boldsymbol{a}\in\mathcal{V}\\ \alpha\in\Lambda_{\boldsymbol{a}}^2}} \check{a}(u_{\boldsymbol{a},\alpha}, v_{\boldsymbol{a},\alpha}) + \sum_{\gamma\in\mathcal{E}} \check{a}(u_\gamma, v_\gamma).$$

The next result bounds the condition number.

Theorem 3.5.3. *Under the assumptions of Theorem 3.3.2, there exists positive constants C_1, C_2 independent of p and h such that*

$$C_1 \check{c}(u,u) \le B(u,u) \le C_2(1+\log^3 p)\check{c}(u,u). \tag{3.5.14}$$

Proof. Owing to the equivalences (3.2.2) and (3.5.13), it suffices to consider the single element case as in Section 3.4. The proof closely mirrors the one used to prove Theorem 3.4.1. In particular, (3.4.4) holds with "11" replaced by a positive constant C thanks to (3.5.13). Similarly, the estimate (3.4.6) may be replaced by

$$\check{a}_K(u_I, u_I) \le \check{a}_K(u,u) \le C a_K(u,u)$$

and (3.4.5) may be replaced by

$$\check{c}_K(u,u) \le C\bar{c}_K(u,u) \le C(1+\log^3 p)a_K(u,u)$$

owing to (3.5.13). The remainder of the proof of (3.5.14) is identical to that of Theorem 3.4.1. $\square$

It remains to verify that the construction of the basis functions in Section 3.5.3, in which $a(\cdot,\cdot)$ is replaced by $\check{a}(\cdot,\cdot)$, $\boldsymbol{A}$ is replaced by $\hat{\boldsymbol{A}}$, etc. still results in functions that satisfy (3.3.5) to (3.3.7). Examining the foregoing arguments reveals that Lemma 3.5.2 still holds (with different constants) due to (3.5.13), and so the same construction is valid. The action of the preconditioner on a residual $\vec{r}$ is then given in Algorithm 3.

Algorithm 3 Matrix form of preconditioner with approximate solves $\quad \vec{r} \mapsto (\vec{\alpha}_I, \vec{\alpha}_B)$

(i) $\tilde{\vec{\alpha}}_I = \check{\boldsymbol{A}}_{II}^{-1}\vec{r}_I$

(ii) $$\begin{cases} \vec{\alpha}_c = \widetilde{\check{\boldsymbol{A}}}_c^{-1}\left(\vec{r}_c - \check{\boldsymbol{A}}_{cI}\tilde{\vec{\alpha}}_I\right) \\ \vec{\alpha}_{\boldsymbol{a},\alpha} = \widetilde{\check{\boldsymbol{A}}}_{\boldsymbol{a},\alpha}^{-1}\left(\vec{r}_{\boldsymbol{a},\alpha} - \check{\boldsymbol{A}}_{\boldsymbol{a},\alpha I}\tilde{\vec{\alpha}}_I\right) \\ \vec{\alpha}_\gamma = \widetilde{\check{\boldsymbol{A}}}_\gamma^{-1}\left(\vec{r}_\gamma - \check{\boldsymbol{A}}_{\gamma I}\tilde{\vec{\alpha}}_I\right) \end{cases}$$

(iii) $$\begin{aligned} \vec{\alpha}_B &= \begin{bmatrix}\vec{\alpha}_c & (\vec{\alpha}_{\boldsymbol{a},\alpha})_{\boldsymbol{a}\in\mathcal{V},\alpha\in\Upsilon^2_{\boldsymbol{a}}} & (\vec{\alpha}_\gamma)_{\gamma\in\mathcal{E}}\end{bmatrix} \\ \vec{\alpha}_I &= \tilde{\vec{\alpha}}_I - \check{\boldsymbol{A}}_{II}^{-1}\check{\boldsymbol{A}}_{IB}\vec{\alpha}_B \end{aligned}$$

As mentioned above, $\check{\boldsymbol{A}}_{II}$ is block diagonal where all of the blocks are equal up to a scaling factor h_K^{-2}. Specifically, if $\vec{\hat{\Phi}}_I$ defines the interior basis functions on $\hat{T}$ and the basis for the interior space on each element is taken to be $\vec{\Phi}_I = \vec{\hat{\Phi}}_I \circ \boldsymbol{F}_K$, then,

$$\breve{\boldsymbol{A}}_{II} = \text{blockdiag}(h_K^{-2}\hat{\boldsymbol{A}}_{II} : K \in \mathcal{T}), \quad \text{where} \quad \hat{\boldsymbol{A}}_{II} := (D^2\vec{\hat{\Phi}}_I, D^2\vec{\hat{\Phi}}_I^T)_{\hat{T}}.$$

Thus, $\hat{\boldsymbol{A}}_{II}$ may be computed and factorized offline. The factorization is then used to compute that action $\breve{\boldsymbol{A}}_{II}^{-1}\vec{r}_I$. Moreover, we need not compute $\tilde{\boldsymbol{B}}_{BB}$ or $\tilde{\boldsymbol{B}}_{BI}$, since only

$$\widetilde{\breve{\boldsymbol{A}}}_{BB} = \breve{\boldsymbol{A}}_{BB} - \breve{\boldsymbol{A}}_{BI}\breve{\boldsymbol{A}}_{II}^{-1}\breve{\boldsymbol{A}}_{IB},$$

is needed. This means that the setup cost for Algorithm 3 is a one-time, offline cost of $\mathcal{O}(p^6)$, a $\mathcal{O}(|\mathcal{T}|p^5)$ cost to assemble the matrix $\widetilde{\breve{\boldsymbol{A}}}_{BB}$, and a $\mathcal{O}(|\mathcal{V}|^3 + |\mathcal{E}|p^3)$ cost to factor the matrices $\widetilde{\breve{\boldsymbol{A}}}_c$ and $\widetilde{\breve{\boldsymbol{A}}}_\gamma$. Thus, the overall setup cost is $\mathcal{O}(|\mathcal{V}|^3 + |\mathcal{E}|p^3 + |\mathcal{T}|p^5)$ operations, which is an improvement over the setup cost of Algorithm 2. The storage costs and the application costs are of the same complexity as Algorithm 2.

3.6 Numerical Examples

In this section $\tilde{\boldsymbol{B}}$ and $\boldsymbol{C}$ denote the stiffness matrices associated with the bilinear forms $B(\cdot,\cdot)$ and $c(\cdot,\cdot)$, respectively relative to the basis defined in Section 3.2.

3.6.1 Airy Stress Tensor Problem

If an elastic plate is subjected to traction boundary conditions in the absence of any body force, then the resulting stresses may be written in the form [110, §4]

$$\boldsymbol{\sigma} = \mathbb{A}(\varphi) = \begin{bmatrix} \varphi_{yy} & -\varphi_{xy} \\ -\varphi_{xy} & \varphi_{xx} \end{bmatrix}.$$

The scalar valued function φ is known as Airy stress function and satisfies a variational problem of the form (3.2.1) with $X = \{v \in H^2(\Omega) : \int_\Omega vq \, dx = 0 \; \forall q \in \mathcal{P}^1(\Omega)\}$,

$$B(u,v) = \int_K \mathbb{A}(u) : \mathbb{A}(v) \, dx = (D^2 u, D^2 v)_\Omega,$$

and $L(v)$ depends on the prescribed tractions. Note that $B(\cdot,\cdot)$ trivially satisfies condition (3.5.7). We consider the case $\Omega = K$, a single triangle.

Table 3.1 and Figure 3.1 show the smallest eigenvalue λ_{min} and the largest eigenvalue λ_{max} of the matrix $\boldsymbol{C}^{-1/2}\tilde{\boldsymbol{B}}\boldsymbol{C}^{-1/2}$. Observe that without preconditioning, the condition number of the stiffness matrix $\tilde{\boldsymbol{B}}$ would grow exponentially fast with p. However, with our preconditioner, the growth of the condition numbers exhibits $1 + \log^3 p$ growth consistent with Theorem 3.3.2.

p	λ_{min}	λ_{max}	$\mathrm{cond}(\boldsymbol{C}^{-1/2}\tilde{\boldsymbol{B}}\boldsymbol{C}^{-1/2})$	$\mathrm{cond}(\tilde{\boldsymbol{B}})$
5	2.941e-02	6.734	231.07	8.94e+03
6	1.224e-02	4.726	386.13	1.30e+05
7	8.522e-03	4.155	487.64	4.90e+05
8	6.001e-03	3.777	629.28	1.58e+06
9	4.890e-03	3.647	745.73	4.40e+06
10	4.036e-03	3.527	873.96	1.10e+07
11	3.527e-03	3.475	985.30	2.67e+07
12	3.102e-03	3.420	1102.20	6.32e+07
13	2.811e-03	3.394	1207.03	1.53e+08
14	2.558e-03	3.362	1314.36	3.71e+08
15	2.369e-03	3.347	1412.87	9.32e+08
16	2.200e-03	3.328	1512.29	2.34e+09
17	2.068e-03	3.319	1605.01	6.23e+09
18	1.947e-03	3.306	1697.82	1.66e+10
19	1.849e-03	3.300	1785.33	4.48e+10
20	1.758e-03	3.291	1872.50	1.38e+11
21	1.682e-03	3.288	1955.08	4.34e+11
22	1.610e-03	3.282	2037.64	1.34e+12
23	1.551e-03	3.279	2113.74	4.54e+12
24	1.494e-03	3.275	2192.33	1.55e+13

Table 3.1: Condition numbers for preconditioned and non-preconditioned stiffness matrix for Airy stress tensor problem.

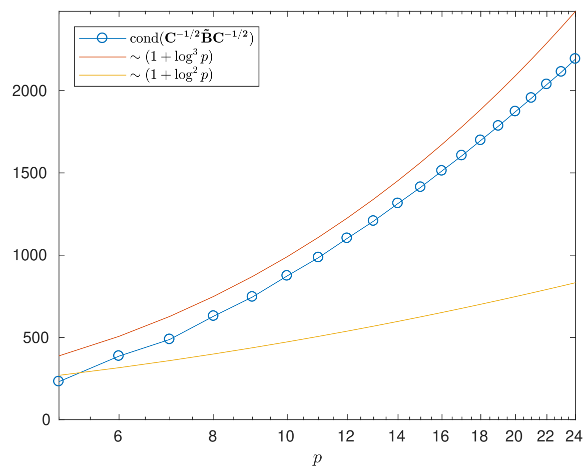

Figure 3.1: Condition numbers for preconditioned stiffness matrix for the Airy stress tensor projection problem. Observe the $1 + \log^3 p$ growth consistent with Theorem 3.3.2.

3.6.2 Stokes Problem

We now apply the preconditioner in Algorithm 1 to the Stokes' equations [55] in a cavity with parabolic inflow and outflow velocity profiles of $y(1-y)$:

$$
\begin{aligned}
\Delta^2 \psi &= 0 && \text{in } \Omega \\
\psi\left(\pm\frac{3}{2}, y\right) &= \frac{1}{2}y^2 - \frac{1}{3}y^3 && 0 \le y \le 1 \\
\psi &= \frac{1}{6} && \text{on } \Gamma_T \\
\psi &= 0 && \text{on } \Gamma_B \\
\partial_n \psi &= 0 && \text{on } \partial\Omega,
\end{aligned}
$$

where Γ_T and Γ_B are the top and bottom boundaries of the cavity in Figure 3.2. The weak form of the equations satisfy (3.2.1) with $X = H_0^2(\Omega)$,

$$B(u,v) = (\Delta u, \Delta v),$$

and $L(v)$ depending on the boundary conditions. Note that $B(\cdot,\cdot)$ satisfies (3.5.7): Let $u \in C^\infty(\bar{\Omega})$ and $v \in C_c^\infty(\Omega)$. Integrating by parts,

$$\begin{aligned} B(u,v) &= \sum_{i,j=1}^{2} \int_\Omega \partial_{x_i}^2 u \; \partial_{x_j}^2 v \; dx = -\sum_{i,j=1}^{2} \int_\Omega \partial_{x_i}^2 \partial_{x_j} u \; \partial_{x_j} v \; dx \\ &= \sum_{i,j=1}^{2} \int_\Omega \partial_{x_i}\partial_{x_j} u \; \partial_{x_i}\partial_{x_j} v \; dx = a(u,v). \end{aligned} \tag{3.6.2}$$

By the density of $C^\infty(\bar{\Omega})$ in $H^2(\Omega)$ and $C_c^\infty(\Omega)$ in $H_0^2(\Omega)$, $B(u,v) = a(u,v)$ for all $u \in H^2(\Omega)$ and $v \in H_0^2(\Omega)$.

In Figure 3.2, we see that the approximation obtained using degree $p = 14$ is able to capture one level of eddies in the bottom corners, and nearly captures the second with only two elements. The condition numbers are given in Figure 3.3. We again observe $1 + \log^3 p$ growth rate in condition number as predicted by Theorem 3.3.2.

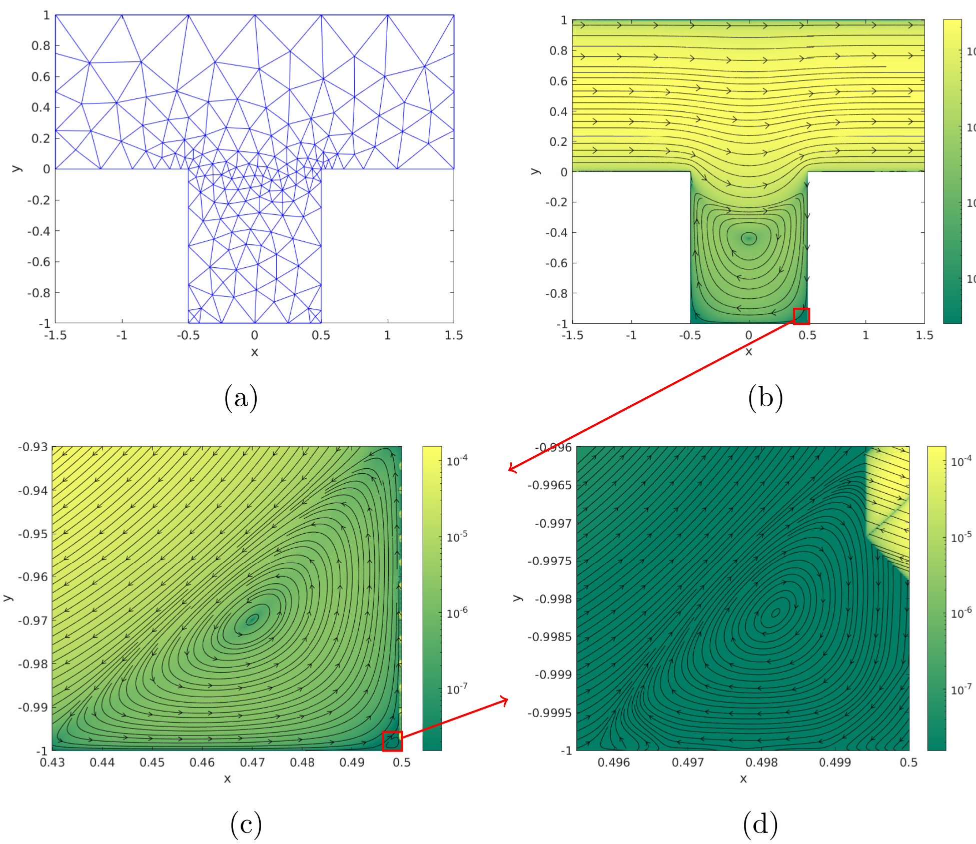

Figure 3.2: $p = 14$ numerical solution for Stokes problem with magnitude of fluid velocity as background color. Observe the resolution of small scale features. (a) Mesh - 316 elements, (b) Numerical solution, (c) Zoom 1 - different color scale, (d) Zoom 2 - different color scale.

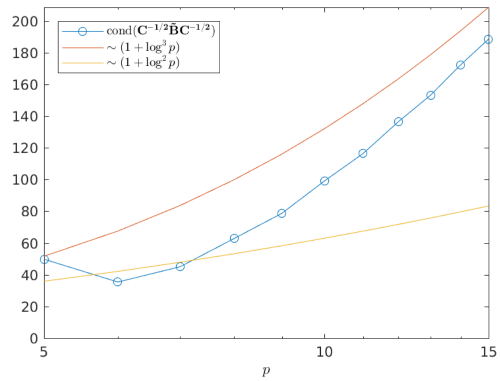

Figure 3.3: Condition numbers for the preconditioned stiffness matrix for the Stokes problem. Observe the $1 + \log^3 p$ growth consistent with Theorem 3.3.2.

3.6.3 Plate Problem

We now apply the preconditioner in Algorithm 1 to the simply supported plate problem [110, §5] on a L-shaped domain with point loading:

$$\begin{aligned} \Delta^2 u &= 10\delta_z && \text{in } \Omega, \\ u = \Delta u - (1-\nu)\partial_{tt} u &= 0 && \text{on } \partial\Omega, \end{aligned}$$

where u is the displacement, $\nu = 0.3$ and z is taken to be the point inside the red circle shown in Figure 3.4. The weak form of the equations satisfy (3.2.1) with $X = H_0^1(\Omega) \cap H^2(\Omega)$,

$$B(u,v) = (\Delta u, \Delta v) - (1-\nu) \int_\Omega (\partial_{x_1}^2 u \; \partial_{x_2}^2 v + \partial_{x_2}^2 u \; \partial_{x_1}^2 v - 2\partial_{x_1}\partial_{x_2} u \; \partial_{x_1}\partial_{x_2} v) \; dx_1 \; dx_2,$$

and $L(v) = v(z)$. Again note that $B(\cdot,\cdot)$ satisfies (3.5.7): Let $u \in C^\infty(\bar{\Omega})$ and $v \in C_c^\infty(\Omega)$. Integrating by parts,

$$\int_\Omega \partial_{x_1}^2 u \ \partial_{x_2}^2 v \ dx \ dy = -\int_\Omega \partial_{x_1}\partial_{x_2} u \ \partial_{x_2} v \ dx_1 \ dx_2 = \int_\Omega \partial_{x_1}\partial_{x_2} u \ \partial_{x_1}\partial_{x_2} v \ dx_1 \ dx_2.$$

Reversing the roles of x_1 and x_2, there holds

$$\int_\Omega \partial_{x_2}^2 u \ \partial_{x_1}^2 v \ dx \ dy = \int_\Omega \partial_{x_1}\partial_{x_2} u \ \partial_{x_1}\partial_{x_2} v \ dx \ dy,$$

and so thanks to (3.6.2), $B(u,v) = a(u,v)$. By the density of $C^\infty(\bar{\Omega})$ in $H^2(\Omega)$ and $C_c^\infty(\Omega)$ in $H_0^2(\Omega)$, $B(u,v) = a(u,v)$ for all $u \in H^2(\Omega)$ and $v \in H_0^2(\Omega)$.

The mesh is chosen so than an element vertex is located at z. The point evaluation functional $L : v \mapsto 10v(z)$ is continuous on the space $H^2(\Omega)$ which means that the problem is well posed (this would not be the case were a standard mixed formulation [34] used). The approximation obtained using degree $p = 14$ are shown in Figure 3.4, where the color represents the displacement u in the negative z-axis. Observe that, whilst the load acts in the $-z$ direction, positive displacements are in the upper left corner consistent with what is observed in practice. The condition numbers for the preconditioned system with varying p are given in Figure 3.5. Again we see condition number growth on the order of $1 + \log^3 p$.

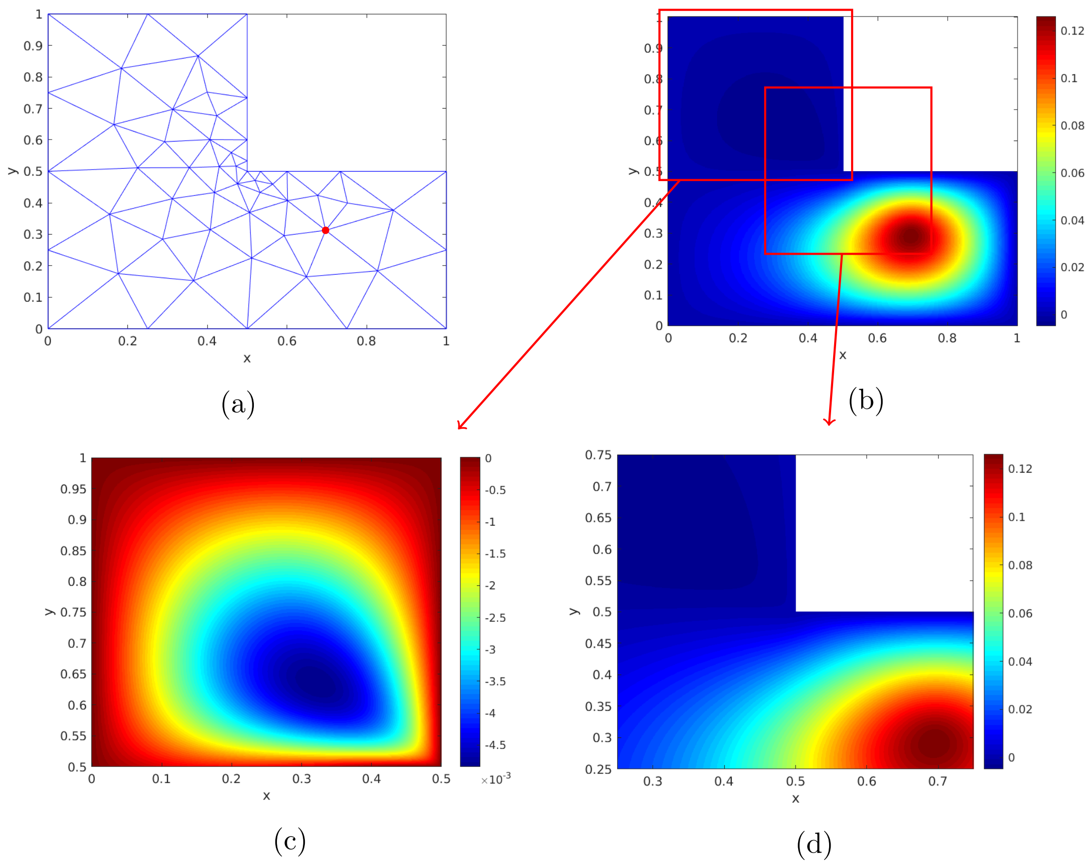

Figure 3.4: $p = 14$ numerical solution of the simply supported plate problem. Observe the deflection in the upper left region. (a) Mesh - 86 elements, (b) Numerical solution, (c) Zoom 1 - different color scale, (d) Zoom 2 - original color scale.

3.7 Traces of C^2 Vertex Functions

We start with a lemma that defines some univariate functions which are used to construct C^2 vertex functions satisfying the condition (3.3.7).

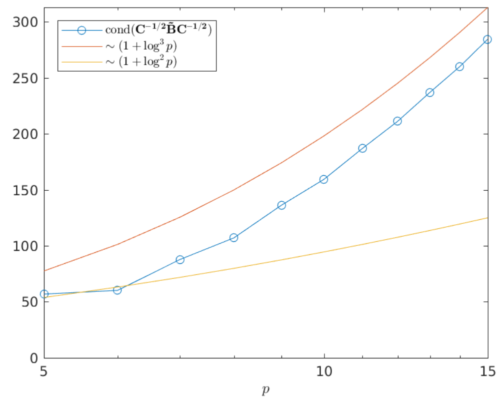

Figure 3.5: Condition numbers for the simply supported plate problem. Observe the $1 + \log^3 p$ growth consistent with Theorem 3.3.2.

Lemma 3.7.1. *Let $m, p \in \mathbb{N}$, $\beta > -1$. Define $\gamma := 2m - 1 + \beta$ and*

$$\psi_{p,m,\beta}(x) := \left(\frac{1-x}{2}\right)\left(\frac{1-x^2}{2}\right)^{m-1} P_p^{(\gamma,\gamma)}(x).$$

Then, $\psi_{p,m,\beta}^{(j)}(\pm 1) = 0$ for $j = 0, 1, \ldots, m-2$, $\psi_{p,m,\beta}^{(m-1)}(1) = 0$, and $\psi_{p,m,\beta}^{(m-1)}(-1) \neq 0$. Moreover,

$$\begin{aligned}\frac{1}{\psi_{p,m,\beta}^{(m-1)}(-1)^2}\int_{-1}^{1}(1-x^2)^{\beta}\psi_{p,m,\beta}(x)^2\ dx &\leq \frac{2^{2m-1-2\beta}\Gamma(\gamma+1)\Gamma(\gamma)p!}{(m-1)!(m-1)!\Gamma(p+2\gamma+1)} \\ &\sim p^{-2(2m-1+\beta)}.\end{aligned}$$

Proof. Let $\psi_p := \psi_{p,m,\beta}$. We first bound

$$
\begin{aligned}
4^\beta \int_{-1}^{1} \left(\frac{1-x^2}{4}\right)^\beta \psi_p(x)^2\ dx &= \int_{-1}^{1} \left(\frac{1-x}{2}\right)^{\gamma+1} \left(\frac{1+x}{2}\right)^{\gamma-1} P_p^{(\gamma,\gamma)}(x)^2\ dx \\
&\le \int_{-1}^{1} \left(\frac{1-x}{2}\right)^{\gamma} \left(\frac{1-x}{2}\right)^{\gamma-1} P_p^{(\gamma,\gamma)}(x)^2\ dx \\
&=: Q_p.
\end{aligned}
$$

Now, using the identity [108, §4]:

$$
(2p+2\gamma-1)P_p^{(\gamma,\gamma-1)} = (p+2\gamma)P_p^{(\gamma,\gamma)} + (p+\gamma)P_{p-1}^{(\gamma,\gamma)}
$$

we get

$$
P_p^{(\gamma,\gamma)} = \mu_p P_p^{(\gamma,\gamma-1)} - \nu_p P_{p-1}^{(\gamma,\gamma)} \qquad \text{with} \quad \mu_p = \frac{2(p+\gamma)}{p+2\gamma} \quad \text{and} \quad \nu_p = \frac{p+\gamma}{p+2\gamma}.
$$

Using this identity and orthogonality, there holds

$$
\begin{aligned}
Q_p = \nu_p^2 &\int_{-1}^{1} \left(\frac{1-x}{2}\right)^{\gamma} \left(\frac{1+x}{2}\right)^{\gamma-1} P_{p-1}^{(\gamma,\gamma)}(x)^2\ dx \\
&+ \mu_p^2 \int_{-1}^{1} \left(\frac{1-x}{2}\right)^{\gamma} \left(\frac{1+x}{2}\right)^{\gamma-1} P_p^{(\gamma,\gamma-1)}(x)^2\ dx \\
=:&\ \nu_p^2 Q_{p-1} + \mu_p^2 T_p. \qquad (3.7.1)
\end{aligned}
$$

First note that

$$
T_p = \frac{1}{p+\gamma} \frac{\Gamma(p+\gamma+1)\Gamma(p+\gamma)}{\Gamma(p+2\gamma)p!} = \frac{\Gamma(p+\gamma)^2}{\Gamma(p+2\gamma)p!}.
$$

We now claim

$$Q_p \leq \frac{\Gamma(p+\gamma+1)^2}{\Gamma(p+2\gamma+1)!p!} \cdot \frac{2}{\gamma}. \tag{3.7.2}$$

For $p = 0$, we have

$$Q_0 = \int_{-1}^{1} \left(\frac{1-x}{2}\right)^{\gamma} \left(\frac{1+x}{2}\right)^{\gamma-1} dx = \frac{\Gamma(\gamma)^2}{\Gamma(2\gamma)p!},$$

and (3.7.2) holds as an equality in the case $p = 0$. Now suppose the result holds true for $p = q - 1$. Then, by (3.7.1),

$$(q+2\gamma)^2 Q_q = (q+\gamma)^2 Q_{q-1} + 4(q+\gamma)^2 T_q.$$

Direct computation gives

$$Q_q \leq \frac{(q+\gamma)^2}{(q+2\gamma)^2} \cdot \frac{\Gamma(q+\gamma)^2}{\Gamma(q+2\gamma)q!} \cdot \frac{2}{\gamma}(q+2\gamma) = \frac{\Gamma(q+\gamma+1)^2}{\Gamma(q+2\gamma+1)q!} \cdot \frac{2}{\gamma}$$

and (3.7.2) follows by induction. Again using identities from [108, §4]

$$\psi_p^{(m-1)}(-1) = \frac{(m-1)!}{2^{m-1}} P_p^{(\gamma,\gamma)}(-1) = \frac{(-1)^p (m-1)!\Gamma(p+\gamma+1)}{2^{m-1}\Gamma(\gamma+1)p!}.$$

Thus,

$$\frac{1}{\psi_p^{(m-1)}(-1)^2} \int_{-1}^{1} (1-x^2)^{\beta} \psi_p(x)^2 \, dx = 2^{2m-1-2\beta} \frac{\Gamma(\gamma+1)\Gamma(\gamma)p!}{(m-1)!(m-1)!\Gamma(p+2\gamma+1)}.$$

By Stirling's formula, $\frac{p!}{\Gamma(p+2\gamma+1)} \sim p^{-2(2m-1+\beta)}$. $\square$

Next, we record a scale-invariant version of the H^2-stable polynomial extension theorem established in Chapter 2:

Corollary 3.7.2. *Let $f, g : \partial K \to \mathbb{R}$ be such that $f_i := f|_{\gamma_i} \in \mathcal{P}_p(\gamma_i)$ and $g_i := g|_{\gamma_i} \in \mathcal{P}_{p-1}(\gamma_i)$ for $p \geq 1$. Assume further that f and g satisfy the compatibility conditions* (2.2.10) *at the vertices. Then, there exists a polynomial $U \in \mathcal{P}_p(K)$ such that*

1. *U has trace (f, g): $U|_{\gamma_i} = f_i$, $\partial_n U|_{\gamma_i} = g_i$, and*
2. *U depends continuously on f and g:*

$$\begin{aligned} &h_K^{-1}\|U\|_{L^2(K)} + |U|_{H^1(K)} + h_K|U|_{H^2(K)} \\ &\qquad \leq C\left(h_K^{-1/2}\|f\|_{L^2(\partial K)} + h_K^{1/2}\|\boldsymbol{\sigma}(f,g)\|_{L^2(\partial K)} + h_K|\boldsymbol{\sigma}(f,g)|_{H^{1/2}(\partial K)}\right) \end{aligned} \tag{3.7.3}$$

where $\boldsymbol{\sigma}(f, g) = (\partial_t f)\hat{\boldsymbol{n}} - g\hat{\boldsymbol{t}}$, and C is independent of p and h_K.

Proof. The existence of a polynomial U satisfying the required conditions is given by Corollary 2.2.3 where the estimate (3.7.3) is also established in the case $h_K = 1$. Employing the usual scaling argument gives the estimate (3.7.3). $\square$

Let $\boldsymbol{a} \in \mathcal{V}$. Thanks to Corollary 3.7.2, we only need to specify the boundary values of $\Phi_{\boldsymbol{a}}^{\alpha}$ on each $K \in \mathcal{T}_{\boldsymbol{a}}$. We first consider the case $\Upsilon_{\boldsymbol{a}}^2 = \{(\hat{\boldsymbol{e}}_1, \hat{\boldsymbol{e}}_1), (\hat{\boldsymbol{e}}_1, \hat{\boldsymbol{e}}_2), (\hat{\boldsymbol{e}}_2, \hat{\boldsymbol{e}}_2)\}$

and summarize the boundary values below. Let $K \in \mathcal{T}_{\boldsymbol{a}}$ and label K as in Figure 2.3 so that $\boldsymbol{a}_1 := \boldsymbol{a}$. Let $F : [-1,1] \to \mathbb{R}$ and $G : [-1,1] \to \mathbb{R}$ be given by

$$F(t) = \frac{\psi_{p-5,3,0}(t)}{\psi''_{p-5,3,0}(-1)} \qquad \text{and} \qquad G(t) = \frac{\psi_{p-4,2,0}(t)}{\psi'_{p-4,2,0}(-1)},$$

where $\psi_{p,m,\beta}$ is given by Lemma 3.7.1. Now, we define the traces f and g as follows:

$\alpha = (2,0)$:

$$\begin{aligned}
f_1(t) &= 0 & g_1(t) &= 0 \\
f_2(t) &= \frac{1}{4}|\gamma_2|^2 (t_2^x)^2 F\left(1 - \frac{2t}{|\gamma_2|}\right) & g_2(t) &= -\frac{1}{2}|\gamma_2| t_2^x n_2^x G\left(1 - \frac{2t}{|\gamma_2|}\right) \\
f_{i+2}(t) &= \frac{1}{4}|\gamma_3|^2 (t_3^x)^2 F\left(\frac{2t}{|\gamma_3|} - 1\right) & g_3(t) &= \frac{1}{2}|\gamma_3| t_3^x n_3^x G\left(\frac{2t}{|\gamma_3|} - 1\right)
\end{aligned} \tag{3.7.4}$$

$\alpha = (1,1)$:

$$\begin{aligned}
f_1(t) &= 0 & g_1(t) &= 0 \\
f_2(t) &= \frac{1}{2}|\gamma_2|^2 t_2^x t_2^y F\left(1 - \frac{2t}{|\gamma_2|}\right) & g_2(t) &= -\frac{1}{2}|\gamma_2| (t_2^x n_2^y + t_2^y n_2^x) G\left(1 - \frac{2t}{|\gamma_2|}\right) \\
f_3(t) &= \frac{1}{2}|\gamma_3|^2 t_3^x t_3^y F\left(\frac{2t}{|\gamma_3|} - 1\right) & g_3(t) &= \frac{1}{2}|\gamma_3| (t_3^x n_3^y + t_3^y n_3^x) G\left(\frac{2t}{|\gamma_3|} - 1\right)
\end{aligned} \tag{3.7.5}$$

$\alpha = (0,2)$:

$$\begin{aligned}
f_1(t) &= 0 & g_1(t) &= 0 \\
f_2(t) &= \frac{1}{4}|\gamma_2|^2 (t_2^y)^2 F\left(1 - \frac{2t}{|\gamma_2|}\right) & g_2(t) &= -\frac{1}{2}|\gamma_2| t_2^y n_2^y G\left(1 - \frac{2t}{|\gamma_2|}\right) \\
f_3(t) &= \frac{1}{4}|\gamma_3|^2 (t_3^y)^2 F\left(\frac{2t}{|\gamma_3|} - 1\right) & g_3(t) &= \frac{1}{2}|\gamma_3| t_3^y n_3^y G\left(\frac{2t}{|\gamma_3|} - 1\right)
\end{aligned} \tag{3.7.6}$$

Since F and G vanish to order 2 and 1, respectively, f and g satisfy the compatibility conditions in Corollary 3.7.2. Let $\bar{\Phi}_{\boldsymbol{a}}^{\alpha}$ be the extension of f and g given by Corollary 3.7.2. First note that we have the desired interpolation properties:

$$D^{\beta}\bar{\Phi}_{\boldsymbol{a}}^{\alpha}(\boldsymbol{a}_i) = \delta_{\alpha\beta}\delta_{1i} \qquad \forall|\beta| \leq 2,\ 1 \leq i \leq 3.$$

Moreover, for $m \in \{0,1,2\}$ there holds,

$$\begin{aligned} h_K^{m-1}|\bar{\Phi}_{\boldsymbol{a}}^{\alpha}|_{H^m(K)} &\leq C\sum_{i=2}^{3}\Big\{h_K^{-1/2}\|f_i\|_{L^2(\gamma_i)} + h_K^{1/2}\left(|f_i|_{H^1(\gamma_i)} + \|g_i\|_{L^2(\gamma_i)}\right) \\ &\qquad\qquad + h_K\left(|f_i'|_{H^{1/2}_{00}(\gamma_i)} + |g_i|_{H^{1/2}_{00}(\gamma_i)}\right)\Big\} \\ &\leq Ch_K^2\left(\|F\|_{H^{3/2}_{00}(-1,1)} + \|G\|_{H^{1/2}_{00}(-1,1)}\right). \end{aligned}$$

Now, thanks to inverse estimates [25, Corollary 3.4] and Lemma 3.7.1, we have

$$\|F\|_{H^k(-1,1)} + \|G\|_{H^{k-1}(-1,1)} \leq Cp^{2k}\left(\|F\|_{L^2(-1,1)} + p^{-2}\|G\|_{L^2(-1,1)}\right) \leq Cp^{-5+2k}.$$

By interpolation,

$$|\bar{\Phi}_{\boldsymbol{a}}^{\alpha}|_{H^m(K)} \leq Ch_K^{3-m}\left(\|F\|_{H^{3/2}_{00}(-1,1)} + \|G\|_{H^{1/2}_{00}(-1,1)}\right) \leq Ch_K^{3-m}p^{-2}. \tag{3.7.7}$$

In the general case $\Upsilon_{\boldsymbol{a}}^2 = \{(\hat{\boldsymbol{\eta}}_1, \hat{\boldsymbol{\eta}}_2), (\hat{\boldsymbol{\rho}}_1, \hat{\boldsymbol{\rho}}_2), (\hat{\boldsymbol{\omega}}_2, \hat{\boldsymbol{\omega}}_2)\}$, the C^2 vertex functions may be construction from $\bar{\Phi}_{\boldsymbol{a}}^{(2,0)}$, $\bar{\Phi}_{\boldsymbol{a}}^{(1,1)}$, and $\bar{\Phi}_{\boldsymbol{a}}^{(0,2)}$ by the following transformation:

$$\begin{bmatrix} \bar{\Phi}_{\boldsymbol{a}}^{(\hat{\boldsymbol{\eta}}_1,\hat{\boldsymbol{\eta}}_2)} \\ \bar{\Phi}_{\boldsymbol{a}}^{(\hat{\boldsymbol{\rho}}_1,\hat{\boldsymbol{\rho}}_2)} \\ \bar{\Phi}_{\boldsymbol{a}}^{(\hat{\boldsymbol{\omega}}_1,\hat{\boldsymbol{\omega}}_2)} \end{bmatrix} = \begin{bmatrix} \eta_1^x\eta_2^x & \rho_1^x\rho_2^x & \omega_1^x\omega_2^x \\ \eta_1^x\eta_2^y + \eta_1^y\eta_2^x & \rho_1^x\rho_2^y + \rho_1^y\rho_2^x & \omega_1^x\omega_2^y + \omega_1^y\omega_2^x \\ \eta_1^y\eta_2^y & \rho_1^y\rho_2^y & \omega_1^y\omega_2^y \end{bmatrix}^{-1} \begin{bmatrix} \bar{\Phi}_{\boldsymbol{a}}^{(2,0)} \\ \bar{\Phi}_{\boldsymbol{a}}^{(1,1)} \\ \bar{\Phi}_{\boldsymbol{a}}^{(0,2)} \end{bmatrix}. \tag{3.7.8}$$

Direct verification reveals that

$$\partial_\beta \bar{\Phi}_{\boldsymbol{a}}^\alpha(\boldsymbol{a}_i) = \delta_{\alpha\beta}\delta_{1i} \qquad \forall \alpha, \beta \in \Upsilon_{\boldsymbol{a}}^2,\ 1 \le i \le 3,$$

and the triangle inequality and (3.7.7) give

$$|\bar{\Phi}_{\boldsymbol{a}}^\alpha|_{H^m(K)} \le C h_K^{3-m} p^{-2} \qquad \forall \alpha \in \Upsilon_{\boldsymbol{a}}^2,\ m \in \{0,1,2\}. \tag{3.7.9}$$

3.8 Conclusions

This chapter constructed the first nonoverlapping domain decomposition preconditioner for the stiffness matrix arising from the discretization of fourth order elliptic problems by high order Argyris elements. A careful selection of the coarse space and C^2 vertex functions controlled the condition number growth of the preconditioner system with an asymptotic bound of $\mathcal{O}(1 + \log^3 p)$ independent of h. The preconditioner was also modified to allow for inexact solvers on each of the subspaces, resulting in a more computationally efficient method. The special rapidly decaying functions in Lemma 3.7.1 will appear in each of the remaining chapters to play a similar role as in the construction of the C^2 vertex functions in Section 3.7. Combining the 1D polynomials in Lemma 3.7.1 with an appropriate polynomial preserving extension theorem gives the existence of a bivariate polynomials on triangles interpolating derivatives of a given order with rapid decay in Sobolev norms; see e.g. Lemmas 4.5.1, 5.4.3 and 6.9.7.

There are a variety of future research directions regarding preconditioning high order elements. One is to construct overlapping preconditioners in 2D and 3D for the high order Argyris elements in the spirit of [95] to obtain h- and p-independent condition numbers. Another direction is to adopt the techniques in [6, 7] construct uniform-in-p preconditioner for the mass matrix using the high order Argyris elements, which is useful for time-dependent fourth order problems like the Cahn-Hilliard equations [36]. In magnetohydrodynamics applications [52], C^1 elements are often used in potential methods, as the main quantity of interest is the gradient or curl of the solution, even though the PDEs are *second* order. For these applications, the results for the preconditioner above do not directly apply, necessitating additional theory. Finally, one may generalize the methodology in this chapter to $2m^{\text{th}}$-order elliptic problems discretized by C^{m-1}-conforming elements for $m \geq 3$.

Chapter Four

Mass Conserving Mixed hp-FEM Approximations to Stokes Flow. Part I: Uniform Stability

4.1 Introduction

The Stokes equations on a simply connected polygon Ω with boundary $\Gamma = \partial\Omega$ describe incompressible flow dominated by viscous forces [55]:

$$-\nu\Delta\boldsymbol{u} + \nabla p = \boldsymbol{f} \qquad \text{in } \Omega, \tag{4.1.1a}$$

$$\operatorname{div}\boldsymbol{u} = 0 \qquad \text{in } \Omega, \tag{4.1.1b}$$

$$\boldsymbol{u} = \boldsymbol{0} \qquad \text{on } \Gamma, \tag{4.1.1c}$$

where $\boldsymbol{u} = (u_1, u_2)$ is the fluid velocity, p the pressure, $\boldsymbol{f}$ the body force, and $\nu > 0$ the kinematic viscosity. For simplicity, we assume ν is constant and $\boldsymbol{f} \in \boldsymbol{L}^2(\Omega)$. The weak form of (4.1.1) reads as follows: Find $(\boldsymbol{u}, p) \in \boldsymbol{H}_0^1(\Omega) \times L_0^2(\Omega)$ such that

$$a(\boldsymbol{u},\boldsymbol{v}) + b(\boldsymbol{v}, p) = (\boldsymbol{f},\boldsymbol{v}) \qquad \forall\boldsymbol{v} \in \boldsymbol{H}_0^1(\Omega), \tag{4.1.2a}$$

$$b(\boldsymbol{u}, q) = 0 \qquad \forall q \in L_0^2(\Omega), \tag{4.1.2b}$$

where

$$a(\boldsymbol{u},\boldsymbol{v}) := \nu(\nabla\boldsymbol{u}, \nabla\boldsymbol{v}), \quad b(\boldsymbol{v}, p) := -(\operatorname{div}\boldsymbol{v}, p),$$

and $L_0^2(\Omega)$ the (closed) subspace of square integrable functions with vanishing average value:

$$L_0^2(\Omega) := \left\{ q \in L^2(\Omega) : \int_\Omega q \, d\boldsymbol{x} = 0 \right\}.$$

We are interested in finding conforming high order polynomial, mixed finite element discretizations of (4.1.2) where k (rather than the usual choice p) will denote the polynomial order for the remainder of this thesis, while p denotes the pressure: Find $(\boldsymbol{u}_{hk}, p_{hk}) \in \boldsymbol{V}_0 \times Q_0$ such that

$$a(\boldsymbol{u}_{hk}, \boldsymbol{v}) + b(\boldsymbol{v}, p_{hk}) = (\boldsymbol{f}, \boldsymbol{v}) \qquad \forall \boldsymbol{v} \in \boldsymbol{V}_0 \tag{4.1.3a}$$

$$b(\boldsymbol{u}_{hk}, q) = 0 \qquad \forall q \in Q_0, \tag{4.1.3b}$$

where $\boldsymbol{V}_0 \subset \boldsymbol{H}_0^1(\Omega)$ and $Q_0 \subset L_0^2(\Omega)$ are spaces of piecewise polynomials of degree k and $k-1$ defined later on a triangulation of Ω denoted by $\mathcal{T}$.

The construction of finite element subspaces that satisfy exact sequence properties has received much attention recently; see the review paper [66] and references therein. One example of an exact sequence [50, 55] is the following:

$$\mathbb{R} \xrightarrow{\subset} H^2(\Omega) \xrightarrow{\mathbf{curl}} \boldsymbol{H}^1(\Omega) \xrightarrow{\mathrm{div}} L^2(\Omega) \longrightarrow 0, \tag{4.1.4}$$

where the rotated gradient operator is defined by $\mathbf{curl}\,\phi = (\nabla\phi)^\perp$ with $\boldsymbol{t}^\perp = (t_y, -t_x)$ for a vector $\boldsymbol{t} \in \mathbb{R}^2$. By saying the sequence (4.1.4) is exact, we mean that kernel of each operator in the sequence equals the range of the preceding operator. For example, the second inclusion means that if $\operatorname{div} \boldsymbol{u} \equiv 0$ for $\boldsymbol{u} \in \boldsymbol{H}^1(\Omega)$, then $\boldsymbol{u}$ can be written as $\boldsymbol{u} = \mathbf{curl}\, \psi$ for some $\psi \in H^2(\Omega)$. The following sequence, considered by [50, 55], is also exact and corresponds to homogeneous boundary conditions:

$$0 \xrightarrow{\subset} H_0^2(\Omega) \xrightarrow{\mathbf{curl}} \boldsymbol{H}_0^1(\Omega) \xrightarrow{\operatorname{div}} L_0^2(\Omega) \longrightarrow 0. \tag{4.1.5}$$

Observe that the Stokes system (4.1.2) involves the spaces $\boldsymbol{H}_0^1(\Omega)$ and $L_0^2(\Omega)$ which appear in this sequence.

The exactness of the sequence (4.1.5) means, among other things that, since the velocity $\boldsymbol{u} \in \boldsymbol{H}_0^1(\Omega)$, then $q = \operatorname{div} \boldsymbol{u} \in L_0^2(\Omega)$. As a consequence, (4.1.2b) implies $\| \operatorname{div} \boldsymbol{u}\|^2 = 0$ or $\operatorname{div} \boldsymbol{u} \equiv 0$. If the finite element spaces $\Sigma_0 \subset H_0^2(\Omega)$, $\boldsymbol{V}_0$ and Q_0 also form an exact sequence

$$0 \xrightarrow{\subset} \Sigma_0 \xrightarrow{\mathbf{curl}} \boldsymbol{V}_0 \xrightarrow{\operatorname{div}} Q_0 \longrightarrow 0. \tag{4.1.6}$$

then the same argument can be carried out at the discrete level to conclude that the resulting approximation (4.1.3) will be pointwise mass conserving, i.e. $\operatorname{div} \boldsymbol{u}_{hk} \equiv 0$ in Ω. Furthermore, the exactness of the discrete sequence (4.1.6) then implies $\boldsymbol{u}_{hk} = \mathbf{curl}\, \phi_{hk}$ for some $\phi_{hk} \in \Sigma_0$. Consequently, since $\boldsymbol{u} = \mathbf{curl}\, \phi$ for some $\phi \in H_0^2(\Omega)$, we have

$$\|\boldsymbol{u} - \boldsymbol{u}_{hk}\|_{\boldsymbol{H}^1(\Omega)} = \| \mathbf{curl}(\phi - \phi_{hk})\|_{\boldsymbol{H}^1(\Omega)} \leq C\|\phi - \phi_{hk}\|_{H^2(\Omega)}$$

which shows that the accuracy of the velocity approximation is in fact dictated by the approximation properties of Σ_0 in $H_0^2(\Omega)$.

In principle, one could ensure the inclusion $\operatorname{div} \boldsymbol{V}_0 \subset Q_0$ holds by choosing a sufficiently large space Q_0. However, it is known [29, 31, 55] that the stability and accuracy of (4.1.3) depends on whether the inf-sup condition (also known as the Babuška-Brezzi condition)

$$\sup_{\mathbf{0} \neq \boldsymbol{v} \in \boldsymbol{V}_0} \frac{b(\boldsymbol{v}, q)}{\|\boldsymbol{v}\|_{\boldsymbol{H}^1(\Omega)}} \geq \beta(h,k) \|q\|_{L^2(\Omega)} \qquad \forall q \in Q_0 \tag{4.1.7}$$

holds for some $\beta(h,k) > 0$. The fact that the inf-sup condition must hold for *all* $q \in Q_0$ means that the space Q_0 cannot be chosen to be too large. Alternatively, one can satisfy (4.1.7) by choosing the velocity space $\boldsymbol{V}_0$ sufficiently large, but choosing $\boldsymbol{V}_0$ too large may violate the inclusion $\operatorname{div} \boldsymbol{V}_0 \subseteq Q_0$. As such, the selection of appropriate pairs for the finite element discretization of Stokes flow involves a delicate balance between maintaining stability (4.1.7) versus preserving the exact sequence property (4.1.6). Many choices [66] for the pair $\boldsymbol{V}_0 \times Q_0$ are known to satisfy the inf-sup condition with a constant $\beta(h,k)$ independent of h. Such choices are suitable for h-version FEM where $k \in \mathbb{N}$ is maintained at a constant, fixed, value. However, it is more often than not the case that $\beta(h,k) \to 0$ as k is increased for these spaces which, at the very least, makes these spaces unattractive for p- or hp-version FEM in which convergence is sought by raising the polynomial order k. For instance, the inf-sup constant $\beta(h,k)$ appears in the denominator of a priori error estimates, affects the conditioning of the resulting linear system, and affects the performance of preconditioners.

In this chapter, we consider a particular choice of Σ_0, $\boldsymbol{V}_0$, and Q_0 which satisfies the exact sequence property (4.1.6), and which was shown in [50] to be uniformly stable in h, i.e. $\beta(h,k)$ is independent of h for each given $\mathbb{N} \ni k \geq 4$. In Section 4.2, we describe sets of degrees of freedom for the spaces and give necessary and sufficient conditions on the mesh under which the spaces satisfy the exact sequence property (4.1.6). In Section 4.3, we prove that in fact, $\beta(h,k) \geq \beta_0 > 0$ where β_0 is *independent of both h and k*. The main tool is the construction of a continuous right inverse of the divergence operator on the space Q_0 which is bounded uniformly in of both h and k. In Section 4.4, we compute the actual values of the inf-sup constant $\beta(h,k)$ on a sequence of meshes. This chapter concludes with auxiliary technical results in Section 4.5 and a discussion on the extension of the results to more general boundary conditions in Section 4.6.

The current chapter is the first part of a three part series of chapters in which we study these spaces from the point of view of high order finite element approximation. In Chapter 5, we establish approximation properties of the spaces which are optimal in both the mesh size h *and* the polynomial degree k. In the Chapter 6, we discuss implementation aspects of the method and construct a block diagonal preconditioner for the indefinite linear system arising from the discrete equations (4.1.3). In summary, this means that *the pair $\boldsymbol{V}_0 \times Q_0$ is (a) pointwise mass conserving, (b) uniformly inf-sup stable in both h and k, and (c) gives optimal error estimates in both h and k.* At the time of writing, these seem to be the only choice of conforming spaces on triangles shown to satisfy (a)-(c). For instance, although the $\boldsymbol{\mathcal{Q}}_k \times \mathcal{P}_{k-1}$ elements for quadrilaterals satisfy (b)-(c) [28], they do not satisfy (a). The work in [4] considered the $\boldsymbol{\mathcal{Q}}_k \times \mathcal{Q}'_{k-1}$ elements with continuous pressures; the resulting spaces again satisfy (b-c) but not (a). The $\boldsymbol{\mathcal{P}}_k \times \mathcal{P}_{k-2}$ triangular element was shown to satisfy $\beta(h,k) \geq Ck^{-3}$ [99, 104], which is insufficient to establish (b)-(c). The work of [105] proves the analogue of the $\boldsymbol{\mathcal{Q}}_k \times \mathcal{Q}_{k-2}$ element on triangles satisfies $\beta(h,k) \geq Ck^{-1/2}$ which is again insufficient to establish (b)-(c). The Scott-Vogelius $\boldsymbol{\mathcal{P}}_k \times \mathcal{P}_{k-1}$ elements [100, 113] on meshes with no singular vertices satisfy (a); however, it was only shown that $\beta(h,k) \geq Ck^{-r}$ for some integer r sufficiently large, which is again insufficient to establsh (b)-(c). Boillat [30] showed that the $\beta(h,k) \geq Ck^{-2}\log^{-1/2} k$ for the Taylor-Hood elements and numerical computations in [29] also suggest that these elements are not uniformly inf-sup stable in k. If one is willing to relax the $\boldsymbol{H}^1(\Omega)$-smoothness requirement of the velocity approximation to $\boldsymbol{H}(\mathrm{div};\Omega)$, then the $\boldsymbol{H}(\mathrm{div};\Omega)$-conforming scheme of [73] was shown to satisfy (a)-(c) on triangles.

4.2 Finite Element Spaces

Let $\mathcal{T}$ be a shape-regular (3.2.3) partition of the domain Ω into triangles such that the nonempty intersection of any two distinct elements from $\mathcal{T}$ is either a single common vertex or a single common edge of both elements. We partition the element vertices $\mathcal{V}$ into: (i) $\mathcal{V}_C$ the set of element vertices located at a vertex of the polygonal domain Ω, (ii) $\mathcal{V}_B$ the set of remaining element vertices on the domain boundary Γ which are not corner vertices and (iii) $\mathcal{V}_I$ the set of element vertices in the interior of domain Ω. Similarly, $\mathcal{E}_I$ the denotes the set of interior edges. Given a vertex $\boldsymbol{a} \in \mathcal{V}$, $\mathcal{E}_{\boldsymbol{a}}$ denotes the set of edges having $\boldsymbol{a}$ as an endpoint, and, given an element $K \in \mathcal{T}$, $\mathcal{T}_K$ denotes the set of elements sharing a vertex or edge with $K \in \mathcal{T}$.

We consider the following finite element spaces for $\mathbb{N} \ni k \geq 4$:

$$\Sigma := \{\phi \in C^1(\bar{\Omega}) : \phi|_K \in \mathcal{P}_{k+1}(K)\ \forall K \in \mathcal{T},\ \phi \text{ is } C^2 \text{ at noncorner vertices}\}, \tag{4.2.1a}$$

$$\boldsymbol{V} := \{\boldsymbol{v} \in \boldsymbol{C}^0(\bar{\Omega}) : \boldsymbol{v}|_K \in \boldsymbol{\mathcal{P}}_k(K)\ \forall K \in \mathcal{T},\ \boldsymbol{v} \text{ is } \boldsymbol{C}^1 \text{ at noncorner vertices}\}, \tag{4.2.1b}$$

$$Q := \{q \in L^2(\Omega) : q|_K \in \mathcal{P}_{k-1}(K)\ \forall K \in \mathcal{T},\ q \text{ is } C^0 \text{ at noncorner vertices}\}, \tag{4.2.1c}$$

where $\boldsymbol{\mathcal{P}}_k(K) = [\mathcal{P}_k(K)]^2$. The spaces Σ, $\boldsymbol{V}$, and Q are somewhat non-standard owing to the differing smoothness requirements imposed at corner and noncorner vertices of the physical domain Ω. The space Σ may be regarded as a modification of the TUBA finite element space [11] which requires C^2 continuity at all vertices and used in Chapter 3, whereas the velocity space $\boldsymbol{V}$ is more akin to Hermite elements [38, §2] which require C^1 continuity at all vertices. The pressure space Q resembles discontinuous elements subject to the constraint that functions are continuous at noncorner vertices. We shall give global sets of degrees of freedom for these nonstandard spaces and conditions under which they form an exact sequence.

4.2.1 Degrees of Freedom

The following results establish a set of global degrees of freedom for each of the above spaces (4.2.1). For the purpose of counting dimensions, we use the following notation:

- $V := |\mathcal{V}|$ the total number of vertices in the mesh,
- $V_I := |\mathcal{V}_I|$ the number of interior mesh vertices,
- $V_B := |\mathcal{V}_B|$ the number of vertices on the boundary of the domain which are not corners of the domain,
- $V_C := |\mathcal{V}_C|$ the number of corners of the domain,
- $E := |\mathcal{E}|$ the number of edges in the mesh,
- $E_I := |\mathcal{E}_I|$ the number of interior edges in the mesh, and
- $T := |\mathcal{T}|$ the number of elements.

A special role will be played by the edges attached to vertices $\boldsymbol{a} \in \mathcal{V}_C$ located at the corners of the polygonal domain Ω. Let $E_C := \sum_{\boldsymbol{a}\in\mathcal{V}_C} |\mathcal{E}_{\boldsymbol{a}}|$. If no element has vertices at two consecutive corners of the domain, then E_C is the total number of edges attached the to corner vertices.

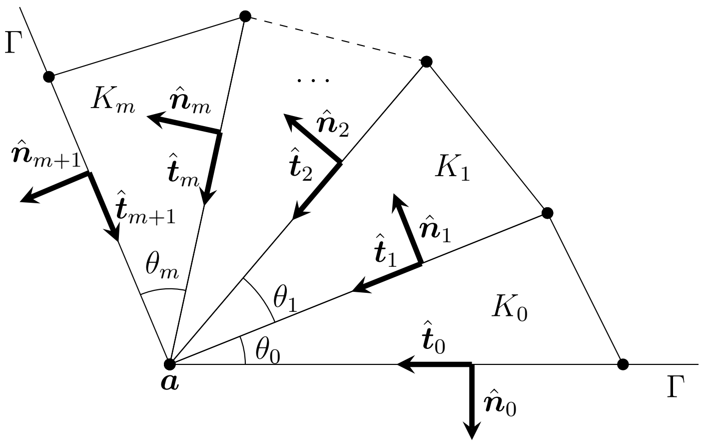

Figure 4.1: Notation for mesh around a corner boundary vertex $\boldsymbol{a} \in \mathcal{V}_C$ with $m = |\mathcal{E}_{\boldsymbol{a}}| - 2$ interior edges.

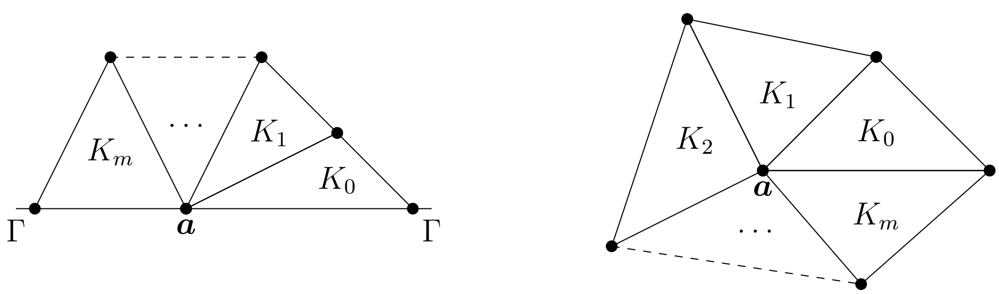

Figure 4.2: Notation for mesh around a noncorner vertex $\boldsymbol{a} \in \mathcal{V} \backslash \mathcal{V}_C$ with $m = |\mathcal{T}_{\boldsymbol{a}}| - 1$.

Lemma 4.2.1. *The pressure space Q has dimension*

$$\dim Q = V + \frac{1}{2}(k-2)(k+3)T + E_C - 2V_C, \tag{4.2.2}$$

and is unisolvent with respect to the following set of global degrees of freedom for $q \in Q$:

(i) One functional value $q(\boldsymbol{a})$ at each noncorner vertex $\boldsymbol{a} \in \mathcal{V} \setminus \mathcal{V}_C = \mathcal{V}_I \cup \mathcal{V}_B$.

(ii) $|\mathcal{E}_{\boldsymbol{a}}|-1$ *functional values* $q_i(\boldsymbol{a})$, $i = 0, \dots, |\mathcal{E}_{\boldsymbol{a}}|-2$, *at each corner vertex* $\boldsymbol{a} \in \mathcal{V}_C$, *with* $q_i = q|_{K_i}$ *as in Figure 4.1.*

(iii) $\frac{1}{2}(k-2)(k+3)$ *interior moment degrees of freedom*

$$\int_K qr \; d\boldsymbol{x} \qquad \forall r \in \mathcal{P}_{k-1}(K) : r(\boldsymbol{a}) = 0, \; \forall \boldsymbol{a} \in \mathcal{V}_K$$

on each element $K \in \mathcal{T}$.

Proof. We start with an upper bound for the dimension of Q. Let $q \in Q$ be given. For each $K \in \mathcal{T}$, the local space $\mathcal{P}_{k-1}(K)$ is unisolvent with respect to the $\frac{k}{2}(k+1)$ local degrees of freedom (illustrated in Figure 4.4)

$$q(\boldsymbol{a}) \qquad \forall \boldsymbol{a} \in \mathcal{V}_K \quad \text{and} \quad \int_K qr \; d\boldsymbol{x} \qquad \forall r \in \mathcal{P}_{k-1}(K) : r(\boldsymbol{a}) = 0, \; \forall \boldsymbol{a} \in \mathcal{V}_K. \tag{4.2.3}$$

Assume that all of the global degrees of freedom corresponding to q vanish. In particular, the local degrees of freedom (4.2.3) on each element are identically zero, and, by local unisolvance, $q|_K \equiv 0$. Thus, $q \equiv 0$ on Ω, and so

$$\dim Q \leq V + \left(\frac{k}{2}(k+1) - 3\right) T + E_C - 2V_C. \tag{4.2.4}$$

Now assume that values for each of the degrees of freedom described in the statement of the lemma have been given. For each $K \in \mathcal{T}$, define $q_K \in \mathcal{P}_{k-1}(K)$

by assigning these given values to the local degrees of freedom (4.2.3). Then, the function q defined by the rule $q|_K = q_K$ $\forall K \in \mathcal{T}$ is clearly continuous at noncorner vertices, and so $q \in Q$. Thus, (4.2.4) holds as an equality. $\square$

Lemma 4.2.2. *The velocity space* $\boldsymbol{V}$ *has dimension*

$$\dim \boldsymbol{V} = 2\left[3V + (k-3)E + \frac{1}{2}(k-2)(k-1)T + E_C - 2V_C\right], \tag{4.2.5}$$

and is unisolvent with respect to the following set of global degrees of freedom for $\boldsymbol{v} \in \boldsymbol{V}$*:*

(i) 2 *values of* $\boldsymbol{v}(\boldsymbol{a})$ *at each vertex* $\boldsymbol{a} \in \mathcal{V}$*.*

(ii) 4 *values of* $D^\alpha \boldsymbol{v}(\boldsymbol{a})$*,* $|\alpha| = 1$*, at each noncorner vertex* $\boldsymbol{a} \in \mathcal{V} \setminus \mathcal{V}_C$*.*

(iii) $2|\mathcal{E}_{\boldsymbol{a}}|$ *tangential derivative values at each corner vertex* $\boldsymbol{a} \in \mathcal{V}_C$*:*

$$\partial_{t_i} \boldsymbol{v}|_{\gamma_i}(\boldsymbol{a}), \quad i = 1, \ldots, m, \qquad \partial_{t_0} \boldsymbol{v}_0(\boldsymbol{a}), \quad \textit{and} \quad \partial_{t_{m+1}} \boldsymbol{v}_m(\boldsymbol{a}),$$

with $\boldsymbol{v}_i = \boldsymbol{v}|_{K_i}$*,* $m := |\mathcal{E}_{\boldsymbol{a}}| - 2$*, and* $\hat{\boldsymbol{t}}_i$ *the unit tangent vector of* $\gamma_i \in \mathcal{E}_{\boldsymbol{a}}$ *oriented as in Figure 4.1.*

(iv) $2(k-3)$ *moment degrees of freedom on each edge* $\gamma \in \mathcal{E}$*:*

$$\int_\gamma \boldsymbol{v} \cdot \boldsymbol{r} \; dS \qquad \forall \boldsymbol{r} \in \boldsymbol{\mathcal{P}}_{k-4}(\gamma). \tag{4.2.6}$$

(v) $(k-2)(k-1)$ *interior moment degrees of freedom on each element* $K \in \mathcal{T}$*:*

$$\int_K \boldsymbol{v} \cdot \boldsymbol{r}\, d\boldsymbol{x} \qquad \forall \boldsymbol{r} \in \boldsymbol{\mathcal{P}}_{k-3}(K).$$

Proof. Let $\boldsymbol{v} \in \boldsymbol{V}$. For each $K \in \mathcal{T}$, the local space $\boldsymbol{\mathcal{P}}_k(K)$ may be equipped with $(k+1)(k+2)$ local degrees of freedom (illustrated in Figure 4.4)

$$\begin{aligned} &D^\alpha \boldsymbol{v}(\boldsymbol{a}) && \forall \boldsymbol{a} \in \mathcal{V}_K,\ \forall |\alpha| \le 1, && \int_\gamma \boldsymbol{v} \cdot \boldsymbol{r}\, dS && \forall \boldsymbol{r} \in \boldsymbol{\mathcal{P}}_{k-4}(\gamma),\ \forall \gamma \in \mathcal{E}_K, \\ &\int_K \boldsymbol{v} \cdot \boldsymbol{r}\, d\boldsymbol{x} && \forall r \in \boldsymbol{\mathcal{P}}_{k-3}(K). \end{aligned} \tag{4.2.7}$$

Assume that all of the global degrees corresponding to $\boldsymbol{v}$ vanish. The local degrees of freedom (4.2.7) on each element $K \in \mathcal{T}$ are identically zero, and, by local unisolvance, $\boldsymbol{v}|_K \equiv \boldsymbol{0}$. Thus, $\boldsymbol{v} \equiv \boldsymbol{0}$ on Ω, and so

$$\dim \boldsymbol{V} \le 2\left[3V + (k-3)E + \frac{1}{2}(k-1)(k-2)T + E_C - 2V_C\right]. \tag{4.2.8}$$

Now assume that values for each of the degrees of freedom in the statement of the lemma have been given. For each $K \in \mathcal{T}$, define $\boldsymbol{v}_K \in \boldsymbol{\mathcal{P}}_k(K)$ by assigning these given values to the local degrees of freedom (4.2.7). We claim that the function $\boldsymbol{v}$ defined by the rule $\boldsymbol{v}|_K = \boldsymbol{v}_K$ on each $K \in \mathcal{T}$ satisfies $\boldsymbol{v} \in \boldsymbol{V}$. We clearly have that $\boldsymbol{v}$ is continuous at every vertex and $\boldsymbol{v}$ is C^1 at every non-corner vertex. Let $\mathcal{E} \ni \gamma = K \cap K'$ be given, and define $\boldsymbol{\mathcal{P}}_k(\gamma) \ni \boldsymbol{w} := \boldsymbol{v}|_K - \boldsymbol{v}|_{K'}$ on γ. The degrees of freedom (i-iii) ensure that $\boldsymbol{w}|_{\partial\gamma} = \partial_{t_\gamma}\boldsymbol{w}|_\gamma = 0$, while (iv) gives

$$\int_\gamma \boldsymbol{w}\cdot\boldsymbol{r}\; dS = 0 \qquad \forall \boldsymbol{r} \in \boldsymbol{\mathcal{P}}_{k-4}(\gamma).$$

These $2(k+1)$ linearly independent conditions on $\boldsymbol{w}$ mean that $\boldsymbol{w} = \boldsymbol{0}$. As a result, $\boldsymbol{v}$ is globally continuous, and hence $\boldsymbol{v} \in \boldsymbol{V}$. Thus, (4.2.8) holds as an equality. □

Lemma 4.2.3. *The modified TUBA space Σ has dimension*

$$\dim\Sigma = 6V + (2k-7)E + \frac{1}{2}(k-3)(k-4)T + E_C - 2V_C, \tag{4.2.9}$$

and is unisolvent with respect to the following set of global degrees of freedom for $\phi \in \Sigma$:

(i) 3 values of $D^\alpha\phi(\boldsymbol{a})$, $|\alpha| \le 1$, at each vertex $\boldsymbol{a} \in \mathcal{V}$.

(ii) 3 values of $D^\alpha\phi(\boldsymbol{a})$, $|\alpha| = 2$, at each noncorner vertex $\boldsymbol{a} \in \mathcal{V}\setminus\mathcal{V}_C$.

(iii) $|\mathcal{E}_{\boldsymbol{a}}| + 1$ second derivative values for each corner vertex $\boldsymbol{a} \in \mathcal{V}_C$:

$$\partial_{t_it_i}\phi_i(\boldsymbol{a}),\quad i\in\{1,2,\ldots,m\},\quad \partial_{t_0t_0}\phi_0(\boldsymbol{a}),\quad \partial_{t_0t_1}\phi_0(\boldsymbol{a}),\quad \textit{and}\quad \partial_{t_{m+1}t_{m+1}}\phi_m(\boldsymbol{a}), \tag{4.2.10}$$

with $\phi_i := \phi|_{K_i}$, $m := |\mathcal{E}_{\boldsymbol{a}}| - 2$ and $\hat{\boldsymbol{t}}_i$ the unit tangent vectors of $\gamma_i \in \mathcal{E}_{\boldsymbol{a}}$ oriented as in Figure 4.1.

(iv) $2k-7$ moments degrees of freedom on each edge $\gamma \in \mathcal{E}$:

$$\int_\gamma \phi r \; dS \qquad \forall r \in \mathcal{P}_{k-5}(\gamma) \quad \textit{and} \quad \int_\gamma (\partial_n \phi) r \; dS \qquad \forall r \in \mathcal{P}_{k-4}(\gamma). \quad (4.2.11)$$

(v) $\frac{1}{2}(k-3)(k-4)$ moments degrees of freedom on each element $K \in \mathcal{T}$:

$$\int_K \phi r \; d\boldsymbol{x} \qquad \forall r \in \mathcal{P}_{k-5}(K).$$

Proof. Let $\phi \in \Sigma$. For each $K \in \mathcal{T}$, the local space $\mathcal{P}_{k+1}(K)$ may be equipped with $\frac{1}{2}(k+2)(k+3)$ local degrees of freedom (illustrated in Figure 4.4)

$$\begin{aligned} &D^\alpha \phi(\boldsymbol{a}) && \forall \boldsymbol{a} \in \mathcal{V}_K, \; \forall |\alpha| \leq 2, && \int_\gamma \phi r \; dS && \forall r \in \mathcal{P}_{k-5}(\gamma), \; \forall \gamma \in \mathcal{E}_K, \\ &\int_\gamma (\partial_n \phi) r \; dS && \forall r \in \mathcal{P}_{k-4}(\gamma), \; \forall \gamma \in \mathcal{E}_K, && \int_K \phi r \; d\boldsymbol{x} && \forall r \in \mathcal{P}_{k-5}(K). \end{aligned} \quad (4.2.12)$$

Let $\phi \in \Sigma$ and assume all of the global degrees of freedom corresponding to ϕ vanish. It immediately follows at all of the local degrees of freedom (4.2.12) vanish with the exception of the values of the local hessians $D^2\phi|_K(\boldsymbol{a})$ at each corner vertex $\boldsymbol{a} \in \mathcal{V}_C$. Since $\phi \in C^1(\bar{\Omega})$, the second derivatives of ϕ satisfy the following conditions:

$$\partial_{t_i t_i} \phi|_i(\boldsymbol{a}) = \partial_{t_i t_i} \phi|_{i-1}(\boldsymbol{a}), \qquad 1 \leq i \leq m, \quad (4.2.13a)$$

$$\partial_{t_i n_i} \phi|_i(\boldsymbol{a}) = \partial_{t_i n_i} \phi|_{i-1}(\boldsymbol{a}), \qquad 1 \leq i \leq m, \quad (4.2.13b)$$

where the elements $K_i \in \mathcal{T}_{\boldsymbol{a}}$ are ordered as in Figure 4.1. Expressing the mixed tangential derivatives in terms of the derivatives appearing in (4.2.13) gives the following set of equivalent, but linearly independent conditions

$$\partial_{t_i t_i}\phi_i(\boldsymbol{a}) = \partial_{t_i t_i}\phi_{i-1}(\boldsymbol{a}), \qquad 1 \le i \le m, \tag{4.2.14a}$$

$$\partial_{t_i t_{i+1}}\phi_i(\boldsymbol{a}) = \frac{(\cot\theta_{i-1} + \cot\theta_i)\partial_{t_i t_i}\phi_i(\boldsymbol{a}) - \csc\theta_{i-1}\partial_{t_{i-1} t_i}\phi_{i-1}(\boldsymbol{a})}{\csc\theta_i}, \quad 1 \le i \le m. \tag{4.2.14b}$$

Starting with K_0 and using (4.2.14a), we have $\partial_{t_0 t_0}\phi_0(\boldsymbol{a}) = \partial_{t_0 t_1}\phi_0(\boldsymbol{a}) = \partial_{t_1 t_1}\phi_0(\boldsymbol{a}) = 0$, and so $D^2\phi_0(\boldsymbol{a}) = \mathbf{0}$. Moving to K_1 and using (4.2.14a), we have $\partial_{t_1 t_1}\phi_1(\boldsymbol{a}) = \partial_{t_2 t_2}\phi_1(\boldsymbol{a}) = 0$. The mixed derivative $\partial_{t_1 t_2}\phi_1(\boldsymbol{a})$ also vanishes by (4.2.14b), and so $D^2\phi_1(\boldsymbol{a}) = \mathbf{0}$. We may bootstrap this argument element-by-element to conclude that $D^2\phi_i(\boldsymbol{a}) = 0$ for $0 \le i \le m$. As a result, all of the local degrees of freedom (4.2.12) vanish and so $\phi \equiv 0$ on Ω. Thus,

$$\dim\Sigma \le 6V + (2k-7)E + \frac{1}{2}(k-3)(k-4)T + E_C - 2V_C \tag{4.2.15}$$

Now assume that values for each of the degrees of freedom in the statement of the lemma have been given. For each $K \in \mathcal{T}$, define $\phi_K \in \mathcal{P}_{k+1}(K)$ by assigning these given values to the local degrees of freedom (4.2.12), using the relations (4.2.14) to assign the second order derivatives at corner vertices. We claim that the function ϕ defined by the rule $\phi|_K = \phi_K$ on each $K \in \mathcal{T}$ satisfies $\phi \in \Sigma$. We clearly have that ϕ is C^1 at every vertex and ϕ is C^2 at every non-corner vertex. Let $\mathcal{E} \ni \gamma = K \cap K'$

be given, and define $\mathcal{P}_{k+1}(\gamma) \ni \psi := \phi|_K - \phi|_{K'}$ and $\mathcal{P}_k(\gamma) \ni \rho := \partial_{n_\gamma}\phi|_K - \partial_{n_\gamma}\phi|_{K'}$ on γ. The degrees of freedom (i-iii) and the equivalence between relations (4.2.13) and (4.2.14) ensure that $\partial^j_{t_\gamma}\psi|_{\partial\gamma} = 0$ for $0 \le j \le 2$ and $\partial^l_{t_\gamma}\rho|_{\partial\gamma} = 0$ for $0 \le l \le 1$, while (iv) gives

$$\int_\gamma \psi r \; dS = 0 \qquad \forall r \in \mathcal{P}_{k-5}(\gamma) \quad \text{and} \quad \int_\gamma \rho s \; dS = 0 \qquad \forall s \in \mathcal{P}_{k-4}(\gamma).$$

These $k+2$ linearly independent conditions on ψ and $k+1$ linearly independent conditions on ρ mean that $\psi \equiv \rho \equiv 0$. As a result, ϕ is globally C^1, and hence $\phi \in \Sigma$. Thus, (4.2.15) holds as an equality. $\square$

Figure 4.3: Types of singular corner vertices

Lemmas 4.2.1 to 4.2.3 characterize the global FEM spaces Q, $\boldsymbol{V}$, and Σ. The corresponding spaces satisfying homogeneous essential boundary conditions are defined by:

$$\Sigma_0 := \Sigma \cap H^2_0(\Omega), \quad \boldsymbol{V}_0 := \boldsymbol{V} \cap \boldsymbol{H}^1_0(\Omega), \quad \text{and} \quad Q_0 := Q \cap L^2_0(\Omega), \tag{4.2.16}$$

and are identical to the corresponding spaces proposed in [50]. However, it is worth noting that the spaces without boundary conditions differ from these considered in [50]. In order to count the dimension of the modified TUBA space, we recall the notion of a *singular corner vertex*, as defined in [83, 100, 113]. A corner vertex $\boldsymbol{a} \in \mathcal{V}_C$ is *singular* if all element edges meeting at $\boldsymbol{a}$ fall on two straight lines, or, equally well, if $\theta_i + \theta_{i+1} = \pi$ for $0 \leq i \leq |\mathcal{T}_{\boldsymbol{a}}| - 2$, using the notation in Figure 4.1; otherwise, the $\boldsymbol{a}$ is *nonsingular*. The two cases are illustrated in Figure 4.3. Let $\mathcal{V}_C^S$ denote the set of singular corner vertices with $V_C^S := |\mathcal{V}_C^S|$. It is now a simple matter to count the dimensions of the spaces (4.2.16):

Lemma 4.2.4. *The dimension of the boundary condition spaces is as follows:*

$$\dim Q_0 = \dim Q - 1 = V + \frac{1}{2}(k-2)(k+3)T - 1 + E_C - 2V_C, \tag{4.2.17}$$

$$\dim \boldsymbol{V}_0 = 2\left(3V_I + (k-3)E_I + \frac{1}{2}(k-1)(k-2)T + V_B + E_C - 2V_C\right), \tag{4.2.18}$$

$$\dim \Sigma_0 = 6V_I + (2k-7)E_I + \frac{1}{2}(k-4)(k-3)T + V_B + E_C - 3V_C + V_C^S. \tag{4.2.19}$$

Proof. (4.2.17) follows on noting that the single constraint is that $\int_\Omega q \; d\boldsymbol{x} = 0$ for $q \in Q_0$.

Now let $\boldsymbol{v} \in \boldsymbol{V}_0$. Clearly all of the edge moments (4.2.6) must vanish for boundary edges. Moreover, at noncorner boundary vertices $\boldsymbol{a} \in \mathcal{V}_B$, $\partial_t \boldsymbol{v}(\boldsymbol{a}) = \boldsymbol{0}$, while $\partial_n \boldsymbol{v}(\boldsymbol{a})$ is unconstrained, where $\hat{\boldsymbol{t}}$ and $\hat{\boldsymbol{n}}$ are the unit tangent and normal vectors on Γ at $\boldsymbol{a}$. For corner vertices $\boldsymbol{a} \in \mathcal{V}_C$, $\boldsymbol{v}(\boldsymbol{a}) = \boldsymbol{0}$ and $\partial_{t_0} \boldsymbol{v}_0(\boldsymbol{a}) = \partial_{t_{m+1}} \boldsymbol{v}_m(\boldsymbol{a}) = \boldsymbol{0}$ using the notation in Figure 4.1. Thus, $|\mathcal{E}_{\boldsymbol{a}}| - 2$ degrees of freedom are unconstrained per corner vertex. (4.2.18) immediately follows.

Let $\phi \in \Sigma_0$. Then, on each boundary edge γ, $\phi = \partial_n \phi = 0$, and so all moment degrees of freedom on γ (4.2.11) must vanish. For a noncorner boundary vertex $\boldsymbol{a}$, $\phi(\boldsymbol{a}) = \partial_t \phi(\boldsymbol{a}) = \partial_n \phi(\boldsymbol{a}) = \partial_{tt} \phi(\boldsymbol{a}) = \partial_{tn} \phi(\boldsymbol{a}) = 0$ where $\hat{\boldsymbol{t}}$ and $\hat{\boldsymbol{n}}$ are the unit tangent and normal vectors along the boundary Γ at $\boldsymbol{a}$. The only unconstrained vertex degree of freedom is $\partial_{nn}\phi(\boldsymbol{a})$. For a corner vertex $\boldsymbol{a} \in \mathcal{V}_C$, there holds $\phi(\boldsymbol{a}) = 0$, and $\nabla \phi(\boldsymbol{a}) = \mathbf{0}$. Using the notation in Figure 4.1 and Lemma 4.2.3,

$$
\begin{aligned}
0 &= \partial_{t_0 t_0} \phi_0(\boldsymbol{a}) = \partial_{t_{m+1} t_{m+1}} \phi_m(\boldsymbol{a}), \\
0 &= \left(\partial_{t_0 t_0} \phi_0(\boldsymbol{a}) \hat{\boldsymbol{t}}_0 + \partial_{t_0 n_0} \phi_0(\boldsymbol{a}) \hat{\boldsymbol{n}}_0\right) \cdot \hat{\boldsymbol{t}}_1 = \partial_{t_0 t_1} \phi_0(\boldsymbol{a}), \\
0 &= \left(\partial_{t_{m+1} t_{m+1}} \phi_m(\boldsymbol{a}) \hat{\boldsymbol{t}}_{m+1} + \partial_{t_{m+1} n_{m+1}} \phi_m(\boldsymbol{a}) \hat{\boldsymbol{n}}_{m+1}\right) \cdot \hat{\boldsymbol{t}}_m = \partial_{t_m t_{m+1}} \phi_m(\boldsymbol{a}),
\end{aligned}
$$

where $m = |\mathcal{E}_{\boldsymbol{a}}| - 2$. By summing (4.2.14b) over $i \in \{1, \ldots, m\}$, we rewrite the last constraint in terms of the the degrees of freedom (4.2.10):

$$
0 = \sum_{i=1}^{m} (-1)^i [\cot \theta_{i-1} + \cot \theta_i] \partial_{t_i t_i} \phi_i(\boldsymbol{a}). \tag{4.2.20}
$$

Since $\cot \theta_{i-1} + \cot \theta_i = 0$ for all $1 \leq i \leq m$ if and only if $\theta_{i-1} + \theta_i = \pi$ for all $1 \leq i \leq m$, the constraint (4.2.20) is automatically satisfied if $\boldsymbol{a} \in \mathcal{V}_C^S$ but is nontrivial for $\boldsymbol{a} \in \mathcal{V}_C \setminus \mathcal{V}_C^S$. Thus, there are 3 constraints for every $\boldsymbol{a} \in \mathcal{V}_C^S$ and 4 constraints for every $\boldsymbol{a} \in \mathcal{V}_C \setminus \mathcal{V}_C^S$. (4.2.19) follows immediately. $\square$

Observe that, contrary to the usual practice, we have chosen to define the spaces directly in terms of *global degrees of freedom* since the degrees of freedom at element vertices differ according to the location of the vertex relative to the boundary of the (global) domain Ω. Nevertheless, one could also work with the local degrees of freedom for the finite element spaces as illustrated in Figure 4.4. In fact, one can [50] construct global finite element spaces by piecing together the elements in Figure 4.4 in the usual way [38, §2], where the resulting spaces have the same degree of continuity at every vertex. However, if the corresponding homogeneous spaces were to be defined by taking the intersections with the spaces $H_0^2(\Omega)$, $\boldsymbol{H}_0^1(\Omega)$, and $L_0^2(\Omega)$, similarly to (4.2.16), then the exact sequence property would *not* hold since the divergence of the velocity space is a *proper subset* of the pressure space. Further details will be found in [50, §3.2].

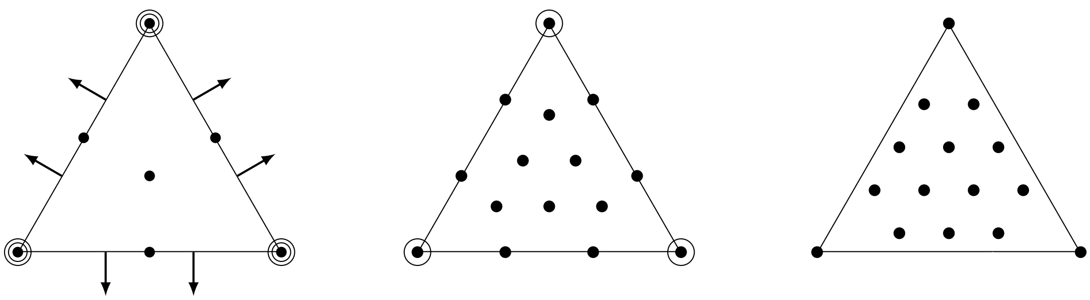

(a) Σ (b) $\boldsymbol{V}$ (c) Q

Figure 4.4: Local degrees of freedom for the finite element spaces in the case $k = 5$.

4.2.2 Exact Sequence Properties

We now establish necessary and sufficient conditions under which the spaces defined above give exact sequences. The unconstrained case is simple.

Lemma 4.2.5. *The following sequence is exact:*

$$\mathbb{R} \xrightarrow{\ \subset\ } \Sigma \xrightarrow{\ \mathbf{curl}\ } \boldsymbol{V} \xrightarrow{\ \mathrm{div}\ } Q \longrightarrow 0. \tag{4.2.21}$$

Proof. The inclusions $\mathbf{curl}\,\Sigma \subset \boldsymbol{V}$, $\mathrm{div}\,\boldsymbol{V} \subset Q$, and $\mathbf{curl}\,\Sigma \subset \mathrm{Ker}\,\mathrm{div}$ follow by definition. Here, we consider div as a linear operator $\boldsymbol{V} \to Q$. Moreover, $\mathbf{curl}\,\phi = \mathbf{0}$ if and only if $\phi \in \mathbb{R}$ and so $\dim \mathbf{curl}\,\Sigma = \dim \Sigma - 1$. Using the dimension counts (4.2.2), (4.2.5) and (4.2.9) and the relation $V + T - E = 1$ reveals that

$$\dim \Sigma + \dim Q = \dim \boldsymbol{V} + V + T - E = \dim \boldsymbol{V} + 1.$$

Moreover, by the rank-nullity theorem, we have

$$\dim \boldsymbol{V} = \dim \mathrm{Im}\,\mathrm{div} + \dim \mathrm{Ker}\,\mathrm{div} \geq \dim Q + \dim \Sigma - 1 = \dim \boldsymbol{V},$$

and so $\mathrm{Im}\,\mathrm{div} = Q$ and $\mathrm{Ker}\,\mathrm{div} = \mathbf{curl}\,\Sigma$. Thus, the sequence (4.2.21) is exact. $\square$

Lemma 4.2.5 deals with the unconstrained spaces. However, the situation regarding the spaces with homogeneous boundary conditions is less straightforward. An indication of the difficulties is provided by noting that (using the same arguments as in Lemma 4.2.5) the sequence

$$0 \xrightarrow{\ \subset\ } \Sigma_0 \xrightarrow{\ \mathbf{curl}\ } \boldsymbol{V}_0 \xrightarrow{\ \mathrm{div}\ } Q_0 \longrightarrow 0. \tag{4.2.22}$$

is exact if and only if

$$\dim \Sigma_0 + \dim Q_0 - \dim \boldsymbol{V}_0 = 0. \tag{4.2.23}$$

Using Lemma 4.2.4 gives

$$\dim \Sigma_0 + \dim Q_0 - \dim \boldsymbol{V}_0 = V - V_B - V_C - E_I + T - 1 + V_C^S$$

and then, since $E_I = E - V + V_I = E - V_B - V_C$ and $V + T - E = 1$, we arrive at

$$\dim \Sigma_0 + \dim Q_0 - \dim \boldsymbol{V}_0 = V_C^S. \tag{4.2.24}$$

In view of (4.2.23) and (4.2.24), the sequence (4.2.22) is exact if and only if

$$V_C^S = 0. \tag{4.2.25}$$

The condition $V_C^S = 0$ appears in the stability of the Taylor Hood elements [30]. Condition (4.2.25) means that there are at least two elements attached to every corner vertex of the polygonal domain Ω, and if $\boldsymbol{a} \in \mathcal{V}_C$ coincides with a re-entrant corner of the domain and $|\mathcal{T}_{\boldsymbol{a}}| = 3$, then the elements are *not* configured as in Figure 4.3b. A mesh $\mathcal{T}$ having this property is said to be *corner-split*. The above discussion leads to the following result:

Theorem 4.2.6. *The sequence*

$$0 \xrightarrow{\subset} \Sigma_0 \xrightarrow{\mathbf{curl}} \boldsymbol{V}_0 \xrightarrow{\text{div}} Q_0 \longrightarrow 0$$

is exact if and only if the mesh is corner-split.

In light of Theorem 4.2.6, we will henceforth assume *the mesh $\mathcal{T}$ is corner-split.*

4.3 Uniform Stability of Elements

One of the main results of [50] is that the pair $\boldsymbol{V}_0 \times Q_0$ satisfies the inf-sup condition (4.1.7) with a constant uniformly bounded below in h for each fixed polynomial degree $k \in \mathbb{N}$ [50, Lemma 3.3]. However, if one wishes to use high order approximation schemes, such as the p-version of the finite element method, then one would like to understand the dependence of the inf-sup constant $\beta(h,k)$ on the polynomial order k. For instance the bound $\beta(h,k) \geq Ck^{-r}$ for some $r > 7$ follows from [113, Lemma 2.5], which (if this estimate were to be sharp) would mean that the stability of the associated mixed scheme is rather sensitive to the order k. In particular, it would lead to an a priori error bound for the scheme which is suboptimal by at least $r > 7$ orders in k.

Our main theorem establishes that, in fact, $\beta(h,k)$ is bounded below *indepen-*

dently of the polynomial order. An important quantity that appears in the stability estimates is the following measure of how close a corner vertex is to being singular:

$$\xi(\boldsymbol{a}) := \max_{0 \le i \le |\mathcal{T}_{\boldsymbol{a}}|-2} |\sin(\theta_i + \theta_{i+1})|, \qquad \boldsymbol{a} \in \mathcal{V}_C, \tag{4.3.1}$$

using the notation in Figure 4.1. In particular, if $\boldsymbol{a}$ is a singular vertex, then $\xi(\boldsymbol{a}) = 0$. Likewise, the quantity

$$\xi(\mathcal{T}) := \min_{\boldsymbol{a} \in \mathcal{V}_C} \xi(\boldsymbol{a}) \tag{4.3.2}$$

measures how close the mesh is to containing singular corner nodes. Note that on a corner-split mesh, $\xi(\boldsymbol{a}) > 0$ for all $\boldsymbol{a} \in \mathcal{V}_C$ since there exists at least one pair of consecutive angles satisfying $\theta_i + \theta_{i+1} \neq \pi$. The key result, proved at the end of this section, reads as follows:

Theorem 4.3.1. *If the mesh $\mathcal{T}$ is corner-split, then for every $q \in Q$ there exists $\boldsymbol{v} \in \boldsymbol{V}$ with*

$$\operatorname{div} \boldsymbol{v} = q \quad \text{in } \Omega \qquad \text{and} \qquad \|\boldsymbol{v}\|_{\boldsymbol{H}^1(\Omega)} \le C\xi(\mathcal{T})^{-1}\|q\|_{L^2(\Omega)}, \tag{4.3.3}$$

where C is independent of k, h, and q. Moreover, if $q \in Q_0$, then there exists $\boldsymbol{v} \in \boldsymbol{V}_0$ satisfying (4.3.3).

Theorem 4.3.1 shows that there exists a right inverse of the divergence operator on the space Q whose continuity is independent of both h and k. An immediate consequence of Theorem 4.3.1 is the following uniform bound on the discrete inf-sup condition for the associated mixed scheme:

Corollary 4.3.2. *If the mesh $\mathcal{T}$ is corner-split, then the spaces $\boldsymbol{V} \times Q$ and $\boldsymbol{V}_0 \times Q_0$ are uniformly inf-sup stable in h and k. That is, there exist positive constants $\beta > 0$ and $\beta_0 > 0$ independent of both h and k such that*

$$\sup_{\mathbf{0} \neq \boldsymbol{v} \in \boldsymbol{V}} \frac{b(\boldsymbol{v}, q)}{\|\boldsymbol{v}\|_{\boldsymbol{H}^1(\Omega)}} \geq \beta \xi(\mathcal{T}) \|q\|_{L^2(\Omega)} \qquad \forall q \in Q, \tag{4.3.4a}$$

$$\sup_{\mathbf{0} \neq \boldsymbol{v} \in \boldsymbol{V}_0} \frac{b(\boldsymbol{v}, q_0)}{\|\boldsymbol{v}\|_{\boldsymbol{H}^1(\Omega)}} \geq \beta_0 \xi(\mathcal{T}) \|q_0\|_{L^2(\Omega)} \qquad \forall q_0 \in Q_0. \tag{4.3.4b}$$

Proof. Let $q \in Q$ (respectively $q \in Q_0$). By Theorem 4.3.1, there exists $\boldsymbol{u} \in \boldsymbol{V}$ (respectively $\boldsymbol{u} \in \boldsymbol{V}_0$) such that $\operatorname{div} \boldsymbol{u} = -q$ in Ω and $\|\boldsymbol{u}\|_{\boldsymbol{H}^1(\Omega)} \leq C\|q\|_{L^2(\Omega)}$. Hence,

$$\frac{b(\boldsymbol{u}, q)}{\|\boldsymbol{u}\|_{\boldsymbol{H}^1(\Omega)}} = \frac{\|q\|^2_{L^2(\Omega)}}{\|\boldsymbol{u}\|_{\boldsymbol{H}^1(\Omega)}} \geq \frac{\xi(\mathcal{T})}{C} \|q\|_{L^2(\Omega)},$$

and (4.3.4) follows after taking the supremum over $\boldsymbol{v} \in \boldsymbol{V}$ (respectively $\boldsymbol{v} \in \boldsymbol{V}_0$). □

Remark 4.3.3. Corollary 4.3.2 fails to hold for the spaces $\boldsymbol{V}_0 \times Q_0$ on meshes which are not corner-split. For example, consider the case where the domain is a triangle $\Omega = K$ (see Figure 4.5a) where the mesh $\mathcal{T}$ consists of a single element K. In this case, $\boldsymbol{V}_0 = \boldsymbol{\mathcal{P}}_k(K) \cap \boldsymbol{H}^1_0(K)$ and, in particular, the divergence of a function $\boldsymbol{v} \in \boldsymbol{V}_0$ automatically vanishes at the vertices of K. This means that the image of $\boldsymbol{V}_0$ under the divergence operator is a strict proper subset of Q_0:

$$\operatorname{div} \boldsymbol{V}_0 \subseteq \left\{ q \in \mathcal{P}_{k-1}(K) \cap L^2_0(K) : q(\boldsymbol{a}) = 0 \ \forall \boldsymbol{a} \in \mathcal{V}_K \right\} \subsetneq Q_0$$

since the value of $q \in Q_0$ at corner vertices $q(\boldsymbol{a})$, $\boldsymbol{a} \in \mathcal{V}_K$, need not necessarily vanish. Thus, the orthogonal complement

$$(\operatorname{div} \boldsymbol{V}_0)^{\perp} = \{q \in Q_0 : (q, \operatorname{div} \boldsymbol{v}) = 0 \ \forall \boldsymbol{v} \in \boldsymbol{V}_0\}$$

is nonempty. In particular, there exists a nonzero $q \in (\operatorname{div} \boldsymbol{V}_0)^{\perp}$, $b(\boldsymbol{v}, q) = 0 \ \forall \boldsymbol{v} \in \boldsymbol{V}_0$, and so the inf-sup constant for the spaces $\boldsymbol{V}_0 \times Q_0$ is identically zero for all k.

4.3.1 Right Inverse of the Divergence Operator on a Single Element

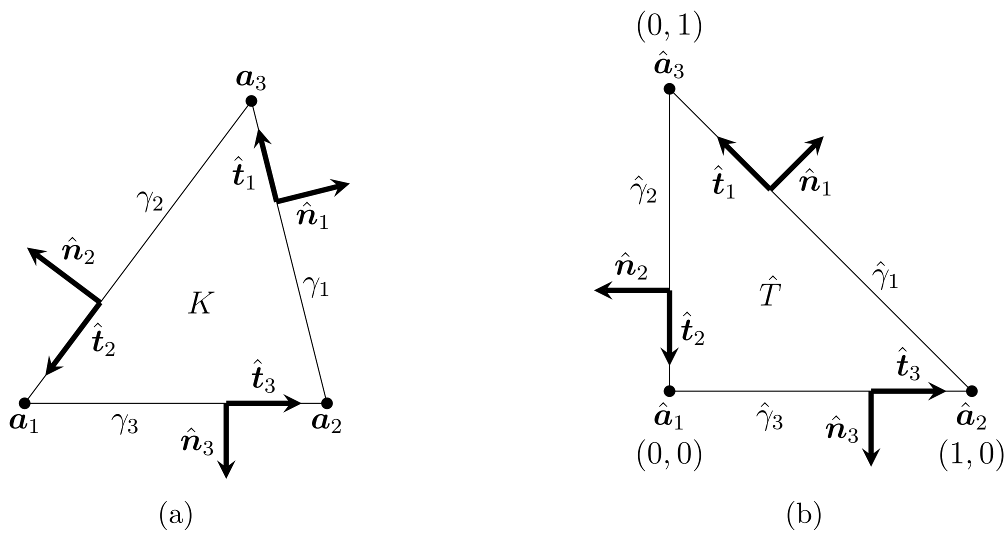

Figure 4.5: Scheme for (a) general triangle K and (b) reference triangle $\hat{T}$.

Let $K \in \mathcal{T}$ be labeled as in Figure 4.5a with diameter h_K and define local finite element spaces as follows:

$$\boldsymbol{V}_0(K) := \boldsymbol{\mathcal{P}}_k(K) \cap \boldsymbol{H}_0^1(K)$$
$$Q_0(K) := \left\{ q \in \mathcal{P}_{k-1}(K) \cap L_0^2(K) : q(\boldsymbol{a}) = 0,\ \boldsymbol{a} \in \mathcal{V}_K \right\}.$$

The following analog of Theorem 4.3.1 holds in the case of a single element:

Theorem 4.3.4. *Let $q \in Q_0(K)$. Then, there exists $\boldsymbol{v} \in \boldsymbol{V}_0(K)$ satisfying* $\operatorname{div} \boldsymbol{v} = q$ *in K, and*

$$h_K^{-1} \|\boldsymbol{v}\|_{\boldsymbol{L}^2(K)} + |\boldsymbol{v}|_{\boldsymbol{H}^1(K)} \leq C \|q\|_{L^2(K)}, \tag{4.3.5}$$

where C is independent of k, h_K, and q.

The proof of Theorem 4.3.4 is postponed until later in this section. However, an immediate consequence of Theorem 4.3.4 is the following analogue of Corollary 4.3.2:

Corollary 4.3.5. *The spaces $\boldsymbol{V}_0(K) \times Q_0(K)$ are uniformly inf-sup stable in k: For all $q \in Q_0(K)$,*

$$\sup_{\boldsymbol{0} \neq \boldsymbol{v} \in \boldsymbol{V}_0(K)} \frac{b(\boldsymbol{v}, q)}{\|\boldsymbol{v}\|_{\boldsymbol{H}^1(K)}} \geq \beta_0 \|q\|_{L^2(K)} \tag{4.3.6}$$

where β_0 is independent of k, h_K, and q.

In order to prove Theorem 4.3.4, we need the following result concerning the extension of certain polynomial vector fields on a reference element $\hat{T}$ (see Figure 4.5b):

Lemma 4.3.6. *Let* $\boldsymbol{u} \in \boldsymbol{\mathcal{P}}_k(\hat{T}) : \operatorname{div} \boldsymbol{u} \in Q_0(\hat{T})$. *Then, there exists* $\psi \in \mathcal{P}_{k+1}(\hat{T})$ *such that*

$$\mathbf{curl}\, \psi|_{\partial \hat{T}} = \boldsymbol{u}|_{\partial \hat{T}} \qquad \textit{and} \qquad \|\psi\|_{H^2(\hat{T})} \leq C \|\boldsymbol{u}\|_{\boldsymbol{H}^1(\hat{T})},$$

where C *is independent of* k *and* $\boldsymbol{u}$.

Proof. The condition $\mathbf{curl}\, \psi|_{\partial \hat{T}} = \boldsymbol{u}|_{\partial \hat{T}}$ holds provided $\psi = f$ and $\partial_n \psi = g$ on $\partial \hat{T}$, where f and g are defined by

$$f(t) := \int_0^t \boldsymbol{u} \cdot \hat{\boldsymbol{n}}\, dS \qquad \text{and} \qquad g(t) := -\boldsymbol{u}(t) \cdot \hat{\boldsymbol{t}},$$

and t is a parametrization of $\partial \hat{T}$. These functions satisfy the following *compatibility* conditions:

1. Since $\int_{\partial \hat{T}} \boldsymbol{u} \cdot \hat{\boldsymbol{n}}\, dS = \int_{\hat{T}} \operatorname{div} \boldsymbol{u}\, d\boldsymbol{x} = 0$ by hypothesis, f is continuous on $\partial \hat{T}$.

2. Since $\partial_t f = \boldsymbol{u} \cdot \hat{\boldsymbol{n}}$ on $\partial \hat{T}$, we have

$$\boldsymbol{u} = (\boldsymbol{u} \cdot \hat{\boldsymbol{t}})\hat{\boldsymbol{t}} + (\boldsymbol{u} \cdot \hat{\boldsymbol{n}})\hat{\boldsymbol{n}} = \partial_t f \hat{\boldsymbol{n}} - g\hat{\boldsymbol{t}} \quad \text{on } \partial \hat{T}.$$

Hence $\partial_t f \hat{\boldsymbol{n}} - g\hat{\boldsymbol{t}}$ is continuous at the element vertices since $\boldsymbol{u} \in \boldsymbol{\mathcal{P}}_k(\hat{T})$.

3. Let f_i and g_i denote the restrictions of f and g to $\hat{\gamma}_i$. From 2. we have

$$\left[\partial_{tt} f_{i+1}(\hat{\boldsymbol{a}}_i)\hat{\boldsymbol{t}}_{i+1} + \partial_t g_{i+1}(\hat{\boldsymbol{a}}_i)\hat{\boldsymbol{n}}_{i+1}\right] \cdot \hat{\boldsymbol{t}}_{i+2} = \partial_{t_{i+1}} \boldsymbol{u}^{\perp}(\hat{\boldsymbol{a}}_i) \cdot \hat{\boldsymbol{t}}_{i+2} = \partial_{t_{i+1}} \boldsymbol{u}(\hat{\boldsymbol{a}}_i) \cdot \hat{\boldsymbol{n}}_{i+2} \tag{4.3.7}$$

and similarly,

$$\left[\partial_{tt} f_{i+2}(\hat{\boldsymbol{a}}_i)\hat{\boldsymbol{t}}_{i+2} + \partial_t g_{i+2}(\hat{\boldsymbol{a}}_i)\hat{\boldsymbol{n}}_{i+2}\right] \cdot \hat{\boldsymbol{t}}_{i+1} = \partial_{t_{i+2}} \boldsymbol{u}(\hat{\boldsymbol{a}}_i) \cdot \hat{\boldsymbol{n}}_{i+1}. \tag{4.3.8}$$

Since $\hat{\boldsymbol{n}}_{i+1}$ and $\hat{\boldsymbol{n}}_{i+2}$ are linearly independent, we may write

$$\boldsymbol{u} = \alpha_{i+1}\hat{\boldsymbol{n}}_{i+1} + \alpha_{i+2}\hat{\boldsymbol{n}}_{i+2},$$

where the scalars $\alpha_{i+1}, \alpha_{i+2}$ can be determined by taking dot products with $\hat{\boldsymbol{t}}_{i+1}$ an $\hat{\boldsymbol{t}}_{i+2}$, and simplifying to arrive at

$$\boldsymbol{u} = (\hat{\boldsymbol{t}}_{i+1} \cdot \hat{\boldsymbol{n}}_{i+2})^{-1} \left[(\boldsymbol{u} \cdot \hat{\boldsymbol{t}}_{i+1})\hat{\boldsymbol{n}}_{i+2} - (\boldsymbol{u} \cdot \hat{\boldsymbol{t}}_{i+2})\hat{\boldsymbol{n}}_{i+1})\right].$$

Thus, we have the identity

$$\operatorname{div} \boldsymbol{u} = (\hat{\boldsymbol{t}}_{i+1} \cdot \hat{\boldsymbol{n}}_{i+2})^{-1} \left[\partial_{t_{i+1}} \boldsymbol{u} \cdot \hat{\boldsymbol{n}}_{i+2} - \partial_{t_{i+2}} \boldsymbol{u} \cdot \hat{\boldsymbol{n}}_{i+1}\right], \tag{4.3.9}$$

and recalling that $\operatorname{div} \boldsymbol{u} \in Q_0(\hat{T})$, so that $\operatorname{div} \boldsymbol{u}(\hat{\boldsymbol{a}}_i) = 0$, we have

$$\partial_{t_{i+1}} \boldsymbol{u}(\hat{\boldsymbol{a}}_i) \cdot \hat{\boldsymbol{n}}_{i+2} - \partial_{t_{i+2}} \boldsymbol{u}(\hat{\boldsymbol{a}}_i) \cdot \hat{\boldsymbol{n}}_{i+1} = 0,$$

which combined with (4.3.7) and (4.3.8) means that the compatibility condition

$$\left[\partial_{tt} f_{i+1}(\hat{\boldsymbol{a}}_i)\hat{\boldsymbol{t}}_{i+1} + \partial_t g_{i+1}(\hat{\boldsymbol{a}}_i)\hat{\boldsymbol{n}}_{i+1}\right] \cdot \hat{\boldsymbol{t}}_{i+2} = \left[\partial_{tt} f_{i+2}(\hat{\boldsymbol{a}}_i)\hat{\boldsymbol{t}}_{i+2} + \partial_t g_{i+2}(\hat{\boldsymbol{a}}_i)\hat{\boldsymbol{n}}_{i+2}\right] \cdot \hat{\boldsymbol{t}}_{i+1}$$

is satisfied.

Since f and g enjoy the above properties, Corollary 2.2.3 shows that there exists a polynomial $\psi \in \mathcal{P}_{k+1}(\hat{T})$ satisfying $\psi = f$ and $\partial_n \psi = g$ on $\partial \hat{T}$ and, in addition,

$$\|\psi\|_{H^2(\hat{T})} \leq C \left(\|f\|_{L^2(\partial \hat{T})} + \|\partial_t f \hat{\boldsymbol{n}} - g \hat{\boldsymbol{t}}\|_{\boldsymbol{H}^{1/2}(\partial \hat{T})} \right).$$

Noting that $\partial_t f \hat{\boldsymbol{n}} - g\hat{\boldsymbol{t}} = \boldsymbol{u}$ on $\partial \hat{T}$ and applying the trace theorem then gives

$$\|\psi\|_{H^2(\hat{T})} \leq C \left(\|\boldsymbol{u} \cdot \hat{\boldsymbol{n}}\|_{L^2(\partial \hat{T})} + \|\boldsymbol{u}\|_{\boldsymbol{H}^{1/2}(\partial \hat{T})} \right) \leq C \|\boldsymbol{u}\|_{\boldsymbol{H}^1(\hat{T})}$$

and the result follows. $\square$

A result similar to Lemma 4.3.6 is proved in [73, Theorem 3.1], but the extension constructed therein need *not* satisfy the condition $\mathbf{curl}\, \psi \cdot \hat{\boldsymbol{t}} = \boldsymbol{u} \cdot \hat{\boldsymbol{t}}$ on $\partial \hat{T}$, and, as such, is unsuitable for our current purposes. We now prove Theorem 4.3.4.

Proof of Theorem 4.3.4. We start with the case where K is the reference element $\hat{T}$

(see Figure 4.5b). Let $q \in Q_0(\hat{T})$ be given and define

$$\boldsymbol{v}_0(\boldsymbol{x}) := -\int_{\hat{T}} \theta(\boldsymbol{y})\boldsymbol{L}_y(q)(\boldsymbol{x})\ d\boldsymbol{y}, \quad \boldsymbol{x} \in \hat{T},$$

where $\theta \in C_c^\infty(\hat{T})$ is any smooth function with compact support on $\hat{T}$ satisfying $\int_{\hat{T}} \theta\ d\boldsymbol{x} = 1$, and $\boldsymbol{L}_y : \mathcal{P}_{k-1}(\hat{T}) \to \boldsymbol{\mathcal{P}}_k(\hat{T})$ is the Poincaré operator defined by

$$\boldsymbol{L}_y(q)(\boldsymbol{x}) := (\boldsymbol{x} - \boldsymbol{y}) \int_0^1 tq(\boldsymbol{y} + t(\boldsymbol{x} - \boldsymbol{y}))\ dt, \quad \boldsymbol{x} \in \hat{T}.$$

By [39, Corollary 3.4]

$$\operatorname{div} \boldsymbol{v}_0 = q \qquad \text{and} \qquad \|\boldsymbol{v}_0\|_{\boldsymbol{H}^1(\hat{T})} \le C\|q\|_{L^2(\hat{T})}. \tag{4.3.10}$$

Clearly $\boldsymbol{L}_y(q)$ is a polynomial of degree k in $\boldsymbol{x}$ and, as a result, $\boldsymbol{v}_0 \in \boldsymbol{V}_0^k(\hat{T})$, $\operatorname{div} \boldsymbol{v}_0 \in Q_0^k(\hat{T})$ and, thanks to Lemma 4.3.6, there exists $\psi \in \mathcal{P}_{k+1}(\hat{T})$ such that

$$\mathbf{curl}\, \psi|_{\partial \hat{T}} = \boldsymbol{v}_0 \qquad \text{and} \qquad \|\psi\|_{H^2(\hat{T})} \le C\|\boldsymbol{v}_0\|_{\boldsymbol{H}^1(\hat{T})} \le C\|q\|_{L^2(\hat{T})}.$$

Let $\boldsymbol{v} := \boldsymbol{v}_0 - \mathbf{curl}\, \psi \in \boldsymbol{\mathcal{P}}_k(\hat{T})$. Then, $\operatorname{div} \boldsymbol{v} = \operatorname{div} \boldsymbol{v}_0 = q$ and $\boldsymbol{v}|_{\partial \hat{T}} = (\boldsymbol{v}_0 - \mathbf{curl}\, \psi)|_{\partial \hat{T}} = \mathbf{0}$ so that $\boldsymbol{v} \in \boldsymbol{V}_0(\hat{T})$, and

$$\|\boldsymbol{v}\|_{\boldsymbol{H}^1(\hat{T})} \le C\|\boldsymbol{v}_0\|_{\boldsymbol{H}^1(\hat{T})} + \|\psi\|_{H^2(\hat{T})} \le C\|q\|_{L^2(\hat{T})},$$

which completes the proof in the case of the reference element.

We extend the result to a general triangle K via the Piola transformation as follows. Let $\boldsymbol{F}_K : \hat{T} \to K$ be an affine, invertible, transformation such that $\boldsymbol{F}_K(\hat{T}) = K$ and define $\hat{q} : \hat{T} \to \mathbb{R}$ by $\hat{q} := |D\boldsymbol{F}_K| q \circ \boldsymbol{F}_K$ where $|D\boldsymbol{F}_K|$ denotes the determinant of the Jacobian of $\boldsymbol{F}_K$. Then, $\hat{q} \in Q_0(\hat{T})$, $\|\hat{q}\|_{L^2(\hat{T})} \leq Ch_K \|q\|_{L^2(K)}$, and (as above) there exists $\hat{\boldsymbol{v}} \in \boldsymbol{V}_0(\hat{T})$ satisfying

$$\operatorname{div} \hat{\boldsymbol{v}} = \hat{q} \qquad \text{and} \qquad \|\hat{\boldsymbol{v}}\|_{\boldsymbol{H}^1(\hat{T})} \leq C \|\hat{q}\|_{L^2(\hat{T})}.$$

Now, let $\boldsymbol{v} := |D\boldsymbol{F}_K|^{-1} (D\boldsymbol{F}_K \hat{\boldsymbol{v}}) \circ \boldsymbol{F}_K^{-1}$ be the Piola transform [29, p.59-60] of $\hat{\boldsymbol{v}}$ so that

$$\|\boldsymbol{v}\|_{\boldsymbol{L}^2(K)} \leq C \|\hat{\boldsymbol{v}}\|_{\boldsymbol{L}^2(\hat{T})}, \qquad |\boldsymbol{v}|_{\boldsymbol{H}^1(K)} \leq Ch_K^{-1} |\hat{\boldsymbol{v}}|_{\boldsymbol{H}^1(\hat{T})},$$

and $\operatorname{div} \boldsymbol{v} = |D\boldsymbol{F}_K|^{-1} \operatorname{div} \hat{\boldsymbol{v}} = |D\boldsymbol{F}_K|^{-1} \hat{q} = q$. Then,

$$h_K^{-1} \|\boldsymbol{v}\|_{\boldsymbol{L}^2(K)} + |\boldsymbol{v}|_{\boldsymbol{H}^1(K)} \leq Ch_K^{-1} \|\hat{\boldsymbol{v}}\|_{\boldsymbol{H}^1(\hat{T})} \leq Ch_K^{-1} \|\hat{q}\|_{L^2(\hat{T})} \leq C \|q\|_{L^2(K)}$$

which gives the result claimed. $\square$

4.3.2 Extension to a Corner-Split Mesh

The next step towards proving Theorem 4.3.1 is to extend the single element result Theorem 4.3.4 to a corner-split mesh. We begin with an auxiliary lemma which establishes the existence of a polynomial from $\boldsymbol{V}_0$ with certain properties. The idea stems from a similar construction used in the proof of [50, Lemma 3.1 and Lemma 3.3]; the construction presented below, while more intricate than the one presented in [50], is shown to be uniformly bounded in the polynomial degree k:

Lemma 4.3.7. *Suppose that $\mathcal{T}$ is corner-split and let $q \in Q$. Then, there exists $\boldsymbol{v}_h \in \boldsymbol{V}$ satisfying*

$$\operatorname{div} \boldsymbol{v}_h(\boldsymbol{a}) = q(\boldsymbol{a}) \qquad \forall \boldsymbol{a} \in \mathcal{V}, \tag{4.3.11a}$$

$$\int_K \operatorname{div} \boldsymbol{v}_h \; d\boldsymbol{x} = \int_K q \; d\boldsymbol{x} \qquad \forall K \in \mathcal{T}, \tag{4.3.11b}$$

$$\|\boldsymbol{v}_h\|_{\boldsymbol{H}^1(\Omega)} \leq C\xi(\mathcal{T})^{-1}\|q\|_{L^2(\Omega)}, \tag{4.3.11c}$$

where $\xi(\mathcal{T})$ is defined in (4.3.2)*, and C is independent of q, h and k. Moreover, if $q \in Q_0$, then there exists $\boldsymbol{v}_h \in \boldsymbol{V}_0$ satisfying* (4.3.11)*.*

Proof. Let $q \in Q$. Then there exists $\boldsymbol{w} \in \boldsymbol{H}^1(\Omega)$ such that $\operatorname{div} \boldsymbol{w} = q$ and $\|\boldsymbol{w}\|_{\boldsymbol{H}^1(\Omega)} \leq C\|q\|_{L^2(\Omega)}$. For instance, $\boldsymbol{w}$ may be constructed by extending q by zero to a ball $B_R \supset \Omega$, for R sufficiently large, and taking $\boldsymbol{w} = \nabla\psi$ where $\psi \in H^2(B_R) \cap H^1_0(B_R)$ is the unique $H^1_0(B_R)$ solution to $\Delta\psi = q$ as in [12, §1]. If $q \in Q_0$, then we instead take $\boldsymbol{w} \in \boldsymbol{H}^1_0(\Omega)$ [55, Corollary 2.4].

Let $\boldsymbol{w}_h$ be a continuous and piecewise linear function on the mesh $\mathcal{T}$ satisfying the conditions:

$$\|\boldsymbol{w}_h\|_{\boldsymbol{H}^1(\Omega)} \le C\|\boldsymbol{w}\|_{\boldsymbol{H}^1(\Omega)}, \tag{4.3.12a}$$

$$h_K^{-1}\|\boldsymbol{w}-\boldsymbol{w}_h\|_{\boldsymbol{L}^2(K)} + h_K^{-1/2}\|\boldsymbol{w}-\boldsymbol{w}_h\|_{\boldsymbol{L}^2(\partial K)} \le C\|\boldsymbol{w}\|_{\boldsymbol{H}^1(\mathcal{T}_K)} \qquad \forall K\in\mathcal{T}, \tag{4.3.12b}$$

where C is independent of h_K and $\boldsymbol{w}$. In addition, if $q \in Q_0$, so that $\boldsymbol{w} \in \boldsymbol{H}_0^1(\Omega)$, then we require $\boldsymbol{w}_h \in \boldsymbol{H}_0^1(\Omega)$. Various choices for $\boldsymbol{w}_h$ are possible, e.g. the Scott-Zhang interpolant [101] of $\boldsymbol{w}$.

Let $\boldsymbol{\psi} \in \boldsymbol{V}_0$ be given by Theorem 4.5.3 and define $\boldsymbol{v}_4 \in \boldsymbol{V}^4 := \{\boldsymbol{v}\in\boldsymbol{V} : \boldsymbol{v}|_K \in \boldsymbol{\mathcal{P}}_4(\Omega)\ \forall K\in\mathcal{T}\}$ by assigning the following values to the degrees of freedom for the space $\boldsymbol{V}^4$ listed in Lemma 4.2.2:

$$\boldsymbol{v}_4(\boldsymbol{a}) = \boldsymbol{w}_h(\boldsymbol{a}) \qquad \forall \boldsymbol{a}\in\mathcal{V}, \tag{4.3.13a}$$

$$D\boldsymbol{v}_4|_K(\boldsymbol{a}) = \boldsymbol{0} \qquad \forall \boldsymbol{a}\in\mathcal{V}_K,\ \forall K\in\mathcal{T}, \tag{4.3.13b}$$

$$\int_\gamma \boldsymbol{v}_4\cdot\boldsymbol{r}\ dS = \int_\gamma (\boldsymbol{w}-\boldsymbol{\psi})\cdot\boldsymbol{r}\ dS \qquad \forall \boldsymbol{r}\in\boldsymbol{\mathcal{P}}_0(\gamma),\ \forall\gamma\in\mathcal{E}, \tag{4.3.13c}$$

$$\int_K \boldsymbol{v}_4\cdot\boldsymbol{r}\ d\boldsymbol{x} = \int_K (\boldsymbol{w}-\boldsymbol{\psi})\cdot\boldsymbol{r}\ d\boldsymbol{x} \qquad \forall \boldsymbol{r}\in\boldsymbol{\mathcal{P}}_1(K),\ \forall K\in\mathcal{T}. \tag{4.3.13d}$$

Now, we take $\boldsymbol{v}_h := \boldsymbol{v}_4 + \boldsymbol{\psi}$.

Observe that by (4.3.13b) and (4.5.18b), $\operatorname{div}\boldsymbol{v}_h(\boldsymbol{a}) = \operatorname{div}\boldsymbol{\psi}(\boldsymbol{a}) = q(\boldsymbol{a})$, and thus,

$\boldsymbol{v}_h$ satisfies (4.3.11a). Furthermore, thanks to (4.3.13c),

$$\int_K \operatorname{div} \boldsymbol{v}_h \, d\boldsymbol{x} = \sum_{\gamma \in \mathcal{E}_K} \int_\gamma \boldsymbol{v}_h \cdot \hat{\boldsymbol{n}}_\gamma \, dS = \sum_{\gamma \in \mathcal{E}_K} \int_\gamma \boldsymbol{w} \cdot \hat{\boldsymbol{n}}_\gamma \, dS = \int_K \operatorname{div} \boldsymbol{w} \, d\boldsymbol{x} = \int_K q \, d\boldsymbol{x}$$

for all $K \in \mathcal{T}$. Moreover, if $q \in Q_0$, then $\boldsymbol{w}$ and $\boldsymbol{w}_h \in \boldsymbol{H}_0^1(\Omega)$ and hence $\boldsymbol{v}_h \in \boldsymbol{V}_0$.

It remains to establish continuity (4.3.11c). Now, let $\boldsymbol{z} := \boldsymbol{v}_4 - \boldsymbol{w}_h$. Let $K \in \mathcal{T}$ and $\hat{\boldsymbol{z}} = \boldsymbol{z} \circ \boldsymbol{F}_K$. The degrees of freedom

$$D^\alpha \hat{\boldsymbol{z}}(\hat{\boldsymbol{a}}), \qquad \forall \hat{\boldsymbol{a}} \in \mathcal{V}_{\hat{T}}, \ |\alpha| \le 1, \qquad \int_{\hat{\gamma}} \hat{\boldsymbol{z}} \cdot \boldsymbol{r} \, dS \qquad \forall \boldsymbol{r} \in \boldsymbol{\mathcal{P}}_0(\hat{\gamma}), \ \forall \hat{\gamma} \in \mathcal{E}_{\hat{T}},$$

$$\int_{\hat{T}} \hat{\boldsymbol{z}} \cdot \boldsymbol{r} \, d\boldsymbol{x} \qquad \forall r \in \boldsymbol{\mathcal{P}}_1(\hat{T}),$$

are unisolvent on $\boldsymbol{\mathcal{P}}_4(\hat{T})$, and thanks to the equivalence of norms on $\boldsymbol{\mathcal{P}}_4(\hat{T})$, there holds

$$\|\hat{\boldsymbol{z}}\|^2_{\boldsymbol{H}^1(\hat{T})} \approx \sum_{\boldsymbol{a} \in \mathcal{V}_{\hat{T}}} |\nabla \hat{\boldsymbol{z}}(\boldsymbol{a})|^2 + \sum_{\hat{\gamma} \in \mathcal{E}_{\hat{T}}} \left| \sup_{\substack{\boldsymbol{r} \in \boldsymbol{\mathcal{P}}_0(\hat{\gamma}) \\ \|\boldsymbol{r}\|_{\boldsymbol{L}^2(\hat{\gamma})} = 1}} \int_{\hat{\gamma}} \hat{\boldsymbol{z}} \cdot \boldsymbol{r} \, dS \right|^2 + \left| \sup_{\substack{\boldsymbol{r} \in \boldsymbol{\mathcal{P}}_1(\hat{T}) \\ \|\boldsymbol{r}\|_{\boldsymbol{L}^2(\hat{T})} = 1}} \int_{\hat{T}} \hat{\boldsymbol{z}} \cdot \boldsymbol{r} \, d\boldsymbol{x} \right|^2,$$

where we used that $\hat{\boldsymbol{z}}$ vanishes at the vertices of $\hat{T}$. Applying standard scaling arguments, we bound the vertex contribution using [6, Lemma 6.1] applied to $\nabla \hat{\boldsymbol{z}}$:

$$\sum_{\boldsymbol{a} \in \mathcal{V}_{\hat{T}}} |\nabla \hat{\boldsymbol{z}}(\boldsymbol{a})|^2 = \sum_{\boldsymbol{a} \in \mathcal{V}_{\hat{T}}} |\nabla (\boldsymbol{w}_h \circ \boldsymbol{F}_K)(\boldsymbol{a})|^2 \le C |\boldsymbol{w}_h \circ \boldsymbol{F}_K|^2_{\boldsymbol{H}^1(\hat{T})} \le C \|\boldsymbol{w}_h\|^2_{\boldsymbol{H}^1(K)},$$

where C is independent of k because $\boldsymbol{w}_h$ is a fixed degree polynomial. Similarly, we use edge the degrees of freedom (4.3.13c) to bound the edge contribution:

$$\begin{aligned}
\sum_{\hat{\gamma}\in\mathcal{E}_{\hat{T}}} \left| \sup_{\substack{\boldsymbol{r}\in\boldsymbol{\mathcal{P}}_0(\hat{\gamma})\\ \|\boldsymbol{r}\|_{\boldsymbol{L}^2(\hat{\gamma})}=1}} \int_{\hat{\gamma}} \hat{\boldsymbol{z}}\cdot\boldsymbol{r}\, dS \right|^2 &\leq Ch_K^{-2} \sum_{\gamma\in\mathcal{E}_K} \left| \sup_{\substack{\boldsymbol{r}\in\boldsymbol{\mathcal{P}}_0(\gamma)\\ \|\boldsymbol{r}\|_{\boldsymbol{L}^2(\gamma)}=1}} \int_{\gamma} \boldsymbol{z}\cdot\boldsymbol{r}\, dS \right|^2 \\
&= Ch_K^{-1} \sum_{\gamma\in\mathcal{E}_K} \left| \sup_{\substack{\boldsymbol{r}\in\boldsymbol{\mathcal{P}}_0(\gamma)\\ \|\boldsymbol{r}\|_{\boldsymbol{L}^2(\gamma)}=1}} \int_{\gamma} (\boldsymbol{w}-\boldsymbol{w}_h-\boldsymbol{\psi})\cdot\boldsymbol{r}\, dS \right|^2 \\
&\leq Ch_K^{-1} \sum_{\gamma\in\mathcal{E}_K} \left(\|\boldsymbol{w}-\boldsymbol{w}_h\|^2_{\boldsymbol{L}^2(\gamma)} + \|\boldsymbol{\psi}\|^2_{\boldsymbol{L}^2(\gamma)} \right) \\
&\leq C\left(h_K^{-1}\|\boldsymbol{w}-\boldsymbol{w}_h\|^2_{\boldsymbol{L}^2(\partial K)} + \xi(\mathcal{T})^{-2}\|q\|^2_{L^2(\mathcal{T}_K)} \right),
\end{aligned}$$

where we used the trace theorem with scaling

$$h_K^{-1}\|\boldsymbol{\psi}\|^2_{\boldsymbol{L}^2(\partial K)} \leq C\left(h_K^{-2}\|\boldsymbol{\psi}\|^2_{\boldsymbol{L}^2(K)} + |\boldsymbol{\psi}|^2_{\boldsymbol{H}^1(K)} \right)$$

and (4.5.18c) in the final line. The interior contribution may be controlled using analogous arguments:

$$\left| \sup_{\substack{\boldsymbol{r}\in\boldsymbol{\mathcal{P}}_1(\hat{T})\\ \|\boldsymbol{r}\|_{\boldsymbol{L}^2(\hat{T})}=1}} \int_{\hat{T}} \hat{\boldsymbol{z}}\cdot\boldsymbol{r}\, d\boldsymbol{x} \right|^2 \leq Ch_K^{-2}\left(\|\boldsymbol{w}-\boldsymbol{w}_h\|^2_{\boldsymbol{L}^2(K)} + \|\boldsymbol{\psi}\|^2_{\boldsymbol{L}^2(K)} \right).$$

Collecting results and using (4.3.12b) and (4.5.18c), we arrive at

$$h_K^{-2}\|\boldsymbol{z}\|^2_{\boldsymbol{L}^2(K)} + |\boldsymbol{z}|^2_{\boldsymbol{H}^1(K)} \leq C\left(\|\boldsymbol{w}_h\|^2_{\boldsymbol{H}^1(K)} + \|\boldsymbol{w}\|^2_{\boldsymbol{H}^1(\mathcal{T}_K)} + \xi(\mathcal{T})^{-2}\|q\|^2_{L^2(\mathcal{T}_K)} \right).$$

By the triangle inequality, (4.3.12a), and (4.5.18c),

$$\begin{aligned}\|\boldsymbol{v}\|^2_{\boldsymbol{H}^1(\Omega)} &\leq C \sum_{K\in\mathcal{T}} \left(\|\boldsymbol{w}_h\|^2_{\boldsymbol{H}^1(K)} + \|\boldsymbol{w}\|^2_{\boldsymbol{H}^1(\mathcal{T}_K)} + \xi(\mathcal{T})^{-2}\|q\|^2_{L^2(\mathcal{T}_K)} \right) \\ &\leq C \left(\|\boldsymbol{w}\|^2_{\boldsymbol{H}^1(\Omega)} + \xi(\mathcal{T})^{-2}\|q\|^2_{L^2(\Omega)} \right).\end{aligned}$$

(4.3.11c) now follows since $\|\boldsymbol{w}\|_{\boldsymbol{H}^1(\Omega)} \leq C\|q\|_{L^2(\Omega)}$. $\square$

Finally, we are in a position to provide the proof of the main result:

Proof of Theorem 4.3.1. Let $q \in Q$ and let $\boldsymbol{v}_h \in \boldsymbol{V}$, with $\boldsymbol{v}_h \in \boldsymbol{V}_0$ if $q \in Q_0$, be chosen as in Lemma 4.3.7. Define $r := q - \operatorname{div} \boldsymbol{v}_h$ so that, thanks to properties (4.3.11),

- r vanishes at all the vertices:

$$r(\boldsymbol{a}) = q(\boldsymbol{a}) - \operatorname{div} \boldsymbol{v}_h(\boldsymbol{a}) = 0 \qquad \forall \boldsymbol{a} \in \mathcal{V}. \tag{4.3.14}$$

- r has zero mean on each element:

$$\int_K r \; d\boldsymbol{x} = \int_K (q - \operatorname{div} \boldsymbol{v}_h) \; d\boldsymbol{x} = 0 \qquad \forall K \in \mathcal{T}. \tag{4.3.15}$$

- there exists a constant C independent of h and k such that

$$\|r\|_{L^2(\Omega)} \leq C\xi(\mathcal{T})^{-1}\|q\|_{L^2(\Omega)}. \tag{4.3.16}$$

In view of (4.3.14) and (4.3.15), we may apply the single element result Theorem 4.3.4 on each element separately to give $\boldsymbol{v}_K \in \boldsymbol{V}_0(K)$, $K \in \mathcal{T}$, satisfying

$$\operatorname{div} \boldsymbol{v}_K = r|_K \quad \text{and} \quad \|\boldsymbol{v}_K\|_{\boldsymbol{H}^1(K)} \leq C\|r\|_{L^2(K)}, \tag{4.3.17}$$

where C is independent of h and k. Define $\boldsymbol{v} \in \boldsymbol{V}$ by the rule

$$\boldsymbol{v}|_K = \boldsymbol{v}_h + \boldsymbol{v}_K \qquad \forall K \in \mathcal{T}.$$

When $q \in Q_0$, $\boldsymbol{v}_h \in \boldsymbol{V}_0$, and so $\boldsymbol{v} \in \boldsymbol{V}_0$. On each element $K \in \mathcal{T}$, we have

$$\operatorname{div} \boldsymbol{v} = \operatorname{div} \boldsymbol{v}_h + \operatorname{div} \boldsymbol{v}_K = \operatorname{div} \boldsymbol{v}_h + q - \operatorname{div} \boldsymbol{v}_h = q,$$

and combining (4.3.11), (4.3.16) and (4.3.17) gives

$$\|\boldsymbol{v}\|^2_{\boldsymbol{H}^1(\Omega)} \leq C\left(\|\boldsymbol{v}_h\|^2_{\boldsymbol{H}^1(\Omega)} + \sum_{K\in\mathcal{T}} \|\boldsymbol{v}_K\|^2_{\boldsymbol{H}^1(K)}\right) \leq C\xi(\mathcal{T})^{-2}\|q\|^2_{L^2(\Omega)},$$

which completes the proof. $\square$

4.4 Evaluation of Inf-Sup Constant

In this section, we explicitly compute the values of the inf-sup constant β for the reference element spaces $\boldsymbol{V}_0(\hat{T}) \times Q_0(\hat{T})$, which played a crucial role in constructing a right-continuous inverse of the divergence operator on a mesh in Section 4.3, and for the multi-element spaces $\boldsymbol{V}_0 \times Q_0$ on a typical corner-split mesh. Corollaries 4.3.2 and 4.3.5 assert that in both cases $\beta \geq \beta_0$, β_0 is independent of h and k. The inf-sup constant β is given by the square root of the smallest eigenvalue of the following generalized eigenvalue problem:

$$\boldsymbol{B}\boldsymbol{A}^{-1}\boldsymbol{B}^T\boldsymbol{p} = \lambda \boldsymbol{C}\boldsymbol{p},$$

where

$$A_{ij} = (\nabla \boldsymbol{\Phi}_i, \nabla \boldsymbol{\Phi}_j), \quad B_{jl} = b(\boldsymbol{\Phi}_l, \psi_j), \quad C_{lm} = (\psi_l, \psi_m),$$

and $\{\boldsymbol{\Phi}_i\}$ and $\{\psi_l\}$ are bases for the velocity and pressure spaces. Let $\Omega = [0,1]^2$ to be the unit square $(0,1) \times (0,1)$ with the triangulation $\mathcal{T}$ shown in Figure 4.6a. Figure 4.6b displays the computed values of β for $4 \leq k \leq 20$. As expected, β is uniformly bounded below as the polynomial degree is increased. We then perform uniform refinements of the mesh $\mathcal{T}$ by subdividing each triangle into four congruent subtriangles and compare the inf-sup constants for polynomial order $k = 4, 6, 8$ in Figure 4.7. Again, β does not decay as the mesh is refined.

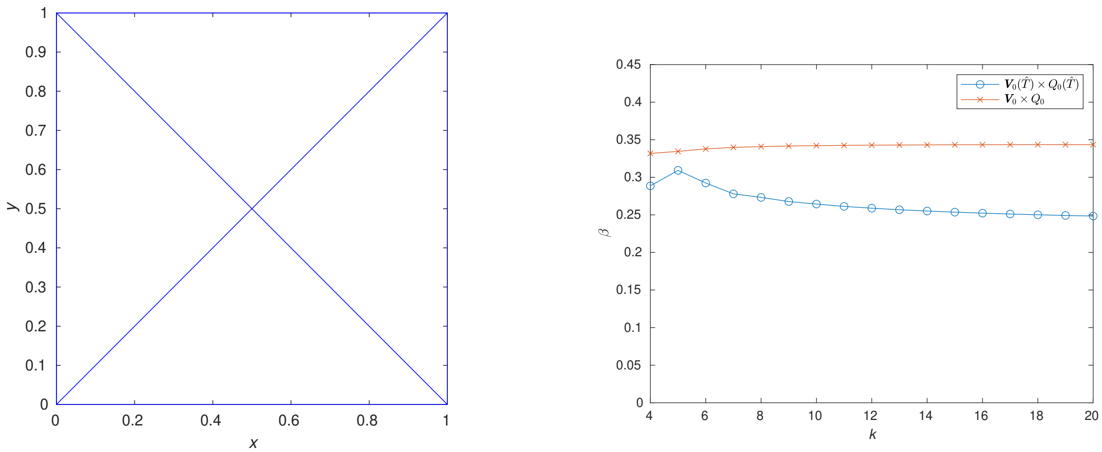

(a) (b)

Figure 4.6: (a) Domain Ω with mesh $\mathcal{T}$ and (b) inf-sup constants for the spaces $\boldsymbol{V}_0(\hat{T}) \times Q_0(\hat{T})$ and $\boldsymbol{V}_0 \times Q_0$. Notice that β does not decay as k grows as predicted by Corollaries 4.3.2 and 4.3.5.

4.5 Auxiliary Technical Results

Given $q \in Q$, we want to construct an interpolant $\boldsymbol{\psi} \in \boldsymbol{V}$ satisfying

$$\operatorname{div} \boldsymbol{\psi}|_K(\boldsymbol{a}) = q|_K(\boldsymbol{a}) \qquad \forall \boldsymbol{a} \in \mathcal{V}_K,\ \forall K \in \mathcal{T}, \tag{4.5.1a}$$

$$\|\boldsymbol{\psi}\|_{\boldsymbol{H}^1(\Omega)} \leq C\|q\|_{L^2(\Omega)}, \tag{4.5.1b}$$

where C is independent of h, k, and q. It suffices to construct $\boldsymbol{\psi}_{\boldsymbol{a}} \in \boldsymbol{V}$, $\boldsymbol{a} \in \mathcal{V}$, satisfying

$$\begin{aligned} &\operatorname{supp} \boldsymbol{\psi}_{\boldsymbol{a}} \subseteq \mathcal{T}_{\boldsymbol{a}}, && && \boldsymbol{\psi}_{\boldsymbol{a}}(\boldsymbol{b}) = \boldsymbol{0} && \forall \boldsymbol{b} \in \mathcal{V}, \\ &D\boldsymbol{\psi}_{\boldsymbol{a}}(\boldsymbol{b}) = \boldsymbol{0} && \forall \boldsymbol{b} \in \mathcal{V} \setminus \{\boldsymbol{a}\}, && \operatorname{div} \boldsymbol{\psi}_{\boldsymbol{a}}|_K(\boldsymbol{a}) = q|_K(\boldsymbol{a}) && \forall K \in \mathcal{T}_{\boldsymbol{a}}, \end{aligned}$$

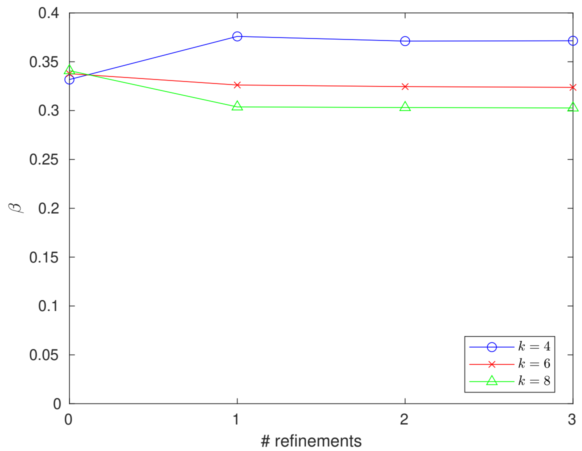

Figure 4.7: Values of the inf-sup constant β for $k = 4, 6, 8$ on uniform refinements of the mesh in Figure 4.6a.

and

$$h_K^{-1} \|\boldsymbol{\psi}_{\boldsymbol{a}}\|_{\boldsymbol{L}^2(K)} + |\boldsymbol{\psi}_{\boldsymbol{a}}|_{\boldsymbol{H}^1(K)} \leq C\|q\|_{L^2(\mathcal{T}_{\boldsymbol{a}})} \qquad \forall K \in \mathcal{T}_{\boldsymbol{a}},$$

where C is independent of h, k, and q, since then the function $\boldsymbol{\psi} := \sum_{\boldsymbol{a} \in \mathcal{V}} \boldsymbol{\psi}_{\boldsymbol{a}}$ satisfies (4.5.1).

We begin with a lemma concerning the existence of vertex functions that interpolate derivatives and possess appropriate decay properties in the polynomial order k:

Lemma 4.5.1. *Let $K \in \mathcal{T}$, $\boldsymbol{a} \in \mathcal{V}_K$, and $\boldsymbol{F}_K : \hat{T} \to K$ an invertible affine transformation be given. For every $k \geq 3$ and pair of linearly independent unit vectors $\hat{\boldsymbol{\mu}}_1$,*

$\hat{\boldsymbol{\mu}}_{\mathbf{2}}$, *there exist* $\phi_{\boldsymbol{a}}^{\hat{\boldsymbol{\mu}}_i} \in \mathcal{P}_k(K)$, $i = 1, 2$, *such that*

$$\phi_{\boldsymbol{a}}^{\hat{\boldsymbol{\mu}}_i}(\boldsymbol{b}) = 0 \qquad \forall \boldsymbol{b} \in \mathcal{V}_K, \tag{4.5.2a}$$

$$\partial_{\mu_j}\phi_{\boldsymbol{a}}^{\hat{\boldsymbol{\mu}}_i}(\boldsymbol{b}) = \delta_{ij}\delta_{\boldsymbol{ab}} \qquad \forall \boldsymbol{b} \in \mathcal{V}_K,\ j = 1, 2, \tag{4.5.2b}$$

$$\phi_{\boldsymbol{a}}^{\hat{\boldsymbol{\mu}}_i}|_{\gamma_{\boldsymbol{a}}} = 0, \tag{4.5.2c}$$

$$\|\phi_{\boldsymbol{a}}^{\hat{\boldsymbol{\mu}}_i} \circ \boldsymbol{F}_K\|_{H^1(\hat{T})} \leq Ck^{-2}|\hat{\boldsymbol{\mu}}_1 \cdot \hat{\boldsymbol{\mu}}_2^{\perp}|^{-1}\|D\boldsymbol{F}_K\|_{L^\infty(\hat{T})}, \tag{4.5.2d}$$

where $\gamma_{\boldsymbol{a}} \in \mathcal{E}_K$ *is the edge opposite vertex* $\boldsymbol{a}$, *and* C *is independent of* K, $\boldsymbol{a}$, $\boldsymbol{F}_K$, $\hat{\boldsymbol{\mu}}_1$, $\hat{\boldsymbol{\mu}}_2$, *and* k. *Moreover, if* $\hat{\boldsymbol{\mu}}_1 = \pm\hat{\boldsymbol{t}}_\gamma$ *where* $\boldsymbol{a}$ *is a vertex of* $\gamma \in \mathcal{E}_K$, *then*

$$\phi_{\boldsymbol{a}}^{\hat{\boldsymbol{\mu}}_2}|_\gamma = 0. \tag{4.5.3}$$

Similarly, if $\hat{\boldsymbol{\mu}}_2 = \pm\hat{\boldsymbol{t}}_\gamma$ *where* $\boldsymbol{a}$ *is a vertex of* $\gamma \in \mathcal{E}_K$, *then*

$$\phi_{\boldsymbol{a}}^{\hat{\boldsymbol{\mu}}_1}|_\gamma = 0. \tag{4.5.4}$$

Proof. By Lemma 3.7.1, there exists $F_k \in \mathcal{P}_k(I)$ such that

$$F_k(-1) = F_k(1) = F_k'(1) = 0, \quad F_k'(-1) = 1, \quad \text{and} \quad \|F_k\|_{L^2(I)} \leq Ck^{-3},$$

where $I = (-1, 1)$ and C is independent of k. By interpolation, and the inverse estimate $\|F_k'\|_{L^2(I)} \leq Ck^2\|F_k\|_{L^2(I)}$ [25, Corollary 3.4], we obtain the following $H^{1/2}_{00}(I)$

bound for F_k:

$$\|F_k\|_{H^{1/2}_{00}(I)} \le C\|F_k\|^{1/2}_{L^2(I)}\|F_k\|^{1/2}_{H^1(I)} \le Ck^{-2}. \tag{4.5.5}$$

Define the function $f \in L^2(\partial\hat{T})$, where $\hat{T}$ is the reference element in Figure 4.5b, by

$$f_1(s) = f_2(s) = 0, \quad f_3(s) = \frac{|\hat{\gamma}_3|}{2} F_k\left(\frac{2s}{|\hat{\gamma}_3|} - 1\right),$$

where $f_i = f|_{\hat{\gamma}_i}$ and s is the arc length parametrization of $\hat{\gamma}_i$ oriented as in Figure 4.5b, $1 \le i \le 3$. Since f is continuous at the vertices $\hat{\boldsymbol{a}}_j$, $1 \le j \le 3$, [13, Theorem 7.4] asserts the existence of $\hat{\phi}_1^{(1,0)} \in \mathcal{P}_k(\hat{T})$ such that

$$\hat{\phi}_1^{(1,0)}|_{\partial\hat{T}} = f \quad \text{and} \quad \|\hat{\phi}_1^{(1,0)}\|_{H^1(\hat{T})} \le C\|f\|_{H^{1/2}(\partial\hat{T})},$$

with C independent of k. Using that $f_i \in H^{1/2}_{00}(\gamma_i)$ and (4.5.5), we have

$$\|f\|_{H^{1/2}(\partial\hat{T})} \le C\sum_{i=1}^{3}\|f_i\|_{H^{1/2}_{00}(\gamma_i)} \le C\|F_k\|_{H^{1/2}_{00}(I)} \le Ck^{-2}.$$

Using similar arguments, we construct $\hat{\phi}_1^{(0,1)} \in \mathcal{P}_k(\hat{T})$ satisfying

$$\hat{\phi}_1^{(0,1)}|_{\hat{\gamma}_1} = \hat{\phi}_1^{(0,1)}|_{\hat{\gamma}_3} = 0, \quad \hat{\phi}_1^{(0,1)}|_{\hat{\gamma}_2}(s) = -\frac{|\hat{\gamma}_2|}{2} F_k\left(1 - \frac{2s}{|\hat{\gamma}_2|}\right)$$

and $\|\hat{\phi}_1^{(0,1)}\|_{H^1(\hat{T})} \le Ck^{-2}$. Thus, for $|\alpha| = 1$,

$$\|\hat{\phi}_1^{\alpha}\|_{H^1(\hat{T})} + k\|\hat{\phi}_1^{\alpha}\|_{L^2(\partial\hat{T})} \le Ck^{-2}, \tag{4.5.6}$$

and it is simple to verify that for $1 \leq j \leq 3$, there holds

$$D^{\beta}\hat{\phi}_1^{\alpha}(\hat{\boldsymbol{a}}_j) = \delta_{1j}\delta_{\alpha\beta} \qquad \forall |\beta| \leq 1. \tag{4.5.7}$$

Analogous arguments give the existence of $\hat{\phi}_i^{\alpha} \in \mathcal{P}_k(\hat{T})$, $i = 2, 3$, $|\alpha| = 1$ satisfying (4.5.6) and (4.5.7) with "1" replaced by "i".

We define

$$\begin{bmatrix} \phi_{\boldsymbol{a}}^{\hat{\boldsymbol{\mu}}_1} \\ \phi_{\boldsymbol{a}}^{\hat{\boldsymbol{\mu}}_2} \end{bmatrix} := \begin{bmatrix} \hat{\boldsymbol{\mu}}_1 & \hat{\boldsymbol{\mu}}_2 \end{bmatrix}^{-1} D\boldsymbol{F}_K^T \begin{bmatrix} \hat{\phi}_i^{(1,0)} \circ \boldsymbol{F}_K^{-1} \\ \hat{\phi}_i^{(0,1)} \circ \boldsymbol{F}_K^{-1} \end{bmatrix}, \tag{4.5.8}$$

where $\boldsymbol{a} = \boldsymbol{F}_K(\hat{\boldsymbol{a}}_i)$. A straightforward computation shows that $\phi_{\boldsymbol{a}}^{\hat{\boldsymbol{\mu}}_i}$, $i = 1, 2$, satisfy (4.5.2a) to (4.5.2c). (4.5.2d) follows easily from (4.5.6) and (4.5.8) on noting that

$$\left\| \begin{bmatrix} \hat{\boldsymbol{\mu}}_1 & \hat{\boldsymbol{\mu}}_2 \end{bmatrix}^{-1} \right\|_2 \leq \sqrt{2} |\hat{\boldsymbol{\mu}}_1 \cdot \hat{\boldsymbol{\mu}}_2^{\perp}|^{-1},$$

where $\|\cdot\|_2$ is the induced 2-norm.

We now examine $\phi_{\boldsymbol{a}}^{\hat{\boldsymbol{\mu}}_i}|_{\gamma}$ for $\gamma \in \mathcal{E}_K$ with $\boldsymbol{a}$ a vertex of γ. On parameterizing γ by $t \in [-1, 1]$ so that $t = -1$ corresponds to $\boldsymbol{a}$, we see that

$$\phi_{\boldsymbol{a}}^{\hat{\boldsymbol{\mu}}_i}|_{\gamma}(t) \propto F_k(t), \tag{4.5.9}$$

thanks to (4.5.8) and the construction of $\{\hat{\phi}_i^{\alpha}\}$. If $\hat{\boldsymbol{\mu}}_1 = \pm\hat{\boldsymbol{t}}_{\gamma}$, then (4.5.3) follows from (4.5.9) and the condition $\partial_{t_\gamma}\phi_{\boldsymbol{a}}^{\hat{\boldsymbol{\mu}}_2}(\boldsymbol{a}) = 0$. Equation (4.5.4) follows from similar arguments. $\square$

The next step is to construct a piecewise polynomial that is locally supported and interpolates the divergence at a single vertex:

Lemma 4.5.2. *Suppose that $\mathcal{T}$ is corner-split. Let $q \in Q$, $k \geq 4$. For each $\boldsymbol{a} \in \mathcal{V}$, there exists $\boldsymbol{\psi}_{\boldsymbol{a}} \in \boldsymbol{V}_0$ satisfying the following properties:*

$$\operatorname{supp} \boldsymbol{\psi}_{\boldsymbol{a}}|_{K'} \subseteq \mathcal{T}_{\boldsymbol{a}}, \tag{4.5.10a}$$

$$\boldsymbol{\psi}_{\boldsymbol{a}}(\boldsymbol{b}) = \boldsymbol{0} \qquad \forall \boldsymbol{b} \in \mathcal{V}, \tag{4.5.10b}$$

$$D\boldsymbol{\psi}_{\boldsymbol{a}}(\boldsymbol{b}) = \boldsymbol{0} \qquad \forall \boldsymbol{b} \in \mathcal{V} \setminus \{\boldsymbol{a}\}, \tag{4.5.10c}$$

and for $K \in \mathcal{T}_{\boldsymbol{a}}$, there holds

$$\operatorname{div} \boldsymbol{\psi}_{\boldsymbol{a}}|_K(\boldsymbol{a}) = q|_K(\boldsymbol{a}) \tag{4.5.11a}$$

$$h_K^{-1}\|\boldsymbol{\psi}_{\boldsymbol{a}}\|_{\boldsymbol{L}^2(K)} + |\boldsymbol{\psi}_{\boldsymbol{a}}|_{\boldsymbol{H}^1(K)} \leq C\xi(\mathcal{T})^{-1}\|q\|_{L^2(\mathcal{T}_{\boldsymbol{a}})}, \tag{4.5.11b}$$

where $\xi(\mathcal{T})$ is defined in (4.3.2) and C depends only on Ω and the shape regularity parameter.

Proof. Let $q \in Q$ and $\boldsymbol{a} \in \mathcal{V}$ be given. (a) Assume first that $\boldsymbol{a} \in \mathcal{V}_I$. Let $\phi_{\boldsymbol{a}}^{\hat{\mathbf{e}}_1}, \phi_{\boldsymbol{a}}^{\hat{\mathbf{e}}_2} \in \mathcal{P}_k(K)$ be given by Lemma 4.5.1 with $\hat{\boldsymbol{\mu}}_1 = \hat{\boldsymbol{e}}_1$, $\hat{\boldsymbol{\mu}}_2 = \hat{\boldsymbol{e}}_2$, where $\{\hat{\boldsymbol{e}}_1, \hat{\boldsymbol{e}}_2\}$ is the standard basis for $\mathbb{R}^2$. Define $\boldsymbol{\psi}_{\boldsymbol{a}}$ by assigning derivative values $\partial_x \boldsymbol{\psi}_{\boldsymbol{a}}(\boldsymbol{a}) \cdot \hat{\boldsymbol{e}}_1 =$

$\partial_y \boldsymbol{\psi}_{\boldsymbol{a}}(\boldsymbol{a}) \cdot \hat{\boldsymbol{e}}_2 = \frac{1}{2} q(\boldsymbol{a})$:

$$\boldsymbol{\psi}_{\boldsymbol{a}} = \begin{cases} \frac{1}{2} q(\boldsymbol{a}) \left[\phi_{\boldsymbol{a}}^{\hat{\mathbf{e}}_1} \hat{\boldsymbol{e}}_1 + \phi_{\boldsymbol{a}}^{\hat{\mathbf{e}}_2} \hat{\boldsymbol{e}}_2 \right] & \text{on } K \in \mathcal{T}_{\boldsymbol{a}}, \\ \mathbf{0} & \text{otherwise.} \end{cases} \tag{4.5.12}$$

By (4.5.2b),

$$\operatorname{div} \boldsymbol{\psi}_{\boldsymbol{a}}|_K(\boldsymbol{a}) = \partial_x \phi_{\boldsymbol{a}}^{\hat{\mathbf{e}}_1}(\boldsymbol{a}) + \partial_y \phi_{\boldsymbol{a}}^{\hat{\mathbf{e}}_2}(\boldsymbol{a}) = q(\boldsymbol{a}) \qquad \forall K \in \mathcal{T}_{\boldsymbol{a}},$$

and so $\boldsymbol{\psi}_{\boldsymbol{a}}$ satisfies (4.5.11a). Additionally, (4.5.2a) to (4.5.2c), (4.5.3) and (4.5.4) means that $\boldsymbol{\psi}_{\boldsymbol{a}} \in \boldsymbol{V}_0$ and satisfies (4.5.10a) to (4.5.10c).

We now show that $\boldsymbol{\psi}_{\boldsymbol{a}}$ given by (4.5.12) depends continuously on q (4.5.11b). Let $K \in \mathcal{T}_{\boldsymbol{a}}$ and define $\hat{\boldsymbol{\psi}}_{\boldsymbol{a}} = \boldsymbol{\psi}_{\boldsymbol{a}} \circ \boldsymbol{F}_K$. By (4.5.2d),

$$\|\hat{\boldsymbol{\psi}}_{\boldsymbol{a}}\|_{\boldsymbol{H}^1(\hat{T})} \leq C |q(\boldsymbol{a})| \sum_{j=1,2} \|\phi_{\boldsymbol{a}}^{\hat{\mathbf{e}}_j} \circ \boldsymbol{F}_K\|_{\boldsymbol{H}^1(\hat{T})} \leq C k^{-2} \|D\boldsymbol{F}_{K_l}\|_{L^\infty(\hat{T})} |q(\boldsymbol{a})|.$$

By [6, Lemma 6.1], there holds

$$k^{-2} |q|_K(\boldsymbol{a})| = k^{-2} |(q|_K \circ \boldsymbol{F}_K)(\hat{\boldsymbol{a}})| \leq C \|q \circ \boldsymbol{F}_K\|_{L^2(\hat{T})} \leq C h_K^{-1} \|q\|_{L^2(K)} \qquad \forall K \in \mathcal{T}_{\boldsymbol{a}},$$

where $\hat{\boldsymbol{a}} := \boldsymbol{F}_K^{-1}(\boldsymbol{a})$. By shape regularity, $\|D\boldsymbol{F}_K\|_{L^\infty(\hat{T})} \leq C h_K$, and thus,

$$h_K^{-1} \|\boldsymbol{\psi}_{\boldsymbol{a}}\|_{\boldsymbol{L}^2(K)} + |\boldsymbol{\psi}_{\boldsymbol{a}}|_{\boldsymbol{H}^1(K)} \leq C \|\hat{\boldsymbol{\psi}}_{\boldsymbol{a}}\|_{\boldsymbol{H}^1(\hat{T})} \leq C \|q\|_{L^2(K)},$$

with C independent of k and h_K. Equation (4.5.11b) now follows on noting that $0 < \xi(\mathcal{T}) \leq 1$.

(b) Now consider the case $\boldsymbol{a} \in \mathcal{V}_B$. Let $\phi_{\boldsymbol{a}}^{\hat{\boldsymbol{n}}}, \phi_{\boldsymbol{a}}^{\hat{\boldsymbol{t}}} \in \mathcal{P}_k(K)$ be given by Lemma 4.5.1 with $\hat{\boldsymbol{\mu}}_1 = \hat{\boldsymbol{n}}$, $\hat{\boldsymbol{\mu}}_2 = \hat{\boldsymbol{t}}$ the unit outward normal and unit tangent vectors to Γ at $\boldsymbol{a}$. Define $\boldsymbol{\psi}_{\boldsymbol{a}}$ by assigning derivative values $\partial_t \boldsymbol{\psi}_{\boldsymbol{a}}(\boldsymbol{a}) = \boldsymbol{0}$ and $\partial_n \boldsymbol{\psi}_{\boldsymbol{a}}(\boldsymbol{a}) = q(\boldsymbol{a})\hat{\boldsymbol{n}}$:

$$\boldsymbol{\psi}_{\boldsymbol{a}} = \begin{cases} q(\boldsymbol{a})\phi_{\boldsymbol{a}}^{\hat{\boldsymbol{n}}}\hat{\boldsymbol{n}} & \text{on } K \in \mathcal{T}_{\boldsymbol{a}}, \\ \boldsymbol{0} & \text{otherwise.} \end{cases} \tag{4.5.13}$$

By (4.5.2b),

$$\operatorname{div} \boldsymbol{\psi}_{\boldsymbol{a}}|_K(\boldsymbol{a}) = \partial_t \boldsymbol{\psi}_{\boldsymbol{a}}|_K(\boldsymbol{a}) \cdot \hat{\boldsymbol{t}} + \partial_n \boldsymbol{\psi}_{\boldsymbol{a}}|_K(\boldsymbol{a}) \cdot \hat{\boldsymbol{n}} = q(\boldsymbol{a})\partial_n \phi_{\boldsymbol{a}}^{\hat{\boldsymbol{n}}}(\boldsymbol{a}) = q(\boldsymbol{a}),$$

and so $\boldsymbol{\psi}_{\boldsymbol{a}}$ satisfies (4.5.11a). The remaining properties (4.5.10a) to (4.5.10c) and (4.5.11b) follow similar arguments to the previous case on noting that $\boldsymbol{\psi}_{\boldsymbol{a}}|_\Gamma = \boldsymbol{0}$ by the choice $\hat{\boldsymbol{\mu}}_2 = \hat{\boldsymbol{t}}$ and (4.5.4).

(c) Finally, consider the case $\boldsymbol{a} \in \mathcal{V}_C$. Orient the elements as in Figure 4.1 and let $\alpha_i := q|_{K_i}(\boldsymbol{a})$, $0 \le i \le m := |\mathcal{T}_{\boldsymbol{a}}| - 1$. We define the vectors $\{\boldsymbol{d}_i\}_{i=0}^{m+1}$ as follows:

$$\boldsymbol{d}_0 = \boldsymbol{d}_{m+1} = \boldsymbol{0}, \tag{4.5.14a}$$

$$\boldsymbol{d}_i = (\alpha_{i-1} - \boldsymbol{d}_{i-1} \cdot \hat{\boldsymbol{t}}_{i-1})\hat{\boldsymbol{t}}_i, \qquad 1 \le i \le s-1, \tag{4.5.14b}$$

$$\boldsymbol{d}_i = (\alpha_i - \boldsymbol{d}_{i+1} \cdot \hat{\boldsymbol{t}}_{i+1})\hat{\boldsymbol{t}}_i, \qquad s+1 \le i \le m, \tag{4.5.14c}$$

$$\boldsymbol{d}_s = \frac{\sin\theta_s\alpha_s + \boldsymbol{d}_{s+1} \cdot \hat{\boldsymbol{n}}_s}{\sin(\theta_{s-1} + \theta_s)}\hat{\boldsymbol{t}}_{s-1} + \frac{(\sin\theta_{s-1})\alpha_{s-1} - \boldsymbol{d}_{s-1} \cdot \hat{\boldsymbol{n}}_s}{(\sin(\theta_{s-1}) + \theta_s)}\hat{\boldsymbol{t}}_{s+1}, \tag{4.5.14d}$$

where $s := \arg\max_{1 \le i \le m-1} |\sin(\theta_{i-1} + \theta_i)|$. Since $\mathcal{T}$ is corner-split, $\boldsymbol{d}_s$, and thus $\{\boldsymbol{d}_i\}$, are well-defined. A simple computation reveals that

$$q|_{K_i}(\boldsymbol{a}) = \alpha_i = \csc\theta_i \left[\boldsymbol{d}_i \cdot \hat{\boldsymbol{n}}_{i+1} - \boldsymbol{d}_{i+1} \cdot \hat{\boldsymbol{n}}_i\right], \qquad 0 \le l \le m, \tag{4.5.15}$$

with the estimate

$$|\boldsymbol{d}_i| \le C\xi(\boldsymbol{a})^{-1} \sum_{i=0}^{m} |q|_{K_i}(\boldsymbol{a})|, \tag{4.5.16}$$

where $\xi(\boldsymbol{a})$ is defined in (4.3.1).

For each $K_i \in \mathcal{T}_{\boldsymbol{a}}$, let $\phi_{\boldsymbol{a}}^{\hat{\boldsymbol{t}}_i}, \phi_{\boldsymbol{a}}^{\hat{\boldsymbol{t}}_{i+1}} \in \mathcal{P}_k(K_i)$ be given by Lemma 4.5.1 with $\hat{\boldsymbol{\mu}}_1 = \hat{\boldsymbol{t}}_i$,

$\hat{\boldsymbol{\mu}}_2 = \hat{\boldsymbol{t}}_{i+1}$. Define $\boldsymbol{\psi}_{\boldsymbol{a}}$ by assigning tangential derivative values $\partial_{t_i}\boldsymbol{\psi}_{\boldsymbol{a}}|_{K_i}(\boldsymbol{a}) = \boldsymbol{d}_i$:

$$\boldsymbol{\psi}_{\boldsymbol{a}} = \begin{cases} \phi_{\boldsymbol{a}}^{\hat{\boldsymbol{t}}_i}\boldsymbol{d}_i + \phi_{\boldsymbol{a}}^{\hat{\boldsymbol{t}}_{i+1}}\boldsymbol{d}_{i+1} & \text{on } K_i \in \mathcal{T}_{\boldsymbol{a}}, \\ \boldsymbol{0} & \text{otherwise,} \end{cases} \tag{4.5.17}$$

where. By construction, $\partial_{t_i}\boldsymbol{\psi}_{\boldsymbol{a}}|_{K_i}(\boldsymbol{a}) = \boldsymbol{d}_i$, and so $\boldsymbol{\psi}_{\boldsymbol{a}}$ satisfies (4.5.11a) by the identity (4.3.9) and (4.5.15). Additionally, (4.5.2a) to (4.5.2c), (4.5.3) and (4.5.4) means that $\boldsymbol{\psi}_{\boldsymbol{a}} \in \boldsymbol{V}$ and satisfies (4.5.10a) to (4.5.10c). Since $\boldsymbol{d}_0 = \boldsymbol{d}_{m+1} = \boldsymbol{0}$, $\boldsymbol{\psi}_{\boldsymbol{a}} = \boldsymbol{0}$ on Γ by properties (4.5.3), (4.5.4) and (4.5.10a), and so $\boldsymbol{\psi}_{\boldsymbol{a}} \in \boldsymbol{V}_0$.

Finally, we show that $\boldsymbol{\psi}_{\boldsymbol{a}}$ given by (4.5.17) depends continuously on q (4.5.11b). Let $K \in \mathcal{T}_{\boldsymbol{a}}$. Using the estimate (4.5.16) and arguing similarly as above, we obtain

$$h_K^{-2}\|\boldsymbol{\psi}_{\boldsymbol{a}}\|_{\boldsymbol{L}^2(K)}^2 + |\boldsymbol{\psi}_{\boldsymbol{a}}|_{\boldsymbol{H}^1(K)}^2 \leq C\xi(\boldsymbol{a})^{-2}h_K^2\sum_{i=0}^{m} h_{K_i}^{-2}\|q\|_{L^2(K_i)}^2,$$

where we used shape regularity to uniformly bound $|\hat{\boldsymbol{t}}_i \cdot \hat{\boldsymbol{t}}_{i+1}^{\perp}|^{-1} = \csc\theta_i$. Again using shape regularity, $h_{K_i} \approx h_K$ and so (4.5.11b) follows on noting that $\xi(\boldsymbol{a})^{-1} \leq \xi(\mathcal{T})^{-1}$. $\square$

We now obtain the existence of the interpolant $\boldsymbol{\psi}$ summing the individual vertex contributions $\boldsymbol{\psi}_{\boldsymbol{a}}$:

Theorem 4.5.3. *Suppose that $\mathcal{T}$ is corner-split and let $q \in Q$, $k \geq 4$. The function*

$\boldsymbol{\psi} \in \boldsymbol{V}_0$ defined by the rule

$$\boldsymbol{\psi} := \sum_{\boldsymbol{a}\in\mathcal{V}} \boldsymbol{\psi}_{\boldsymbol{a}},$$

where $\boldsymbol{\psi}_{\boldsymbol{a}}$ are given in Lemma 4.5.2, satisfies the following properties:

$$\boldsymbol{\psi}(\boldsymbol{a}) = \mathbf{0} \qquad \forall \boldsymbol{a} \in \mathcal{V}, \tag{4.5.18a}$$

$$\operatorname{div} \boldsymbol{\psi}|_K(\boldsymbol{a}) = q|_K(\boldsymbol{a}) \qquad \forall \boldsymbol{a} \in \mathcal{V}_K,\ K \in \mathcal{T}, \tag{4.5.18b}$$

$$h_K^{-2}\|\boldsymbol{\psi}\|^2_{\boldsymbol{L}^2(K)} + |\boldsymbol{\psi}|^2_{\boldsymbol{H}^1(K)} \le C\xi(\mathcal{T})^{-2}\|q\|^2_{L^2(\mathcal{T}_K)} \qquad \forall K \in \mathcal{T}, \tag{4.5.18c}$$

where $\xi(\mathcal{T})$ is defined in (4.3.2) *and C is independent of h, k, and q.*

4.6 Mixed Boundary Conditions

We now outline how to modify the finite element spaces in the presence of more general boundary conditions. Let $\{\boldsymbol{A}_i\}$ be the W vertices of the domain Ω, and let $\{\Gamma_i\}$ be the open edge connecting vertices $\boldsymbol{A}_i$ and $\boldsymbol{A}_{i+1}$, $1 \le i \le W$, as illustrated in Figure 4.8. The boundary $\Gamma = \partial\Omega$ is partitioned into subsets Γ_D and Γ_N as follows:

$$\Gamma_D = \bigcup_{i\in\mathcal{D}} \Gamma_i \quad \text{and} \quad \Gamma_N = \bigcup_{i\in\mathcal{N}} \Gamma_i$$

for disjoint indexing sets $\mathcal{D}, \mathcal{N} \subseteq \{1, \ldots, W\}$ with $\mathcal{D} \neq \emptyset$ and $\mathcal{N} \neq \emptyset$. We consider boundary conditions of the form

$$\boldsymbol{u} = \boldsymbol{0} \qquad \text{on } \Gamma_D \quad \text{and} \quad \nu \partial_n \boldsymbol{u} - p\hat{\boldsymbol{n}} = 0 \qquad \text{on } \Gamma_N,$$

where vertices are located where there is a change in boundary condition type (see e.g. $\boldsymbol{A}_2$ in Figure 4.8). The corresponding variational form of the Stokes equations is then:

$$\begin{aligned} a(\boldsymbol{u}, \boldsymbol{v}) + b(\boldsymbol{v}, p) &= (\boldsymbol{f}, \boldsymbol{v}) \qquad && \forall \boldsymbol{v} \in \boldsymbol{H}^1_D(\Omega), \\ b(\boldsymbol{u}, q) &= 0 && \forall q \in L^2(\Omega), \end{aligned}$$

where $\boldsymbol{H}^1_D(\Omega) := \{\boldsymbol{u} \in \boldsymbol{H}^1(\Omega) : \boldsymbol{u}|_{\Gamma_D} = \boldsymbol{0}\}$.

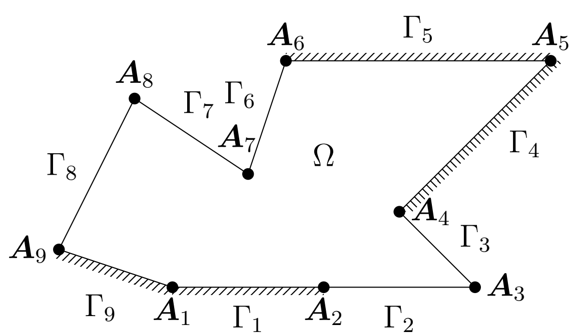

Figure 4.8: Example domain Ω and boundary partition $\mathcal{D} = \{1, 4, 5, 9\}$ and $\mathcal{N} = \{2, 3, 6, 7, 8\}$.

Let $\{\Gamma_D^{(j)}\}_{j=1}^J$ denote the connected components of Γ_D and define

$$H_D^2(\Omega) := \{\phi \in H^2(\Omega) : \phi|_{\Gamma_D^{(1)}} = 0,\ \phi|_{\Gamma_D^{(j)}} \text{ is constant},\ 2 \le j \le J,\ \text{and } \partial_n\phi|_{\Gamma_D} = 0\}.$$

A simple calculation reveals that $\mathbf{curl}\, H_D^2(\Omega) \subset \boldsymbol{H}_D^1(\Omega)$. In fact, we have the following exact sequence property:

Lemma 4.6.1. *The sequence*

$$0 \xrightarrow{\subset} H_D^2(\Omega) \xrightarrow{\mathbf{curl}} \boldsymbol{H}_D^1(\Omega) \xrightarrow{\mathrm{div}} L^2(\Omega) \longrightarrow 0, \tag{4.6.1}$$

is exact.

Proof. (i) If $\phi \in H_D^2(\Omega)$ and $\mathbf{curl}\,\phi = 0$, then ϕ is constant in Ω. The condition $\phi|_{\Gamma_D^{(1)}} = 0$ then means that $\phi \equiv 0$.

(ii) Let $\boldsymbol{u} \in \boldsymbol{H}_D^1(\Omega)$ be divergence free. By the exactness of (4.1.4), there exists $\psi \in H^2(\Omega)$ such that $\mathbf{curl}\,\psi = \boldsymbol{u}$. Since $\mathbf{curl}\,\psi|_{\Gamma_D} = \mathbf{0}$, $\nabla\psi|_{\Gamma_D} = \mathbf{0}$. As a result,

$$\psi \in \{\phi \in H^2(\Omega) : \phi|_{\Gamma_D^{(j)}} \text{ is constant},\ 1 \le j \le J,\ \text{and } \partial_n\phi|_{\Gamma_D} = 0\},$$

and so $\phi = \psi - \psi|_{\Gamma_D^{(1)}}$ satisfies $\phi \in H_D^2(\Omega)$ with $\mathbf{curl}\,\phi = \mathbf{curl}\,\psi = \boldsymbol{u}$.

(iii) By [79, Lemma 11.1.1], $\mathrm{div}\,\boldsymbol{H}_D^1(\Omega) = L^2(\Omega)$. $\square$

The finite element spaces Σ, $\boldsymbol{V}$, Q are defined as above (4.2.1), where corner vertices now also include vertices of the domain where boundary conditions change type. The corresponding spaces satisfying homogeneous mixed boundary conditions are defined by:

$$\Sigma_D := \Sigma \cap H^2_D(\Omega), \quad \boldsymbol{V}_D := \boldsymbol{V} \cap \boldsymbol{H}^1_D(\Omega), \quad \text{and} \quad Q_D := Q. \tag{4.6.2}$$

To count the dimension of these spaces, we partition the boundary edges and vertices further. Let $\mathcal{E}_B := \mathcal{E} \setminus \mathcal{E}_I$ be partitioned into $\mathcal{E}_B^D$ consisting of all element edges coinciding with Γ_D and $\mathcal{E}_B^N$ the remaining boundary edges. Similarly, let $\mathcal{V}_C^D \subset \mathcal{V}_C$ denote the corner vertices with both boundary edges coinciding with Γ_D, $\mathcal{V}_C^{DN}$ the corner vertices where boundary conditions change type, and $\mathcal{V}_C^N$ the remaining corner vertices. The set $\mathcal{V}_B$ is analogously partitioned into $\mathcal{V}_B^D$ and $\mathcal{V}_B^N$. The quantities E_B^D, V_C^D, etc. as defined analogously as in Section 4.2. We then have the following result:

Lemma 4.6.2. *The dimension of the mixed boundary condition spaces is as follows:*

$$\dim \boldsymbol{V}_D = \dim \boldsymbol{V} - 2[(k-3)E_B^D + 2V_B^D + 3V_C^D + 2V_C^{DN}], \tag{4.6.3}$$

$$\dim \Sigma_D = \dim \Sigma - [(2k-7)E_B^D + 5V_B^D + 7V_C^D - |\mathcal{V}_C^S \cap \mathcal{V}_C^D| + 5V_C^{DN}] + J - 1 \tag{4.6.4}$$

Proof. Let $\boldsymbol{v} \in \boldsymbol{V}_D$. The same arguments as in the proof of Lemma 4.2.4 hold for $\gamma \in \mathcal{E}_B^D$, $\boldsymbol{a} \in \mathcal{V}_B^D$, and $\boldsymbol{a} \in \mathcal{V}_C^D$. For $\boldsymbol{a} \in \mathcal{V}_C^{DN}$, $\boldsymbol{v}(\boldsymbol{a}) = \boldsymbol{0}$ and $\partial_{t_\gamma} \boldsymbol{v}|_\gamma(\boldsymbol{a}) = \boldsymbol{0}$ for $\gamma \in \mathcal{E}_{\boldsymbol{a}} \cap \mathcal{E}_B^D$. Equation (4.6.3) now follows.

Let $\tilde{\Sigma}_D := \{\phi \in \Sigma : \phi|_{\Gamma_D} = \partial_n \phi|_{\Gamma_D} = 0\}$ and $\phi \in \tilde{\Sigma}_D$. Again, the same arguments as in the proof of Lemma 4.2.4 hold for $\gamma \in \mathcal{E}_B^D$, $\boldsymbol{a} \in \mathcal{V}_B^D$, and $\boldsymbol{a} \in \mathcal{V}_C^D$. For $\boldsymbol{a} \in \mathcal{V}_C^{DN}$, $\phi(\boldsymbol{a}) = 0$, $\nabla\phi(\boldsymbol{a}) = \mathbf{0}$, and $\partial_{t_\gamma t_\gamma}\phi|_\gamma(\boldsymbol{a}) = \partial_{t_\gamma n_\gamma}\phi|_\gamma(\boldsymbol{a}) = 0$. Thus,

$$\dim \tilde{\Sigma}_D = \dim \Sigma - [(2k-7)E_B^D + 5V_B^D + 7V_C^D - |\mathcal{V}_C^S \cap \mathcal{V}_C^D| + 5V_C^{DN}].$$

Clearly Σ_D has an additional $J-1$ degrees of freedom for the value of $\phi|_{\Gamma_D^{(j)}}$, $2 \leq j \leq J$, and so (4.6.4) follows. $\square$

The analogue of Theorem 4.2.6 is the following:

Theorem 4.6.3. *The sequence*

$$0 \xrightarrow{\subset} \Sigma_D \xrightarrow{\mathbf{curl}} \boldsymbol{V}_D \xrightarrow{\mathrm{div}} Q \longrightarrow 0 \tag{4.6.5}$$

is exact if and only if the mesh is corner-split at Dirichlet vertices, i.e. $|\mathcal{V}_C^S \cap \mathcal{V}_C^D| = 0$.

Proof. Arguing as in Section 4.2.2, the sequence (4.6.5) is exact if and only if

$$\dim \Sigma_D + \dim Q - \dim \boldsymbol{V}_D = 0.$$

Using Lemmas 4.2.5 and 4.6.2 gives

$$\dim \Sigma_D + \dim Q - \dim \boldsymbol{V}_D = E_B^D - V_B^D - V_C^D - V_C^{DN} + J + |\mathcal{V}_C^S \cap \mathcal{V}_C^D|$$

Moreover,

$$E_B^D = \sum_{j=1}^{J} |\mathcal{E}_B^D \cap \Gamma_D^{(j)}| = \sum_{j=1}^{J} \{|(\mathcal{V}_B^D \cup \mathcal{V}_C^D \cup \mathcal{V}_C^{DN}) \cap \bar{\Gamma}_D^{(j)}| - 1\} = V_B^D + V_C^D + \mathcal{V}_C^{DN} - J,$$

where we used Euler's identity on each connected component $\Gamma_D^{(j)}$ in the second step: $|\mathcal{E}_B^D \cap \Gamma_D^{(j)}| = |\mathcal{V} \cap \bar{\Gamma}_D^{(j)}| - 1$. Consequently, there holds

$$\dim \Sigma_D + \dim Q - \dim \boldsymbol{V}_D = |\mathcal{V}_C^S \cap \mathcal{V}_C^D|,$$

which completes the proof. $\square$

The results of [8] may be used to pick the vectors $\{\boldsymbol{d}_i\}$ for vertices $\boldsymbol{a} \in \mathcal{V}_C^{DN} \cup \mathcal{V}_C^N \cup \mathcal{V}_B^N$ in the construction of $\boldsymbol{\psi}_{\boldsymbol{a}}$ in Lemma 4.5.2 to obtain the following:

Lemma 4.6.4. *Suppose that $\mathcal{T}$ is corner-split at Dirichlet vertices. Let $q \in Q$, $k \geq 4$. For each $\boldsymbol{a} \in \mathcal{V}$, there exists $\boldsymbol{\psi}_{\boldsymbol{a}} \in \boldsymbol{V}_D$ satisfying the following properties:*

$$\begin{aligned} \operatorname{supp} \boldsymbol{\psi}_{\boldsymbol{a}}|_{K'} \subseteq \mathcal{T}_{\boldsymbol{a}}&, \\ \boldsymbol{\psi}_{\boldsymbol{a}}(\boldsymbol{b}) = \boldsymbol{0} & \qquad \forall \boldsymbol{b} \in \mathcal{V}, \\ D\boldsymbol{\psi}_{\boldsymbol{a}}(\boldsymbol{b}) = \boldsymbol{0} & \qquad \forall \boldsymbol{b} \in \mathcal{V} \setminus \{\boldsymbol{a}\}, \end{aligned}$$

and for $K \in \mathcal{T}_{\boldsymbol{a}}$, there holds

$$\operatorname{div} \boldsymbol{\psi}_{\boldsymbol{a}}|_K(\boldsymbol{a}) = q|_K(\boldsymbol{a})$$
$$h_K^{-1} \|\boldsymbol{\psi}_{\boldsymbol{a}}\|_{\boldsymbol{L}^2(K)} + |\boldsymbol{\psi}_{\boldsymbol{a}}|_{\boldsymbol{H}^1(K)} \leq C \xi_D(\mathcal{T})^{-1} \|q\|_{L^2(\mathcal{T}_{\boldsymbol{a}})},$$

where $\xi_D(\mathcal{T}) := \min_{\boldsymbol{a} \in \mathcal{V}_C^D} \xi(\boldsymbol{a})$ and C depends only on Ω and the shape regularity parameter.

A continuous right inverse of the divergence operator and uniform inf-sup stability of the spaces $\boldsymbol{V}_D \times Q$ may then be established using exactly the same arguments as in Section 4.3.

The method may also be extended to the case where conditions are imposed on $\boldsymbol{u} \cdot \hat{\boldsymbol{t}}$ and $\boldsymbol{u} \cdot \hat{\boldsymbol{n}}$ separately and to the symmetric gradient bilinear form $\nu(\boldsymbol{\varepsilon}(\boldsymbol{u}), \boldsymbol{\varepsilon}(\boldsymbol{v}))$. We refer to [8] for the details in the more general case of the Scott-Vogelius elements, where uniform in h and k stability estimates are established.

Chapter Five

Mass Conserving Mixed *hp*-FEM Approximations to Stokes Flow. Part II: Optimal Convergence

5.1 Introduction

This chapter is the second part in a series discussing a mass conserving, high order, mixed finite element method for Stokes flow on a simply connected polygon Ω (4.1.2). Problem (4.1.2) is approximated using mixed, high order, finite elements as follows: Find $(\boldsymbol{u}_{hk}, p_{hk}) \in \boldsymbol{V}_0 \times Q_0$ such that

$$a(\boldsymbol{u}_{hk}, \boldsymbol{v}) + b(\boldsymbol{v}, p_{hk}) = (\boldsymbol{f}, \boldsymbol{v}) \qquad \forall \boldsymbol{v} \in \boldsymbol{V}_0, \tag{5.1.1a}$$

$$b(\boldsymbol{u}_{hk}, q) = 0 \qquad \forall q \in Q_0, \tag{5.1.1b}$$

where the finite element spaces are chosen for $k \geq 4$ as in the previous chapter (4.2.16). In addition, we assume that the mesh $\mathcal{T}$ is *corner-split* which, roughly speaking, means that every element $K \in \mathcal{T}$ has at most one edge lying on the domain boundary Γ; for a precise definition, see Section 4.2.2.

One of the main results shown in Chapter 4 is that these elements are uniformly inf-sup stable in the mesh size h and polynomial order k if the mesh $\mathcal{T}$ is corner-split.

Theorem 5.1.1 (Corollary 4.3.2)**.** *If the mesh $\mathcal{T}$ is corner-split, then there exists a positive constant β independent of both h and k such that*

$$\sup_{\mathbf{0} \neq \boldsymbol{v} \in \boldsymbol{V}_0} \frac{b(\boldsymbol{v}, q)}{\|\boldsymbol{v}\|_{\boldsymbol{H}^1(\Omega)}} \geq \beta \|q\|_{L^2(\Omega)} \qquad \forall q \in Q_0. \tag{5.1.2}$$

Strictly speaking, Corollary 4.3.2 shows that β depends on the mesh-dependent quantity $\xi(\mathcal{T})$ defined in (4.3.2), but is nevertheless bounded independently of the mesh size h and the polynomial degree k. In the current work, we establish optimal error estimates for the hp-finite element approximation to (4.1.3).

We begin with the error in the velocity. In particular, the exactness of the following sequence [55]

$$0 \xrightarrow{\subset} H_0^2(\Omega) \xrightarrow{\mathbf{curl}} \boldsymbol{H}_0^1(\Omega) \xrightarrow{\text{div}} L_0^2(\Omega) \longrightarrow 0, \tag{5.1.3}$$

means that, since the velocity $\boldsymbol{u} \in \boldsymbol{H}_0^1(\Omega)$, then $q = \operatorname{div} \boldsymbol{u} \in L_0^2(\Omega)$. As a consequence, (4.1.3b) implies $\|\operatorname{div} \boldsymbol{u}\|^2 = 0$ or $\operatorname{div} \boldsymbol{u} \equiv 0$. Using the exactness of the sequence (5.1.3) again then gives $\boldsymbol{u} = \mathbf{curl}\, \phi$ for some $\phi \in H_0^2(\Omega)$. Taking $\boldsymbol{v} = \mathbf{curl}\, \psi$ in (4.1.3a) leads to the standard *stream-function formulation* of the Stokes equations [55, Theorem 5.5]:

$$(\boldsymbol{f}, \mathbf{curl}\, \psi) = \nu(\nabla\, \mathbf{curl}\, \phi, \nabla\, \mathbf{curl}\, \psi) = \nu(D^2\phi, D^2\psi) = \nu(\Delta\phi, \Delta\psi) \qquad \forall \psi \in H_0^2(\Omega), \tag{5.1.4}$$

thanks to the identity $(D^2\phi, D^2\psi) = (\Delta\phi, \Delta\psi)$ for $\phi, \psi \in H_0^2(\Omega)$. As shown in the previous chapter Theorem 4.2.6 and in [50, p.1315-1316], the finite element spaces (4.2.16) satisfy a discrete analogue of (5.1.3) provided that the mesh $\mathcal{T}$ is corner-split:

$$0 \xrightarrow{\subset} \Sigma_0 \xrightarrow{\mathbf{curl}} \boldsymbol{V}_0 \xrightarrow{\text{div}} Q_0 \longrightarrow 0. \tag{5.1.5}$$

The same argument that lead to (5.1.4) can be carried out at the discrete level to conclude that the resulting approximation (5.1.1) will be pointwise mass conserving; i.e., $\operatorname{div} \boldsymbol{u}_{hk} \equiv 0$ in Ω, and $\boldsymbol{u}_{hk} = \mathbf{curl}\, \phi_{hk}$ where $\phi_{hk} \in \Sigma_0$ is the Σ_0 finite element approximation of ϕ:

$$\nu(\Delta\phi_{hk}, \Delta\psi) = (\boldsymbol{f}, \mathbf{curl}\, \psi) \quad \forall\psi \in \Sigma_0.$$

A standard application of Céa's Lemma [38, Theorem 2.4.1] gives following error estimate:

$$\|\boldsymbol{u} - \boldsymbol{u}_{hk}\|_{\boldsymbol{H}^1(\Omega)} = \|\,\mathbf{curl}(\phi - \phi_{hk})\|_{\boldsymbol{H}^1(\Omega)} \le \sqrt{2}\|\phi - \phi_{hk}\|_{H^2(\Omega)} \le C \inf_{\psi\in\Sigma_0} |\phi - \psi|_{H^2(\Omega)},$$

where C is a constant that depends only on the *diameter* of the domain Ω which shows that the accuracy of the velocity approximation in $\boldsymbol{H}_0^1(\Omega)$ using the space $\boldsymbol{V}_0$ is in fact dictated by the approximation properties of Σ_0 in $H_0^2(\Omega)$ and is *independent* of the error of the pressure approximation and the viscosity ν [66].

We now turn to the error in the pressure. A consequence of the inf-sup condition (5.1.2) is the well known result [66, Lemma 4.4]

$$\beta\|P_Q p - p_{hk}\|_{L^2(\Omega)} \le \sup_{\mathbf{0}\ne\boldsymbol{v}\in\boldsymbol{V}_0} \frac{b(\boldsymbol{v}, P_Q p - p_{hk})}{\|\boldsymbol{v}\|_{\boldsymbol{H}^1(\Omega)}} \le \nu|\boldsymbol{u} - \boldsymbol{u}_{hk}|_{\boldsymbol{H}^1(\Omega)},$$

where $P_Q : L_0^2(\Omega) \to Q_0$ is the $L_0^2(\Omega)$ projection of p onto Q_0. Employing the triangle inequality and properties of a projection gives

$$\begin{aligned}\|p - p_{hk}\|_{L^2(\Omega)} &\le \|p - P_Q p\|_{L^2(\Omega)} + \frac{\nu}{\beta}|\boldsymbol{u} - \boldsymbol{u}_{hk}|_{\boldsymbol{H}^1(\Omega)} \\ &\le \inf_{q \in Q_0} \|p - q\|_{L^2(\Omega)} + \frac{\nu}{\beta}|\boldsymbol{u} - \boldsymbol{u}_{hk}|_{\boldsymbol{H}^1(\Omega)}.\end{aligned}$$

Crucial here is that the discrete inf-sup constant β is independent of h and k, which means that, together with the above discussion, we obtain the following quasi-optimal error estimate:

Lemma 5.1.2. *If the mesh $\mathcal{T}$ is corner-split, then the finite element approximation $(\boldsymbol{u}_{hk}, p_{hk})$ to the Stokes problem* (5.1.1) *satisfies*

$$\|\boldsymbol{u} - \boldsymbol{u}_{hk}\|_{\boldsymbol{H}^1(\Omega)} \le C \inf_{\psi \in \Sigma_0} \|\phi - \psi\|_{H^2(\Omega)}, \tag{5.1.6}$$

where $\phi \in H_0^2(\Omega) : \mathbf{curl}\, \phi = \boldsymbol{u}$, and

$$\|p - p_{hk}\|_{L^2(\Omega)} \le \inf_{q \in Q_0} \|p - q\|_{L^2(\Omega)} + \frac{\nu}{\beta}|\boldsymbol{u} - \boldsymbol{u}_{hk}|_{\boldsymbol{H}^1(\Omega)} \tag{5.1.7}$$

with C depending only on the diameter of Ω.

The error estimates (5.1.6) and (5.1.7) reveal two important properties of the particular choices of $\boldsymbol{V}_0$ and Q_0. First, the error in the velocity approximation is *independent* of the error in the pressure approximation, and the constant C in (5.1.6) is *independent* of the viscosity ν. Second, the error estimate for the pressure (5.1.7) is quasi-optimal in h and k – the constants are independent of h and k since the inf-sup constant β is uniformly bounded below thanks to Theorem 5.1.1.

To obtain estimates for the convergence rate, we derive approximation properties of the spaces Σ_0 and Q_0 for two classes of functions: (1) functions with general Sobolev regularity, for which we establish algebraic convergence rates using locally quasi-uniform meshes and (2) functions exhibiting the usual singularities at corners of the polygonal domain Ω, which belong to countably normed (weighted) spaces for which we obtain exponential convergence using geometrically graded meshes. Some approximation properties for the (slightly) smoother subspaces

$$\tilde{\Sigma}_0 := \{\phi \in \Sigma_0 : \phi \text{ is } C^2 \text{ at all vertices}\} \quad \text{and} \quad \tilde{Q}_0 := \{q \in Q_0 : q \text{ is } C^0 \text{ at all vertices}\}$$

are already known in the literature. The algebraic convergence of p-version methods using the finite element space $\tilde{\Sigma}_0$ for variational problems posed in $H_0^2(\Omega)$ was first shown in [68] and later improved in [106] in the setting of finite element approximation of general $2m$-th order elliptic equations. However, the approximation result [106, Theorem 4.1] only applies in the case that the true solution belongs to $H^s(\Omega)$ for some $s > \frac{7}{2}$, whereas standard arguments only establish the existence of a solution in $H^s(\Omega)$ for some $s > 2$ in general. We augment the existing approximation theory for the space $\tilde{\Sigma}_0$ by requiring only minimal regularity $s > 2$ (rather than $s > \frac{7}{2}$ as in [106]) and exhibiting the dependence on the mesh size explicitly. Exponential convergence of hp-methods for general $2m$-th order elliptic equations was proved in [57]. In particular, the results in [57] imply exponential convergence of approximations in Σ_0 to solutions belonging to countably normed spaces using geometrically graded meshes. However, hp-estimates of algebraic or exponential type have yet to be established for the space Q_0. We develop the hp-approximation theory for the space Q_0 in both Sobolev spaces, which leads to algebraic convergence, and in countably normed spaces, which leads to exponential convergence using geometrically graded meshes. In fact, we will actually construct optimal Sobolev space approximations in $\tilde{Q}_0$, which clearly implies optimal approximation properties of the space Q_0.

The remainder for the paper is organized as follows. In Section 5.2, we formally state the main assumptions and results. In Section 5.3, we introduce two key results used to establish optimal algebraic hp-error estimates. We build $L_0^2(\Omega)$ approximations in $\tilde{Q}_0$ in Section 5.4 and $H_0^2(\Omega)$ approximations in $\tilde{\Sigma}_0$ in Section 5.5. In Section 5.6, we state and prove auxiliary lemmas needed to show exponential convergence on geometrically graded meshes for singular solutions belonging to particular countably normed spaces. Finally, in Section 5.7, we present two numerical examples to showcase the power of the method: Moffatt eddies in a wedge and parabolic flow in a T-shaped cavity.

5.2 Assumptions and Statement of Main Results

We continue to use the same notation for mesh entities as in previous chapters. Given an edge $\gamma \in \mathcal{E}$, let $\mathcal{T}_\gamma$ denote the elements with γ as an edge; i.e., $\mathcal{T}_\gamma := \{K \in \mathcal{T} : \gamma \in \mathcal{E}_K\}$. We recall that shape regularity (3.2.3) implies that $h_K \approx h_L$ for $L \in \mathcal{T}_K$

where the equivalence constants depend only on κ. For a positive real number $s \geq 0$ and subset $\omega \subseteq \Omega$, let $\|D^s u\|_{H^0(\omega)} := |u|_{H^s(\omega)}$.

5.2.1 Approximation in Sobolev Spaces

The first set of results deals with the approximation of functions known only to belong to a Sobolev space $H^s(\Omega)$ for some $s > 0$. In the absence of any additional information on the nature of the solution, the mesh is assumed to be locally quasi-uniform with no specific local refinements. The following theorem, proved in Section 5.4 and Section 5.5, establishes the existence of global approximations with optimal local approximation power:

Theorem 5.2.1. *Let $\phi \in H^{s+1}(\Omega) \cap H_0^2(\Omega)$ and $q \in H^{s-1}(\Omega) \cap L_0^2(\Omega)$, $s > 1$. Then, there exists $\phi_{hk} \in \tilde{\Sigma}_0$ and $q_{hk} \in \tilde{Q}_0$ such that*

$$\|\phi - \phi_{hk}\|_{H^2(K)} \leq C h_K^{\min(k,s-1)} k^{-(s-1)} \|D^{m+1}\phi\|_{H^{s-m}(\mathcal{T}_K)} \qquad \forall K \in \mathcal{T}, \tag{5.2.1}$$

and

$$\|q - q_{hk}\|_{L^2(K)} \leq C h_K^{\min(k,s-1)} k^{-(s-1)} \|D^{m-1}q\|_{H^{s-m}(\mathcal{T}_K)} \qquad \forall K \in \mathcal{T}, \tag{5.2.2}$$

where $m = \min(k+1, s)$ and C depends only on s, Ω, and the shape regularity parameter κ.

As an immediate consequence of the approximation result Theorem 5.2.1, we obtain the following optimal a priori error estimate for the finite element approximation of the Stokes problem:

Theorem 5.2.2. *Suppose that the solution to* (4.1.3) *satisfies* $\boldsymbol{u} \in \boldsymbol{H}^s(\Omega) \cap \boldsymbol{H}_0^1(\Omega)$ *and* $p \in H^{s-1}(\Omega) \cap L_0^2(\Omega)$ *for some* $s > 1$*, and let* $(\boldsymbol{u}_{hk}, p_{hk})$ *be the finite element approximation defined by* (5.1.1)*. If the mesh* $\mathcal{T}$ *is corner-split, then*

$$\|\boldsymbol{u} - \boldsymbol{u}_{hk}\|_{\boldsymbol{H}^1(\Omega)}^2 \leq C \sum_{K \in \mathcal{T}} h_K^{2\min(k,s-1)} k^{-2(s-1)} \|D^m \boldsymbol{u}\|_{\boldsymbol{H}^{s-m}(\mathcal{T}_K)}^2 \tag{5.2.3a}$$

$$\begin{aligned}\|p - p_{hk}\|_{L^2(\Omega)}^2 \leq C\Bigg(&\sum_{K \in \mathcal{T}} h_K^{2\min(k,s-1)} k^{-2(s-1)} \|D^{m-1} p\|_{H^{s-m}(\mathcal{T}_K)}^2 \\ &+ \nu^2 \sum_{K \in \mathcal{T}} h_K^{2\min(k,s-1)} k^{-2(s-1)} \|D^m \boldsymbol{u}\|_{\boldsymbol{H}^{s-m}(\mathcal{T}_K)}^2 \Bigg),\end{aligned} \tag{5.2.3b}$$

where $m = \min(k+1, s)$ *and* C *is independent of* h*,* k*,* ν*,* $\boldsymbol{u}$*, and* p*.*

Proof. Recall that $\boldsymbol{u} = \mathbf{curl}\,\phi$ for some $\phi \in H_0^2(\Omega)$, and so $D^{m+1}\phi = D^m \boldsymbol{u}^\perp$ where $m = \min(k+1, s)$. By Poincaré's inequality,

$$\|\phi\|_{H^{s+1}(\Omega)} \leq C\|D^2\phi\|_{H^{s-1}(\Omega)} = C\|D\boldsymbol{u}^\perp\|_{\boldsymbol{H}^{s-1}(\Omega)} < \infty,$$

where C depends only on the domain Ω. Applying (5.1.6) and (5.2.1), we have

$$\begin{aligned}\|\boldsymbol{u}-\boldsymbol{u}_{hk}\|^2_{\boldsymbol{H}^1(\Omega)} &\le C\sum_{K\in\mathcal{T}} h_K^{2\min(k,s-1)}k^{-2(s-1)}\|D^{m+1}\phi\|^2_{H^{s-m}(\mathcal{T}_K)}\\ &\le C\sum_{K\in\mathcal{T}} h_K^{2\min(k,s-1)}k^{-2(s-1)}\|D^{m}\boldsymbol{u}\|^2_{\boldsymbol{H}^{s-m}(\mathcal{T}_K)},\end{aligned}$$

which gives (5.2.3a). In a similar vein, (5.2.3b) follows from (5.1.7), (5.2.2) and (5.2.3a) since the inf-sup constant β is independent of h and k by Theorem 5.1.1. $\square$

The approximation properties established in Theorem 5.2.1 also give the following result for finite element approximations of variational problems posed in $H_0^2(\Omega)$ using the space $\tilde{\Sigma}_0$:

Theorem 5.2.3. *Suppose that $\phi \in H^{s+1}(\Omega)\cap H_0^2(\Omega)$, $s>1$, is the unique solution to the following problem: Find $\phi\in H_0^2(\Omega)$ such that*

$$c(\phi,\psi)=\mathcal{L}(\psi) \qquad \forall\psi\in H_0^2(\Omega),$$

where $c(\cdot,\cdot) : H_0^2(\Omega)\times H_0^2(\Omega)\to\mathbb{R}$ is a coercive and continuous bilinear form on $H_0^2(\Omega)$ and $\mathcal{L} : H_0^2(\Omega)\to\mathbb{R}$ is a continuous linear functional. Then, the finite element approximation $\phi_{hk}\in\tilde{\Sigma}_0$ defined by

$$c(\phi_{hk},\psi)=\mathcal{L}(\psi) \qquad \forall\psi\in\tilde{\Sigma}_0$$

satisfies

$$\|\phi - \phi_{hk}\|^2_{H^2(\Omega)} \leq C \sum_{K \in \mathcal{T}} h_K^{2\min(k,s-1)} k^{-2(s-1)} \|D^{m+1}\phi\|^2_{H^{s-m}(\mathcal{T}_K)},$$

where $m = \min(k+1, s)$ *and* C *depends only on* s*,* Ω*, and the shape regularity parameter* κ*.*

Theorem 5.2.3 augments the previous best known result in [106, Theorem 4.1] by requiring only minimal regularity $s > 2$ (rather than $s > \frac{7}{2}$ as in [106]) and exhibiting the dependence on the mesh size explicitly.

5.2.2 Approximation in Countably Normed Spaces $\mathcal{B}^m_\delta(\Omega)$

The second set of results deals with exponential convergence of singular solutions on geometrically graded meshes. The appropriate spaces in which to work are now the countably normed spaces $B^m_\delta(\Omega)$ defined, for instance, as in [60, §2] in which δ counterbalances the usual algebraic singularities that appear in the neighborhood of vertices of the domain. In particular, by [60, Remark 5.9] if the body force is analytic, $\boldsymbol{f} \in \boldsymbol{\mathcal{B}}^0_\delta(\Omega)$, for some $0 < \delta < 1$, then the solution to the Stokes problem (4.1.3) satisfies $\boldsymbol{u} \in \boldsymbol{\mathcal{B}}^2_\delta(\Omega) \cap \boldsymbol{H}^1_0(\Omega)$ and $p \in \mathcal{B}^1_\delta(\Omega) \cap L^2_0(\Omega)$. It is easy to see that the associated stream function $\phi \in \mathcal{B}^3_\delta(\Omega) \cap H^2_0(\Omega)$. We emphasize that the presence of weights in the definitions of the spaces $B^m_\delta(\Omega)$ means that p, $\boldsymbol{u}$, and ϕ may have the usual singular behavior at the corners of the domain Ω. Nevertheless, Corollary 5.2.5

shows that the finite element approximation to (5.1.1) on properly chosen geometric meshes converges exponentially fast in terms of total number of degrees of freedom.

Let $\{\mathcal{T}^{n,\sigma} : n \in \mathbb{N}_0\}$, denote a sequence of geometrically graded meshes where $n \in \mathbb{N}_0$ denotes the number of layers and $\sigma \in (0,1)$ is the mesh grading factor as in [57, §5]. The associated finite element spaces on these meshes are given by

$$\begin{aligned}
\Sigma_0^n &:= \{\phi \in C^1(\bar{\Omega}) : \phi|_K \in \mathcal{P}_{2n+5}(K),\ \forall K \in \mathcal{T}^{n,\sigma}, \\
&\qquad\qquad \phi \text{ is } C^2 \text{ at noncorner vertices}\} \cap H_0^2(\Omega), \\
\boldsymbol{V}_0^n &:= \{\boldsymbol{v} \in \boldsymbol{C}(\bar{\Omega}) : \boldsymbol{v}|_K \in \boldsymbol{\mathcal{P}}_{2n+4}(K),\ \forall K \in \mathcal{T}^{n,\sigma}, \\
&\qquad\qquad \boldsymbol{v} \text{ is } \boldsymbol{C}^1 \text{ at noncorner vertices}\} \cap \boldsymbol{H}_0^1(\Omega), \\
Q_0^n &:= \{q \in L^2(\Omega) : q|_K \in \mathcal{P}_{2n+3}(K),\ \forall K \in \mathcal{T}^{n,\sigma}, \\
&\qquad\qquad q \text{ is } C^0 \text{ at noncorner vertices}\} \cap L_0^2(\Omega),
\end{aligned}$$

We have the following theorem:

Theorem 5.2.4. *Suppose $\psi \in \mathcal{B}_\delta^3(\Omega)$ and $q \in \mathcal{B}_\delta^1(\Omega)$. Then, there exist $\psi_n \in \Sigma_0^n$ and $q_n \in Q_0^n$ such that*

$$\|\psi - \psi_n\|_{H^2(\Omega)} \leq C \exp(-bN_\Sigma^{1/3}), \tag{5.2.4a}$$

$$\|q - q_n\|_{L^2(\Omega)} \leq C \exp(-bN_Q^{1/3}), \tag{5.2.4b}$$

where $N_\Sigma = \dim \Sigma_0^n$, $N_Q = \dim Q_0^n$, and C and b are independent of n.

Proof. (5.2.4a) is a special case of [57, Theorem 5.1] choosing $m = 2$ and using a uniform degree vector. Theorem 5.6.7 along with standard arguments e.g. [57, Theorem 5.1], gives the existence of a function

$$r_n \in \{q \in L^2(\Omega) : q|_K \in \mathcal{P}_{2n+3}(K),\ \forall K \in \mathcal{T}^{n,\sigma},\ q \text{ is } C^0 \text{ at noncorner vertices}\}$$

satisfying $\|q - r_n\|_{L^2(\Omega)} \leq C \exp(-bN_Q^{1/3})$. Although $r_n \notin L_0^2(\Omega)$ in general, defining $q_n \in L_0^2(\Omega)$ by

$$q_n = r_n - \frac{1}{|\Omega|} \int_\Omega r_n \; d\boldsymbol{x}$$

and then noting

$$q_n = r_n - \frac{1}{|\Omega|} \int_\Omega (q - r_n) \; d\boldsymbol{x}$$

followed by applying the Cauchy-Schwarz inequality gives (5.2.4b). □

Observing $\dim Q_0^n \approx \dim \boldsymbol{V}_0^n \approx \dim \Sigma_0^n$, we have the following corollary:

Corollary 5.2.5. *Suppose* $(\boldsymbol{u}, p) \in \boldsymbol{\mathcal{B}}_\delta^2(\Omega) \cap \boldsymbol{H}_0^1(\Omega) \times \mathcal{B}_\delta^1(\Omega) \cap L_0^2(\Omega)$, $0 < \beta < 1$, *solves the Stokes problem* (4.1.3). *If the mesh* $\mathcal{T}^{n,\sigma}$ *is corner-split, then the finite element approximation* $(\boldsymbol{u}_n, p_n) \in \boldsymbol{V}_0^n \times Q_0^n$ *to* (5.1.1) *satisfies*

$$\|\boldsymbol{u} - \boldsymbol{u}_n\|_{\boldsymbol{H}^1(\Omega)} + \|p - p_n\|_{L^2(\Omega)} \leq C \exp(-bN^{1/3}) \tag{5.2.5}$$

where $N = \dim \boldsymbol{V}_0^n + \dim Q_0^n$, *and* C *and* b *are positive constants independent of* n.

5.3 Notation and Preliminaries for $\tilde{Q}_0$ and $\tilde{\Sigma}_0$ Constructions

While the proofs of (5.2.1) and (5.2.2) each follow the same general approach found in [16, 17, 106], the details of the actual construction differ. The first step is to construct a (discontinuous) polynomial approximation having optimal approximation power on each element. The following result, taken from [106, Lemma 3.1], provides a useful starting point:

Lemma 5.3.1 (Lemma 3.1 [106]). *There exists a family of operators* $\hat{\Pi}_k$, $k = 1, 2, \ldots$, $\hat{\Pi}_k : H^s(\hat{T}) \to \mathcal{P}_k(\hat{T})$ *such that for any* $u \in H^s(\hat{T})$, $s \geq 0$, *the following estimates hold where, in each case,* C *is independent of* u *and* k*:*

1. *for* $0 \leq l \leq s$,

$$\left\| u - \hat{\Pi}_k u \right\|_{H^l(\hat{T})} \leq C k^{-(s-l)} \|u\|_{H^s(\hat{T})}; \tag{5.3.1}$$

2. *for* $|\alpha| < s - \frac{1}{2}$, $0 \leq l \leq s - |\alpha| - \frac{1}{2}$, $\gamma \in \mathcal{E}_{\hat{T}}$,

$$\left\| D^\alpha \left(u - \hat{\Pi}_k u \right) \right\|_{H^l(\gamma)} \leq C k^{-(s-|\alpha|-l-\frac{1}{2})} \|u\|_{H^s(\hat{T})}; \tag{5.3.2}$$

3. and for $|\alpha| < s-1$ *and* $\boldsymbol{x} \in \hat{T}$,

$$\left| D^{\alpha} \left(u - \hat{\Pi}_k u \right) (\boldsymbol{x}) \right| \leq C k^{-(s-|\alpha|-1)} \|u\|_{H^s(\hat{T})}. \tag{5.3.3}$$

Moreover, if $u \in \mathcal{P}_k(\hat{T})$, *then* $\hat{\Pi}_k u = u$.

Although Lemma 5.3.1 is stated for approximation error over the reference element, the fact that the projections $\hat{\Pi}_k$ preserve polynomials gives the following corollary on a general element in which the dependence on the element diameter h_K is made explicit:

Corollary 5.3.2. *Let* $K \in \mathcal{T}$ *and* $k \in \mathbb{N}$. *Then, there exists an operator* Π_k^K : $H^s(K) \to \mathcal{P}_k(K)$ *such that for any* $u \in H^s(K)$, $s \geq 0$, *the following estimates hold:*

1. For $0 \leq l \leq s$,

$$\left\| u - \Pi_k^K u \right\|_{H^l(K)} \leq C \frac{h_K^{\min(k+1,s)-l}}{k^{s-l}} \|D^m u\|_{H^{s-m}(K)}; \tag{5.3.4}$$

2. For $|\alpha| < s - \frac{1}{2}$, $0 \leq l \leq s - |\alpha| - \frac{1}{2}$, $\gamma \in \mathcal{E}_K$,

$$\left\| D^{\alpha} \left(u - \Pi_k^K u \right) \right\|_{H^l(\gamma)} \leq C \frac{h_K^{\min(k+1,s)-l-|\alpha|-\frac{1}{2}}}{k^{s-|\alpha|-l-\frac{1}{2}}} \|D^m u\|_{H^{s-m}(K)}; \tag{5.3.5}$$

3. For $|\alpha| < s-1$ *and* $\boldsymbol{x} \in K$*,*

$$\left|D^\alpha \left(u - \Pi_k^K u\right)(\boldsymbol{x})\right| \leq C \frac{h_K^{\min(k+1,s)-|\alpha|-1}}{k^{s-|\alpha|-1}} \|D^m u\|_{H^{s-m}(K)}; \tag{5.3.6}$$

where $m = \min(k+1, s)$ *and* C *is independent of* u*,* h_K*, and* k*. Moreover, if* $u \in \mathcal{P}_k(K)$*, then* $\Pi_k^K u = u$*.*

Proof. Let $\hat{u} \in H^s(\hat{T})$, $s \geq 0$. If $s \geq 1$, then $m = \min(k+1, s) \geq 1$. By Lemma 5.3.1, there holds

$$\|\hat{u} - \hat{\Pi}_k \hat{u}\|_{H^l(\hat{T})} = \|\hat{u} - p - \hat{\Pi}_k(\hat{u} - p)\|_{H^l(\hat{T})} \leq C k^{-(s-l)} \|\hat{u} - p\|_{H^s(\hat{T})} \qquad \forall p \in \mathcal{P}_k(\hat{T})$$

since $\hat{\Pi}_k p = p$. Taking the infimum over $p \in \mathcal{P}_k(\hat{T})$ gives

$$\|\hat{u} - \hat{\Pi}_k \hat{u}\|_{H^l(\hat{T})} \leq C k^{-(s-l)} \inf_{p \in \mathcal{P}_k(\hat{T})} \|\hat{u} - p\|_{H^s(\hat{T})},$$

and then applying the quotient norm equivalence (see e.g. [86, Theorem 7.2] for the case of integer s and [65, Lemma 2.3] for real s) gives

$$\begin{aligned}\inf_{p \in \mathcal{P}_k(\hat{T})} \|\hat{u} - p\|_{H^s(\hat{T})} &\leq C \begin{cases} \inf_{p \in \mathcal{P}_{\lfloor s \rfloor}} \|\hat{u} - p\|_{H^s(\hat{T})} & s \leq k+1, \\ \|D^m \hat{u}\|_{H^{s-m}(\hat{T})} + \inf_{p \in \mathcal{P}_k(\hat{T})} \|\hat{u} - p\|_{H^{m-1}(\hat{T})} & s > k+1, \end{cases} \\ &\leq C \|D^m \hat{u}\|_{H^{s-m}(\hat{T})}.\end{aligned}$$

Summarizing, for $s \geq 0$, there holds

$$\|\hat{u} - \hat{\Pi}_k \hat{u}\|_{H^l(\hat{T})} \leq C k^{-(s-l)} \|D^m \hat{u}\|_{H^{s-m}(\hat{T})}, \qquad \text{where} \quad m = \min(k+1, s). \quad (5.3.7)$$

For a general triangle K and $u \in H^s(K)$, $s \geq 0$, we define

$$\Pi_k^K u = \left[\hat{\Pi}_k \hat{u}\right] \circ \boldsymbol{F}_K^{-1},$$

where we recall that $\boldsymbol{F}_K : \hat{T} \to K$ is an invertible affine transformation such that $\boldsymbol{F}_K(\hat{T}) = K$ and $\hat{u} := u \circ \boldsymbol{F}_K$. (5.3.4) now follows from (5.3.7) by a standard scaling argument. Analogous arguments give (5.3.6). □

5.4 Approximation Theory for $\tilde{Q}_0$

We now build $L_0^2(\Omega)$ approximations in $\tilde{Q}_0$. For $q \in L_0^2(\Omega)$, the piecewise polynomial r defined by $r|_K = \Pi_k^K q$, where Π_k^K is the operator in Corollary 5.3.2 for $K \in \mathcal{T}$, is *not* necessarily continuous at element vertices (nor does it have mean value zero). To remedy this, we adjust r element by element so that it is continuous at the vertices and interpolates the average value of q. In order to make the adjustments, we will need certain specially constructed nodal functions:

Lemma 5.4.1. *For every $k \geq 2$ and $K \in \mathcal{T}$, there exists $\Psi_{\boldsymbol{a}} \in \mathcal{P}_k(K) \cap L_0^2(K)$,*

$\boldsymbol{a} \in \mathcal{V}_K$, such that

$$\Psi_{\boldsymbol{a}}(\boldsymbol{b}) = \delta_{\boldsymbol{ab}}, \qquad \forall \boldsymbol{b} \in \mathcal{V}_K \quad \textit{and} \quad \|\Psi_{\boldsymbol{a}}\|_{L^2(K)} \le C h_K k^{-2}, \tag{5.4.1}$$

where C is independent of h_K and k.

The proof of Lemma 5.4.1 is postponed to Section 5.8. The nodal functions in Lemma 5.4.1 are used to adjust $\Pi_k^K q$ element by element to interpolate the average value of q over K and to be continuous at the element vertices.

Lemma 5.4.2. *Let $q \in H^s(\Omega)$, $s > 0$, and let $\{\Upsilon_{\boldsymbol{a}}\}_{\boldsymbol{a} \in \mathcal{V}}$ be given constants. Then, for $k \ge 4$, there exists $z \in \tilde{Q}_0$ satisfying*

$$z(\boldsymbol{a}) = \Upsilon_{\boldsymbol{a}} \qquad \forall \boldsymbol{a} \in \mathcal{V},$$

and

$$\|q - z\|_{L^2(K)} \le C \left\{ h_K^{\min(k,s)} k^{-s} \|D^m q\|_{H^{s-m}(K)} + h_K k^{-2} \max_{\boldsymbol{a} \in \mathcal{V}_K} |\Upsilon_{\boldsymbol{a}} - \Pi_k^K q(\boldsymbol{a})| \right\} \tag{5.4.2}$$

where $m = \min(k+1, s)$ where C is independent of q, h_K, and k.

Proof. Let $K \in \mathcal{T}$ and $\mathbb{N} \ni l \geq 3$ be given. Define polynomials $v, w \in \mathcal{P}_l(K)$ by

$$v := \Pi_l^K q + \left[\frac{1}{|K|}\int_K (q - \Pi_l^K q)\, d\boldsymbol{x}\right]\left(1 - \sum_{\boldsymbol{a}\in\mathcal{V}_K} \Psi_{\boldsymbol{a}}\right)$$
$$w := \sum_{\boldsymbol{a}\in\mathcal{V}_K} (\Upsilon_{\boldsymbol{a}} - \Pi_l^K q(\boldsymbol{a}))\Psi_{\boldsymbol{a}},$$

where $\Psi_{\boldsymbol{a}} \in \mathcal{P}_l(K) \cap L_0^2(K)$, are taken as in Lemma 5.4.1. By (5.3.4) and (5.4.1) and the Cauchy-Schwarz inequality,

$$\begin{aligned}\|q - v\|_{L^2(K)} &\leq C\left\{h_K^{-1}\left(h_K + \sum_{\boldsymbol{a}\in\mathcal{V}_K} \|\Psi_{\boldsymbol{a}}\|_{L^2(K)}\right) + 1\right\}\|q - \Pi_l^K q\|_{L^2(K)} \\ &\leq C h_K^{\min(l+1,s)} l^{-s} \|D^m q\|_{H^{s-m}(K)},\end{aligned}$$

where $m = \min(l+1, s)$. Moreover, using that $\Psi_{\boldsymbol{a}} \in L_0^2(K)$ and (5.4.1), there holds

$$\int_K v\, d\boldsymbol{x} = \int_K q\, d\boldsymbol{x}, \qquad v(\boldsymbol{a}) = \Pi_l^K q(\boldsymbol{a}) \qquad \forall \boldsymbol{a} \in \mathcal{V}_K, \quad \text{and} \quad \int_K w\, d\boldsymbol{x} = 0$$

with the estimate

$$\|w\|_{L^2(K)} \leq \sum_{\boldsymbol{a}\in\mathcal{V}_K} |\Upsilon_{\boldsymbol{a}} - \Pi_l^K q(\boldsymbol{a})| \cdot \|\Psi_{\boldsymbol{a}}\|_{L^2(K)} \leq C h_K l^{-2} \max_{\boldsymbol{a}\in\mathcal{V}_K} |\Upsilon_{\boldsymbol{a}} - \Pi_l^K q(\boldsymbol{a})|.$$

Finally, we define z on element K by the rule $z|_K = v + w$. Owing to the triangle inequality, z satisfies (5.4.2). Moreover,

$$z|_K(\boldsymbol{a}) = v(\boldsymbol{a}) + w(\boldsymbol{a}) = \Pi_l^K q(\boldsymbol{a}) + \Upsilon_{\boldsymbol{a}} - \Pi_l^K q(\boldsymbol{a}) = \Upsilon_{\boldsymbol{a}} \qquad \forall \boldsymbol{a} \in \mathcal{V}_K.$$

In addition, $\int_K z\ d\boldsymbol{x} = \int_K q\ d\boldsymbol{x}$ for all K which gives $\int_\Omega z\ d\boldsymbol{x} = \int_\Omega q\ d\boldsymbol{x} = 0$, and hence taking $l = k-1$ gives $z \in \tilde{Q}_0$. □

We are now faced with the problem of choosing the nodal values specified by the constants $\{\Upsilon_{\boldsymbol{a}}\}$ in Lemma 5.4.2 so that the bound (5.2.2) holds. If q is continuous, then choosing $\Upsilon_{\boldsymbol{a}} = q(\boldsymbol{a})$ is the natural choice, whilst if q is discontinuous, then we take $\Upsilon_{\boldsymbol{a}} = \Pi_k^L q(\boldsymbol{a})$ where $L \in \mathcal{T}_{\boldsymbol{a}}$ is an arbitrarily chosen, but fixed, element in the neighborhood of $\boldsymbol{a}$. We shall need similar results when we consider approximation properties of the spaces $\tilde{\Sigma}_0$ in the next section, in which even greater continuity requirements are imposed. The following result shows that these choices ensure that the resulting approximation satisfies the bound (5.2.2) and prepares the way for generalization to the spaces $\tilde{\Sigma}_0$ later:

Lemma 5.4.3. *Let $q \in H^s(\Omega) \cap H_0^l(\Omega)$, $s \geq l \in \mathbb{N}_0$. For $k = l+3, l+4, \ldots$, define constants $\{\Upsilon_{\boldsymbol{a}}^\alpha : |\alpha| = l,\ \boldsymbol{a} \in \mathcal{V}\}$ as follows:*

(i) For interior vertices $\boldsymbol{a} \in \mathcal{V}_I$,

$$\Upsilon_{\boldsymbol{a}}^\alpha = \begin{cases} D^\alpha \Pi_k^L q(\boldsymbol{a}) & l \leq s \leq l+1 \\ D^\alpha q(\boldsymbol{a}) & s > l+1 \end{cases}$$

where $L \in \mathcal{T}_{\boldsymbol{a}}$ is any fixed but arbitrarily chosen element in the neighborhood of $\boldsymbol{a}$.

(ii) *For non-corner boundary vertices $\boldsymbol{a} \in \mathcal{V}_B$,*

$$\Upsilon_{\boldsymbol{a}}^{\alpha} = \hat{n}_x^{\alpha_1} \hat{n}_y^{\alpha_2} \cdot \begin{cases} \partial_n^l \Pi_k^L q(\boldsymbol{a}) & l \le s \le l+1 \\ \partial_n^l q(\boldsymbol{a}) & s > l+1 \end{cases}$$

where $\hat{\boldsymbol{n}}$ is the unit normal vector of Γ at $\boldsymbol{a}$ and $L \in \mathcal{T}_{\boldsymbol{a}}$ is any fixed but arbitrarily chosen element in the neighborhood of $\boldsymbol{a}$ such that L has an edge on the domain boundary, i.e. $L \cap \Gamma \in \mathcal{E}$.

(iii) *For corner vertices $\boldsymbol{a} \in \mathcal{V}_C$,*

$$\Upsilon_{\boldsymbol{a}}^{\alpha} = \begin{cases} \Pi_k^L q(\boldsymbol{a}) & l = 0,\ 0 \le s \le 1 \\ q(\boldsymbol{a}) & l = 0,\ s > 1 \\ 0 & l \ge 1 \end{cases}$$

where $L \in \mathcal{T}_{\boldsymbol{a}}$ is any fixed but arbitrarily chosen element in the neighborhood of $\boldsymbol{a}$.

Then, $\Upsilon_{\boldsymbol{a}}^{\alpha}$ satisfies the estimate

$$|\Upsilon_{\boldsymbol{a}}^{\alpha} - D^{\alpha} \Pi_k^K q(\boldsymbol{a})| \le C h_K^{\min(k-l, s-l-1)} k^{-(s-l-2)} \|D^m q\|_{H^{s-m}(\mathcal{T}_{\boldsymbol{a}})} \qquad \forall K \in \mathcal{T}_{\boldsymbol{a}}, \quad (5.4.3)$$

where $m = \min(k+1, s)$ and C is independent of q, h_K, and k.

Proof. First let $s = l$. For $\boldsymbol{a} \in \mathcal{V}_I \cup \mathcal{V}_B$, or $\boldsymbol{a} \in \mathcal{V}_C$ and $l = 0$, and $K \in \mathcal{T}_{\boldsymbol{a}}$, we apply the inverse estimate [6, Lemma 6.1] and (5.3.4) to obtain

$$|\Upsilon_{\boldsymbol{a}}^{\alpha} - D^{\alpha}\Pi_k^K q(\boldsymbol{a})| \leq C h_K^{-1} k^2 \left(\|D^l \Pi_k^L q\|_{L^2(L)} + \|D^l \Pi_k^K q\|_{L^2(K)} \right) \leq C h_K^{-1} k^2 \|D^l q\|_{L^2(\mathcal{T}_{\boldsymbol{a}})}. \tag{5.4.4}$$

Estimate (5.4.3) then follows on noting that $\min(k - l, s - l - 1) = -1$. For $\boldsymbol{a} \in \mathcal{V}_C$, we replace $\Pi_k^L q$ with 0 and apply the same argument as above.

Now let $s = l + 1$. For $\gamma \in \mathcal{E}$, let

$$|||v|||_{1/2,\gamma} := |\gamma|^{-1/2} \|v\|_{L^2(\gamma)} + |v|_{H^{1/2}(\gamma)}$$

denote a scale-invariant $H^{1/2}(\gamma)$ norm. For $\boldsymbol{a} \in \mathcal{V}_I$, or $\boldsymbol{a} \in \mathcal{V}_C$ and $l = 0$, and $K \in \mathcal{T}_{\boldsymbol{a}}$, we label the elements in $\mathcal{T}_{\boldsymbol{a}}$ as in Figure 5.1 and apply [13, Theorem 6.2] to obtain

$$|D^{\alpha}(\Pi_k^{K_j} q - \Pi_k^{K_{j+1}} q)(\boldsymbol{a})| \leq C(1 + \log^{1/2} k) \left|\left|\left| D^{\alpha}(\Pi_k^{K_j} q - \Pi_k^{K_{j+1}} q) \right|\right|\right|_{1/2,\gamma_j}$$

where $\gamma_j = K_j \cap K_{j+1}$. Since $D^{\alpha} q|_{\gamma_j} \in H^{1/2}(\gamma_j)$ by the trace theorem, we use the triangle inequality and (5.3.5) to arrive at

$$\left|\left|\left| D^{\alpha}(\Pi_k^{K_j} q - \Pi_k^{K_{j+1}} q) \right|\right|\right|_{1/2,\gamma_j} \leq \sum_{i=0}^{2} \left|\left|\left| D^{\alpha}(q - \Pi_k^{K_{j+i}} q) \right|\right|\right|_{1/2,\gamma_j} \leq C \|D^{l+1} q\|_{L^2(\mathcal{T}_{\gamma_j})}.$$

Thus, we have the bound

$$|D^\alpha(\Pi_k^L q - \Pi_k^K q)(\boldsymbol{a})| \leq \sum_{j=0}^{n-1} |D^\alpha(\Pi_k^{K_j} q - \Pi_k^{K_{j+1}} q)(\boldsymbol{a})| \leq C(1+\log^{1/2} k)\|D^{l+1}q\|_{L^2(\mathcal{T}_{\boldsymbol{a}})}.$$

Estimate (5.4.3) then follows on noting that $\min(k-l, s-l-1) = 0$ and $1+\log^{1/2} k \leq Ck$.

For $\boldsymbol{a} \in \mathcal{V}_B$ and $K \in \mathcal{T}_{\boldsymbol{a}}$, we use an analogous argument to arrive at

$$\begin{aligned} |\Upsilon_{\boldsymbol{a}}^\alpha - D^\alpha \Pi_k^K q(\boldsymbol{a})| &\leq |\Upsilon_{\boldsymbol{a}}^\alpha - D^\alpha \Pi_k^L q(\boldsymbol{a})| + \sum_{j=0}^{n-1} |D^\alpha(\Pi_k^{K_j} q - \Pi_k^{K_{j+1}} q)(\boldsymbol{a})| \\ &\leq |\Upsilon_{\boldsymbol{a}}^\alpha - D^\alpha \Pi_k^L q(\boldsymbol{a})| + Ck\|D^{l+1}q\|_{L^2(\mathcal{T}_{\boldsymbol{a}})}. \end{aligned}$$

Let $\gamma \in \mathcal{E}_L \cap \mathcal{E}_{\boldsymbol{a}}$ be such that $\gamma \subset \Gamma$. Applying [13, Theorem 6.2] again gives

$$\begin{aligned} |\Upsilon_{\boldsymbol{a}}^\alpha - D^\alpha \Pi_k^L q(\boldsymbol{a})| &\leq C(1+\log^{1/2} k) \left|\left|\left| \hat{n}_x^{\alpha_1} \hat{n}_y^{\alpha_2} \partial_n^l \Pi_k^L q - D^\alpha \Pi_k^L q \right|\right|\right|_{1/2,\gamma} \\ &\leq Ck \left(\left|\left|\left| \hat{n}_x^{\alpha_1} \hat{n}_y^{\alpha_2} \partial_n^l \Pi_k^L q - D^\alpha q \right|\right|\right|_{1/2,\gamma} + \left|\left|\left| D^\alpha(\Pi_k^L q - q) \right|\right|\right|_{1/2,\gamma} \right). \end{aligned}$$

Since $q \in H^s(\Omega) \cap H_0^l(\Omega)$, $\partial_t^i \partial_n^{l-i} q|_\gamma = 0$ for $1 \leq i \leq l$, and so

$$D^\alpha q = \hat{n}_x^{\alpha_1} \hat{n}_y^{\alpha_2} \partial_n^l q \quad \text{on } \gamma. \tag{5.4.5}$$

Thus, estimate (5.4.3) now follows from (5.3.6).

If $\boldsymbol{a} \in \mathcal{V}_C$ and $l \geq 1$, then $\boldsymbol{a} = \gamma_1 \cap \gamma_2$ for some $\gamma_1, \gamma_2 \subset \Gamma$, and there exists constants $c^{\alpha}_{i,j}$, $i = 1, 2$, $j = 1, \dots, l$ such that

$$D^{\alpha} q = \sum_{i=1}^{2} \sum_{j=1}^{l} c^{\alpha}_{i,j} \partial^{j}_{t_i} \partial^{l-j}_{n_i} q \tag{5.4.6}$$

where $\hat{\boldsymbol{n}}_i$ and $\hat{\boldsymbol{t}}_i$ are the unit normal and tangent vectors on γ_i, $i = 1, 2$. Using [13, Theorem 6.2], we obtain

$$\begin{aligned} |D^{\alpha} \Pi^{K}_{k} q(\boldsymbol{a})| &\leq C(1 + \log^{1/2} k) \sum_{i=1}^{2} \sum_{j=1}^{l} c^{\alpha}_{i,j} \left|\left|\left| \partial^{j}_{t_i} \partial^{l-j}_{n_i} \Pi^{K}_{k} q \right|\right|\right|_{1/2,\gamma_i} \\ &= C(1 + \log^{1/2} k) \sum_{i=1}^{2} \sum_{j=1}^{l} c^{\alpha}_{i,j} \left|\left|\left| \partial^{j}_{t_i} \partial^{l-j}_{n_i} (\Pi^{K}_{k} q - q) \right|\right|\right|_{1/2,\gamma_i} \end{aligned}$$

since $\partial^{i}_{t} \partial^{l-i}_{n} q|_{\gamma_1} = \partial^{i}_{t} \partial^{l-i}_{n} q|_{\gamma_2} = 0$ for $1 \leq i \leq l$, Estimate (5.4.3) now follows from analogous arguments as above.

For $l < s < l + 1$, we view $\Upsilon_{\boldsymbol{a}}$ as a (linear) function of q, and the mapping $q \mapsto \Upsilon^{\alpha}_{\boldsymbol{a}}(q)$ has the following property: $\Upsilon^{\alpha}_{\boldsymbol{a}}(q+p) = \Upsilon^{\alpha}_{\boldsymbol{a}}(q) + p(\boldsymbol{a})$ for all $p \in \mathcal{P}_k(\mathcal{T}_{\boldsymbol{a}})$. Thus, we use a standard interpolation argument to the operator $q \mapsto \Upsilon^{\alpha}_{\boldsymbol{a}}(q) - D^{\alpha} \Pi^{K}_{k} q(\boldsymbol{a})$ to obtain

$$|\Upsilon^{\alpha}_{\boldsymbol{a}}(q) - D^{\alpha} \Pi^{K}_{k} q(\boldsymbol{a})| \leq C h_K^{s-l-1} k^{-(s-l-2)} \|q\|_{H^s(\mathcal{T}_{\boldsymbol{a}})}.$$

Equation (5.4.3) now follows from a quotient space argument with [65, Lemma 2.3]:

$$\begin{aligned}
|\Upsilon^{\alpha}_{\boldsymbol{a}}(q) - D^{\alpha}\Pi^K_k q(\boldsymbol{a})| &= \inf_{p\in\mathcal{P}_k(\mathcal{T}_{\boldsymbol{a}})} |\Upsilon^{\alpha}_{\boldsymbol{a}}(q-p) - D^{\alpha}\Pi^K_k(q-p)(\boldsymbol{a})| \\
&\le C h_K^{s-l-1} k^{-(s-l-2)} \inf_{p\in\mathcal{P}_{\lfloor s\rfloor}(\mathcal{T}_{\boldsymbol{a}})} \|q-p\|_{H^s(\mathcal{T}_{\boldsymbol{a}})} \\
&\le C h_K^{s-l-1} k^{-(s-l-2)} |q|_{H^s(\mathcal{T}_{\boldsymbol{a}})}.
\end{aligned}$$

In the case $s > l+1$. (5.4.3) follows from (5.3.6), (5.4.5) and (5.4.6). $\square$

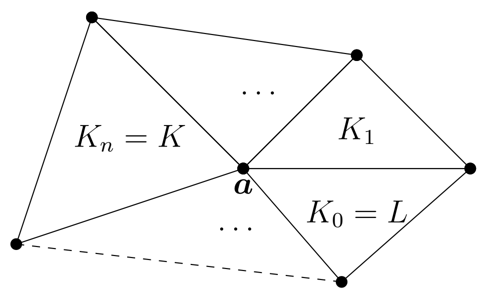

Figure 5.1: Schema for the proof of Lemma 5.4.3.

The estimate (5.2.2) now follows as a simple consequence of Lemma 5.4.2 on choosing the constants $\Upsilon^{\alpha}_{\boldsymbol{a}}$ as in Lemma 5.4.3 in the special case $l = 0$.

5.5 Approximation Theory for $\tilde{\Sigma}_0$

Let $\phi \in H^s(\Omega)$, $s > 2$, be given. The discontinuous polynomials $\Pi^K_{k+1}\phi$ from Corollary 5.3.2 again provide the starting point for constructing an approximation from the space $\tilde{\Sigma}_0$. However, this time we need to adjust $\Pi^K_{k+1}\phi$ in order to obtain C^2 continuity at element vertices. We first carry out nodal adjustments similar to the one used in the case of $\tilde{Q}_0$ to obtain C^0 continuity at the vertices. The Sobolev embedding theorem means that ϕ and $D\phi$ are continuous at the vertices, so we adjust $\Pi^K_{k+1}\phi$ to interpolate ϕ and $D\phi$ at the vertices. However, since ϕ is not necessarily C^2, similarly to the argument used for $\tilde{Q}_0$, we adjust $\Pi^K_{k+1}\phi$ to obtain an approximation where second order derivatives at the vertices are given by constants $\Upsilon^\alpha_{\boldsymbol{a}} : |\alpha| = 2$. The values of the constants $\Upsilon^\alpha_{\boldsymbol{a}}$ are chosen as in Lemma 5.4.3. In order to make the corrections, we require the analogue of the Ψ functions in Lemma 5.4.1. Fortunately, we constructed such functions in Section 3.7. Note that we also give estimates in the $H^{1/2}_{00}$ and $H^{3/2}_{00}$ norms on element edges (see Section 2.3 for the definition of these spaces), which will be used later to further modify the construction to ensure global C^1 continuity across edges.

Lemma 5.5.1. *Let $\phi \in H^{s+1}(\Omega) \cap H^2_0(\Omega)$ with $s > 1$ and $k \geq 4$. Then, there exists*

$$z \in \{\psi \in L^2(\Omega) : \psi|_K \in \mathcal{P}_{k+1}(K)\ \forall K \in \mathcal{T},\ \psi \textit{ is } C^2 \textit{ at all vertices}\}$$

such that

$$D^\alpha z(\boldsymbol{a}) = \begin{cases} D^\alpha \phi(\boldsymbol{a}) & |\alpha| \leq 1 \\ \Upsilon^\alpha_{\boldsymbol{a}} & |\alpha| = 2 \end{cases} \qquad \forall \boldsymbol{a} \in \mathcal{V}, \tag{5.5.1}$$

where $\Upsilon_{\boldsymbol{a}}^{\alpha}$ *are given by Lemma 5.4.3 with* $l = 2$*, and for all* $K \in \mathcal{T}$ *and* $\gamma \in \mathcal{E}_K$*,*

$$\|\phi - z\|_{H^2(K)} \leq C h_K^{\min(k,s-1)} k^{-(s-1)} \|D^{m+1}\phi\|_{H^{s-m}(\mathcal{T}_K)}, \tag{5.5.2}$$

$$\|\phi - z|_K\|_{H_{00}^{3/2}(\gamma)} + \|\partial_n(\phi - z|_K)\|_{H_{00}^{1/2}(\gamma)} \leq C h_K^{\min(k,s-1)} k^{-(s-1)} \|D^{m+1}\phi\|_{H^{s-m}(\mathcal{T}_K)}, \tag{5.5.3}$$

where $m = \min(k+1, s)$ *and* C *is independent of* ϕ*,* h_K*, and* k*.*

Proof. Let $K \in \mathcal{T}$ be given. For $|\alpha| \leq 1$, let $\Phi_{\boldsymbol{a}}^{\alpha}$ denote the degree 5 polynomial satisfying

$$D^{\beta}\Phi_{\boldsymbol{a}}^{\alpha}(\boldsymbol{b}) = \delta_{\alpha\beta}\delta_{\boldsymbol{ab}} \quad \text{and} \quad \partial_n \Phi_{\boldsymbol{a}}^{\alpha}(\boldsymbol{m}_j) = 0 \qquad \forall |\beta| \leq 2,\ \forall \boldsymbol{b} \in \mathcal{V}_K,\ 1 \leq j \leq 3,$$

where $\boldsymbol{m}_j$ is the midpoint on γ_j. It is simple to verify for $0 \leq l \leq 2$,

$$\|\Phi_{\boldsymbol{a}}^{\alpha}\|_{H^l(K)} \leq C h_K^{|\alpha|-l+1} \quad \text{and} \quad \|\Phi_{\boldsymbol{a}}^{\alpha}\|_{H^l(\gamma_j)} \leq C h_K^{|\alpha|-l+\frac{1}{2}}. \tag{5.5.4}$$

For $|\alpha| = 2$, let $\Phi_{\boldsymbol{a}}^{\alpha}$ denote the degree $k+1$ polynomial in Section 3.7 which satisfies

$$D^{\beta}\Phi_{\boldsymbol{a}}^{\alpha}(\boldsymbol{b}) = \delta_{\alpha\beta}\delta_{\boldsymbol{ab}} \qquad \forall |\beta|,\ \forall \boldsymbol{b} \in \mathcal{V}_K, \qquad D^{\beta}\Phi_{\boldsymbol{a}}^{\alpha}|_{\gamma_{\boldsymbol{a}}} = 0 \qquad \forall |\beta| \leq 1,$$

and

$$\|\Phi_{\boldsymbol{a}}^{\alpha}\|_{H^2(K)} \leq C \sum_{\gamma \in \mathcal{E}_K} \left(\|\Phi_{\boldsymbol{a}}^{\alpha}\|_{H_{00}^{3/2}(\gamma)} + \|\partial_n \Phi_{\boldsymbol{a}}^{\alpha}\|_{H_{00}^{1/2}(\gamma)} \right) \leq C h_K k^{-2}. \tag{5.5.5}$$

Define the polynomials $v, w \in \mathcal{P}_{k+1}(K)$ by

$$v := \Pi_{k+1}^K \phi + \sum_{\substack{\boldsymbol{a} \in \mathcal{V}_K \\ |\alpha| \leq 1}} D^{\alpha} \left(\phi - \Pi_{k+1}^K \phi \right) (\boldsymbol{a}) \Phi_{\boldsymbol{a}}^{\alpha} \quad \text{and} \quad w := \sum_{\substack{\boldsymbol{a} \in \mathcal{V}_K \\ |\alpha| = 2}} \left(\Upsilon_{\boldsymbol{a}}^{\alpha} - D^{\alpha} \Pi_{k+1}^K \phi(\boldsymbol{a}) \right) \Phi_{\boldsymbol{a}}^{\alpha}.$$

Since $s+1 > 2$, $\phi \in C^1(\bar{K})$ and so v and w are well-defined. By (5.3.4), (5.3.6) and (5.5.4),

$$\begin{aligned}
\|\phi - v\|_{H^2(K)} &\leq \|\phi - \Pi_{k+1}^K \phi\|_{H^2(K)} + \sum_{\substack{\boldsymbol{a} \in \mathcal{V}_K \\ |\alpha| \leq 1}} \left| D^{\alpha} \left(\phi - \Pi_{k+1}^K \phi \right) (\boldsymbol{a}) \right| \cdot \|\Phi_{\boldsymbol{a}}^{\alpha}\|_{H^2(K)} \\
&\leq C h_K^{\min(k,s-1)} \left(k^{-(s-1)} + \sum_{\substack{\boldsymbol{a} \in \mathcal{V}_K \\ |\alpha| \leq 1}} k^{-(s-|\alpha|)} \right) \|D^{m+1} \phi\|_{H^{s-m}(K)} \\
&\leq C h_K^{\min(k,s-1)} k^{-(s-1)} \|D^{m+1} \phi\|_{H^{s-m}(K)},
\end{aligned}$$

where $m = \min(k+1, s)$, and by (5.4.3) and (5.5.5)

$$\begin{aligned}
\|w\|_{H^2(K)} &\leq \sum_{\substack{\boldsymbol{a} \in \mathcal{V}_K \\ |\alpha| = 2}} \left| \Upsilon_{\boldsymbol{a}}^{\alpha} - D^{\alpha} \Pi_{k+1}^K \phi(\boldsymbol{a}) \right| \cdot \|\Phi_{\boldsymbol{a}}^{\alpha}\|_{H^2(K)} \\
&\leq C h_K^{\min(k,s-1)} k^{-(s-1)} \|D^{m+1} \phi\|_{H^{s-m}(K)}.
\end{aligned}$$

Let $\gamma \in \mathcal{E}_K$. $D^\alpha \phi(\boldsymbol{a}) = D^\alpha v(\boldsymbol{a})$, $\forall |\alpha| \le 1$, $\forall \boldsymbol{a} \in \mathcal{V}_K$, and so $\phi - v \in H^{3/2}_{00}(\gamma)$. By (5.3.6) and (5.5.4),

$$\begin{aligned} \|\phi - v\|_{H^t(\gamma)} &\le \|\phi - \Pi^K_{k+1}\phi\|_{H^t(\gamma)} + \sum_{\substack{\boldsymbol{a}\in\mathcal{V}_K \\ |\alpha|\le 1}} \left|D^\alpha \left(\phi - \Pi^K_{k+1}\phi\right)(\boldsymbol{a})\right| \cdot \|\Phi^\alpha_{\boldsymbol{a}}\|_{H^t(\gamma)} \\ &\le C h_K^{\min(k,s-1)-t-\frac{1}{2}} k^{-\left(s-t+\frac{1}{2}\right)} \|D^{m+1}\phi\|_{H^{s-m}(K)}, \end{aligned}$$

for $0 \le t \le s + \frac{1}{2}$. Since $s + \frac{1}{2} > \frac{3}{2}$, we may use [74, Theorem 6.1] to conclude

$$H^{3/2}_{00}(\gamma) = (H^1_0(\gamma), H^2_0(\gamma))_{\frac{1}{2},2} = (H^1_0(\gamma), H^{s+1/2}_0(\gamma))_{\theta,2}, \quad \text{where} \quad \theta = \frac{1}{2s-1},$$

and so

$$\begin{aligned} \|\phi - v\|_{H^{3/2}_{00}(\gamma)} &\le C \|\phi - v\|^{1-\theta}_{H^1(\gamma)} \|\phi - v\|^{\theta}_{H^{s+1/2}_0(\gamma)} \\ &\le C h_K^{\min(k,s-1)} k^{-(s-1)} \|D^{m+1}\phi\|_{H^{s-m}(K)}. \end{aligned}$$

Using an analogous argument, we have $\partial_n(\phi - v) \in H^{1/2}_{00}(\gamma)$ with

$$\|\partial_n(\phi - v)\|_{H^{1/2}_{00}(\gamma)} \le C h_K^{\min(k,s-1)} k^{-(s-1)} \|D^{m+1}\phi\|_{H^{s-m}(K)}.$$

Similarly, $\Phi^\alpha_{\boldsymbol{a}} \in H^{3/2}_{00}(\gamma)$, $\partial_n \Phi^\alpha_{\boldsymbol{a}} \in H^{1/2}_{00}(\gamma)$, $\forall |\alpha| = 2$, $\forall \boldsymbol{a} \in \mathcal{V}_K$, and by (5.4.3) and (5.5.5),

$$\|w\|_{H^{3/2}_{00}(\gamma)} + \|\partial_n w\|_{H^{1/2}_{00}(\gamma)} \le C h_K^{\min(k,s-1)} k^{-(s-1)} \|D^{m+1}\phi\|_{H^{s-m}(K)}.$$

Now, we define z on element K by the rule $z|_K = v + w$. Owing to the triangle inequality, z satisfies (5.5.2) and (5.5.3) and owing to the interpolation properties of $\Phi_{\boldsymbol{a}}^{\alpha}$, $|\alpha| \leq 2$, $\boldsymbol{a} \in \mathcal{V}_K$, z satisfies (5.5.1). $\square$

The approximation defined in Lemma 5.5.1 is C^2 at the vertices. However, the approximant is not necessarily globally C^1, nor does it have vanishing trace and vanishing normal derivative trace. We remedy this issue by applying edge corrections. The key ingredients are the error estimates on the edges (5.5.3) and a polynomial extension theorem Corollary 2.2.3 and its scale-invariant version Corollary 3.7.2:

Proof of (5.2.1). Let $\phi \in H^{s+1}(\Omega) \cap H_0^2(\Omega)$, $s > 1$. By Lemma 5.5.1, there exists

$$z \in \{\phi \in L^2(\Omega) : \phi|_K \in \mathcal{P}_{k+1}(K)\ \forall K \in \mathcal{T},\ \phi \text{ is } C^2 \text{ at vertices}\}$$

satisfying (5.5.1) to (5.5.3). For each $\gamma \in \mathcal{E}$, we let $\hat{\boldsymbol{n}}_\gamma$ denote a unit vector normal to γ. Let $K_\gamma, L_\gamma \in \mathcal{T}$ denote the two elements such that $K_\gamma \cap L_\gamma = \gamma$ if $\gamma \in \mathcal{E}_I$ and K_γ the element such that $K_\gamma \cap \Gamma = \gamma$ and $L_\gamma = \emptyset$ if $\gamma \subset \Gamma$. Define the polynomials $f_\gamma \in \mathcal{P}_{k+1}(\gamma)$ and $g_\gamma \in \mathcal{P}_k(\gamma)$ by the rule

$$f_\gamma = \left(z|_{L_\gamma} - z|_{K_\gamma}\right)|_\gamma, \quad \text{and} \quad g_\gamma = \partial_n \left(z|_{L_\gamma} - z|_{K_\gamma}\right)|_\gamma,$$

where $z|_{L_\gamma} = 0$ if $L_\gamma = \emptyset$. For $\boldsymbol{a} \in \partial\gamma$, the following relations hold by (5.5.1) and Lemma 5.4.3:

(i) $D^\alpha z|_{L_\gamma}(\boldsymbol{a}) = D^\alpha z|_{K_\gamma}(\boldsymbol{a}) = D^\alpha \phi(\boldsymbol{a})$ for $|\alpha| \le 1$.

(ii) For $\boldsymbol{a} \in \mathcal{V}_I$, $D^\alpha z|_{L_\gamma}(\boldsymbol{a}) = D^\alpha z|_{K_\gamma}(\boldsymbol{a})$, $|\alpha| = 2$.

(iii) For $\boldsymbol{a} \in \mathcal{V}_B$,

$$\partial_{tt} z|_{K_\gamma}(\boldsymbol{a}) = \hat{t}_x^2 \partial_{xx} z|_{K_\gamma}(\boldsymbol{a}) + 2\hat{t}_x \hat{t}_y \partial_{xy} z|_{K_\gamma}(\boldsymbol{a}) + \hat{t}_y^2 \partial_{yy} z|_{K_\gamma}(\boldsymbol{a}) = (\hat{\boldsymbol{t}} \cdot \hat{\boldsymbol{n}})^2 d_{\boldsymbol{a}} = 0,$$

where $\hat{\boldsymbol{t}}$ and $\hat{\boldsymbol{n}}$ are the unit tangent and normal vectors to Γ at $\boldsymbol{a}$ and

$$d_{\boldsymbol{a}} = \begin{cases} \partial_n^2 \Pi_k^L \phi(\boldsymbol{a}) & 1 < s \le 2, \\ \partial_n^2 \phi(\boldsymbol{a}) & s > 2, \end{cases}$$

where $L \in \mathcal{T}$ is defined in Lemma 5.4.3. Similarly, $\partial_{nt} z|_{K_\gamma}(\boldsymbol{a}) = (\hat{\boldsymbol{t}} \cdot \hat{\boldsymbol{n}}) d_{\boldsymbol{a}} = 0$.

(iv) For $\boldsymbol{a} \in \mathcal{V}_C$, $D^\alpha z|_{K_\gamma}(\boldsymbol{a}) = 0$ for $|\alpha| = 2$.

Thus, $f_\gamma \in H_0^3(\gamma)$ and $g_\gamma \in H_0^2(\gamma)$. By (5.5.3),

$$\|f_\gamma\|_{H_{00}^{3/2}(\gamma)} + \|g_\gamma\|_{H_{00}^{1/2}(\gamma)} \le C h_{K_\gamma}^{\min(k,s-1)} k^{-(s-1)} \|D^{m+1}\phi\|_{H^{s-m}(K_\gamma \cup L_\gamma)}, \tag{5.5.6}$$

where $m = \min(k+1, s)$.

We now construct $\phi_{hk} \in \Sigma_0$ element by element. Let $K \in \mathcal{T}$ and $\gamma \in \mathcal{E}_K$ be given. If $K = K_\gamma$, we define the functions $F_\gamma \in L^2(\partial K)$, $G_\gamma \in L^2(\partial K)$ by the rule

$$F_\gamma|_{\gamma'} = f_\gamma \delta_{\gamma\gamma'}, \quad G_\gamma|_{\gamma'} = g_\gamma \delta_{\gamma\gamma'}, \quad \gamma' \in \mathcal{E}_K.$$

$D^\alpha F_\gamma(\boldsymbol{a}) = D^\beta G_\gamma(\boldsymbol{a}) = 0$ for $|\alpha| \le 2$, $|\beta| \le 1$, $\boldsymbol{a} \in \mathcal{V}_K$, and so Corollary 3.7.2 asserts the existence of $w_\gamma \in \mathcal{P}_{k+1}(K)$ such that

$$w_\gamma = F_\gamma \quad \text{and} \quad \partial_n w_\gamma| = G_\gamma \quad \text{on } \partial K$$

and

$$\|w_\gamma\|_{H^2(K)} \le C\big(h_K^{-3/2}\|F_\gamma\|_{L^2(\partial K)} + h_K^{-1/2}\|\partial_t F\hat{\boldsymbol{n}} - G\hat{\boldsymbol{t}}\|_{\boldsymbol{L}^2(\partial K)} + |\partial_t F\hat{\boldsymbol{n}} - G\hat{\boldsymbol{t}}|_{\boldsymbol{H}^{1/2}(\partial K)}\big).$$

Since F and G are supported only on γ and $f_\gamma \in H_0^3(\gamma)$ and $g_\gamma \in H_0^2(\gamma)$, we use Poincaré's inequality to arrive at

$$\|w_\gamma\|_{H^2(K)} \le C\left(|f_\gamma|_{H_{00}^{3/2}(\gamma)} + |g_\gamma|_{H_{00}^{1/2}(\gamma)}\right). \tag{5.5.7}$$

If $K = L_\gamma$, we take $w_\gamma = 0$. By (5.5.6) and (5.5.7),

$$\|w_\gamma\|_{H^2(K)} \le Ch_K^{\min(k,s-1)} k^{-(s-1)} \|D^{m+1}\phi\|_{H^{s-m}(\mathcal{T}_\gamma)}. \tag{5.5.8}$$

Now, we define ϕ_{hk} on element K by

$$\phi_{hk} = z + \sum_{\gamma \in \mathcal{E}_K} w_\gamma \quad \text{on } K.$$

By construction, $\phi_{hk} \in C^1(\bar{\Omega}) \cap H_0^2(\Omega)$ and is C^2 at *all* vertices. Thus, $\phi_{hk} \in \tilde{\Sigma}_0$. Moreover, (5.2.1) follows from (5.5.2) and (5.5.8). $\square$

5.6 Approximation Theory for Q_0^n

In this section, we turn to approximation in countably normed spaces and begin by establishing some technical results that are needed to prove exponential convergence of the finite element method using geometrically graded meshes. To this end, we define the weighted Sobolev spaces $H_\delta^{k,l}(\hat{T})$, $k \geq l \geq 0$, $0 < \delta < 1$ on the reference element $\hat{T}$ (see Figure 5.2) to be the completion of smooth functions under the norm

$$\|u\|^2_{H_\delta^{k,l}(\hat{T})} := \sum_{j=0}^{l-1} \int_{\hat{T}} r^{2\delta} |D^j u|^2 \, d\boldsymbol{x} + \sum_{j=l}^{k} \int_{\hat{T}} r^{2(\delta+j-l)} |D^j u|^2 \, d\boldsymbol{x},$$

where $r = |\boldsymbol{x}|$. Such spaces have been widely studied, e.g. [14, 15, 57, 60, 98], for various choices of parameters k and l. Unfortunately, the extra smoothness of functions in Q_0^n at the noncorner vertices means that the choices of k and l we need do work not fall within previously studied cases, and some additional results will be required.

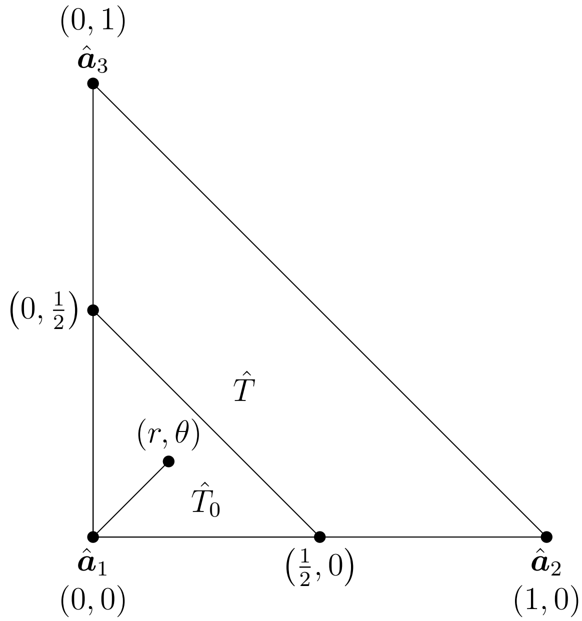

Figure 5.2: Reference triangles $\hat{T}$ and $\hat{T}_0$ and polar coordinates (r, θ).

We begin with a result inspired by [15, Lemma 4.3]:

Lemma 5.6.1. *Let $\delta > 0$ and u be a measurable function on $\hat{T}$ such that*

$$\int_{\hat{T}} r^{2\delta} |Du|^2 \; d\boldsymbol{x} + \int_{\hat{T}\setminus\hat{T}_0} |u|^2 \; d\boldsymbol{x} < \infty,$$

where $\hat{T}$ and $\hat{T}_0$ are as shown in Figure 5.2. Then, there exists a constant $a(u) \in \mathbb{R}$ such that

$$\int_{\hat{T}} r^{2\delta-2} |u - a(u)|^2 \; d\boldsymbol{x} \leq C \int_{\hat{T}} r^{2\delta} |Du|^2 \; d\boldsymbol{x} \tag{5.6.1}$$

with

$$|a(u)| \leq C \left(\int_{\hat{T}} r^{2\delta} |Du|^2 \; d\boldsymbol{x} + \int_{\hat{T} \setminus \hat{T}_0} |u|^2 \; d\boldsymbol{x} \right)^{1/2} \tag{5.6.2}$$

and C independent of u.

Proof. The proof of [15, Lemma 4.3] gives (5.6.1) with the reference triangle $\hat{T}$ replaced by the sector $S = \{(r, \theta) : 0 \leq r \leq 1, \; 0 \leq \theta \leq \pi/2\}$ and

$$a(u) = \frac{2}{\pi} \int_0^{\pi/2} u(1, \theta) \; d\theta,$$

where (r, θ) denote polar coordinates. Using the trace theorem, there holds

$$|a(u)|^2 \leq C \int_0^{\pi/2} u^2(1, \theta) \; d\theta \leq C \|u\|^2_{H^1(S \setminus S_0)},$$

where $S_0 = \{(r, \theta) : 0 \leq r \leq 1/2, \; 0 \leq \theta \leq \pi/2\}$. Transforming to $\hat{T}$ and $\hat{T}_0$ using the (smooth) mapping $(r, \theta) \mapsto (r(\cos\theta + \sin\theta), \theta)$ gives (5.6.1) and (5.6.2). $\square$

Using this result, we have the following lemma which allows us to trade powers of r for derivatives of u at the expense of an additional term involving the L^2 norm of u on a set excluding the singularity in u:

Lemma 5.6.2. *Let $u \in H^{1,0}_\delta(\hat{T})$, $0 < \delta < 1$. Then,*

$$\int_{\hat{T}} r^{2\delta} |u|^2 \; d\boldsymbol{x} \leq C \left\{ \int_{\hat{T}} r^{2\delta+2} |Du|^2 \; d\boldsymbol{x} + \int_{\hat{T} \setminus \hat{T}_0} |u|^2 \; d\boldsymbol{x} \right\},$$

and C is independent of u.

Proof. Applying Lemma 5.6.1, we have

$$\int_{\hat{T}} r^{2\delta}|u|^2 \; d\boldsymbol{x} \leq 2\int_{\hat{T}} r^{2\delta}(|u-a|^2+|a|^2) \; d\boldsymbol{x} \leq C\left\{ \int_{\hat{T}} r^{2\delta+2}|Du|^2 \; d\boldsymbol{x} + \int_{\hat{T}\setminus\hat{T}_0} |u|^2 \; d\boldsymbol{x} \right\}.$$

□

The next two results concern the compact embedding properties of the spaces $H^{1,1}_\delta(\hat{T})$ and $H^{2,1}_\delta(\hat{T})$.

Lemma 5.6.3. *The space $H^{1,1}_\delta(\hat{T})$, $0<\delta<1$, is compactly embedded in $L^2(\hat{T})$.*

Proof. Let $u \in H^{1,1}_\delta(\hat{T})$ with $a(u)=0$, where $a(u)$ is given by Lemma 5.6.1, and (r,θ) be polar coordinates centered at the origin as in Figure 5.2. Then, $v = r^\delta u$ satisfies

$$\partial_\theta v = r^\delta \partial_\theta u \quad \text{and} \quad \partial_r v = r^\delta \partial_r u + \delta r^{\delta-1} u.$$

Since $a(u)=0$, (5.6.1) gives $\|r^{\delta-1}u\|_{L^2(\hat{T})} \leq C\|u\|_{H^{1,1}_\delta(\hat{T})}$, and so $v \in H^1(\hat{T})$ with $\|v\|_{H^1(\hat{T})} \leq C\|u\|_{H^{1,1}_\delta(\hat{T})}$.

Let $\{u_k\}_{k=1}^\infty$ be a bounded sequence in $H^{1,1}_\delta(\hat{T})$ with $a(u_k)=0$. Then, $v_k = r^\delta u_k$, $k=1,2,\ldots$, is a uniformly bounded sequence in $H^1(\hat{T})$ and there exists a subsequence $\{v_{k_j}\}_{j=1}^\infty$ converging weakly in $H^1(\hat{T})$ to $v \in H^1(\hat{T})$. Since $H^1(\hat{T})$ is compactly embedded in $L^q(\hat{T})$ for $1 \le q < \infty$, $v_{k_j} \to v$ strongly in $L^q(\hat{T})$. Define $u := r^{-\delta} v$. By Hölder's inequality, we obtain

$$\|u\|_{L^2(\hat{T})} \le \|r^{-\delta p}\|_{L^2(\hat{T})}^{1/p} \|v^q\|_{L^2(\hat{T})}^{1/q} \le \|r^{-\delta p}\|_{L^2(\hat{T})}^{1/p} \|v\|_{L^{2q}(\hat{T})},$$

where $p^{-1} + q^{-1} = 1$. Choosing q such that $1 < p < \delta^{-1}$ gives $u \in L^2(\hat{T})$. An analogous argument shows that $u_k \in L^2(\hat{T})$ and $\|u_{k_j} - u\|_{L^2(\hat{T})} \le C\|v_{k_j} - v\|_{L^{2q}(\hat{T})}$; thus, $u_{k_j} \to u$ strongly in $L^2(\hat{T})$.

We extend the result to a general bounded sequence as follows. Let $\{u_k\}_{k=1}^{\infty}$ be a bounded sequence in $H_\delta^{1,1}(\hat{T})$ and define $\tilde{u}_k = u_k - a(u_k)$. Then, $a(\tilde{u}_k) = 0$ by definition and $\|\tilde{u}_k\|_{H_\delta^{1,1}(\hat{T})} + |a(u_k)| \le C\|u\|_{H_\delta^{1,1}(\hat{T})}$ by (5.6.2). Thus, there exists a subsequence such that $\tilde{u}_{k_j} \to \tilde{u} \in L^2(\hat{T})$ and $a(u_{k_j}) \to \tilde{a}$. Then, $u_{k_j} \to u := \tilde{u} + \tilde{a}$ in $L^2(\hat{T})$ by the triangle inequality:

$$\|u_{k_j} - \bar{u}\|_{L^2(\hat{T})} \le \|\tilde{u}_{k_j} - \tilde{u}\|_{L^2(\hat{T})} + \|a(u_{k_j}) - \tilde{a}\|_{L^2(\hat{T})} \to 0.$$

$\square$

Lemma 5.6.4. *The space $H_\delta^{2,1}(\hat{T})$, $0 < \delta < 1$, is compactly embedded in $H_{\delta^*}^{1,1}(\hat{T})$ for any $\delta^* \in (\delta, 1)$.*

Proof. Let $u \in H_\delta^{2,1}(\hat{T})$ with $a(u) = 0$, where $a(u)$ is given by Lemma 5.6.1, and define $v = r^{\delta+1}u$. Then,

$$\begin{aligned}
\partial_\theta^m v &= r^{\delta+1}\partial_\theta u, && 0 \le m \le 2,\\
\partial_\theta^n \partial_r v &= (\delta+1)r^\delta \partial_\theta^n u + r^{\delta+1}\partial_\theta^n \partial_r u, && 0 \le n \le 1,\\
\partial_{rr} v &= \delta(\delta+1)r^{\delta-1}u + 2(\delta+1)r^\delta \partial_r u + r^{\delta+1}\partial_{rr}u.
\end{aligned}$$

By (5.6.1), $\|r^{\delta-1}u\|_{L^2(\hat{T})} \le C\|r^\delta Du\|_{L^2(\hat{T})}$, and so $v \in H^2(\hat{T})$ with the bound $\|v\|_{H^2(\hat{T})} \le C\|u\|_{H^{2,1}_\delta(\hat{T})}$. In particular, v is continuous with $v(0,0) = 0$ since

$$|v(0,0)|^2 = \lim_{\delta\to 0} |S_\delta|^{-1} \int_{S_\delta} |v|^2 \, d\boldsymbol{x} \le C \lim_{\delta\to 0} \int_{S_\delta} r^{2\delta}|u|^2 \, d\boldsymbol{x} = 0,$$

where $S_\delta := \{\boldsymbol{x} \in \hat{T} : |\boldsymbol{x}| < \delta\}$.

Now let $\{u_k\}_{k=1}^\infty$ be a bounded sequence in $H^{2,1}_\delta(\hat{T})$ satisfying $a(u_k) = 0$. Then, $v_k = r^{\delta+1}u_k$, $k = 1, 2, \ldots$, is a uniformly bounded sequence in $H^2(\hat{T})$ satisfying $v_k(0,0) = 0$, and there is a subsequence $\{v_{k_j}\}_{j=1}^\infty$ converging weakly in $H^2(\hat{T})$ to $v \in H^2(\hat{T})$. Moreover, $v(0,0) = 0$ since pointwise evaluation is a continuous linear functional on $H^2(\hat{T})$. Since $H^2(\hat{T})$ is compactly embedded in $W^{1,q}(\hat{T})$ for all $q \in [1,\infty)$, $v_{k_j} \to v$ strongly in $W^{1,q}(\hat{T})$.

Define $u = r^{-(\delta+1)}v$ and let $\delta^* \in (\delta, 1)$. Then,

$$\partial_\theta u = r^{-(\delta+1)}\partial_\theta v \quad \text{and} \quad \partial_r u = -(\delta+1)r^{-(\delta+2)}v + r^{-(\delta+1)}\partial_r \bar{v}.$$

Applying [15, Lemma 4.3] with $\alpha = -2(\delta+1)$ and using that v is continuous with $v(0) = 0$, we have

$$\|u\|_{H^{1,1}_{\delta^*}(\hat{T})} \leq C\left\{\|r^{-(\delta-\delta^*+1)}v\|_{L^2(\hat{T})} + \|r^{-(\delta-\delta^*+1)}Dv\|_{L^2(\hat{T})}\right\}.$$

Using Hölder's inequality, there holds

$$\|u\|_{H^{1,1}_{\delta^*}(\hat{T})} \leq C\|r^{-(\delta-\delta^*+1)}\|_{L^{2p}(\hat{T})}\|v\|_{W^{1,2q}(\hat{T})}.$$

Choosing q such that $1 < p < (\delta - \delta^* + 1)^{-1}$ gives $u \in H^{1,1}_{\delta^*}(\hat{T})$ with $\|u\|_{H^{1,1}_{\delta^*}(\hat{T})} \leq C\|v\|_{W^{1,2q}(\hat{T})}$. By an analogous argument,

$$\|u_{k_j} - u\|_{H^{1,1}_{\delta^*}(\hat{T})} \leq C\|v_{k_j} - v\|_{W^{1,2q}(\hat{T})} \to 0.$$

Thus, $u_{k_j} \to u$ strongly in $H^{1,1}_{\delta^*}(\hat{T})$.

The case $a(u_k) \neq 0$ follows a similar argument to the one used in the proof of Lemma 5.6.3. □

We now construct an affine approximation to functions in $H^{2,1}_{\delta}(K)$ which is continuous with respect to the seminorm defined by

$$|u|^2_{H^{2,1}_{\delta}(\hat{T})} := \int_{\hat{T}} r^{2(\beta+1)}|D^2u|^2 \, d\boldsymbol{x}.$$

The argument uses the foregoing embedding theorems to give an equivalent norm on the space.

Lemma 5.6.5. *Let $u \in H^{2,1}_\delta(\hat{T})$ and let $q \in \mathcal{P}_1(\hat{T})$ be the affine function satisfying $q(\hat{\boldsymbol{a}}_i) = u(\hat{\boldsymbol{a}}_i)$, $i = 2, 3$, and $\int_{\hat{T}}(u - q) = 0$. Then,*

$$\|u - q\|_{L^2(\hat{T})} + \|u - q\|_{H^{2,1}_\delta(\hat{T})} \leq C|u|_{H^{2,1}_\delta(\hat{T})}$$

with C independent of u.

Proof. We first show that

$$|\!|\!|u|\!|\!|^2 := |u|^2_{H^{2,1}_\delta(\hat{T})} + \sum_{i=2}^{3} |u(\hat{\boldsymbol{a}}_i)|^2 + \left(\int_{\hat{T}} u \, d\boldsymbol{x}\right)^2$$

defines a norm on $H^{2,1}_\delta(\hat{T})$. First note that $|\!|\!|\cdot|\!|\!|$ is well-defined since for $u \in H^{2,1}_\delta(\hat{T})$, $u \in H^2(\hat{T} \setminus \hat{T}_0) \subset C^0(\overline{\hat{T} \setminus \hat{T}_0})$ and by Lemma 5.6.3, $u \in L^2(\hat{T})$. Clearly we have $|\!|\!|u|\!|\!| \leq C\|u\|_{H^{2,1}_\delta(\hat{T})}$. We claim that there exists a constant C such that

$$\|u\|_{H^{2,1}_\delta(\hat{T})} \leq C|\!|\!|u|\!|\!|.$$

Indeed, if this were not the case, then there exists a sequence $\{u_k\}$ such that $\|u_k\|_{H^{2,1}_\delta(\hat{T})} = 1$ and $|\!|\!|u_k|\!|\!| \to 0$ and a subsequence $\{u_{k_j}\}$ converging weakly to $\bar{u} \in H^{2,1}_\delta(\hat{T})$. By Lemmas 5.6.3 and 5.6.4, $u_{k_j} \to \bar{u}$ strongly in $L^2(\hat{T})$ and in $H^{1,1}_{\delta^*}(\hat{T})$ for all $\delta^* \in (\delta, 1)$. Moreover,

$$|u_{k_j}|^2_{H^{2,1}_{\delta^*}(\hat{T})} \leq |u_{k_j}|^2_{H^{2,1}_\delta(\hat{T})} \leq |\!|\!|u_{k_j}|\!|\!|^2 \to 0,$$

and so $u_{k_j} \to \bar{u}$ strongly in $H^{2,1}_{\delta^*}(\hat{T})$. $|||\bar{u}||| = 0$ and so $D^2\bar{u} = 0$, or $\bar{u} \in \mathcal{P}_1(\hat{T})$. But $\bar{u}(\boldsymbol{a}_i) = 0$, $i = 2, 3$ and $\int_{\hat{T}} \bar{u} = 0$. Thus, $\bar{u} \equiv 0$. Applying Lemma 5.6.2 to $D^\alpha u$, $|\alpha| = 1$, and using $L^2(\hat{T})$ convergence, there holds

$$\|u_{k_j}\|^2_{H^{2,1}_\delta(\hat{T})} \leq C \left\{ \|u_{k_j}\|^2_{L^2(\hat{T})} + \int_{\hat{T}} r^{2\delta+2} |Du_{k_j}|^2 \, d\boldsymbol{x} + \int_{\hat{T}\setminus\hat{T}_0} |D^2 u_{k_j}|^2 \, d\boldsymbol{x} \right\} \to 0,$$

which contradicts $\|u_{k_j}\|_{H^{2,1}_\delta(\hat{T})} = 1$ for all j.

Now, let q be such that $q(\hat{\boldsymbol{a}}_i) = u(\hat{\boldsymbol{a}}_i)$, $i = 2, 3$ and $\int_{\hat{T}}(u - q) = 0$. Then,

$$\|u - q\|_{L^2(\hat{T})} \leq C\|u - q\|_{H^{2,1}_\delta(\hat{T})} \leq C|||u - q||| = C|u|_{H^{2,1}_\delta(\hat{T})},$$

which completes the proof. □

The following lemma, adapted from [96, Theorem 8.5], is used for constructing approximations to functions on elements away from the physical domain corners, i.e. where the functions are smooth. The two main properties are that the approximation interpolates at the vertices (since the pressure is continuous at the noncorner vertices) and has sufficient decay in higher order Sobolev seminorms.

Lemma 5.6.6. *For every $u \in H^{k+1}(\hat{S})$, $\hat{S} = (-1, 1)^2$, $k \geq 1$, there exists a polynomial q of degree at most k separately in x and y such that $q(\boldsymbol{a}) = u(\boldsymbol{a})$, $\boldsymbol{a}$ vertex of $\hat{S}$, and*

$$\|u - q\|^2_{L^2(\hat{S})} \leq C\frac{(k-s)!}{(k+s)!} \left\{ \|\partial_x^{s+1}\partial_y u\|^2_{L^2(\hat{S})} + \|\partial_x\partial_y^{s+1} u\|^2_{L^2(\hat{S})} \right\}$$

for any $0 < s < k$ *with* C *independent of* k, s, *and* u.

Let $\mathcal{L}_i$, $0 \leq i \leq n$ denote the set of elements of $\mathcal{T}^{n,\sigma}$ that are $n-i$ layers away from the corners of Ω and define

$$\|u\|^2_{H^{k,l}_\delta(\Omega)} := \sum_{j=0}^{l-1} \int_\Omega d_c^{2\delta} |D^j u|^2 \, d\boldsymbol{x} + \sum_{j=l}^{k} \int_\Omega d_c^{2(\delta+j-l)} |D^j u|^2 \, d\boldsymbol{x},$$

where d_c is the Euclidean distance to nearest corner of Ω. Given $u \in H^{m,1}_\delta(\Omega)$, $m \geq n+1$, we construct a polynomial approximation of u, denoted r, on an element $K \in \mathcal{T}^{n,\sigma}$ using the procedure in the proof of [57, Lemma 5.1]. That is, we apply element-wise pullbacks of u to the reference element $\hat{T}$ and use Lemma 5.6.5 if K contains a corner of the physical domain Ω, i.e. $K \in \mathcal{L}_n$ and Lemma 5.6.6 otherwise, i.e. $\mathcal{L}_i$, $0 \leq i \leq n-1$. Analogous arguments to the proof of [57, Lemma 5.1] lead to the following theorem:

Theorem 5.6.7. *For* $u \in H^{m,1}_\delta(\Omega)$, $m \geq n+1$, *there exists*

$$r \in \{q \in L^2(\Omega) : q|_K \in \mathcal{P}_{2n+3}(K),\ \forall K \in \mathcal{T}^{n,\sigma},\ q \text{ is } C^0 \text{ at all noncorner vertices}\}$$

such that

$$\|u - r\|^2_{L^2(\Omega)} \leq C \Bigg\{ \sum_{K \in \mathcal{L}_n} h_K^{2(1-\delta)} \|u\|^2_{H^{2,1}_\delta(\Omega)} + \sum_{i=0}^{n-1} \sum_{K \in \mathcal{L}_i} h_K^{2(1-\delta)} \frac{\lambda^{2s_i}(n-s_i)!}{(n+s_i)!} \|u\|^2_{H^{s_i+2,1}_\delta(\Omega)} \Bigg\}$$

for $0 < s_i < n$ *where* C *and* λ *are positive constants independent of* n, s_i, *and* u.

5.7 Numerical Examples

In this section, we present numerical computations highlighting the convergence properties of the method on two typical test cases: Moffatt eddies in a wedge-shaped domain and parabolic inflow and outflow on a T-shaped domain.

5.7.1 Moffatt Eddies

The first example, due to Moffatt [82], is a common benchmark for higher order method as it contains features on many scales. We take the domain Ω to be the wedge with a fixed mesh shown in Figure 5.3a and prescribe a parabolic flow profile on the top part of the boundary and no flow on the remainder of the boundary:

$$\boldsymbol{u}(x,0) = \begin{bmatrix} 1 - x^2 \\ 0 \end{bmatrix}, \qquad -1 \leq x \leq 1, \quad \text{and} \quad \boldsymbol{u} = \mathbf{0} \text{ on } \Gamma \setminus (-1,1) \times \{0\}.$$

The solution contains an infinite cascade of eddies, each about 400 times weaker than the previous one. Moreover, the pressure also has an infinite cascade of singularities, starting at $(\pm 1, 0)$. The blowup of the pressure combined with the exponentially decreasing strength of the eddies makes this problem challenging for many numerical methods. We use a purely spectral method, that is, we only increase the polynomial degree k and do not refine the mesh. The convergence of the method is displayed

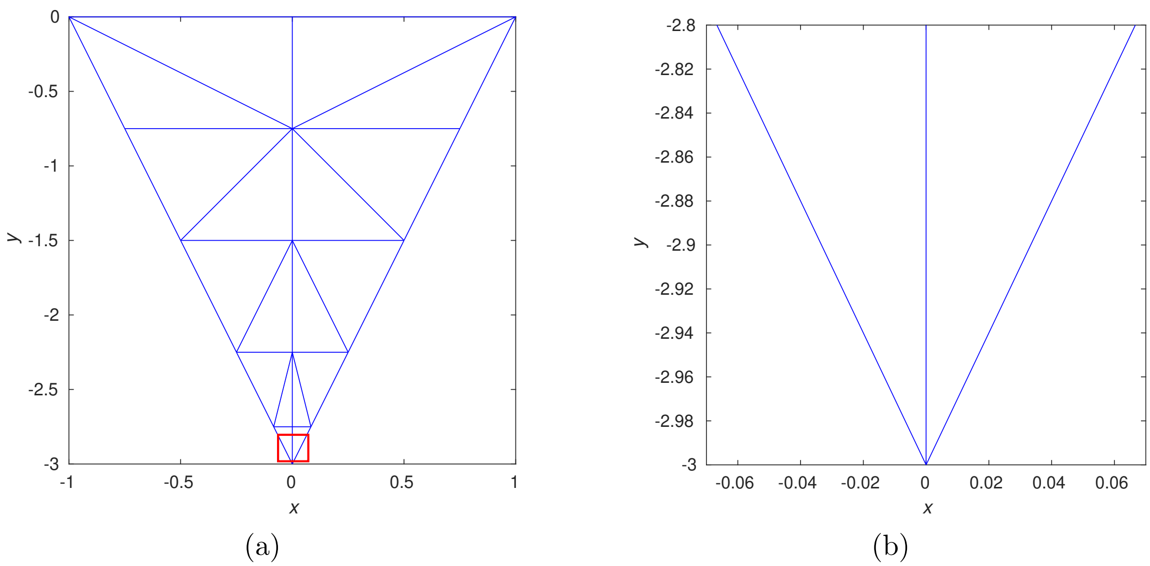

Figure 5.3: (a) 18 element computational mesh and (b) zoom on red box

in Figure 5.4 for $k = 4, \ldots, 10$. The total error is given by $\sqrt{e_u^2 + e_p^2}$, where e_u is the $\boldsymbol{H}^1(\Omega)$ velocity error and e_p is the $L^2(\Omega)$ pressure error, and was computed by comparing to a high order reference solution. As predicted by Theorem 5.2.2, the method convergence at an algebraic rate due to the limited regularity of the solution. Our results for $k = 13$ are displayed in Figure 5.5. We see a good resolution of the streamlines and pressure profile using only 18 elements despite there being no mesh grading near the singularities. On zooming in on Figure 5.6, we see that the bottom two elements completely resolve one eddy and nearly resolve two more eddies. Furthermore, the pressure profile exhibits the expected blow-up of the pressure at the corner vertices. Overall, the method completely resolves four eddies and mostly resolves a fifth, equivalent to a 10^{13} range of scales, while also nicely capturing the pressure profile.

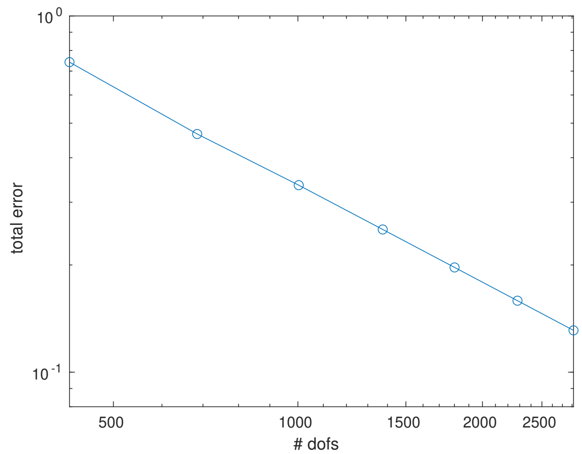

Figure 5.4: Convergence of numerical solution to the Moffatt eddy problem for $k = 4, \ldots, 10$.

5.7.2 T-shape Domain

The next example is a combination of the forward- and backward-facing step benchmark problems considered in [4]. We take the domain Ω to be the T-shaped domain with an example meshes in Figure 5.7, zero body force $\boldsymbol{f} \equiv \mathbf{0}$, parabolic flow profile on the leftmost and rightmost boundaries of the domain, no flow on the remainder of the boundary:

$$\boldsymbol{u}\left(\pm\frac{3}{2}, y\right) = \begin{bmatrix} y(1-y) \\ 0 \end{bmatrix}, \qquad 0 \leq y \leq 1, \quad \text{and} \quad \boldsymbol{u} = \mathbf{0} \qquad \text{on } \Gamma \setminus \left\{\pm\frac{3}{2}\right\} \times (0,1).$$

Since the boundary data is polynomial, the solution $(\boldsymbol{u}, p)$ belongs to the countably normed spaces in Section 5.2.2 despite having limited (unweighted) Sobolev regularity due to the re-entrant corners. We expect that the finite element approxi-

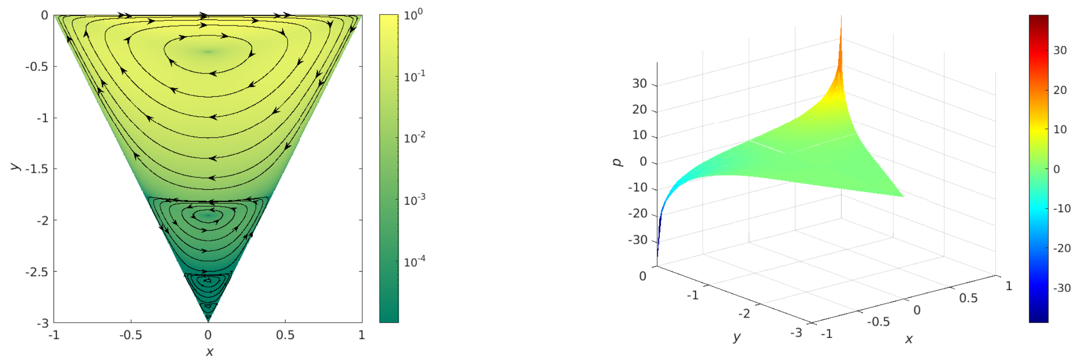

(a) (b)

Figure 5.5: Numerical solution for $k = 13$: (a) Streamlines with $|\boldsymbol{u}|$ background color and (b) pressure p.

mation converges exponentially fast in terms of the total number of degrees of freedom (5.2.5) on a properly graded sequence of meshes. The first mesh in Figure 5.7a consists of one layer of elements around the re-entrant corner and the bottom most corners with $\sigma = 0.08$. We then refine the mesh by successively adding layers of elements such that the inner most layer of elements has a diameter proportional to σ^n, where n is the number of refinements. For example, the mesh corresponding to $n = 3$ is shown in Figures 5.7b and 5.7c.

Figure 5.8 shows the total error of the method on the sequence of meshes described above for polynomial degrees $k = 4, \ldots, 10$. The total error is computed in the same manner as for the Moffatt eddy example. The plots confirm two properties of the method. One, on each fixed mesh, the error decays algebraically (for k sufficiently large) due to the limited Sobolev regularity. Two, the envelope of the curves demonstrates that the method is converging exponentially fast according to (5.2.5),

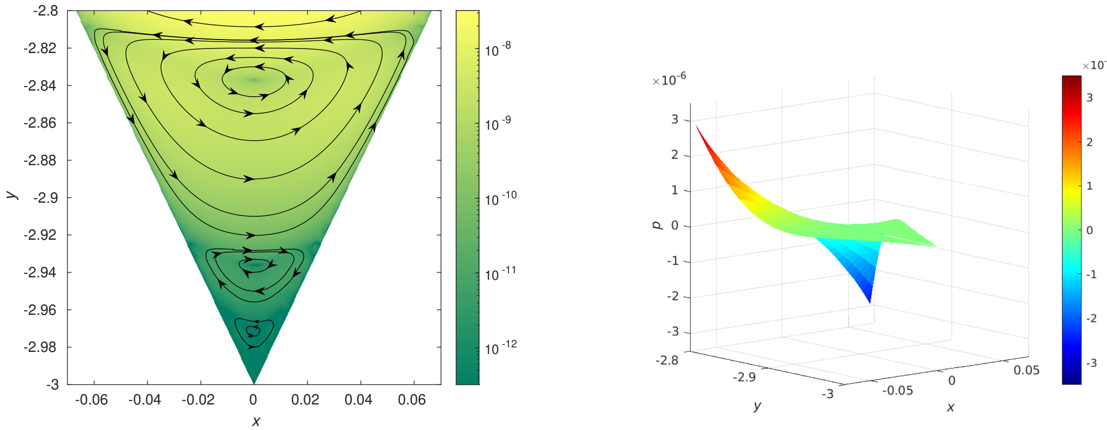

(a) (b)

Figure 5.6: Numerical solution for $k = 13$, zoom on bottom eddies: (a) Streamlines with $|\boldsymbol{u}|$ background color and (b) pressure p.

exhibited by a linear error curve in Figure 5.8b.

Besides convergence of the method, we are also interested in its ability to (visually) resolve two distinctive features of this problem: the pressure blows up at the re-entrant corners, and two infinite cascade of small eddies form on the bottom corners of the domain. We first examine the pressure blow-up. Because the pressure is singular at the re-entrant corners, the numerical solution will never be able to fully resolve it. However, increasing the polynomial order k and further refining the mesh mitigates the pollution of the error. Figure 5.9 displays numerical solution for (k, n) $= (4, 1)$, $(6, 2)$, $(8, 3)$, $(10, 4)$. As the polynomial degree increases and the mesh is further refined, the magnitude of the numerical oscillations away from the corner decrease, the jump across elements decreases (despite no continuity across edges being explicitly enforced by the method), and the spike at the corner is more localized. The magnitude of the spikes also grows as k and n increase – the magnitude of the spikes

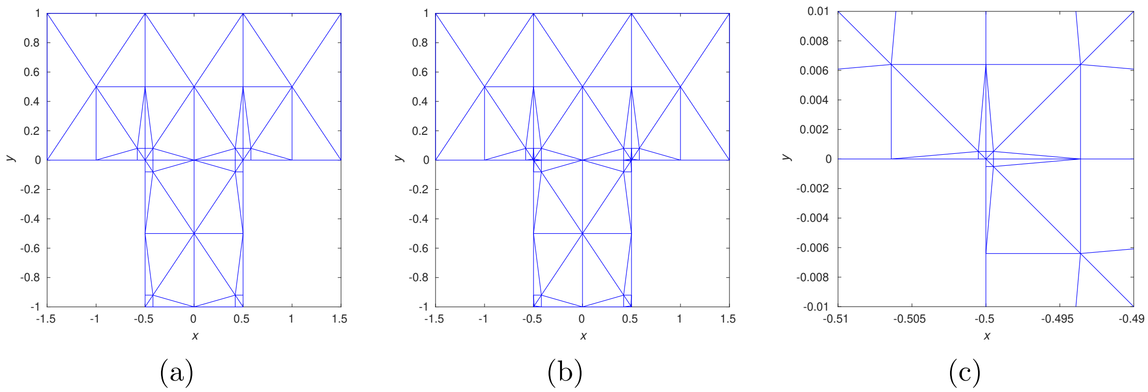

Figure 5.7: Geometrically graded meshes: (a) mesh with $n = 1$ layer of elements, (b) mesh with $n = 3$ layers of elements, and (c) zoom on re-entrant corner of mesh with $n = 3$ layers of elements.

is about 330 for $(k, n) = (10, 4)$, even though the z-axis limits are capped at $z = \pm 15$ for visualization. For these reasons, we focus our attention on the $(k, n) = (10, 4)$ solution shown in Figure 5.10. The streamlines near the re-entrant corner exhibit good resolution and the oscillations in the pressure profile are localized to the few elements around the re-entrant corners. The eddies in the bottom corner of the domains are also resolved to machine precision, as shown in Figure 5.11. Overall, the method is able to limit the pollution of the pressure singularity and resolve the small scale eddies with only a few refinements despite the total error of the method being of the order 10^{-3}.

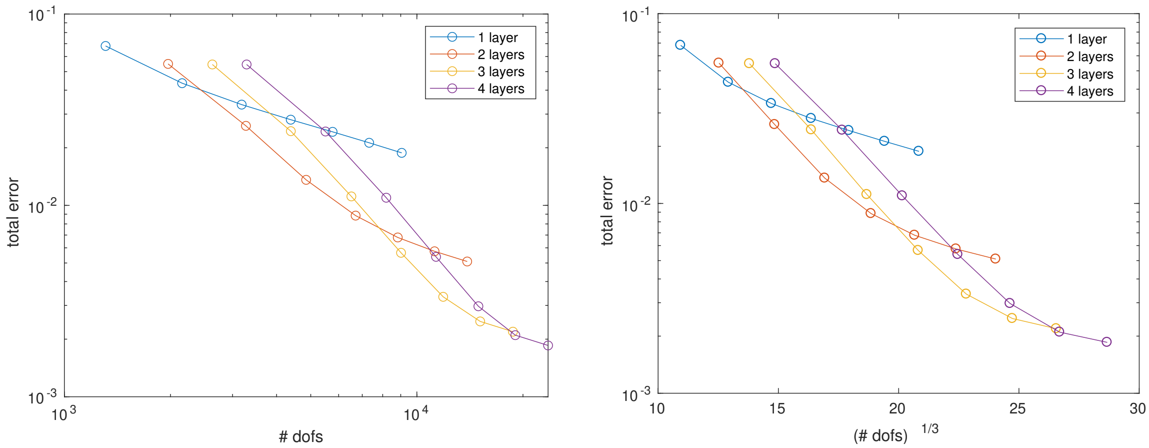

(a) (b)

Figure 5.8: Error of the method on various geometric meshes for $k = 4, \ldots, 10$: (a) Log-log plot and (b) semi-log plot.

5.8 Proof of Lemma 5.4.1

By Lemma 3.7.1, there exists $F_k \in \mathcal{P}_{k+1}(I)$ such that

$$F_k(-1) = F_k(1) = F_k'(1) = 0, \quad F_k'(-1) = 1, \quad \text{and} \quad \|F_k\|_{L^2(I)} \le Ck^{-3},$$

where $I = (-1, 1)$ and C is independent of k. By interpolation, and the inverse estimate $\|F_k'\|_{L^2(I)} \le Ck^2\|F_k\|_{L^2(I)}$ [25, Corollary 3.4], we obtain the following $H_{00}^{1/2}(I)$ bound for F_k:

$$\|F_k\|_{H_{00}^{1/2}(I)} \le C\|F_k\|_{L^2(I)}^{1/2}\|F_k\|_{H^1(I)}^{1/2} \le Ck\|F_k\|_{L^2(I)} \le Ck^{-2}. \tag{5.8.1}$$

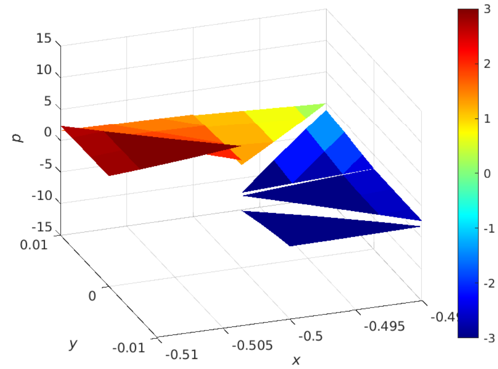

(a) $(k, n) = (4, 1)$ approximation

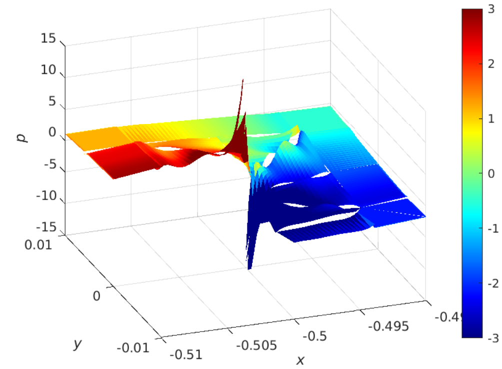

(b) $(k, n) = (6, 2)$ approximation

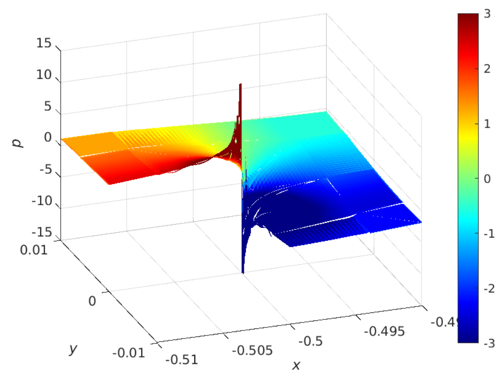

(c) $(k, n) = (8, 3)$ approximation

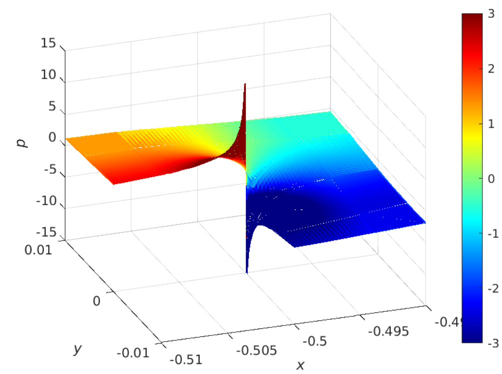

(d) $(k, n) = (10, 4)$ approximation

Figure 5.9: Pressure approximations near re-entrant corner.

Define the function $\boldsymbol{f} \in L^2(\partial \hat{T})$, where $\hat{T}$ is the reference element in Figure 4.5b, by

$$\boldsymbol{f}_1(s) = \mathbf{0}, \quad \boldsymbol{f}_2(s) = -\frac{|\gamma|_2}{4} F_k \left(1 - \frac{2s}{|\gamma_2|}\right) \hat{\boldsymbol{t}}_2, \quad \boldsymbol{f}_3(s) = -\frac{|\gamma_3|}{4} F_k \left(\frac{2s}{|\gamma_3|} - 1\right) \hat{\boldsymbol{t}}_3,$$

where $\boldsymbol{f}_i = \boldsymbol{f}|_{\gamma_i}$ and s is the arc length parametrization of γ_i oriented as in Figure 4.5b, $1 \leq i \leq 3$. Since $\boldsymbol{f}$ is continuous at the vertices $\hat{\boldsymbol{a}}_j$, $1 \leq j \leq 3$, [13, Theorem 7.4] (applied component-wise) asserts the existence of a $\boldsymbol{v} \in \boldsymbol{\mathcal{P}}_{k+1}(\hat{T})$ such

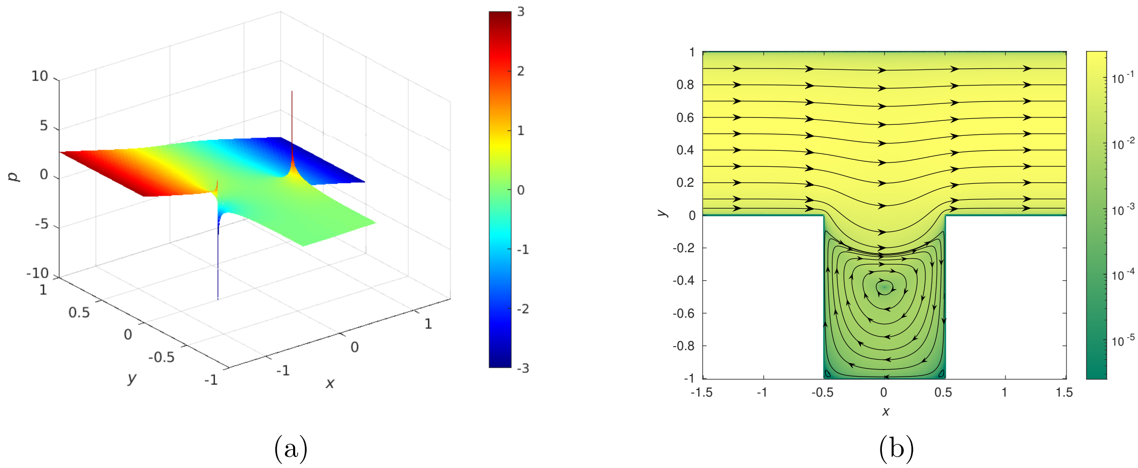

Figure 5.10: Numerical solution for $(k, n) = (10, 4)$: (a) Pressure and (b) streamlines with $|\boldsymbol{u}|$ background color.

that

$$\boldsymbol{v}|_{\partial \hat{T}} = \boldsymbol{f} \quad \text{and} \quad \|\boldsymbol{v}\|_{\boldsymbol{H}^1(\hat{T})} \leq C\|\boldsymbol{f}\|_{\boldsymbol{H}^{1/2}(\partial \hat{T})}$$

with C independent of k. Using that $\boldsymbol{f}_i \in \boldsymbol{H}^{1/2}_{00}(\gamma_i)$ and (5.8.1), we have

$$\|\boldsymbol{f}\|_{\boldsymbol{H}^{1/2}(\partial \hat{T})} \leq C \sum_{i=1}^{3} \|\boldsymbol{f}_i\|_{\boldsymbol{H}^{1/2}_{00}(\gamma_i)} \leq C\|F_k\|_{H^{1/2}_{00}(I)} \leq Ck^{-2}.$$

Define $\hat{\Psi}_1 := \operatorname{div} \boldsymbol{v}$. Using the identity

$$\operatorname{div} \boldsymbol{v} = (\hat{\boldsymbol{t}}_{i+1} \cdot \hat{\boldsymbol{n}}_{i+2})^{-1} \left[\partial_{t_{i+1}} \boldsymbol{v} \cdot \hat{\boldsymbol{n}}_{i+2} - \partial_{t_{i+2}} \boldsymbol{v} \cdot \hat{\boldsymbol{n}}_{i+1}\right], \qquad 1 \leq i \leq 3,$$

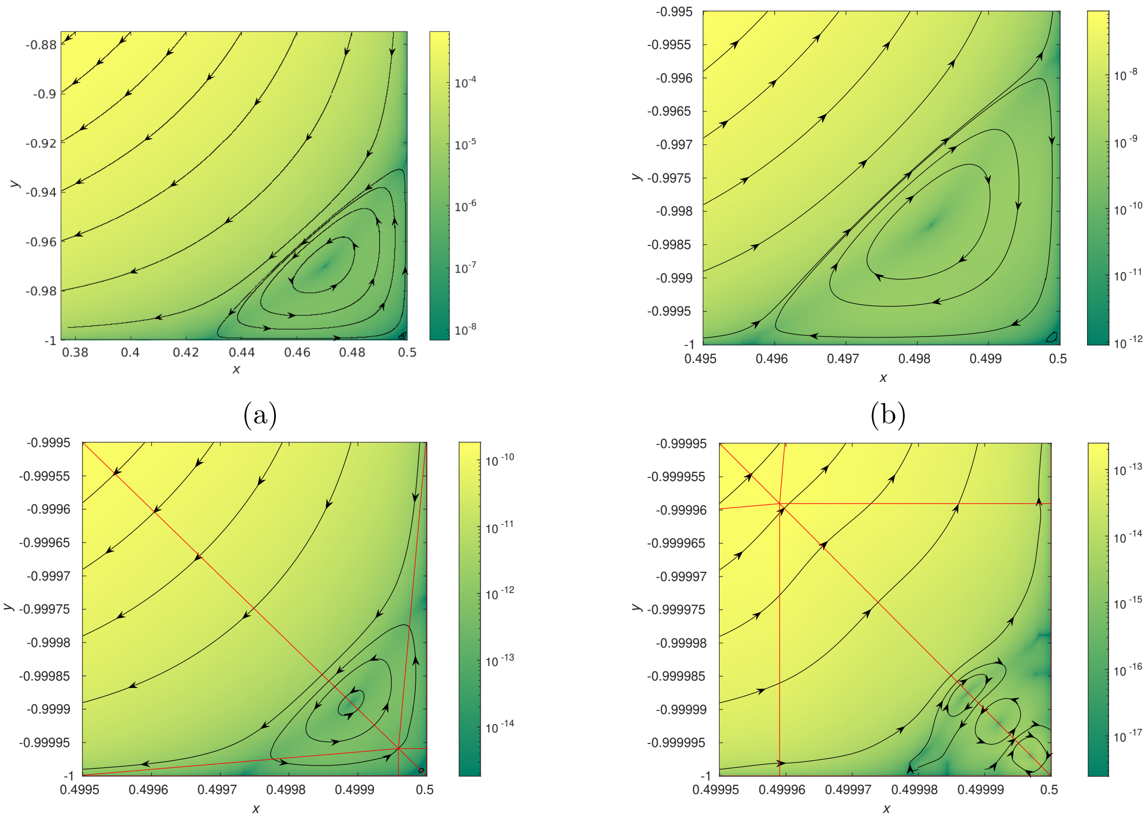

(a) (b) (c) (d)

Figure 5.11: Streamlines with $|\boldsymbol{u}|$ background color for the $(k, n) = (10, 4)$ solution: (a-b) corner zooms 1-2 and (c-d) corner zooms 3-4 with mesh overlay.

gives

$$\hat{\Psi}_1(\hat{\boldsymbol{a}}_1) = (\hat{\boldsymbol{t}}_2 \cdot \hat{\boldsymbol{n}}_3)^{-1} \left[\boldsymbol{f}_2'(|\gamma_2|) \cdot \hat{\boldsymbol{n}}_3 - \boldsymbol{f}_3'(0) \cdot \hat{\boldsymbol{n}}_2\right] = \frac{\hat{\boldsymbol{t}}_2 \cdot \hat{\boldsymbol{n}}_3 + \hat{\boldsymbol{t}}_3 \cdot \hat{\boldsymbol{n}}_2}{2\hat{\boldsymbol{t}}_2 \cdot \hat{\boldsymbol{n}}_3} F_k'(-1) = 1,$$

and similarly, $\hat{\Psi}(\hat{\boldsymbol{a}}_j) = 0$, $j = 2, 3$. By the divergence theorem,

$$\int_{\hat{T}} \hat{\Psi}_1(\boldsymbol{x})\, d\boldsymbol{x} = \int_{\partial \hat{T}} \boldsymbol{v} \cdot \hat{\boldsymbol{n}}\, dS = 0.$$

Moreover, $\|\hat{\Psi}_1\|_{L^2(\hat{T})} \le C\|\boldsymbol{v}\|_{\boldsymbol{H}^1(\hat{T})} \le Ck^{-2}$. Thus $\hat{\Psi}_1$ satisfies (5.4.1) in the case K is the reference triangle $\hat{T}$ and $\boldsymbol{a} = \hat{\boldsymbol{a}}_1$.

We extend the construction to a general triangle K and any vertex as follows. Let $K \in \mathcal{T}$, $i \in \{1, 2, 3\}$, and $\boldsymbol{F}_K : \hat{T} \to K$ be the affine mapping such that $\boldsymbol{F}_K(\hat{T}) = K$ and $\boldsymbol{F}_K(\hat{\boldsymbol{a}}_1) = \boldsymbol{a}$. Define $\Psi_{\boldsymbol{a}} \in \mathcal{P}_k(K)$ by $\Psi_{\boldsymbol{a}} = \hat{\Psi}_1 \circ \boldsymbol{F}_K^{-1}$. Then, $\Psi_{\boldsymbol{a}}(\boldsymbol{b}) = \delta_{\boldsymbol{ab}}$, $\forall \boldsymbol{b} \in \mathcal{V}_K$, $\int_K \Psi \, d\boldsymbol{x} = 0$, and

$$\|\Psi_{\boldsymbol{a}}\|_{L^2(K)} \le Ch_K \|\hat{\Psi}_1\|_{L^2(\hat{T})} \le Ch_K k^{-2},$$

which completes the proof. $\square$

Chapter Six

Mass Conserving Mixed hp-FEM Approximations to Stokes Flow. Part III: Implementation and Preconditioning

6.1 Introduction

This chapter is the final part in a series discussing a mass conserving, high order, mixed finite element method for Stokes flow on a simply connected polygon Ω with boundary $\Gamma = \partial\Omega$ (4.1.2). Problem (4.1.2) is again approximated a using mixed, high order, finite element scheme on a mesh $\mathcal{T}$ as follows: Find $(\boldsymbol{u}_{hk}, p_{hk}) \in \boldsymbol{V}_0 \times Q_0$ such that

$$a(\boldsymbol{u}_{hk}, \boldsymbol{v}) + b(\boldsymbol{v}, p_{hk}) = (\boldsymbol{f}, \boldsymbol{v}) \qquad \forall \boldsymbol{v} \in \boldsymbol{V}_0, \tag{6.1.1a}$$

$$b(\boldsymbol{u}_{hk}, q) = 0 \qquad \forall q \in Q_0, \tag{6.1.1b}$$

where the finite element spaces are chosen for $k \geq 4$ as in the previous two chapters (4.2.16):

$$V := \{v \in C^0(\Omega) : v|_K \in \mathcal{P}_k(K)\ \forall K \in \mathcal{T},\ v \text{ is } C^1 \text{ at noncorner vertices}\},$$

$$Q := \{q \in L^2(\Omega) : q|_K \in \mathcal{P}_{k-1}(K)\ \forall K \in \mathcal{T},\ q \text{ is } C^0 \text{ at noncorner vertices}\},$$

$V_0 := V \cap H_0^1(\Omega)$, $\boldsymbol{V}_0 = V_0 \times V_0$, and $Q_0 = Q \cap L_0^2(\Omega)$. The local degrees of freedom of the spaces V and Q are illustrated in Figure 4.4.

In Part I Chapter 4, it was shown that these elements are uniformly inf-sup stable in the mesh size h and polynomial order k if the mesh $\mathcal{T}$ is corner-split which, roughly speaking, means that every element $K \in \mathcal{T}$ has at most one edge lying on the domain boundary Γ; for a precise definition, see Section 4.2.2.

Theorem 6.1.1 (Theorem 4.3.1 and Corollary 4.3.2)**.** *If the mesh $\mathcal{T}$ is corner-split, then for every $q \in Q_0$, there exists $\boldsymbol{v} \in \boldsymbol{V}_0$ such that* $\operatorname{div} \boldsymbol{v} = q$ *and*

$$\|\boldsymbol{v}\|_{\boldsymbol{H}^1(\Omega)} \leq \beta^{-1} \|q\|_{L^2(\Omega)},$$

where $0 < \beta < 1$ is independent of k and h. Thus, the spaces $\boldsymbol{V}_0 \times Q_0$ are uniformly inf-sup stable:

$$\inf_{0 \neq q \in Q_0} \sup_{\mathbf{0} \neq \boldsymbol{v} \in \boldsymbol{V}_0} \frac{b(\boldsymbol{v}, q)}{\|\boldsymbol{v}\|_{\boldsymbol{H}^1(\Omega)} \|q\|_{L^2(\Omega)}} \geq \beta. \tag{6.1.2}$$

Strictly speaking, Corollary 4.3.2 shows that β depends on the mesh-dependent quantity $\xi(\mathcal{T})$ defined in (4.3.2), but is nevertheless bounded independently of the mesh size h and polynomial degree k. Moreover, the finite element solution $\boldsymbol{u}_{hk}$ will be pointwise divergence free (see e.g. Section 4.1). In Chapter 5, it was shown that these elements have optimal approximation properties in both the mesh size h and the polynomial order k. On locally quasi-uniform meshes, the finite element solution to (6.1.1) converges at the optimal algebraic rate to the solution to (4.1.2) by Theorem 5.2.1. Moreover, if the data $\boldsymbol{f}$ belongs to a particular countably normed space, then the finite element method with properly geometrically graded meshes converges exponentially fast as both the mesh is refined and the polynomial degree is increased Corollary 5.2.5. The spaces $\boldsymbol{V}_0 \times Q_0$ are currently the only known triangular finite element spaces that are uniformly inf-sup stable in h and k, give pointwise divergence free velocities, and posses optimal approximation properties.

In the current chapter, we turn to issues relating to the practical application of the method. In particular, we give explicit bases for the spaces $\boldsymbol{V}$ and Q that result in an efficient preconditioner for the solution of the resulting linear system for (6.1.1), which may be used in conjunction with an iterative solver for indefinite systems, such as MINRES [89]. The preconditioner consists of a standard static condensation, or elimination of the interior degrees of freedom, along with an Additive Schwarz Method (ASM) preconditioner [103, 111] for the resulting Schur complement system associated with the interface degrees of freedom. Thanks to a judicious choice of basis, the condition number grow at most as $\log^3 k$ as k is increased, and is uniform in the mesh size.

The current work finds inspiration in the early works of [32, 69, 102, 114] for h-version methods, [9, 109] for hp-version finite element methods, and [70, 78, 90, 91] for spectral element methods, each of which developed block diagonal and/or block triangular preconditioners in terms of existing preconditioners for second order elliptic problems. Unfortunately, these types of approaches do not readily extend to the mixed finite element scheme (6.1.1) owing to the additional smoothness requirements imposed at element vertices for both the velocity and pressure spaces. Our treatment of these degrees of freedom is similar to the treatment of the second order derivative degrees of freedom in preconditioning the stiffness matrix for $H^2(\Omega)$-conforming methods in Chapter 3 and the treatment of the vertex degrees of freedom in preconditioning the mass matrix for $H^1(\Omega)$ problems [6, 7].

6.2 General Form of a Block-Diagonal Preconditioner

By fixing bases for the spaces $\boldsymbol{V}_0$ and Q, we may express $\boldsymbol{u} \in \boldsymbol{V}_0$ and $p \in Q$ as

$$\boldsymbol{u} = \vec{u}_E^T \vec{\Phi}_E + \vec{u}_I^T \vec{\Phi}_I \quad \text{and} \quad p = \vec{p}_e^T \vec{\psi}_e + \vec{p}_\iota^T \vec{\psi}_\iota,$$

for suitable $\vec{u}_E$, $\vec{u}_I$, $\vec{p}_e$, $\vec{p}_\iota$, where $\vec{\Phi}_E$ is the vector of exterior velocity basis functions (vertex and edge functions), $\vec{\Phi}_I$ the vector of interior velocity basis functions, $\vec{\psi}_e$ the vector of exterior pressure basis functions, and $\vec{\psi}_\iota$ the vector of interior pressure basis functions. Here, the exterior pressure functions consist of vertex functions and a function corresponding to the average value over each element. The variational problem (6.1.1) in matrix form then reads

$$\left[\begin{array}{cc|cc} \boldsymbol{A}_{EE} & \boldsymbol{B}_{Ee} & \boldsymbol{A}_{EI} & \boldsymbol{B}_{E\iota} \\ \boldsymbol{B}_{eE} & \boldsymbol{0} & \boldsymbol{B}_{eI} & \boldsymbol{0} \\ \hline \boldsymbol{A}_{IE} & \boldsymbol{B}_{Ie} & \boldsymbol{A}_{II} & \boldsymbol{B}_{I\iota} \\ \boldsymbol{B}_{\iota E} & \boldsymbol{0} & \boldsymbol{B}_{\iota I} & \boldsymbol{0} \end{array}\right] \left[\begin{array}{c} \vec{u}_E \\ \vec{p}_e \\ \hline \vec{u}_I \\ \vec{p}_\iota \end{array}\right] = \left[\begin{array}{c} \vec{f}_E \\ \vec{0} \\ \hline \vec{f}_I \\ \vec{0} \end{array}\right]. \tag{6.2.1}$$

The matrix appearing in (6.2.1) is symmetric but indefinite, owing to the zero sub-blocks. The pressure variable in problem (6.1.1) is unique up to a constant, meaning that the matrix in (6.2.1) has a one-dimensional null space. Nevertheless, the system (6.2.1) is consistent since the components of the load vector corresponding to pressure basis functions vanish identically and, a fortiori, are orthogonal to constant pressure modes. Consequently, the system (6.2.1) is uniquely solvable up to the addition of a constant in the pressure thanks to the inf-sup condition (6.1.2) and the uniform ellipticity of $a(\cdot,\cdot)$.

The conditioning of the matrix, in common with standard *hp*-finite elements, degenerates rapidly with both the mesh size h and the polynomial order k of the elements. Indeed, almost every practical choice of basis function results in a rapid deterioration of the condition number k, even for symmetric, positive definite systems [5, 88]. We seek a preconditioner for the symmetric, indefinite system (6.2.1) which controls the growth of the conditioning in both h and k.

The first step towards preconditioning is to eliminate, or *statically condense*, the interior degrees of freedom to arrive at the Schur complement system

$$\boldsymbol{S}\begin{bmatrix}\vec{u}_E\\ \vec{p}_e\end{bmatrix} = \begin{bmatrix}\vec{f}^*_E\\ \vec{g}^*_e\end{bmatrix} := \begin{bmatrix}\vec{f}_E\\ \vec{0}\end{bmatrix} - \begin{bmatrix}\boldsymbol{A}_{EI} & \boldsymbol{B}_{E\iota}\\ \boldsymbol{B}_{eI} & \mathbf{0}\end{bmatrix}\begin{bmatrix}\boldsymbol{A}_{II} & \boldsymbol{B}_{I\iota}\\ \boldsymbol{B}_{\iota I} & \mathbf{0}\end{bmatrix}^{-1}\begin{bmatrix}\vec{f}_I\\ \vec{0}\end{bmatrix}, \tag{6.2.2}$$

where

$$\boldsymbol{S} = \begin{bmatrix}\widetilde{\boldsymbol{A}} & \widetilde{\boldsymbol{B}}^T\\ \widetilde{\boldsymbol{B}} & \mathbf{0}\end{bmatrix} = \begin{bmatrix}\boldsymbol{A}_{EE} & \boldsymbol{B}_{Ee}\\ \boldsymbol{B}_{eE} & \mathbf{0}\end{bmatrix} - \begin{bmatrix}\boldsymbol{A}_{EI} & \boldsymbol{B}_{E\iota}\\ \boldsymbol{B}_{eI} & \mathbf{0}\end{bmatrix}\begin{bmatrix}\boldsymbol{A}_{II} & \boldsymbol{B}_{I\iota}\\ \boldsymbol{B}_{\iota I} & \mathbf{0}\end{bmatrix}^{-1}\begin{bmatrix}\boldsymbol{A}_{IE} & \boldsymbol{B}_{Ie}\\ \boldsymbol{B}_{\iota E} & \mathbf{0}\end{bmatrix} \tag{6.2.3}$$

and we have used the fact (see Lemma 6.5.1) that the $(2,2)$ block of Schur complement matrix $\boldsymbol{S}$ reduces to the zero matrix. The inverse of the matrix appearing in

(6.2.2) and (6.2.3) is well-defined by Theorem 6.3.3. After the degrees of freedom on the element interfaces are in hand, the interior degrees of freedom can be recovered by back substitution using the relation

$$\begin{bmatrix} \vec{u}_I \\ \vec{p}_\iota \end{bmatrix} = \begin{bmatrix} \boldsymbol{A}_{II} & \boldsymbol{B}_{I\iota} \\ \boldsymbol{B}_{\iota I} & \boldsymbol{0} \end{bmatrix}^{-1} \left(\begin{bmatrix} \vec{f}_I \\ \vec{0} \end{bmatrix} - \begin{bmatrix} \boldsymbol{A}_{IE} & \boldsymbol{B}_{Ie} \\ \boldsymbol{B}_{\iota E} & \boldsymbol{0} \end{bmatrix} \begin{bmatrix} \vec{u}_E \\ \vec{p}_e \end{bmatrix} \right).$$

The element interface degrees of freedom are obtained by solving the Schur complement system (6.2.2). The matrix $\boldsymbol{S}$ defined in (6.2.3) is symmetric and indefinite, and inherits the one dimensional null space from the full system matrix (6.2.1), again corresponding to the constant pressure mode. Similarly, the right hand side in (6.2.2) inherits the consistency of the load vector meaning that (6.2.2) is uniquely solvable up to a constant pressure mode. The indefiniteness of the problem coupled with the presence of a low dimensional null space suggests using a MINRES iterative solver [89] in conjunction with a suitable preconditioner.

We seek a block diagonal matrix of the form

$$\boldsymbol{P} = \begin{bmatrix} \bar{\boldsymbol{A}} & \boldsymbol{0} \\ \boldsymbol{0} & \nu^{-1}\bar{\boldsymbol{M}} \end{bmatrix} \tag{6.2.4}$$

to precondition $\boldsymbol{S}$, where $\bar{\boldsymbol{A}}$ and $\bar{\boldsymbol{M}}$ are symmetric positive definite matrices. The convergence of the MINRES algorithm with preconditioner $\boldsymbol{P}^{-1}$ depends on the location of the nonzero eigenvalues of $\boldsymbol{P}^{-1}\boldsymbol{S}$ [48, Remark 4.13 and §4.2.4]. In particular, let δ, Δ, θ, and Θ be nonnegative constants such that

$$\delta \leq \frac{\vec{u}_E^T \widetilde{\boldsymbol{A}} \vec{u}_E}{\vec{u}_E^T \bar{\boldsymbol{A}} \vec{u}_E} \leq \Delta \qquad \forall \boldsymbol{u} \in \boldsymbol{V}_0 \quad \text{and} \quad \theta \leq \frac{\vec{q}_e^T \widetilde{\boldsymbol{B}} \widetilde{\boldsymbol{A}}^{-1} \widetilde{\boldsymbol{B}}^T \vec{q}_e}{\nu^{-1} \vec{q}_e^T \bar{\boldsymbol{M}} \vec{q}_e} \leq \Theta \qquad \forall q \in Q_0.$$

Then, by [48, Theorem 4.7 and eq. (4.37)], the eigenvalues of $\boldsymbol{P}^{-1}\boldsymbol{S}$ lie in the set

$$\left[-\Theta, \frac{1}{2}\left(\delta - \sqrt{\delta^2 + 4\delta\theta}\right)\right] \cup \{0\} \cup \left[\delta, \frac{1}{2}\left(\Delta + \sqrt{\Delta^2 + 4\Delta\Theta}\right)\right]. \qquad (6.2.5)$$

In order to use variational techniques like Additive Schwarz Methods to construct $\bar{\boldsymbol{A}}$ and $\bar{\boldsymbol{M}}$, we must first identify the appropriate variational setting of the Schur complement system (6.2.2). In particular, the Schur complement is posed over the subspaces spanned by the external degrees of freedom of $\boldsymbol{V}_0 \times Q$, which are rather non-standard owing to the additional continuity imposed at noncorner vertices. Section 6.3 gives a precise characterization of these spaces including new results showing that they form a discrete exact sequence property (Theorem 6.3.5) and that they, like the spaces $\boldsymbol{V}_0 \times Q_0$, are uniformly inf-sup stable in both h and k (Theorem 6.3.7).

Section 6.4 defines the Stokes extension operator and its relation to the subspace splittings. Section 6.5 uses the results of the previous two sections to relate the matrix form of the Schur complement system to a variational problem. In Section 6.6, we present an explicit set of basis functions on the reference element for the spaces $\boldsymbol{V}$ and Q and then detail how these are used in the construction of the global basis functions. We develop the additive Schwarz theory and construct the matrices $\bar{\boldsymbol{A}}$ and $\bar{\boldsymbol{M}}$ in Section 6.7, which is then applied to three numerical examples demonstrating in Section 6.8. Section 6.9 contains technical lemmas related to the additive Schwarz theory.

6.3 Subspace Splittings, Exact Sequences, and Stability

A key property of the mixed finite element pair $\boldsymbol{V}_0 \times Q_0$ is the exactness of the sequence Theorem 4.2.6 and [50, §3.2]:

$$0 \xrightarrow{\subset} \Sigma_0 \xrightarrow{\mathbf{curl}} \boldsymbol{V}_0 \xrightarrow{\text{div}} Q_0 \longrightarrow 0, \tag{6.3.1}$$

where we recall that $\mathbf{curl} = (\partial_y, -\partial_x)^T$ and Σ_0 is the space of $H^2(\Omega)$-conforming piecewise polynomials given by

$$\Sigma_0 = \{\phi \in C^1(\bar{\Omega}) : \phi|_K \in \mathcal{P}_{k+1}(K)\ \forall K \in \mathcal{T}, \phi \text{ is } C^2 \text{ at noncorner vertices}\} \cap H_0^2(\Omega).$$

The exact sequence property (6.3.1) was used in Theorem 5.2.2 to obtain optimal error estimates for the velocity that were independent of the pressure error. In the remainder of this section, we seek exact sequences analogous to (6.3.1) that respect the separation of interior and exterior degrees of freedom. Such sequences will be used to both identify the variational problem associated with the Schur complement system (6.2.2) and prove its uniform stability.

6.3.1 Interior Subspaces

We first examine the subspaces associated with the interior degrees of freedom given by

$$\begin{aligned}
\Sigma_I &= \{\phi \in \Sigma_0 : \phi|_{\partial K} = \partial_n \phi|_{\partial K} = 0 \ \forall K \in \mathcal{T}\}, \\
\boldsymbol{V}_I &= \{\boldsymbol{v} \in \boldsymbol{V}_0 : \boldsymbol{v}|_{\partial K} = \boldsymbol{0} \ \forall K \in \mathcal{T}\}, \\
Q_I &= \left\{ q \in Q_0 : \int_K q \ d\boldsymbol{x} = 0, \ q|_K(\boldsymbol{a}) = 0 \ \forall \boldsymbol{a} \in \mathcal{V}_K, \ \forall K \in \mathcal{T} \right\},
\end{aligned}$$

which, in turn, may be decomposed into contributions from individual elements:

$$\Sigma_I = \bigoplus_{K\in\mathcal{T}} \Sigma_I(K), \quad \boldsymbol{V}_I = \bigoplus_{K\in\mathcal{T}} \boldsymbol{V}_I(K), \quad \text{and} \qquad Q_I = \bigoplus_{K\in\mathcal{T}} Q_I(K), \tag{6.3.2}$$

where

$$\begin{aligned}
\Sigma_I(K) &:= \mathcal{P}_{k+1}(K) \cap H_0^2(K), \\
\boldsymbol{V}_I(K) &:= \boldsymbol{\mathcal{P}}_k(K) \cap \boldsymbol{H}_0^1(K), \\
Q_I(K) &:= \left\{ q \in \mathcal{P}_{k-1}(K) \cap L_0^2(K) : q(\boldsymbol{a}) = 0, \ \forall \boldsymbol{a} \in \mathcal{V}_K \right\}.
\end{aligned}$$

Here, we follow the usual conventions whereby the above definitions are understood to mean that the functions are defined globally but supported on the single element K. Both the element-level interior spaces and the corresponding interior spaces on a mesh form exact sequences:

Theorem 6.3.1. *The following sequences are exact:*

$$0 \xrightarrow{\subset} \Sigma_I(K) \xrightarrow{\mathbf{curl}} \boldsymbol{V}_I(K) \xrightarrow{\text{div}} Q_I(K) \longrightarrow 0 \qquad \forall K \in \mathcal{T}, \tag{6.3.3}$$

and

$$0 \xrightarrow{\subset} \Sigma_I \xrightarrow{\mathbf{curl}} \boldsymbol{V}_I \xrightarrow{\text{div}} Q_I \longrightarrow 0. \tag{6.3.4}$$

Proof. In view of $\mathbf{curl}\, H_0^2(K) \subset \boldsymbol{H}_0^1(K)$, we have the relations $\mathbf{curl}\, \Sigma_I(K) \subset \boldsymbol{V}_I(K)$, $\mathbf{curl}\, \Sigma_I(K) \subseteq \ker \text{div}$, and by Theorem 4.3.4, $\text{div}\, \boldsymbol{V}_I(K) = Q_I(K)$. Here, we consider div as a linear operator $\boldsymbol{V}_I(K) \to Q_I(K)$. Moreover, for $\phi \in \Sigma_I(K)$, $\mathbf{curl}\, \phi \equiv 0$ if and only if $\phi \equiv 0$ and so $\dim \mathbf{curl}\, \Sigma_I(K) = \dim \Sigma_I(K)$. The dimension counts $\dim \Sigma_I(K) = \frac{k^2-7k+12}{2}$, $\dim \boldsymbol{V}_I(K) = k^2 - 3k + 2$, and $\dim Q_I(K) = \frac{k^2+k-8}{2}$ reveal that $\dim \Sigma_I(K) + \dim Q_I(K) - \dim \boldsymbol{V}_I(K) = 0$. By the rank-nullity theorem, we have

$$\dim \boldsymbol{V}_I(K) = \dim \text{Im div} + \dim \ker \text{div} \geq \dim Q_I(K) + \dim \Sigma_I(K) = \dim \boldsymbol{V}_I(K).$$

and so $\ker \text{div} = \mathbf{curl}\, \Sigma_I(K)$. Thus, the element-level sequence (6.3.3) is exact. The exactness of the global spaces (6.3.4) may be proved along similar lines using the exactness of the element level sequence (6.3.3). $\square$

The inclusions $\mathbf{curl}\, \Sigma_I(K) \subset \boldsymbol{V}_I(K)$ and $\mathbf{curl}\, \Sigma_I \subset \boldsymbol{V}_I$ give a useful decomposition of the interior spaces in terms of the **curl** operator:

Corollary 6.3.2. *The spaces* $\boldsymbol{V}_I(K)$ *and* $\boldsymbol{V}_I$ *admit the following decompositions:*

$$\boldsymbol{V}_I(K) = \mathbf{curl}\,\Sigma_I(K) \oplus \{\boldsymbol{v} \in \boldsymbol{\mathcal{P}}_k(K) \cap \boldsymbol{H}_0^1(K),\ a(\boldsymbol{v}, \mathbf{curl}\,\phi) = 0\ \forall \phi \in \Sigma_I(K)\}$$

and

$$\boldsymbol{V}_I = \mathbf{curl}\,\Sigma_I \oplus \{\boldsymbol{v} \in \boldsymbol{V}_0 : \boldsymbol{v}|_{\partial K} = \mathbf{0}\ \forall K \in \mathcal{T},\ a(\boldsymbol{v}, \mathbf{curl}\,\phi) = 0\ \forall \phi \in \Sigma_I\}. \quad (6.3.5)$$

The next result concerns the stability of the interior mixed finite element pair $\boldsymbol{V}_I \times Q_I$.

Theorem 6.3.3. *Let* $K \in \mathcal{T}$ *and let* β *be the discrete inf-sup constant appearing in* (6.1.2)*. If* $q \in Q_I(K)$*, then there exists* $\boldsymbol{v} \in \boldsymbol{V}_I(K)$ *such that* $\operatorname{div} \boldsymbol{v} = q$ *and*

$$h_K^{-1} \|\boldsymbol{v}\|_{\boldsymbol{L}^2(K)} + |\boldsymbol{v}|_{\boldsymbol{H}^1(K)} \leq \beta^{-1} \|q\|_{L^2(K)}. \quad (6.3.6)$$

Consequently, (i) the spaces $\boldsymbol{V}_I \times Q_I$ *are uniformly inf-sup stable:*

$$\inf_{0 \neq q \in Q_I} \sup_{\mathbf{0} \neq \boldsymbol{v} \in \boldsymbol{V}_I} \frac{b(\boldsymbol{v}, q)}{|\boldsymbol{v}|_{\boldsymbol{H}^1(\Omega)} \|q\|_{L^2(\Omega)}} \geq \beta, \quad (6.3.7)$$

and (ii) the matrix $\begin{bmatrix} \boldsymbol{A}_{II} & \boldsymbol{B}_{I\iota} \\ \boldsymbol{B}_{\iota I} & \mathbf{0} \end{bmatrix}$ *is invertible, and hence the Schur complement* $\boldsymbol{S}$ *appearing in* (6.2.2) *is well-defined by the formula* (6.2.3)*.*

Proof. Let $q \in Q_I(K)$. Then, Theorem 4.3.4 gives the existence of $\boldsymbol{v} \in \boldsymbol{V}_I(K)$ with

$\operatorname{div} \boldsymbol{v} = q$ satisfying the estimate (6.3.6).

Now let $q \in Q_I$ be decomposed as in (6.3.2) so that $q = \sum_{K\in\mathcal{T}} q_K$ with $q_K \in Q_I(K)$. By the first statement in the theorem, there exists $\boldsymbol{v}_K \in \boldsymbol{V}_I(K)$ with $\operatorname{div} \boldsymbol{v}_K = -q_K$ satisfying (6.3.6). Hence, $\boldsymbol{v} := \sum_{K\in\mathcal{T}} \boldsymbol{v}_K$ satisfies $\operatorname{div} \boldsymbol{v} = -q$ and

$$|\boldsymbol{v}|^2_{\boldsymbol{H}^1(\Omega)} = \sum_{K\in\mathcal{T}} |\boldsymbol{v}_K|^2_{\boldsymbol{H}^1(\Omega)} \leq \beta^{-2} \sum_{K\in\mathcal{T}} \|q_K\|^2_{L^2(\Omega)} = \beta^{-2} \|q\|^2_{L^2(\Omega)},$$

from which (6.3.7) immediately follows. (ii) follows at once thanks to the ellipticity of $a(\cdot,\cdot)$ and the inf-sup condition (6.3.7). $\square$

6.3.2 Boundary Subspaces

The subspaces $\tilde{\Sigma}_E$, $\tilde{\boldsymbol{V}}_E$, and $\tilde{Q}_E$ are defined as follows

$$\tilde{\Sigma}_E := \{\phi \in \Sigma_0 : a(\mathbf{curl}\,\phi, \mathbf{curl}\,\psi) = 0 \ \forall \psi \in \Sigma_I\} \tag{6.3.8a}$$

$$\tilde{\boldsymbol{V}}_E := \{\boldsymbol{v} \in \boldsymbol{V}_0 : \operatorname{div} \boldsymbol{v} \in \tilde{Q}_E,\ a(\boldsymbol{v}, \mathbf{curl}\,\psi) = 0 \ \forall \psi \in \Sigma_I\} \tag{6.3.8b}$$

$$\tilde{Q}_E := \{q \in Q_0 : (q, r) = 0 \ \forall r \in Q_I\}, \tag{6.3.8c}$$

and correspond to degrees of freedom on the element boundaries. More precisely, we have:

Theorem 6.3.4. *The following decompositions hold:*

$$\Sigma_0 = \Sigma_I \oplus \tilde{\Sigma}_E, \quad \boldsymbol{V}_0 = \boldsymbol{V}_I \oplus \tilde{\boldsymbol{V}}_E, \quad \textit{and} \quad Q_0 = Q_I \oplus \tilde{Q}_E. \tag{6.3.9}$$

Proof. The decompositions of Σ_0 and Q_0 follow immediately using the orthogonality conditions in the definition of the spaces (6.3.8a) and (6.3.8c). The decomposition of the velocity space $\boldsymbol{V}_0$ is more involved. We first use the exact sequence (6.3.1) to write:

$$\boldsymbol{V}_0 = \mathbf{curl}\,\Sigma_0 \oplus (\mathbf{curl}\,\Sigma_0)^{\perp}, \tag{6.3.10}$$

where $(\mathbf{curl}\,\Sigma_0)^{\perp} := \{\boldsymbol{u} \in \boldsymbol{V}_0 : a(\boldsymbol{u}, \mathbf{curl}\,\psi) = 0\ \forall \psi \in \Sigma_0\}$. Now, let $\boldsymbol{v} \in \boldsymbol{V}_0$ be given. By the decomposition (6.3.10) and the decomposition of Σ_0 in (6.3.9), there exists $\phi_I \in \Sigma_I$, $\tilde{\phi}_E \in \tilde{\Sigma}_E$, and $\boldsymbol{v}_{\perp} \in (\mathbf{curl}\,\Sigma_0)^{\perp}$ such that $\boldsymbol{v} = \mathbf{curl}(\phi_I + \tilde{\phi}_E) + \boldsymbol{v}_{\perp}$. We decompose the divergence analogously: $\operatorname{div} \boldsymbol{v} = q_I + \tilde{q}_E$ with $q_I \in Q_I$ and $\tilde{q}_E \in \tilde{Q}_E$. Thanks to the exact sequence (6.3.4) and the decomposition (6.3.5), there exists $\boldsymbol{w} \in \boldsymbol{V}_I$ such that $\operatorname{div} \boldsymbol{w} = q_I$ and $\boldsymbol{w} \in \{\boldsymbol{v} \in \boldsymbol{V}_I :\ a(\boldsymbol{v}, \mathbf{curl}\,\psi) = 0\ \forall \psi \in \Sigma_I\}$. Then, $\boldsymbol{v}_I := \mathbf{curl}\,\phi_I + \boldsymbol{w}$ satisfies $\boldsymbol{v}_I \in \boldsymbol{V}_I$ and $\operatorname{div} \boldsymbol{v}_I = q_I$. Consequently, $\tilde{\boldsymbol{v}}_E := \boldsymbol{v} - \boldsymbol{v}_I = \mathbf{curl}\,\tilde{\phi}_E + \boldsymbol{v}_{\perp} - \boldsymbol{w}$ satisfies $\operatorname{div} \tilde{\boldsymbol{v}}_E = \operatorname{div}(\boldsymbol{v} - \boldsymbol{v}_I) = \tilde{q}_E \in \tilde{Q}_E$ and

$$a(\tilde{\boldsymbol{v}}_E, \mathbf{curl}\,\psi) = a(\mathbf{curl}\,\tilde{\phi}_E, \mathbf{curl}\,\psi) + a(\boldsymbol{v}_{\perp}, \mathbf{curl}\,\psi) + a(\boldsymbol{w}, \mathbf{curl}\,\psi) = 0 \qquad \forall \psi \in \Sigma_I$$

by construction. Thus, $\tilde{\boldsymbol{v}}_E \in \tilde{\boldsymbol{V}}_E$, which completes the proof. $\square$

Theorem 6.3.4 means that the decompositions in the columns of the following complex (6.3.11) are valid. The next result shows that the rows form exact sequences:

Theorem 6.3.5. *Each row of the following complex is an exact sequence*

$$0 \xrightarrow{\subset} \Sigma_0 \xrightarrow{\mathbf{curl}} \boldsymbol{V}_0 \xrightarrow{\text{div}} Q_0 \longrightarrow 0 \tag{6.3.11a}$$

$$\shortparallel \qquad\qquad \shortparallel \qquad\qquad \shortparallel$$

$$0 \xrightarrow{\subset} \Sigma_I \xrightarrow{\mathbf{curl}} \boldsymbol{V}_I \xrightarrow{\text{div}} Q_I \longrightarrow 0 \tag{6.3.11b}$$

$$\oplus \qquad\qquad \oplus \qquad\qquad \oplus$$

$$0 \xrightarrow{\subset} \tilde{\Sigma}_E \xrightarrow{\mathbf{curl}} \tilde{\boldsymbol{V}}_E \xrightarrow{\text{div}} \tilde{Q}_E \longrightarrow 0 \tag{6.3.11c}$$

where the exterior spaces $\tilde{\Sigma}_E$, $\tilde{\boldsymbol{V}}_E$, *and* $\tilde{Q}_E$ *are given by* (6.3.8).

Proof. Theorem 4.2.6 gives the exactness of (6.3.11a) while Theorem 6.3.1 gives the exactness of (6.3.11b). Moreover, the decomposition (6.3.9) and the exactness the sequences (6.3.11a) and (6.3.11b) imply that $\dim \tilde{\Sigma}_E + \dim \tilde{Q}_E - \dim \tilde{\boldsymbol{V}}_E = 0$. Since $\mathbf{curl}\, \tilde{\Sigma}_E \subset \tilde{\boldsymbol{V}}_E$ and $\text{div}\, \tilde{\boldsymbol{V}}_E \subseteq \tilde{Q}_E$, we conclude that the sequence (6.3.11c) is exact using analogous arguments to those used in Theorem 6.3.1. □

The exactness of the final row in (6.3.11) gives the following analogue of Corollary 6.3.2 for the exterior velocity space:

Corollary 6.3.6. *The exterior velocity space* $\tilde{\boldsymbol{V}}_E$ *admits the following decomposition:*

$$\tilde{\boldsymbol{V}}_E = \mathbf{curl}\,\tilde{\Sigma}_E \oplus \{\boldsymbol{v} \in \boldsymbol{V}_0 : \operatorname{div} \boldsymbol{v} \in \tilde{Q}_E,\ a(\boldsymbol{v}, \mathbf{curl}\,\phi) = 0\ \forall \phi \in \Sigma_0\}.$$

Theorems 6.1.1 and 6.3.3 show that the mixed finite element pairs appearing in the first two rows of (6.3.11) are uniformly inf-sup stable. The next result shows that the boundary spaces are also stable with *the same inf-sup constant as for the full velocity and pressure spaces*:

Theorem 6.3.7. *Let* β *be the discrete inf-sup constant defined in* (6.1.2)*. If* $q \in \tilde{Q}_E$*, then there exists* $\boldsymbol{v} \in \tilde{\boldsymbol{V}}_E$ *such that* $\operatorname{div} \boldsymbol{v} = q$ *and*

$$|\boldsymbol{v}|_{\boldsymbol{H}^1(\Omega)} \le \beta^{-1} \|q\|_{L^2(\Omega)}. \tag{6.3.12}$$

Consequently, the spaces $\tilde{\boldsymbol{V}}_E \times \tilde{Q}_E$ *are uniformly inf-sup stable:*

$$\inf_{0 \ne q \in \tilde{Q}_E} \sup_{\boldsymbol{0} \ne \boldsymbol{v} \in \tilde{\boldsymbol{V}}_E} \frac{b(\boldsymbol{v}, q)}{|\boldsymbol{v}|_{\boldsymbol{H}^1(\Omega)} \|q\|_{L^2(\Omega)}} \ge \beta. \tag{6.3.13}$$

Proof. Let $q \in \tilde{Q}_E$ be given. By Theorem 6.1.1, there exists $\boldsymbol{w} \in \boldsymbol{V}_0$ such that $\operatorname{div} \boldsymbol{w} = q$ and $\|\boldsymbol{w}\|_{\boldsymbol{H}^1(\Omega)} \le \beta^{-1}\|q\|_{L^2(\Omega)}$, where β is independent of h and k. According to Theorem 6.3.4 and (6.3.8b), there exist functions $\boldsymbol{w}_I \in \boldsymbol{V}_I$, $\tilde{\boldsymbol{w}}_E \in \tilde{\boldsymbol{V}}_E$ such that $\boldsymbol{w} = \boldsymbol{w}_I + \tilde{\boldsymbol{w}}_E$. $Q_I \ni \operatorname{div} \boldsymbol{w}_I = \operatorname{div}(\boldsymbol{w} - \tilde{\boldsymbol{w}}_E) \in \tilde{Q}_E$ since $\operatorname{div} \boldsymbol{w} = q \in \tilde{Q}_E$, and so $\operatorname{div} \boldsymbol{w}_I = 0$. By the exact sequence property (6.3.4), $\boldsymbol{w}_I = \mathbf{curl}\,\phi_I$ for some $\phi \in \Sigma_I$, and thus $\boldsymbol{w} = \mathbf{curl}\,\phi_I + \tilde{\boldsymbol{w}}_E$. Note that this decomposition of $\boldsymbol{w}$ is $a(\cdot,\cdot)$ orthogonal by definition: $a(\mathbf{curl}\,\phi_I, \tilde{\boldsymbol{w}}_E) = 0$ and

$$|\boldsymbol{w}|^2_{H^1(\Omega)} = \left[a(\mathbf{curl}\,\phi_I, \mathbf{curl}\,\phi_I) + a(\tilde{\boldsymbol{w}}_E, \tilde{\boldsymbol{w}}_E)\right] = |\,\mathbf{curl}\,\phi_I|^2_{H^1(\Omega)} + |\tilde{\boldsymbol{w}}_E|^2_{H^1(\Omega)}.$$

Define $\boldsymbol{v} := \tilde{\boldsymbol{w}}_E$. Then, $\operatorname{div}\boldsymbol{v} = \operatorname{div}\tilde{\boldsymbol{w}}_E = \operatorname{div}(\tilde{\boldsymbol{w}}_E + \mathbf{curl}\,\phi_I) = \operatorname{div}\boldsymbol{w} = q$, and $|\boldsymbol{v}|_{H^1(\Omega)} \leq |\boldsymbol{w}|_{H^1(\Omega)} \leq \beta^{-1}\|q\|_{L^2(\Omega)}$. (6.3.12) and (6.3.13) follow at once. □

6.4 Stokes Extension Operator

Let $\boldsymbol{V} := V \times V$ denote the discrete velocity space in the absence of essential boundary conditions and $Q_I^\perp$ be the orthogonal complement of Q_I in Q with the corresponding projection $\tilde{\Pi} : Q \to Q_I^\perp$,

$$(\tilde{\Pi}q, r) = (q, r) \qquad \forall r \in Q_I^\perp := \{q \in Q : (q, r) = 0\ \forall r \in Q_I\}. \tag{6.4.1}$$

It is worthwhile noting that (6.4.1) means that $\tilde{Q}_E = Q_I^\perp \cap L^2_0(\Omega)$, so that the space $Q_I^\perp$ corresponds to boundary degrees of freedom. Let $K \in \mathcal{T}$. Then, thanks to standard Babuška-Brezzi theory (see e.g. [55, p. 59 Theorem 4.1]) and Theorem 6.3.3, there exist $\boldsymbol{u}_{S,K} \in \boldsymbol{\mathcal{P}}_k(K)$ and $p_{S,K} \in \mathcal{P}_{k-1}(K)$ satisfying

$$a_K(\boldsymbol{u}_{S,K}, \boldsymbol{v}) + b_K(\boldsymbol{v}, p_{S,K}) = 0 \qquad \forall \boldsymbol{v} \in \boldsymbol{V}_I(K), \tag{6.4.2a}$$

$$b_K(\boldsymbol{u}_{S,K}, q) = 0 \qquad \forall q \in Q_I(K), \tag{6.4.2b}$$

$$\boldsymbol{u}_{S,K} = \boldsymbol{u} \qquad \text{on } \partial K, \tag{6.4.2c}$$

$$p_{S,K}(\boldsymbol{a}) = p|_K(\boldsymbol{a}) \qquad \forall \boldsymbol{a} \in \mathcal{V}_K, \tag{6.4.2d}$$

$$\int_K p_{S,K}\, d\boldsymbol{x} = \int_K p\, d\boldsymbol{x}, \tag{6.4.2e}$$

where $a_K(\cdot,\cdot)$ and $b_K(\cdot,\cdot)$ denote the restrictions of the bilinear forms to element K. We define the Stokes extension map $\boldsymbol{V} \times Q \ni (\boldsymbol{u}, p) \mapsto \mathscr{E}(\boldsymbol{u}, p) =: (\boldsymbol{u}_S, p_S)$ by the rule $\boldsymbol{u}_S = \boldsymbol{u}_{S,K}$ and $p_S = p_{S,K}$ on each element $K \in \mathcal{T}$.

The first result deals with the Stokes extension of a given velocity field paired a zero pressure:

Theorem 6.4.1. *Let* $\boldsymbol{\Pi_V} : \boldsymbol{V} \to \boldsymbol{V}$, $\Pi_Q : \boldsymbol{V} \to Q$ *be defined by the rule*

$$\boldsymbol{V} \ni \boldsymbol{u} \mapsto (\boldsymbol{\Pi_V u}, \Pi_Q \boldsymbol{u}) := \mathscr{E}(\boldsymbol{u}, 0). \tag{6.4.3}$$

Then, $\Pi_Q \boldsymbol{u} \in Q_I$ *and*

$$\|\boldsymbol{\Pi_V u}\|_{\boldsymbol{H}^1(K)} + \nu^{-1} \|\Pi_Q \boldsymbol{u}\|_{L^2(K)} \leq C \|\boldsymbol{u}\|_{\boldsymbol{H}^{1/2}(\partial K)} \qquad \forall K \in \mathcal{T}, \tag{6.4.4}$$

where C is independent of h_K, k, ν, and $\boldsymbol{u}$. In particular, if $\boldsymbol{u} \in \tilde{\boldsymbol{V}}_E$, then $\boldsymbol{\Pi_V u} = \boldsymbol{u}$.

Moreover, the following equivalence of semi-norms holds:

$$C^{-1}|\boldsymbol{u}|_{\boldsymbol{H}^{1/2}(\partial K)} \leq |\boldsymbol{\Pi_V u}|_{\boldsymbol{H}^1(K)} \leq C\beta^{-1}|\boldsymbol{u}|_{\boldsymbol{H}^{1/2}(\partial K)} \qquad \forall K \in \mathcal{T}, \tag{6.4.5}$$

where $C \geq 1$ *is independent of* k*,* h_K*,* β*,* ν*, and* $\boldsymbol{u}$*.*

Proof. Let $K \in \mathcal{T}$ and $\boldsymbol{u} \in \boldsymbol{V}$ be given. Conditions (6.4.2d) and (6.4.2e) imply that $\Pi_Q \boldsymbol{u} \in Q_I$. Let $\boldsymbol{c} = |\partial K|^{-1} \int_{\partial K} \boldsymbol{u}\, dS$. Thanks to [13, Theorem 7.4] and a standard scaling argument, there exists $\tilde{\boldsymbol{w}} \in \boldsymbol{\mathcal{P}}_k(K)$ such that $\tilde{\boldsymbol{w}}|_{\partial K} = (\boldsymbol{u} - \boldsymbol{c})|_{\partial K}$ and

$$h_K^{-1}\|\tilde{\boldsymbol{w}}\|_{\boldsymbol{L}^2(K)} + |\tilde{\boldsymbol{w}}|_{\boldsymbol{H}^1(K)} \leq C\left(h_K^{-1/2}\|\boldsymbol{u} - \boldsymbol{c}\|_{\boldsymbol{L}^2(\partial K)} + |\boldsymbol{u}|_{\boldsymbol{H}^{1/2}(\partial K)}\right),$$

with C independent of h_K, k, and $\boldsymbol{u}$. The polynomial $\boldsymbol{w} := \tilde{\boldsymbol{w}} + \boldsymbol{c}$ satisfies $\boldsymbol{w}|_{\partial K} = \boldsymbol{u}|_{\partial K}$. Moreover, by Poincaré's inequality, $h_K^{-1/2}\|\boldsymbol{u} - \boldsymbol{c}\|_{\boldsymbol{L}^2(\partial K)} \leq C|\boldsymbol{u}|_{\boldsymbol{H}^{1/2}(\partial K)}$, and so

$$\|\boldsymbol{w}\|_{\boldsymbol{H}^1(K)} \leq \|\tilde{\boldsymbol{w}}\|_{\boldsymbol{L}^2(K)} + Ch_K^{1/2}\|\boldsymbol{u}\|_{\boldsymbol{L}^2(\partial K)} + |\tilde{\boldsymbol{w}}|_{\boldsymbol{H}^1(K)} \leq C\|\boldsymbol{u}\|_{\boldsymbol{H}^{1/2}(\partial K)}. \tag{6.4.6}$$

Choosing $\boldsymbol{v} = \boldsymbol{\Pi_V u}|_K - \boldsymbol{w} \in \boldsymbol{V}_I(K)$ in (6.4.2a) gives

$$a_K(\boldsymbol{\Pi_V u}, \boldsymbol{\Pi_V u}) = a_K(\boldsymbol{\Pi_V u}, \boldsymbol{w}) + b_K(\boldsymbol{\Pi_V u} - \boldsymbol{w}, \Pi_Q \boldsymbol{u}).$$

By (6.4.2b), $b_K(\boldsymbol{\Pi_V u}, \Pi_Q \boldsymbol{u}) = 0$ since $\Pi_Q \boldsymbol{u}|_K \in Q_I(K)$, and so, by Cauchy-Schwarz inequality, there holds

$$|\boldsymbol{\Pi}_{\boldsymbol{V}}\boldsymbol{u}|^2_{\boldsymbol{H}^1(K)} \leq \left(|\boldsymbol{\Pi}_{\boldsymbol{V}}\boldsymbol{u}|_{\boldsymbol{H}^1(K)} + \sqrt{2}\nu^{-1}\|\Pi_Q\boldsymbol{u}\|_{L^2(K)}\right)|\boldsymbol{w}|_{\boldsymbol{H}^1(K)}. \tag{6.4.7}$$

Moreover, there exists $\boldsymbol{v} \in \boldsymbol{V}_I(K)$ satisfying $\operatorname{div}\boldsymbol{v} = \Pi_Q\boldsymbol{u}|_K$ and (6.3.6) by Theorem 6.3.3. Consequently,

$$\beta\|\Pi_Q\boldsymbol{u}\|_{L^2(K)} \leq \frac{b_K(\boldsymbol{v}, \Pi_Q\boldsymbol{u})}{|\boldsymbol{v}|_{\boldsymbol{H}^1(K)}} = \frac{a_K(\boldsymbol{\Pi}_{\boldsymbol{V}}\boldsymbol{u}, \boldsymbol{v})}{|\boldsymbol{v}|_{\boldsymbol{H}^1(K)}} \leq \nu|\boldsymbol{\Pi}_{\boldsymbol{V}}\boldsymbol{u}|_{\boldsymbol{H}^1(K)} \tag{6.4.8}$$

thanks to (6.4.2a) and the Cauchy-Schwarz inequality. Collecting results, we obtain

$$|\boldsymbol{\Pi}_{\boldsymbol{V}}\boldsymbol{u}|_{\boldsymbol{H}^1(K)} \leq (1+\sqrt{2}\beta^{-1})|\boldsymbol{w}|_{\boldsymbol{H}^1(K)} \leq C\|\boldsymbol{u}\|_{\boldsymbol{H}^{1/2}(\partial K)}$$

and

$$\|\Pi_Q\boldsymbol{u}\|_{L^2(K)} \leq \nu\beta^{-1}|\boldsymbol{\Pi}_{\boldsymbol{V}}\boldsymbol{u}|_{\boldsymbol{H}^1(K)} \leq C\nu\|\boldsymbol{u}\|_{\boldsymbol{H}^{1/2}(\partial K)},$$

where C is independent of h_K, k, ν, and $\boldsymbol{u}$. Combining the estimate

$$h_K^{-1}\|\boldsymbol{\Pi}_{\boldsymbol{V}}\boldsymbol{u}\|_{\boldsymbol{L}^2(K)} \leq C\left(|\boldsymbol{\Pi}_{\boldsymbol{V}}\boldsymbol{u}|_{\boldsymbol{H}^1(K)} + |\partial K|^{-1}\left|\int_{\partial K}\boldsymbol{\Pi}_{\boldsymbol{V}}\boldsymbol{u}\; dS\right|\right),$$

which follows from [49, Example B.64] and a standard scaling argument, and the

Cauchy-Schwarz inequality then gives

$$\begin{aligned}\|\mathbf{\Pi}_{\boldsymbol{V}}\boldsymbol{u}\|_{\boldsymbol{L}^2(K)} &\le C\left(h_K|\mathbf{\Pi}_{\boldsymbol{V}}\boldsymbol{u}|_{\boldsymbol{H}^1(K)} + h_K^{1/2}\|\mathbf{\Pi}_{\boldsymbol{V}}\boldsymbol{u}\|_{\boldsymbol{L}^2(\partial K)}\right)\\ &\le C\left(|\mathbf{\Pi}_{\boldsymbol{V}}\boldsymbol{u}|_{\boldsymbol{H}^1(K)} + \|\boldsymbol{u}\|_{\boldsymbol{L}^2(\partial K)}\right)\\ &\le C\|\boldsymbol{u}\|_{\boldsymbol{H}^{1/2}(\partial K)}.\end{aligned}$$

Now let $\boldsymbol{u} \in \tilde{\boldsymbol{V}}_E$. Then, $\operatorname{div}\mathbf{\Pi}_{\boldsymbol{V}}\boldsymbol{u} \in \tilde{Q}_E$ by (6.4.2b) and $\boldsymbol{w} := \boldsymbol{u} - \mathbf{\Pi}_{\boldsymbol{V}}\boldsymbol{u} \in \boldsymbol{V}_I$ by (6.4.2c). Moreover, $\operatorname{div}\boldsymbol{w} \in Q_I \cap \tilde{Q}_E$ since $\operatorname{div}\boldsymbol{u}, \operatorname{div}\mathbf{\Pi}_{\boldsymbol{V}}\boldsymbol{u} \in \tilde{Q}_E$. Thus, $\operatorname{div}\boldsymbol{w} = 0$ and $\boldsymbol{w} = \mathbf{curl}\,\phi$ with $\phi \in \Sigma_I$ by the exact sequence property (6.3.4). For any $\psi \in \Sigma_I$, there holds

$$a(\mathbf{curl}\,\phi, \mathbf{curl}\,\psi) = a(\boldsymbol{u}, \mathbf{curl}\,\psi) - a(\mathbf{\Pi}_{\boldsymbol{V}}\boldsymbol{u}, \mathbf{curl}\,\psi) = 0$$

by the definition of $\tilde{\boldsymbol{V}}_E$ and choosing $\boldsymbol{v} = \mathbf{curl}\,\psi$ for $\psi \in \Sigma_I$ in (6.4.2a). Since $a(\mathbf{curl}\,\cdot, \mathbf{curl}\,\cdot)$ is coercive on Σ_I, $\phi \equiv 0$, and $\boldsymbol{u} = \mathbf{\Pi}_{\boldsymbol{V}}\boldsymbol{u}$.

The equivalence (6.4.5) is proved by arguing as in [32, Theorem 4.1]. $\square$

The next result complements Theorem 6.4.1:

Theorem 6.4.2. *For $p \in Q$, $\mathscr{E}(\mathbf{0}, p) = (\mathbf{0}, \tilde{\Pi}p)$ where $\tilde{\Pi}$ is defined in* (6.4.1)*, and*

$$\|\tilde{\Pi}p\|_{L^2(K)} \le \|p\|_{L^2(K)}. \tag{6.4.9}$$

In particular, if $p \in Q_I^\perp$, then $\mathscr{E}(\mathbf{0}, p) = (\mathbf{0}, p)$.

Proof. Let $p \in Q$ and consider the Stokes extension $(\tilde{\boldsymbol{u}}, \tilde{p}) := \mathscr{E}(\mathbf{0}, p)$. Since $Q = Q_I \oplus Q_I^\perp$, the pressure $\tilde{p}$ may be written in the form $\tilde{p} = p_I + \tilde{\Pi} p$. In particular, $p_I \in Q_I$ satisfies

$$b_K(\boldsymbol{v}, p_I) = b_K(\boldsymbol{v}, \tilde{p}) - b_K(\boldsymbol{v}, \tilde{\Pi} p) = b_K(\boldsymbol{v}, \tilde{p}) \qquad \forall \boldsymbol{v} \in \boldsymbol{V}_I(K),\ \forall K \in \mathcal{T},$$

where we used the fact that $b_K(\boldsymbol{v}, \tilde{\Pi} p) = 0$ since $\operatorname{div} \boldsymbol{V}_I(K) = Q_I(K) \perp Q_I^\perp$. Hence,

$$\begin{aligned} a_K(\tilde{\boldsymbol{u}}, \boldsymbol{v}) + b_K(\boldsymbol{v}, p_I) &= 0 \qquad \forall \boldsymbol{v} \in \boldsymbol{V}_I(K), \\ b_K(\tilde{\boldsymbol{u}}, q) &= 0 \qquad \forall q \in Q_I(K). \end{aligned}$$

Equation (6.4.4) then gives $(\tilde{\boldsymbol{u}}, p_I) = \mathscr{E}(\mathbf{0}, 0)$; or, equally well, $\tilde{\boldsymbol{u}} = \mathbf{0}$ and $\tilde{p} = \tilde{\Pi} p$. The estimate (6.4.9) immediately follows since $\tilde{\Pi}$ is a projection. If $p \in Q_I^\perp$, then $\mathscr{E}(\mathbf{0}, p) = (\mathbf{0}, \tilde{\Pi} p) = (\mathbf{0}, p)$. □

Combining Theorems 6.4.1 and 6.4.2 leads to the following result:

Corollary 6.4.3. *The Stokes extension operator $\mathscr{E}(\cdot, \cdot)$ is linear and continuous: For $K \in \mathcal{T}$, there holds*

$$\|\mathscr{E}(\boldsymbol{u}, p)\|_{\boldsymbol{H}^1(K) \times L^2(K)} \leq C \max\{1, \nu\} \|\boldsymbol{u}\|_{\boldsymbol{H}^{1/2}(\partial K)} + \|\tilde{\Pi} p\|_{L^2(K)} \qquad \forall (\boldsymbol{u}, p) \in \boldsymbol{V} \times Q, \tag{6.4.10}$$

where C is independent of h_K, k, and ν. Moreover, $\ker \mathscr{E} = \boldsymbol{V}_I \times Q_I$ *and* $\mathscr{E}(\boldsymbol{u}, p) = (\boldsymbol{\Pi}_{\boldsymbol{V}} \boldsymbol{u}, \Pi_Q \boldsymbol{u} + \tilde{\Pi} p)$.

Proof. The linearity of $\mathscr{E}(\cdot,\cdot)$ is immediate from the definition (6.4.2), and (6.4.10) then follows from (6.4.4) and Theorem 6.4.2 using the triangle inequality. A simple consequence of (6.4.2c) to (6.4.2e) is that $\ker \mathscr{E} \subseteq \boldsymbol{V}_I \times Q_I$. Moreover, (6.4.10) gives that $\boldsymbol{V}_I \times Q_I \subseteq \ker \mathscr{E}$. Thus, $\ker \mathscr{E} = \boldsymbol{V}_I \times Q_I$. $\square$

6.5 Variational Form of the Schur Complement System

The results of the previous two sections are used to study the Schur complement system (6.2.2). The first result relates the Schur complement matrix $\boldsymbol{S}$ to the discrete Stokes extension map:

Lemma 6.5.1. *For all $(\boldsymbol{u}, p), (\boldsymbol{v}, q) \in \boldsymbol{V}_0 \times Q$, the Stokes extension satisfies*

$$a(\boldsymbol{u}_S, \boldsymbol{v}_S) + b(\boldsymbol{v}_S, p_S) + b(\boldsymbol{u}_S, q_S) = \begin{bmatrix} \vec{v}_E \\ \vec{q}_e \end{bmatrix}^T \boldsymbol{S} \begin{bmatrix} \vec{u}_E \\ \vec{p}_e \end{bmatrix} \tag{6.5.1}$$

where $\boldsymbol{S} = \begin{bmatrix} \widetilde{\boldsymbol{A}} & \widetilde{\boldsymbol{B}}^T \\ \widetilde{\boldsymbol{B}} & \widetilde{\boldsymbol{C}} \end{bmatrix}$. *Consequently, the following identities hold:*

$$\vec{u}_E^T \widetilde{\boldsymbol{A}} \vec{v}_E = a(\boldsymbol{\Pi}_{\boldsymbol{V}} \boldsymbol{u}, \boldsymbol{\Pi}_{\boldsymbol{V}} \boldsymbol{v}) \qquad \forall \boldsymbol{u}, \boldsymbol{v} \in \boldsymbol{V}_0, \tag{6.5.2a}$$

$$\vec{p}_e^T \widetilde{\boldsymbol{B}} \vec{u}_E = b(\boldsymbol{\Pi}_{\boldsymbol{V}} \boldsymbol{u}, \tilde{\Pi} p) \qquad \forall p \in Q, \ \boldsymbol{u} \in \boldsymbol{V}_0, \tag{6.5.2b}$$

$$\widetilde{\boldsymbol{C}} = \boldsymbol{0} \quad \textit{and} \quad \vec{g}_e^* = \vec{0}, \tag{6.5.2c}$$

where $\boldsymbol{\Pi}_{\boldsymbol{V}}$ *is defined in* (6.4.3), $\tilde{\Pi}$ *is defined in* (6.4.1), *and* $\vec{g}_e^*$ *is defined in* (6.2.2).

Proof. Let $(\boldsymbol{u}, p) \in \boldsymbol{V}_0 \times Q$. The Stokes extension $(\boldsymbol{u}_S, p_S) = \boldsymbol{\mathcal{E}}(\boldsymbol{u}, p)$ may be written as $\boldsymbol{u}_S = \vec{\Phi}_E^T \vec{u}_E + \vec{\Phi}_I^T \vec{u}_I^*$ and $p_S = \vec{\psi}_e^T \vec{p}_e + \vec{\psi}_\iota^T \vec{p}_\iota^*$ so that $\boldsymbol{u} = \vec{\Phi}_E^T \vec{u}_E + \vec{\Phi}_I^T \vec{u}_I$ and $p = \vec{\psi}_e^T \vec{p}_e + \vec{\psi}_\iota^T \vec{p}_\iota$ for suitable $\vec{u}_E$, $\vec{u}_I$, $\vec{p}_e$, and $\vec{p}_\iota$. Thanks to (6.4.2a) and (6.4.2b), $\vec{u}_I^*$ and $\vec{p}_\iota^*$ are given by

$$\begin{bmatrix} \vec{u}_I^* \\ \vec{p}_\iota^* \end{bmatrix} = - \begin{bmatrix} \boldsymbol{A}_{II} & \boldsymbol{B}_{I\iota} \\ \boldsymbol{B}_{\iota I} & \boldsymbol{0} \end{bmatrix}^{-1} \begin{bmatrix} \boldsymbol{A}_{IE} & \boldsymbol{B}_{Ie} \\ \boldsymbol{B}_{\iota E} & \boldsymbol{0} \end{bmatrix} \begin{bmatrix} \vec{u}_E \\ \vec{p}_e \end{bmatrix}. \tag{6.5.3}$$

Analogous relations hold replacing $(\boldsymbol{u}, p)$ by $(\boldsymbol{v}, q) \in \boldsymbol{V}_0 \times Q$. Now,

$$
\begin{aligned}
&a(\boldsymbol{u}_S, \boldsymbol{v}_S) + b(\boldsymbol{v}_S, p_S) + b(\boldsymbol{u}_S, q_S) \\
&\quad = \left[\begin{array}{c} \vec{v}_E \\ \vec{q}_e \\ \hline \vec{v}_I^* \\ \vec{q}_\iota^* \end{array}\right]^T
\left[\begin{array}{cc|cc} \boldsymbol{A}_{EE} & \boldsymbol{B}_{Ee} & \boldsymbol{A}_{EI} & \boldsymbol{B}_{E\iota} \\ \boldsymbol{B}_{eE} & \boldsymbol{0} & \boldsymbol{B}_{eI} & \boldsymbol{0} \\ \hline \boldsymbol{A}_{IE} & \boldsymbol{B}_{Ie} & \boldsymbol{A}_{II} & \boldsymbol{B}_{I\iota} \\ \boldsymbol{B}_{\iota E} & \boldsymbol{0} & \boldsymbol{B}_{\iota I} & \boldsymbol{0} \end{array}\right]
\left[\begin{array}{c} \vec{u}_E \\ \vec{p}_e \\ \hline \vec{u}_I^* \\ \vec{p}_\iota^* \end{array}\right],
\end{aligned}
$$

and then using (6.5.3), we obtain (6.5.1). Identities (6.5.2) are then obtained from (6.5.1) as follows:

(a) Choose $p = q = 0$. Then, $(\boldsymbol{\Pi_V u}, \Pi_Q \boldsymbol{u}), (\boldsymbol{\Pi_V v}, \Pi_Q \boldsymbol{v}) \in \boldsymbol{V} \times Q_I$ by Theorem 6.4.1, so $b(\boldsymbol{\Pi_V v}, \Pi_Q \boldsymbol{u}) + b(\boldsymbol{\Pi_V u}, \Pi_Q \boldsymbol{v}) = 0$ by (6.4.2b); (6.5.2a) follows.

(b) Choose $p = 0$ and $\boldsymbol{v} = \boldsymbol{0}$. By Theorem 6.4.2, $\mathscr{E}(\boldsymbol{0}, q) = (\boldsymbol{0}, \tilde{\Pi} q)$, and (6.5.2b) follows.

(c) Choose $\boldsymbol{u} = \boldsymbol{v} = \boldsymbol{0}$. By Theorem 6.4.2, $\mathscr{E}(\boldsymbol{0}, p) = (\boldsymbol{0}, \tilde{\Pi} p)$, $\mathscr{E}(\boldsymbol{0}, q) = (\boldsymbol{0}, \tilde{\Pi} q)$, and so $\vec{q}_e^T \widetilde{\boldsymbol{C}} \vec{p}_e = 0$ for all $p, q \in Q$. Thus, $\widetilde{\boldsymbol{C}} = \boldsymbol{0}$. Furthermore, for $\boldsymbol{u} \in \boldsymbol{V}_0$ satisfying (6.1.1), there holds

$$
\vec{q}_e^T \vec{g}_e^* = \vec{q}_e^T \widetilde{\boldsymbol{B}} \vec{u}_E = b(\boldsymbol{\Pi_V u}, \tilde{\Pi} q) = -b(\boldsymbol{u} - \boldsymbol{\Pi_V u}, \tilde{\Pi} q) \qquad \forall q \in Q
$$

by (6.1.1b). Since $\boldsymbol{u}|_{\partial K} = \boldsymbol{\Pi_V u}|_{\partial K}$ for all $K \in \mathcal{T}$, $\operatorname{div}(\boldsymbol{u} - \boldsymbol{\Pi_V u}) \in \operatorname{div} \boldsymbol{V}_I = Q_I \perp Q_I^\perp$, and so $b(\boldsymbol{u} - \boldsymbol{\Pi_V u}, \tilde{q}) = 0$, which completes (6.5.2c). $\square$

The main result of this section relates the Schur complement problem (6.2.2) to a Stokes problem posed on the boundary spaces $\tilde{\boldsymbol{V}}_E \times \tilde{Q}_E$:

Theorem 6.5.2. *The Schur complement system* (6.2.2)*, is equivalent to the following variational problem: Find* $(\boldsymbol{u}, p) \in \tilde{\boldsymbol{V}}_E \times \tilde{Q}_E$ *such that*

$$a(\boldsymbol{u}, \boldsymbol{v}) + b(\boldsymbol{v}, p) = (\boldsymbol{f}, \boldsymbol{v}) \qquad \forall \boldsymbol{v} \in \tilde{\boldsymbol{V}}_E, \tag{6.5.4a}$$

$$b(\boldsymbol{u}, q) = 0 \qquad \forall q \in \tilde{Q}_E. \tag{6.5.4b}$$

Moreover, the nonzero eigenvalues of the generalized eigenvalue problem $\widetilde{\boldsymbol{B}}\widetilde{\boldsymbol{A}}^{-1}\widetilde{\boldsymbol{B}}^T\vec{q}_e = \lambda\nu^{-1}\widetilde{\boldsymbol{M}}\vec{q}_e$ *are contained in the interval* $[\beta^2, 1]$*, where* $\widetilde{\boldsymbol{M}}$ *is the matrix associated with the* $L^2(\Omega)$*-inner product on* $Q_I^{\perp}$ *and* β *is the inf-sup constant in* (6.1.2)*. In particular, the nonzero eigenvalues* λ *are uniformly bounded away from zero in* h *and* k*.*

Proof. Let $(\boldsymbol{u}, p), (\boldsymbol{v}, q) \in \tilde{\boldsymbol{V}}_E \times Q_I^{\perp}$. Substituting the identities in Theorems 6.4.1 and 6.4.2 into (6.5.2) gives

$$\begin{aligned}
\begin{bmatrix} \vec{v}_E \\ \vec{q}_e \end{bmatrix}^T \boldsymbol{S} \begin{bmatrix} \vec{u}_E \\ \vec{p}_e \end{bmatrix} &= \vec{v}_E^T \widetilde{\boldsymbol{A}} \vec{u}_E^T + \vec{q}_e^T \widetilde{\boldsymbol{B}} \vec{u}_E + \vec{v}_E \widetilde{\boldsymbol{B}}^T \vec{p}_e \\
&= a(\boldsymbol{\Pi}_{\boldsymbol{V}}\boldsymbol{u}, \boldsymbol{\Pi}_{\boldsymbol{V}}\boldsymbol{v}) + b(\boldsymbol{\Pi}_{\boldsymbol{V}}\boldsymbol{v}, \tilde{\Pi} p) + b(\boldsymbol{\Pi}_{\boldsymbol{V}}\boldsymbol{u}, \tilde{\Pi} q) \\
&= a(\boldsymbol{u}, \boldsymbol{v}) + b(\boldsymbol{v}, p) + b(\boldsymbol{u}, q).
\end{aligned}$$

(6.5.4) now follows from (6.5.2c) on noting that $\tilde{Q}_E = Q_I^{\perp} \cap L_0^2(\Omega)$. Arguing as in [48, Theorem 3.22], the eigenvalue bound follows from the inf-sup condition (6.3.13). □

6.6 Basis Functions

We first define a basis $\{\phi_i\}$ for the space of scalar-valued functions V. The basis is constructed so that the exclusion of particular functions gives a basis for $V_0 = V \cap H_0^1(\Omega)$, which simplifies both the enforcement of homogeneous boundary conditions and the implementation of the preconditioner. A basis $\{\mathbf{\Phi}_i\}$ for the velocity space $\boldsymbol{V}_0 = V_0 \times V_0$ is then obtained using functions of the form $\phi_j \hat{\boldsymbol{e}}_1$ and $\phi_j \hat{\boldsymbol{e}}_2$, where $\hat{\boldsymbol{e}}_1 = [1,0]^T$ and $\hat{\boldsymbol{e}}_2 = [0,1]^T$. For the pressure space, we only give a basis for Q since the space Q_0 is not used in the actual implementation.

6.6.1 Basis Functions on a Reference Triangle

We begin by defining basis functions for the pressure and velocity spaces on the reference triangle $\hat{T}$ shown in Figure 4.5b.

6.6.1.1 Pressure Basis Functions

Let $\{B_\alpha^k\}_{\alpha\in\mathcal{I}}$ denote the Bernstein polynomials [71]:

$$B_\alpha^k = \frac{k!}{\alpha_1!\alpha_2!\alpha_3!}\lambda_1^{\alpha_1}\lambda_2^{\alpha_2}\lambda_3^{\alpha_3}, \tag{6.6.1}$$

where $\mathcal{I} = \{\alpha \in \mathbb{Z}_+^3 : |\alpha| = k\}$ and $\{\lambda_i,\ 1 \le i \le 3\}$, are the barycentric coordinates on the reference triangle $\hat{T}$. The set $\{B_\alpha^k\}_{\alpha\in\mathcal{I}}$ forms a basis for $\mathcal{P}_k(\hat{T})$ [71]. Each Bernstein polynomial B_α^k can be identified with the domain point $\boldsymbol{x}_\alpha = \frac{\alpha_1}{k}\hat{\boldsymbol{a}}_1 + \frac{\alpha_2}{k}\hat{\boldsymbol{a}}_2 + \frac{\alpha_3}{k}\hat{\boldsymbol{a}}_3$ on the reference triangle. Let $\mathcal{I}_0 = \{\alpha \in \mathcal{I} : \alpha_i < k\}$ denote the subset corresponding to interior (non-vertex) points. Fix any $\beta \in \mathcal{I}_0$; since all the Bernstein polynomials (6.6.1) share the same average value, the set $\{B_\alpha^k - B_\beta^k\}_{\alpha\in\mathcal{I}\setminus\{\beta\}}$ is a basis for $\mathcal{P}_k(\hat{T}) \cap L_0^2(\hat{T})$. This set can be partitioned into:

(i) Vertex functions:

$$\hat{\psi}_i := B_{ke_i}^k - B_\beta^k, \qquad 1 \le i \le 3,$$

satisfying $\int_{\hat{T}} \hat{\psi}_i d\boldsymbol{x} = 0$ and $\hat{\psi}_i(\hat{\boldsymbol{a}}_j) = \delta_{ij}$ for $1 \le i, j \le 3$. Here, $e_i \in \mathbb{Z}_+^3$ is given by $(e_i)_j = \delta_{ij}$, $1 \le i, j \le 3$.

(ii) Interior functions:

$$\hat{\psi}_{\iota,\alpha} := B_\alpha^k - B_\beta^k, \qquad \alpha \in \mathcal{I}_0 \setminus \{\beta\}$$

satisfying $\int_{\hat{T}} \hat{\psi}_{\imath,\alpha} d\boldsymbol{x} = 0$ and $\hat{\psi}_{\imath,\alpha}(\hat{\boldsymbol{a}}_i) = 0$, $1 \le i \le 3$.

In order to obtain a basis for $\mathcal{P}_k(\hat{T})$, we supplement this set with one additional function:

(iii) Average value function

$$\hat{\psi}_{\hat{T}} := 1 - \sum_{i=1}^{3} \hat{\psi}_i. \tag{6.6.2}$$

satisfying $|\hat{T}|^{-1} \int_{\hat{T}} \hat{\psi}_{\hat{T}} d\boldsymbol{x} = 1$ and $\hat{\psi}_{\hat{T}}(\boldsymbol{a}_i) = 0$, $1 \le i \le 3$.

In summary, there are 3 vertex functions, one average value function and $\frac{1}{2}(k+1)(k+2) - 4$ interior functions which total $\frac{1}{2}(k+1)(k+2) = \dim \mathcal{P}_k(\hat{T})$, and form a basis for the pressure space $Q = \mathcal{P}_k(\hat{T})$ on the reference element.

6.6.1.2 Velocity Basis Functions

The construction of the basis functions for the velocity space V is more complicated owing to the higher continuity requirement. In particular, the basis functions $\{\hat{\phi}_i^\beta\}$, $\beta \in \mathbb{Z}_+^2$, $|\beta| = 1$, $i \in \{1,2,3\}$, associated with the derivative degrees of freedom at the vertices should satisfy $D^\alpha \hat{\phi}_i^\beta(\hat{\boldsymbol{a}}_j) = \delta_{\alpha\beta}\delta_{ij}$, $\alpha \in \mathbb{Z}_+^2$, $|\alpha| = 1$, $j \in \{1,2,3\}$. In order to construct these functions, we begin by considering the vector valued function given by

$$\vec{J}_1 := \frac{\lambda_1^2}{P_{k-3}^{(3,3)}(-1)} \begin{bmatrix} \lambda_2 P_{k-3}^{(3,3)}(\lambda_2 - \lambda_1) \\ \lambda_3 P_{k-3}^{(3,3)}(\lambda_3 - \lambda_1) \end{bmatrix}, \tag{6.6.3}$$

where $P_l^{(3,3)}$ is the Jacobi polynomial of degree l [108]. The first component of $\vec{J}_1$ vanishes on edge $\hat{\gamma}_2$ and the gradient at $\hat{\boldsymbol{a}}_1$ is given by $[1 \quad 0]^T$, while the second component vanishes on edge $\hat{\gamma}_3$ and has gradient $[0 \quad 1]^T$ at $\hat{\boldsymbol{a}}_1$. The factor λ_1^2 means that both components of $\vec{J}_1$ and their gradients vanish on the edge $\hat{\gamma}_1$. In summary, since $x = \lambda_2$ and $y = \lambda_3$, we have

$$\vec{J}_1(\hat{\boldsymbol{a}}_i) = \vec{0} \quad \text{and} \quad \begin{bmatrix} \frac{\partial}{\partial x} \\ \frac{\partial}{\partial y} \end{bmatrix} \vec{J}_1^T(\hat{\boldsymbol{a}}_i) = \begin{bmatrix} \frac{\partial}{\partial \lambda_2} \\ \frac{\partial}{\partial \lambda_3} \end{bmatrix} \vec{J}_1^T(\hat{\boldsymbol{a}}_i) = \delta_{i1} \begin{bmatrix} 1 & 0 \\ 0 & 1 \end{bmatrix}. \tag{6.6.4}$$

Defining $\vec{J}_2$ and $\vec{J}_3$ by cyclic permutations of the indices, we conclude that $\vec{J}_2$ and $\vec{J}_3$ vanish at the vertices and that, for $i \in \{1, 2, 3\}$,

$$\begin{bmatrix} \frac{\partial}{\partial \lambda_3} \\ \frac{\partial}{\partial \lambda_1} \end{bmatrix} \vec{J}_2^T(\hat{\boldsymbol{a}}_i) = \delta_{i2} \begin{bmatrix} 1 & 0 \\ 0 & 1 \end{bmatrix} \quad \text{and} \quad \begin{bmatrix} \frac{\partial}{\partial \lambda_1} \\ \frac{\partial}{\partial \lambda_2} \end{bmatrix} \vec{J}_3^T(\hat{\boldsymbol{a}}_i) = \delta_{i3} \begin{bmatrix} 1 & 0 \\ 0 & 1 \end{bmatrix}. \tag{6.6.5}$$

Substituting the identities

$$\begin{bmatrix} \frac{\partial}{\partial \lambda_3} \\ \frac{\partial}{\partial \lambda_1} \end{bmatrix} = \begin{bmatrix} -1 & 1 \\ -1 & 0 \end{bmatrix} \begin{bmatrix} \frac{\partial}{\partial x} \\ \frac{\partial}{\partial y} \end{bmatrix} \quad \text{and} \quad \begin{bmatrix} \frac{\partial}{\partial \lambda_1} \\ \frac{\partial}{\partial \lambda_2} \end{bmatrix} = \begin{bmatrix} 0 & -1 \\ 1 & -1 \end{bmatrix} \begin{bmatrix} \frac{\partial}{\partial x} \\ \frac{\partial}{\partial y} \end{bmatrix}$$

in (6.6.5) and rearranging gives

$$\begin{bmatrix} \frac{\partial}{\partial x} \\ \frac{\partial}{\partial y} \end{bmatrix} \left(\begin{bmatrix} -1 & -1 \\ 1 & 0 \end{bmatrix} \vec{J}_2 \right)^T (\hat{\boldsymbol{a}}_i) = \delta_{i2} \begin{bmatrix} 1 & 0 \\ 0 & 1 \end{bmatrix}, \tag{6.6.6}$$

$$\begin{bmatrix} \frac{\partial}{\partial x} \\ \frac{\partial}{\partial y} \end{bmatrix} \left(\begin{bmatrix} 0 & 1 \\ -1 & -1 \end{bmatrix} \vec{J}_3 \right)^T (\hat{\boldsymbol{a}}_i) = \delta_{i3} \begin{bmatrix} 1 & 0 \\ 0 & 1 \end{bmatrix}. \tag{6.6.7}$$

Armed with (6.6.4), (6.6.6) and (6.6.7), we define the basis functions for the velocity space as follows:

(i) C^0 vertex functions:

$$\hat{\phi}_i = \lambda_i^2(3 - 2\lambda_i), \qquad 1 \le i \le 3,$$

satisfying $\hat{\phi}_i(\hat{\boldsymbol{a}}_j) = \delta_{ij}$, $\nabla\,\hat{\phi}_i(\hat{\boldsymbol{a}}_j) = \mathbf{0}$, and $\hat{\phi}_i|_{\hat{\gamma}_i} = 0$ for $1 \le i, j \le 3$.

(ii) C^1 vertex functions

$$\begin{bmatrix} \hat{\phi}_1^{(1,0)} \\ \hat{\phi}_1^{(0,1)} \end{bmatrix} = \begin{bmatrix} 1 & 0 \\ 0 & 1 \end{bmatrix} \vec{J}_1, \quad \begin{bmatrix} \hat{\phi}_2^{(1,0)} \\ \hat{\phi}_2^{(0,1)} \end{bmatrix} = \begin{bmatrix} -1 & -1 \\ 1 & 0 \end{bmatrix} \vec{J}_2, \quad \text{and} \quad \begin{bmatrix} \hat{\phi}_3^{(1,0)} \\ \hat{\phi}_3^{(0,1)} \end{bmatrix} = \begin{bmatrix} 0 & 1 \\ -1 & -1 \end{bmatrix} \vec{J}_3$$

which, thanks to (6.6.4), (6.6.6) and (6.6.7), satisfy $D^\beta \hat{\phi}_i^\alpha(\hat{\boldsymbol{a}}_j) = \delta_{\alpha\beta}\delta_{ij}$ and $\hat{\phi}_i|_{\hat{\gamma}_i} = 0$ for $1 \le i, j \le 3$, $|\alpha| = 1$, $|\beta| \le 1$.

(iii) Edge functions: Let $\hat{\gamma}$ be the edge connecting vertices $\hat{\boldsymbol{a}}_i$ and $\hat{\boldsymbol{a}}_j$; then the basis functions associated with the edge are defined by

$$\hat{\phi}_{\hat{\gamma},l} = \lambda_i^2 \lambda_j^2 r_l(\lambda_j - \lambda_i), \qquad 1 \le l \le k-3$$

where $\{r_l\}$ is any basis for $\mathcal{P}_{k-4}((-1,1))$. These functions satisfy $D^{\alpha}\hat{\phi}_{\hat{\gamma},l}(\hat{\boldsymbol{a}}_m) = 0$ for $|\alpha| \le 1$, $1 \le m \le 3$, and $\hat{\phi}_{\hat{\gamma},l}|_{\hat{\gamma}'} = \delta_{\hat{\gamma}\hat{\gamma}'}$ for $\hat{\gamma}' \in \mathcal{E}_{\hat{T}}$.

(iv) Interior functions: The basis functions associated with the element interior are defined by

$$\hat{\phi}_{I,l} = \lambda_1 \lambda_2 \lambda_3 s_l, \qquad 1 \le l \le \frac{k^2 - 3k + 2}{2},$$

where $\{s_l\}$ is any basis for $\mathcal{P}_{k-3}(\hat{T})$. These functions satisfy $\hat{\phi}_{I,l}|_{\partial \hat{T}} = 0$ and $\nabla \hat{\phi}_{I,l}(\hat{\boldsymbol{a}}_m)$ $= \mathbf{0}$ for $1 \le m \le 3$.

It is easily seen that the above functions are linearly independent. Furthermore, there are 3 functions per vertex, $\dim \mathcal{P}_{k-4}((-1,1)) = k-3$ functions per edge, and $\dim \mathcal{P}_{k-3}(\hat{T}) = \frac{1}{2}(k-2)(k-1)$ interior functions which total $\frac{1}{2}(k+1)(k+2) = \dim \mathcal{P}_k(\hat{T})$. Hence, the above functions also form a basis for $\mathcal{P}_k(\hat{T})$.

6.6.2 Basis Functions on a Mesh

We now define the global basis functions for the spaces Q and V. The lower continuity requirements imposed at corner vertices $\mathcal{V}_C$ means that extra care must be taken when defining the global basis functions associated with $\mathcal{V}_C$.

6.6.2.1 Pressure Basis Functions

The pressure space Q requires C^0 continuity at all vertices except at corner vertices, where the functions are allowed to be discontinuous. This means that *each element has its own degree of freedom* at vertices $\boldsymbol{a} \in \mathcal{V}_C$, whilst at the remaining vertices $\boldsymbol{a} \in \mathcal{V} \setminus \mathcal{V}_C$, all elements *share a single degree of freedom* at the common vertex as shown in Figure 6.1a. Consequently, any given vertex $\boldsymbol{a} \in \mathcal{V}$ is associated with either (a) *a single* basis function supported on the patch $\mathcal{T}_{\boldsymbol{a}}$ if $\boldsymbol{a} \in \mathcal{V} \setminus \mathcal{V}_C$, or (b) *a collection* of basis functions, each of which is supported on a single element $K \in \mathcal{T}_{\boldsymbol{a}}$ if $\boldsymbol{a} \in \mathcal{V}_C$. The set of supports of the pressure functions associated with a vertex $\boldsymbol{a} \in \mathcal{V}$ is defined by

$$\Omega_{\boldsymbol{a}} = \begin{cases} \{\mathcal{T}_{\boldsymbol{a}}\} & \boldsymbol{a} \in \mathcal{V}_C \\ \{K \in \mathcal{T}_{\boldsymbol{a}}\} & \boldsymbol{a} \in \mathcal{V} \setminus \mathcal{V}_C. \end{cases}$$

That is, the cardinality of these sets is $|\Omega_{\boldsymbol{a}}| = 1$ for noncorner vertices (since there is only one vertex basis function associated to $\boldsymbol{a}$) whilst $|\Omega_{\boldsymbol{a}}| \geq 2$ for corner vertices,

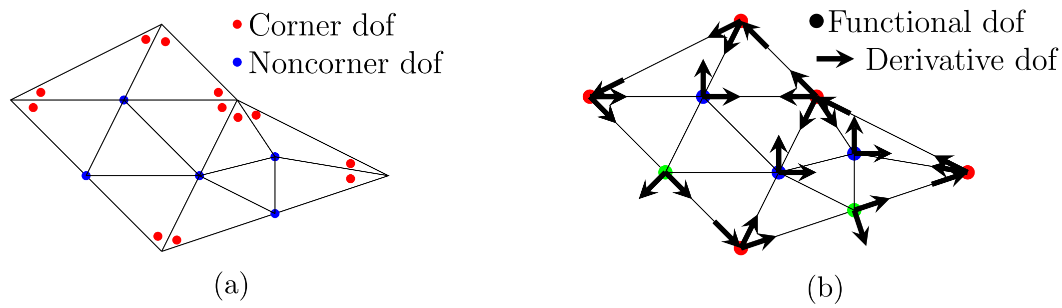

Figure 6.1: (a) The global pressure vertex degrees of freedom and (b) the global velocity vertex degrees of freedom on a mesh of an example domain. Observe that in (a) there are multiple pressure vertex degrees of freedom at corner vertices but only a single degree of freedom at interior vertices and at noncorner boundary vertices and in (b) there are three or more derivative degrees of freedom at corner vertices (red), two derivative degrees of freedom aligned with the domain boundary at noncorner boundary vertices (green), and two derivative degrees of freedom aligned with the coordinate axes at interior vertices (blue).

thanks to the assumption that the mesh is corner-split into at least two elements. The corresponding global vertex functions $\{\psi_{\boldsymbol{a}}^{\omega} : \boldsymbol{a} \in \mathcal{V},\ \omega \in \Omega_{\boldsymbol{a}}\}$ are defined to be pull-backs in the usual way: For each element $K \in \mathcal{T}$, let $\boldsymbol{F}_K : \hat{T} \to K$ be an arbitrary, but fixed, invertible affine transformation. Then,

$$\psi_{\boldsymbol{a}}^{\omega} = \begin{cases} \hat{\psi}_i \circ \boldsymbol{F}_K^{-1} & \text{on } K \subseteq \omega, \\ 0 & \text{otherwise,} \end{cases} \quad \text{and} \quad \psi_K = \begin{cases} \hat{\psi}_{\hat{T}} \circ \boldsymbol{F}_K^{-1} & \text{on } K, \\ 0 & \text{otherwise,} \end{cases} \tag{6.6.8}$$

where i is the index such that $\hat{\boldsymbol{a}}_i = \boldsymbol{F}_K^{-1}(\boldsymbol{a})$.

The average value functions and interior functions are simpler. Each element $K \in \mathcal{T}$ has a single function ψ_K, corresponding to the average value over K, defined by (6.6.8). Similarly, each element $K \in \mathcal{T}$ has $\frac{k}{2}(k+1) - 4$ interior functions also defined to be pull-backs. Thus, there are a total of $\mathcal{O}(|\mathcal{V}| + |\mathcal{T}|k^2)$ global pressure basis functions.

6.6.2.2 Velocity Basis Functions

The velocity space V imposes C^1 continuity at all vertices except at corner vertices, where only C^0-continuity is required to ensure $V \subset H^1(\Omega)$. This means that at corner vertices $\boldsymbol{a} \in \mathcal{V}_C$, each element $K \in \mathcal{T}_{\boldsymbol{a}}$ has two degrees of freedom for the gradient corresponding to the two tangential derivatives corresponding to the two edges of K that meet at $\boldsymbol{a}$. To enforce continuity between two neighboring elements in $\mathcal{T}_{\boldsymbol{a}}$, the tangential derivative corresponding to the common edge must be *shared between the two elements*. In other words, each corner vertex $\boldsymbol{a} \in \mathcal{V}_C$ has *one derivative degree of freedom for each edge* $\gamma \in \mathcal{E}_{\boldsymbol{a}}$. For the remaining noncorner vertices $\boldsymbol{a} \in \mathcal{V} \setminus \mathcal{V}_C$, all elements in $\mathcal{T}_{\boldsymbol{a}}$ *share two degrees of freedom* at the common vertex, corresponding to any two linearly independent directional derivatives as in Figure 6.1b. Consequently, a given vertex $\boldsymbol{a} \in \mathcal{V}$ is associated with either (a) *two* basis functions supported on the patch $\mathcal{T}_{\boldsymbol{a}}$ if $\boldsymbol{a} \in \mathcal{V} \setminus \mathcal{V}_C$, or (b) *a collection* of basis functions, each of which is associated to an edge $\gamma \in \mathcal{E}_{\boldsymbol{a}}$ and supported on the pair of elements sharing the common edge γ if $\boldsymbol{a} \in \mathcal{V}_C$.

The set of unit vectors defining the directional derivative degrees of freedom at a vertex $\boldsymbol{a} \in \mathcal{V}$ are chosen as follows:

$$D_{\boldsymbol{a}} = \begin{cases} \{\hat{\boldsymbol{e}}_1, \hat{\boldsymbol{e}}_2\} & \boldsymbol{a} \in \mathcal{V}_I, \\ \{\hat{\boldsymbol{t}}, \hat{\boldsymbol{n}}\} & \boldsymbol{a} \in \mathcal{V}_B, \\ \{\hat{\boldsymbol{t}}_\gamma : \gamma \in \mathcal{E}_{\boldsymbol{a}}\} & \boldsymbol{a} \in \mathcal{V}_C, \end{cases} \tag{6.6.9}$$

where $\hat{\boldsymbol{t}}$ and $\hat{\boldsymbol{n}}$ are the unit tangent and normal vectors at a noncorner boundary vertex $\boldsymbol{a} \in \mathcal{V}_B$ and $\hat{\boldsymbol{t}}_\gamma$ denotes a unit tangent vector on an edge $\gamma \in \mathcal{E}$ as illustrated in Figure 6.1b. For a given vertex $\boldsymbol{a} \in \mathcal{V}$ and unit vector $\hat{\boldsymbol{\mu}} \in D_{\boldsymbol{a}}$, the global basis function $\phi_{\boldsymbol{a}}^{\hat{\boldsymbol{\mu}}}$ has support

$$\operatorname{supp} \phi_{\boldsymbol{a}}^{\hat{\boldsymbol{\mu}}} = \begin{cases} \{K \in \mathcal{T}_{\boldsymbol{a}} : \exists \gamma \in \mathcal{E}_K \text{ with } \hat{\boldsymbol{t}}_\gamma = \pm \hat{\boldsymbol{\mu}}\} & \boldsymbol{a} \in \mathcal{V}_C, \\ \mathcal{T}_{\boldsymbol{a}} & \boldsymbol{a} \in \mathcal{V} \setminus \mathcal{V}_C. \end{cases}$$

The global C^1 vertex functions come in pairs as follows: Given a noncorner vertex $\boldsymbol{a} \in \mathcal{V}_I \cup \mathcal{V}_B$, let $\hat{\boldsymbol{\mu}}_1$, $\hat{\boldsymbol{\mu}}_2$ be unit vectors such that $D_{\boldsymbol{a}} = \{\hat{\boldsymbol{\mu}}_1, \hat{\boldsymbol{\mu}}_2\}$ as in (6.6.9), and define the basis functions by

$$\begin{bmatrix} \phi_{\boldsymbol{a}}^{\hat{\boldsymbol{\mu}}_1} \\ \phi_{\boldsymbol{a}}^{\hat{\boldsymbol{\mu}}_2} \end{bmatrix} = \begin{bmatrix} \hat{\boldsymbol{\mu}}_1 & \hat{\boldsymbol{\mu}}_2 \end{bmatrix}^{-1} D\boldsymbol{F}_K^T \begin{bmatrix} \hat{\phi}_i^{(1,0)} \circ \boldsymbol{F}_K^{-1} \\ \hat{\phi}_i^{(0,1)} \circ \boldsymbol{F}_K^{-1} \end{bmatrix} \qquad \text{on } K \in \mathcal{T}_{\boldsymbol{a}}, \tag{6.6.10}$$

where i is the index such that $\hat{\boldsymbol{a}}_i = \boldsymbol{F}_K^{-1}(\boldsymbol{a})$ and $D\boldsymbol{F}_K$ is the Jacobian matrix. The above construction ensures that the basis functions are C^1 continuous at the vertex $\boldsymbol{a}$: i.e. $\hat{\boldsymbol{\mu}}_i \cdot \nabla \phi_{\boldsymbol{a}}^{\hat{\boldsymbol{\mu}}_j}(\boldsymbol{a}) = \delta_{ij}$. The case of a corner vertex $\boldsymbol{a} \in \mathcal{V}_C$ is more complicated since, as mentioned above, each edge $\gamma \in \mathcal{E}_{\boldsymbol{a}}$ contributes one independent basis function at the vertex, also defined by the expression (6.6.10), which is supported on the edge patch $\{K \in \mathcal{T}_{\boldsymbol{a}} : \gamma \in \mathcal{E}_K\}$. The unit vectors $\hat{\boldsymbol{\mu}}_1, \hat{\boldsymbol{\mu}}_2$ in (6.6.10) associated with such an element $K \in \mathcal{T}_{\boldsymbol{a}}$ are taken to be the pair of unit tangent vectors on the two edges of K having an endpoint at $\boldsymbol{a}$. This means that the basis functions $\phi_{\boldsymbol{a}}^{\hat{\boldsymbol{\mu}}_1}$ and $\phi_{\boldsymbol{a}}^{\hat{\boldsymbol{\mu}}_2}$ are the only C^1 vertex functions supported on K.

The remaining C^0 vertex functions, edge functions, and interior functions are again defined to be pull-backs of the corresponding functions on the reference element in the usual way: i.e. $\phi_{\boldsymbol{a}} = \hat{\phi}_i \circ \boldsymbol{F}_K^{-1}$ on $K \in \mathcal{T}_{\boldsymbol{a}}$ and $\phi_{\boldsymbol{a}} = 0$ otherwise, where i is the index such that $\hat{\boldsymbol{a}}_i = \boldsymbol{F}_K^{-1}(\boldsymbol{a})$. Similarly, there are $k-3$ edge functions per edge $\gamma \in \mathcal{E}$, supported on the patch of elements containing that edge $\{K \in \mathcal{T} : \gamma \in \mathcal{E}_K\}$, and there are $\frac{1}{2}(k-1)(k-2)$ interior functions per element $K \in \mathcal{T}$. Overall, there are a total of $\mathcal{O}(|\mathcal{V}| + |\mathcal{E}|k + |\mathcal{T}|k^2)$ global velocity basis functions.

6.6.2.3 Velocity Basis Functions with Homogeneous Boundary Conditions

The above construction gives a basis for V in the absence of essential boundary conditions. If nonhomogeneous essential boundary conditions are imposed, then the values of the following basis functions will be constrained by the boundary data:

- the C^0 vertex function $\phi_{\boldsymbol{a}}$, $\boldsymbol{a} \in \mathcal{V} \setminus \mathcal{V}_I$ at each vertex on the domain boundary;

- the C^1 vertex function at each noncorner boundary vertex corresponding to the tangential derivative degree of freedom, i.e. $\phi_{\boldsymbol{a}}^{\hat{\boldsymbol{t}}}$ for $\boldsymbol{a} \in \mathcal{V}_B$;
- the pair of C^1 vertex functions at each corner boundary vertex corresponding to the tangential derivatives along the domain boundary edges: $\phi_{\boldsymbol{a}}^{\hat{\boldsymbol{t}}_\gamma}$, $\phi_{\boldsymbol{a}}^{\hat{\boldsymbol{t}}_{\gamma'}}$ for $\boldsymbol{a} \in \mathcal{V}_C$ where $\gamma, \gamma' \in \mathcal{E}_{\boldsymbol{a}} \cap \Gamma$; and
- all $k-3$ edge functions for each edge on the domain boundary.

If homogeneous essential boundary conditions are imposed, then a basis for $V_0 = V \cap H_0^1(\Omega)$ is obtained by taking the following functions:

- the C^0 vertex function at each interior vertex, i.e. $\phi_{\boldsymbol{a}}$, $\boldsymbol{a} \in \mathcal{V}_I$;
- the following C^1 vertex functions: $\phi_{\boldsymbol{a}}^{\hat{\boldsymbol{\mu}}}$, $\boldsymbol{a} \in \mathcal{V}$, $\hat{\boldsymbol{\mu}} \in \mathring{D}_{\boldsymbol{a}}$ where

$$\mathring{D}_{\boldsymbol{a}} = \begin{cases} \{\hat{\boldsymbol{e}}_1, \hat{\boldsymbol{e}}_2\} & \boldsymbol{a} \in \mathcal{V}_I, \\ \{\hat{\boldsymbol{n}}\} & \boldsymbol{a} \in \mathcal{V}_B, \\ \{\hat{\boldsymbol{t}}_\gamma : \gamma \in \mathcal{E}_{\boldsymbol{a}} \cap \mathcal{E}_I\} & \boldsymbol{a} \in \mathcal{V}_C. \end{cases} \tag{6.6.11}$$

- all $k-3$ edge functions on each interior edge; and
- all interior functions on each element.

Condition (6.6.11) means that we keep both C^1 vertex functions for each interior vertex, the C^1 vertex function associated with the outward normal of Γ for each noncorner boundary vertex, and each C^1 vertex function corresponding to an interior edge unit tangent vector at corner vertices.

6.7 Constructing the Preconditioner Using Additive Schwarz Theory

In Section 6.2, we constructed the stiffness matrix for the Stokes problem (6.2.1) using bases for the spaces $\boldsymbol{V}_0$ and Q and performed static condensation to arrive at the Schur complement system (6.2.2). In Section 6.5, it was shown that the algebraic Schur complement system (6.2.2) was related to the mixed finite element problem (6.5.4) posed on the spaces $\tilde{\boldsymbol{V}}_E \times \tilde{Q}_E$. The alert reader will have noticed a slight discrepancy in the treatment of the average pressure mode over the domain Ω: in Sections 6.2 and 6.6.2, the average pressure modes were included in the discretization (and it was pointed out that these modes span the kernel of the Schur complement) whereas in Section 6.5, the pressure space $\tilde{Q}_E = Q_I^{\perp} \cap L_0^2(\Omega)$ was used, which factors out the singular mode. In order to construct a preconditioner in the form (6.2.4), we formulate an Additive Schwarz Method (ASM) over the spaces $\tilde{\boldsymbol{V}}_E \times Q_I^{\perp}$ rather than the seemingly more natural choice $\tilde{\boldsymbol{V}}_E \times \tilde{Q}_E$ suggested by Theorem 6.5.2.

6.7.1 Pressure ASM

We decompose the pressure space $Q_I^\perp$ as follows:

$$Q_I^\perp = \bigoplus_{\substack{\boldsymbol{a}\in\mathcal{V}\\ \omega\in\Omega_{\boldsymbol{a}}}} \tilde{Q}_{\boldsymbol{a},\omega} \oplus \bigoplus_{K\in\mathcal{T}} \tilde{Q}_K, \tag{6.7.1}$$

where:

(i) the vertex spaces

$$\tilde{Q}_{\boldsymbol{a},\omega} := \mathrm{span}\{\tilde{\psi}_{\boldsymbol{a}}^\omega\}, \qquad \boldsymbol{a}\in\mathcal{V},\ \omega\in\Omega_{\boldsymbol{a}}, \qquad \text{with} \quad \tilde{\psi}_{\boldsymbol{a}}^\omega := \tilde{\Pi}\psi_{\boldsymbol{a}}^\omega$$

are equipped with the inner product

$$m_{\boldsymbol{a},\omega}(p,q) := |\omega| k^{-4} p(\boldsymbol{a}) q(\boldsymbol{a}) \qquad \forall p,q\in\tilde{Q}_{\boldsymbol{a},\omega}.$$

(ii) the element average spaces

$$\tilde{Q}_K := \mathrm{span}\{\tilde{\psi}_K\}, \qquad K\in\mathcal{T}, \qquad \text{with} \quad \tilde{\psi}_K := \tilde{\Pi}\psi_K$$

are equipped with the inner product

$$m_K(p,q) := \frac{1}{|K|}\left(\int_K p\ d\boldsymbol{x}\right)\left(\int_K q\ d\boldsymbol{x}\right) \qquad \forall p,q\in\tilde{Q}_K.$$

Applying the projection $\tilde{\Pi}$ to the formulae for ψ_K (6.6.2) and (6.6.8) gives

$$\tilde{\psi}_K = \begin{cases} 1 - \sum\limits_{\substack{\boldsymbol{a} \in \mathcal{V}_K \\ \Omega_{\boldsymbol{a}} \ni \omega \supseteq K}} \tilde{\psi}_{\boldsymbol{a}}^{\omega} & \text{on } K, \\ 0 & \text{otherwise,} \end{cases}$$

where the functions $\tilde{\psi}_{\boldsymbol{a}}^{\omega}$ are defined in (i) and we use the fact that $\tilde{\Pi}$ preserves constants.

The direct sum decomposition (6.7.1) means that any $q \in Q_I^{\perp}$ may be uniquely expressed in the form

$$q = \sum_{\substack{\boldsymbol{a} \in \mathcal{V} \\ \omega \in \Omega_{\boldsymbol{a}}}} q_{\boldsymbol{a},\omega} + \sum_{K \in \mathcal{T}} q_K,$$

where

$$q_{\boldsymbol{a},\omega} = q|_{\omega}(\boldsymbol{a}) \tilde{\psi}_{\boldsymbol{a}}^{\omega}, \quad \boldsymbol{a} \in \mathcal{V},\ \omega \in \Omega_{\boldsymbol{a}}, \quad \text{and} \quad q_K = \left(\frac{1}{|K|} \int_K q \, d\boldsymbol{x} \right) \tilde{\psi}_K, \quad K \in \mathcal{T}.$$

The action of the associated ASM preconditioner on a residual $g \in L^2(\Omega)$ is given by the solution $p \in Q_I^{\perp}$ of the variational problem $\bar{m}(p,q) = (g,q)\ \forall q \in Q_I^{\perp}$, where

$$\bar{m}(p,q) := \sum_{\substack{\boldsymbol{a} \in \mathcal{V} \\ \omega \in \Omega_{\boldsymbol{a}}}} m_{\boldsymbol{a},\omega}(p_{\boldsymbol{a},\omega}, q_{\boldsymbol{a},\omega}) + \sum_{K \in \mathcal{T}} m_K(p_K, q_K). \tag{6.7.2}$$

The bilinear form $\bar{m}(\cdot,\cdot)$ gives rise to a matrix preconditioner $\bar{\boldsymbol{M}}$ for the pressure space defined by

$$\vec{p}_e^T \bar{\boldsymbol{M}} \vec{q}_e = \bar{m}(\tilde{\Pi} p, \tilde{\Pi} q) \qquad \forall p, q \in Q. \tag{6.7.3}$$

6.7.2 Velocity ASM

We decompose the velocity space $\tilde{\boldsymbol{V}}_E$ as follows:

$$\tilde{\boldsymbol{V}}_E = \tilde{\boldsymbol{V}}_c \oplus \bigoplus_{\substack{\boldsymbol{a}\in\mathcal{V} \\ \hat{\boldsymbol{\mu}}\in\mathring{D}_{\boldsymbol{a}}}} \tilde{\boldsymbol{V}}_{\boldsymbol{a},\hat{\boldsymbol{\mu}}} \oplus \bigoplus_{\gamma\in\mathcal{E}_I} \tilde{\boldsymbol{V}}_\gamma, \tag{6.7.4}$$

where:

(i) the global C^0 vertex space

$$\tilde{\boldsymbol{V}}_c := \operatorname{span}\{\boldsymbol{\Pi_V}(\phi_{\boldsymbol{a}}\hat{\boldsymbol{e}}_1),\ \boldsymbol{\Pi_V}(\phi_{\boldsymbol{a}}\hat{\boldsymbol{e}}_2) : \boldsymbol{a}\in\mathcal{V}_I\},$$

(ii) the C^1 vertex spaces

$$\tilde{\boldsymbol{V}}_{\boldsymbol{a},\hat{\boldsymbol{\mu}}} := \operatorname{span}\{\boldsymbol{\Pi_V}(\phi_{\boldsymbol{a}}^{\hat{\boldsymbol{\mu}}}\hat{\boldsymbol{e}}_1),\ \boldsymbol{\Pi_V}(\phi_{\boldsymbol{a}}^{\hat{\boldsymbol{\mu}}}\hat{\boldsymbol{e}}_2)\}, \qquad \boldsymbol{a}\in\mathcal{V},\ \hat{\boldsymbol{\mu}}\in\mathring{D}_{\boldsymbol{a}},$$

(iii) the edge spaces

$$\tilde{\boldsymbol{V}}_\gamma := \operatorname{span}\{\boldsymbol{\Pi_V}(\phi_{\gamma,j}\hat{\boldsymbol{e}}_1), \boldsymbol{\Pi_V}(\phi_{\gamma,j}\hat{\boldsymbol{e}}_2) : 1 \leq j \leq k-3\}, \qquad \gamma \in \mathcal{E}_I.$$

Each of the velocity subspaces is equipped with the inner product $a(\cdot,\cdot)$ restricted to the appropriate space. The direct sum decomposition (6.7.4) means that any $\boldsymbol{u} \in \tilde{\boldsymbol{V}}_E$ may be uniquely expressed in the form

$$\boldsymbol{u} = \boldsymbol{u}_c + \sum_{\substack{\boldsymbol{a}\in\mathcal{V} \\ \hat{\boldsymbol{\mu}}\in\mathring{D}_{\boldsymbol{a}}}} \boldsymbol{u}_{\boldsymbol{a},\hat{\boldsymbol{\mu}}} + \sum_{\gamma\in\mathcal{E}_I} \boldsymbol{u}_\gamma, \tag{6.7.5}$$

where

$$\boldsymbol{u}_c = \sum_{\boldsymbol{a}\in\mathcal{V}_I} \sum_{i=1}^{2} (\boldsymbol{u}\cdot\hat{\boldsymbol{e}}_i)(\boldsymbol{a})\boldsymbol{\Pi_V}(\phi_{\boldsymbol{a}}\hat{\boldsymbol{e}}_i),$$

$$\boldsymbol{u}_{\boldsymbol{a},\hat{\boldsymbol{\mu}}} = \sum_{i=1}^{2} \partial_{\hat{\boldsymbol{\mu}}}(\boldsymbol{u}|_{K_{\hat{\mu}}}\cdot\hat{\boldsymbol{e}}_i)(\boldsymbol{a})\boldsymbol{\Pi_V}(\phi_{\boldsymbol{a}}^{\hat{\boldsymbol{\mu}}}\hat{\boldsymbol{e}}_i), \quad \boldsymbol{a}\in\mathcal{V}, \quad \hat{\boldsymbol{\mu}}\in\mathring{D}_{\boldsymbol{a}}, \quad K_{\hat{\boldsymbol{\mu}}} \subseteq \operatorname{supp}\phi_{\boldsymbol{a}}^{\hat{\boldsymbol{\mu}}},$$

and for each $\gamma \in \mathcal{E}_I$,

$$\boldsymbol{u}_\gamma = \begin{cases} \boldsymbol{u} - \boldsymbol{u}_c - \sum_{\substack{\boldsymbol{a}\in\mathcal{V} \\ \hat{\boldsymbol{\mu}}\in\mathring{D}_{\boldsymbol{a}}}} \boldsymbol{u}_{\boldsymbol{a},\hat{\boldsymbol{\mu}}} & \text{on } \gamma, \\ \boldsymbol{0} & \text{on the remaining edges in } \mathcal{E}. \end{cases}$$

The action of the associated ASM preconditioner on a residual $\boldsymbol{f} \in \boldsymbol{L}^2(\Omega)$ is given by the solution $\boldsymbol{u} \in \tilde{\boldsymbol{V}}_E$ of the variational problem $\bar{a}(\boldsymbol{u}, \boldsymbol{v}) = (\boldsymbol{f}, \boldsymbol{v})\ \forall \boldsymbol{v} \in \tilde{\boldsymbol{V}}_E$, where

$$\bar{a}(\boldsymbol{u}, \boldsymbol{v}) = a(\boldsymbol{u}_c, \boldsymbol{v}_c) + \sum_{\substack{\boldsymbol{a} \in \mathcal{V} \\ \hat{\boldsymbol{\mu}} \in \mathring{D}_{\boldsymbol{a}}}} a(\boldsymbol{u}_{\boldsymbol{a},\hat{\boldsymbol{\mu}}}, \boldsymbol{v}_{\boldsymbol{a},\hat{\boldsymbol{\mu}}}) + \sum_{\gamma \in \mathcal{E}_I} a(\boldsymbol{u}_\gamma, \boldsymbol{v}_\gamma). \tag{6.7.6}$$

The bilinear form $\bar{a}(\cdot, \cdot)$ gives rise to a matrix preconditioner $\bar{\boldsymbol{A}}$ for the velocity space defined by

$$\vec{u}_E^T \bar{\boldsymbol{A}} \vec{v}_E := \bar{a}(\boldsymbol{\Pi}_{\boldsymbol{V}} \boldsymbol{u}, \boldsymbol{\Pi}_{\boldsymbol{V}} \boldsymbol{v}) \qquad \forall \boldsymbol{u}, \boldsymbol{v} \in \boldsymbol{V}_0. \tag{6.7.7}$$

6.7.3 The Preconditioner and Main Result

Theorem 6.7.1. *Let $\boldsymbol{P}$ be defined as in* (6.2.4) *with $\bar{\boldsymbol{A}}$ given by* (6.7.7) *and $\bar{\boldsymbol{M}}$ given by* (6.7.3), *and let $\vec{r}_n$ denote the residual on the n-th iteration of MINRES with the preconditioner $\boldsymbol{P}^{-1}$. Then,*

$$\|\vec{r}_{2n}\|_{\boldsymbol{P}^{-1}} \leq 2 \left(\frac{\sqrt{\sigma} - 1}{\sqrt{\sigma} + 1} \right)^n \|\vec{r}_0\|_{\boldsymbol{P}^{-1}}, \tag{6.7.8}$$

where $\|\vec{r}\|^2_{\boldsymbol{P}^{-1}} := \vec{r}^T \boldsymbol{P}^{-1} \vec{r}$ and $\sqrt{\sigma} \leq C(1 + \log^3 k)$ with C independent of k and h.

Proof. Thanks to Theorem 6.9.1 and the matrix correspondences (6.7.3) and (6.7.7), there holds

$$\left[C_2\beta^{-2}(1+\log^3 k)\right]^{-1}\bar{\boldsymbol{A}} \le \widetilde{\boldsymbol{A}} \le C_2\bar{\boldsymbol{A}} \quad \text{and} \quad C_1^{-1}\bar{\boldsymbol{M}} \le \widetilde{\boldsymbol{M}} \le C_1\bar{\boldsymbol{M}},$$

where $\widetilde{\boldsymbol{M}}$ is the pressure mass matrix for the space $Q_I^\perp$ and $\boldsymbol{A} \le \boldsymbol{B}$ means that $\boldsymbol{B} - \boldsymbol{A}$ is positive semidefinite. Additionally, the inf-sup condition for the spaces $\tilde{\boldsymbol{V}}_E \times \tilde{Q}_E$ (6.3.13) and the boundedness of the bilinear form $b(\cdot,\cdot)$ can be expressed in matrix form using (6.5.2b) and the same arguments in [48, Theorem 3.22] to arrive at

$$\beta^2 \le \frac{\vec{q}_e^T \widetilde{\boldsymbol{B}} \widetilde{\boldsymbol{A}}^{-1} \widetilde{\boldsymbol{B}}^T \vec{q}_e}{\nu^{-1}\vec{q}_e^T \widetilde{\boldsymbol{M}} \vec{q}_e} \le 1 \qquad \forall \tilde{Q}_E \ni q = \vec{q}_e^T \vec{\psi}_e,$$

where β is the discrete inf-sup constant in (6.1.2). Thus, (6.2.5) holds with $\delta = \beta^2[C_2(1+\log^3 k)]^{-1}$, $\Delta = C_2$, $\theta = \beta^2 C_1^{-1}$, and $\Theta = C_1$. Equation (6.7.8) now follows from applying [48, Theorem 4.14] and using the fact that the inf-sup constant β is bounded below uniformly in k and h gives (6.7.8). $\square$

Theorem 6.7.1 shows that the performance of the preconditioner deteriorates at most as $\log^3 k$ as the polynomial order is increased, but remains bounded as the mesh is refined provided the shape regularity assumption (3.2.3) is satisfied.

6.7.4 Implementation and Cost Analysis of the Preconditioner

To aid in the implementation and cost analysis of computing the actions of $\bar{\boldsymbol{A}}^{-1}$ and $\bar{\boldsymbol{M}}^{-1}$, we assume, for convenience, the interface degrees of freedom are ordered as follows:

(i) velocity C^0 vertex degrees of freedom,

(ii) velocity C^1 vertex degrees of freedom,

(iii) velocity edge degrees of freedom, grouped according to edge,

(iv) pressure vertex degrees of freedom, and

(v) pressure average value degrees of freedom.

This ordering induces a block structure in the matrix $\widetilde{\boldsymbol{A}}$ in which the diagonal sub-blocks are: $\widetilde{\boldsymbol{A}}_c$, corresponding to the global interaction among *all* the global C^0 vertex functions; $\widetilde{\boldsymbol{A}}_{\boldsymbol{a},\hat{\boldsymbol{\mu}}}$, the block-diagonal entry corresponding to the C^1 vertex functions $\{\phi_{\boldsymbol{a}}^{\hat{\boldsymbol{\mu}}}\hat{\boldsymbol{e}}_1, \phi_{\boldsymbol{a}}^{\hat{\boldsymbol{\mu}}}\hat{\boldsymbol{e}}_2\}$; and $\widetilde{\boldsymbol{A}}_\gamma$ corresponding to the interactions among the edge functions associated to γ. The load vectors can be similarly split into subvectors corresponding to the same groupings of degrees of freedom. The block diagonal structure of $\boldsymbol{P}$ is then exploited to compute the action of $\boldsymbol{P}^{-1}$ on a pair of vectors $\vec{f}$, $\vec{g}$ efficiently or in parallel, as described in Algorithm 4. In particular, the matrix $\bar{\boldsymbol{A}}$ given by (6.7.7) is block diagonal and the matrix $\bar{\boldsymbol{M}}$ given by (6.7.3) is diagonal.

Algorithm 4 Action of Preconditioner

Require: $\widetilde{\boldsymbol{A}}$, $\vec{f}$, $\vec{g}$
1: **function**
2: $\quad \vec{u}_c = \widetilde{\boldsymbol{A}}_c^{-1} \vec{f}_c$ $\qquad \triangleright\ \mathcal{O}(|\mathcal{V}|^2)$ velocity C^0 vertex function solve
3: $\quad$ **for** $\boldsymbol{a} \in \mathcal{V}, \hat{\boldsymbol{\mu}} \in \mathring{D}_{\boldsymbol{a}}$, **do** $\qquad \triangleright\ \mathcal{O}(|\mathcal{V}|)$ velocity C^1 vertex function solve
4: $\qquad u_{\boldsymbol{a},\hat{\boldsymbol{\mu}}} = \widetilde{\boldsymbol{A}}_{\boldsymbol{a},\hat{\boldsymbol{\mu}}}^{-1} \vec{f}_{\boldsymbol{a},\hat{\boldsymbol{\mu}}}$
5: $\quad$ **end for**
6: $\quad$ **for** $\gamma \in \mathcal{E}_I$ **do** $\qquad \triangleright\ \mathcal{O}(|\mathcal{E}|k^2)$ velocity edge solve
7: $\qquad \vec{u}_\gamma = \widetilde{\boldsymbol{A}}_\gamma^{-1} \vec{f}_\gamma$
8: $\quad$ **end for**
9: $\quad$ **for** $\boldsymbol{a} \in \mathcal{V}$, $\omega \in \Omega_{\boldsymbol{a}}$ **do** $\qquad \triangleright\ \mathcal{O}(|\mathcal{V}|)$ pressure C^0 vertex function solve
10: $\qquad p_{\boldsymbol{a},\omega} = \nu|\omega|^{-1}k^4 g_{\boldsymbol{a},\omega}$
11: $\quad$ **end for**
12: $\quad$ **for** $K \in \mathcal{T}$ **do** $\qquad \triangleright\ \mathcal{O}(|\mathcal{T}|)$ pressure average value solve
13: $\qquad p_K = \nu|K|^{-1} g_K$
14: $\quad$ **end for**
15: $\quad$ **return** $\vec{u}_c$, $(\vec{u}_{\boldsymbol{a},\hat{\boldsymbol{\mu}}})_{\boldsymbol{a},\hat{\boldsymbol{\mu}}}$, $(\vec{u}_\gamma)_\gamma$, $(p_{\boldsymbol{a},\omega})_{\boldsymbol{a},\omega}$, $(p_K)_K$ $\qquad \triangleright$ Return degrees of freedom
16: **end function**

The cost of computing the action of $\boldsymbol{P}^{-1}$ using Algorithm 4 comprises of two parts: one-time setup costs and recurring costs associated with each application of Algorithm 4. The setup cost is dominated by eliminating the interior degrees of freedom on each element, which takes $\mathcal{O}(|\mathcal{T}|k^6)$ operations needed for the subassembly of the Schur complement. The matrices $\widetilde{\boldsymbol{A}}_c$, $\widetilde{\boldsymbol{A}}_{\boldsymbol{a},\hat{\boldsymbol{\mu}}}$, $\boldsymbol{a} \in \mathcal{V}$, $\hat{\boldsymbol{\mu}} \in \mathring{D}_{\boldsymbol{a}}$, and $\widetilde{\boldsymbol{A}}_\gamma$, $\gamma \in \mathcal{E}$, need only be factored once at a cost of $\mathcal{O}(|\mathcal{V}|^3 + |\mathcal{E}|k^3)$ operations, giving an overall setup cost of $\mathcal{O}(|\mathcal{T}|k^6 + |\mathcal{V}|^3 + |\mathcal{E}|k^3)$.

We now turn to the cost associated with each application of Algorithm 4. Line 2 of Algorithm 4 entails the solution of the linear system $\widetilde{\boldsymbol{A}}_c$ involving all of the C^0 vertex functions which, thanks to the prefactorisation of $\widetilde{\boldsymbol{A}}_c$, costs $\mathcal{O}(|\mathcal{V}|^2)$ operations per solve. Lines 3-5 require the solution of a 2×2 matrix on the velocity C^1 vertex functions for each vertex $\boldsymbol{a} \in \mathcal{V}$ and derivative degree of freedom $\hat{\boldsymbol{\mu}} \in \mathring{D}_{\boldsymbol{a}}$ at a cost of $\mathcal{O}(|\mathcal{V}|)$ operations. Lines 6-8 entail a block diagonal solve over each of the edges which, again thanks to the prefactorisation of $\widetilde{\boldsymbol{A}}_\gamma$, $\gamma \in \mathcal{E}$, can be applied using $\mathcal{O}(|\mathcal{E}|k^2)$ operations. Lines 9-11 require $\mathcal{O}(|\mathcal{V}|)$ operations and lines 12-14 require $\mathcal{O}(|\mathcal{T}|)$ operations by analogous arguments. In summary, the overall cost per application of Algorithm 4 is $\mathcal{O}(|\mathcal{V}|^2 + |\mathcal{E}|k^2 + |\mathcal{T}|)$.

The nonoverlapping domain decomposition method for *hp*-discretizations of the Stokes problem in [9] has a comparable cost. When the subdomains coincide with mesh elements, the preconditioner in [9] consists of static condensation of the interior degrees of freedom, a global vertex solve, decoupled edge solves, and a constant pressure mode solve at a cost of $\mathcal{O}(|\mathcal{T}|k^6 + |\mathcal{V}|^3 + |\mathcal{E}|k^3)$ operations for setup and $\mathcal{O}(|\mathcal{V}|^2 + |\mathcal{E}|k^2 + |\mathcal{T}|)$ operations per application. In the case of spectral methods, other preconditioners for the velocity space, such as the wire basket preconditioners and Neumann-Neumann preconditioners described in the 3D setting in [90, 91], also require static condensation of the interior degrees of freedom, a global coarse solve, decoupled edge solves, and a constant pressure mode solve. The global coarse space consists of $\mathcal{O}(1)$ degrees of freedom per element, while the other spaces are analogous to the ones used in [9]. Thus, the overall cost of these preconditioners is at least $\mathcal{O}(|\mathcal{T}|k^6 + |\mathcal{T}|^3 + |\mathcal{E}|k^3)$ operations for setup and at least $\mathcal{O}(|\mathcal{E}|k^2 + |\mathcal{T}|^2)$ operations per application. For quasi-uniform meshes, $\mathcal{O}(|\mathcal{V}|)$ and $\mathcal{O}(|\mathcal{T}|)$ are of the same order, so the cost of the preconditioners in [9, 90, 91] and the one in Algorithm 4 have similar setup and application costs. However, these methods are not directly comparable to the present one as they use quadrilateral meshes and different underlying finite element spaces which do not satisfy an exact sequence property and, in the case of the $\boldsymbol{\mathcal{Q}}_k \times \mathcal{Q}_{k-2}$ elements, are not uniformly inf-sup stable. More generally, a cost/benefit analysis of different solution methods for both the full discrete Stokes equations (6.2.1), like the one in [47] for low order h-version finite element discretizations, and the Schur complement system (6.2.2) is an active area of research.

It appears that the $\mathcal{O}(|\mathcal{V}|^3)$ cost to factor the matrix $\widetilde{\boldsymbol{A}}_c$ is high in relation to h-version preconditioners. However, we are focused on the scaling of the preconditioner with respect to the polynomial degree. In line with previous works [13, 90, 91], we assume that $|\mathcal{V}|$ is fixed or that $|\mathcal{T}|k^6 + |\mathcal{E}|k^3 \gg |\mathcal{V}|^3$, which means that the cost of eliminating the interior degrees of freedom on each element and the cost of factoring the edge systems dominate the setup cost. In this setting, the $\mathcal{O}(|\mathcal{V}|^3)$ cost is thus negligible.

6.8 Numerical Examples

We illustrate the performance of the preconditioner described in Section 6.7 in three numerical examples. For all examples, we take the viscosity $\nu = 1$.

6.8.1 Moffatt Eddies

In the first example, we revisit the Moffatt problem [82] considered in Section 5.7.1, in which the domain Ω is the wedge with a prescribed parabolic flow profile on the top part of the boundary and no flow on the remainder of the boundary:

$$\boldsymbol{u}(x,0) = \begin{bmatrix} 1-x^2 \\ 0 \end{bmatrix}, \ -1 \leq x \leq 1, \quad \text{and} \quad \boldsymbol{u} = \boldsymbol{0} \text{ on } \Gamma \setminus (-1,1) \times \{0\}.$$

The problem is approximated using a pure p-version finite element scheme on the fixed mesh shown in Figure 6.2a. The results in Section 5.7.1 show that the $k = 13$ solution resolves four to five eddies, equivalent to a 10^{13} range of scales.

Let $\lambda^{\pm}_{min}$ and $\lambda^{\pm}_{max}$ denote the extremal eigenvalues of $\boldsymbol{P}^{-1}\boldsymbol{S}$ so that

$$\sigma(\boldsymbol{P}^{-1}\boldsymbol{S}) \subseteq [-\lambda^{-}_{max}, -\lambda^{-}_{min}] \cup \{0\} \cup [\lambda^{+}_{min}, \lambda^{+}_{max}]. \tag{6.8.1}$$

According to Theorem 6.7.1, $\lambda^{\pm}_{max} \leq C$ and $\lambda^{\pm}_{min} \geq C(1+\log^3 k)^{-1}$ with constant C independent of k and h. Figure 6.2b displays the actual values of the extreme eigenvalues. In agreement with theory, $\lambda^{\pm}_{max}$ is uniformly bounded in k and $\lambda^{+}_{min} \geq C(1+\log^3 k)^{-1}$. However, λ^{-}_{min} appears to remain uniformly bounded in k, which would mean that, in practice, the contraction factor in Theorem 6.7.1 is pessimistic. The residual history for $k \in \{4, 7, 10, 13\}$ for the preconditioned MINRES solver are displayed in Figure 6.2c. The starting vector is taken to be $\vec{x} + \vec{\epsilon}$, where $\vec{x}$ is the true solution of the Schur complement system (6.2.2) and $\vec{\epsilon}$ is a random perturbation with entries uniformly distributed in $(-1, 1)$. Here, and in the remaining examples, the relative residual is given by $\sqrt{(\vec{r}^T \boldsymbol{P}^{-1}\vec{r})/(\vec{r}_0^T \boldsymbol{P}^{-1}\vec{r}_0)}$, where $\vec{r}_0$ is the initial residual vector, and MINRES is terminated when the relative residual is smaller than 10^{-8}. It is observed that, as the polynomial order is raised, the iteration counts grow modestly consistent with the results in Theorem 6.7.1.

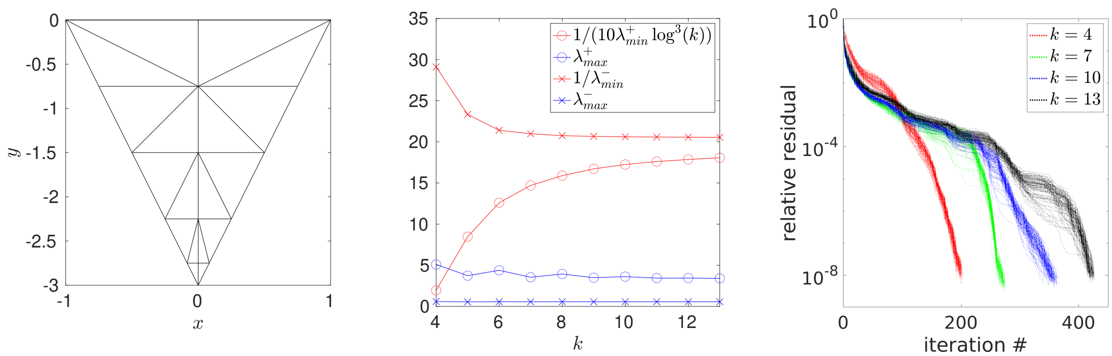

(a) (b) (c)

Figure 6.2: (a) 18 element mesh, (b) extremal eigenvalues of $\boldsymbol{P}^{-1}\boldsymbol{S}$, and (c) MINRES convergence history with $k \in \{4, 7, 10, 13\}$, stopping tolerance 10^{-8} for a sequence of random initial iterates for Moffatt eddies problem. $1/\lambda_{min}^{+}$ grows as $\log^3 k$ while the other extreme eigenvalues remain bounded as the polynomial degree k is increased.

6.8.2 T-shaped Domain

In the next example, we consider the T-shaped domain example [4] where $\boldsymbol{f} \equiv \mathbf{0}$ and boundary conditions are parabolic flow profile on the leftmost and rightmost boundaries of the domain and no flow on the remainder of the boundary:

$$\boldsymbol{u}\left(\pm\frac{3}{2}, y\right) = \begin{bmatrix} y(1-y) \\ 0 \end{bmatrix}, \ 0 \le y \le 1, \quad \text{and} \quad \boldsymbol{u} = \boldsymbol{0} \text{ on } \Gamma \setminus \left\{\pm\frac{3}{2}\right\} \times (0,1).$$

The sequence of meshes is shown in Figure 6.3, in which the elements are geometrically graded and which were shown to give exponential convergence of the finite element solution in Section 5.7.2. The mesh in Figure 6.3a consists of one layer of elements around the re-entrant corner and the most bottom corners, with a grading factor of $\sigma = 0.08$. We then refine the mesh by successively adding layers of elements such that the innermost layer of elements has a diameter proportional to σ^n, where n is the number of refinements. For example, the mesh corresponding to three levels is shown in Figures 6.3b and 6.3c. Observe that, once a mesh contains two or more layers, the shape regularity constant κ (3.2.3) changes from 0.1695 to 0.0829 due to the presence of "needle" elements near the corners, but remains constant on further refinement. In particular, several estimates in the analysis depend on κ, and thus we would expect the performance of the preconditioner to be worse for $n \ge 2$ than for $n = 1$.

As with the previous example, the extremal eigenvalues (6.8.1), displayed in Figure 6.4, remain bounded independently of the number of levels of geometric refinement, whilst $1/\lambda^+_{min}$ increases by a factor of roughly 10 after one level of refinement due to the change in shape regularity mentioned above. This value is an order of magnitude greater than the value of $1/\lambda^+_{min}$ observed for the Moffatt ($\kappa = 0.1508$)

example and accounts for the increase of the resulting iteration counts observed in the residual histories for $k \in \{4, 7, 10, 13\}$ in Figure 6.5. Thus, as one might expect, the preconditioner $\boldsymbol{P}^{-1}$ is less effective on meshes containing high aspect ratio elements owing to the fact that the inf-sup constants and inequalities employed in Section 6.9 all depend on the shape regularity constant appearing in (3.2.3). Nevertheless, similar to the behavior observed in the previous example, for each fixed n, the iteration counts grow modestly in k. For each fixed k, the iteration counts are bounded in n, and remain virtually unchanged for $n \geq 3$.

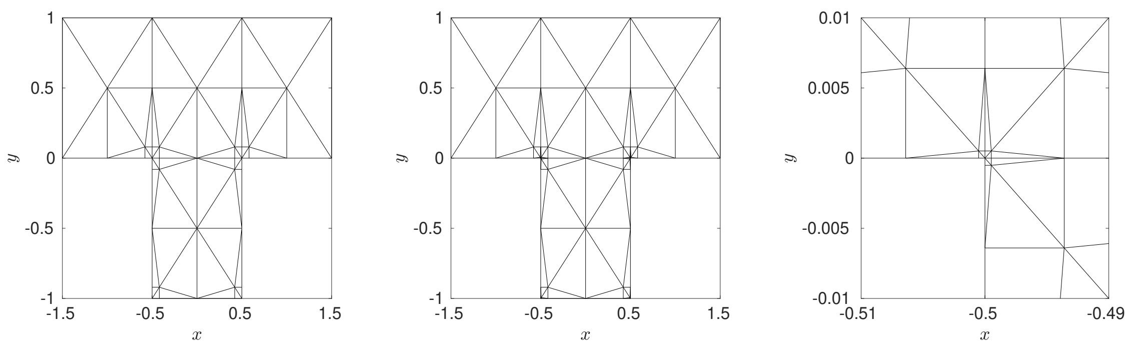

(a) (b) (c)

Figure 6.3: (a) Mesh with $n = 1$ layer of elements, (b) Mesh with $n = 3$ layers of elements, and (c) Zoom on re-entrant corner of mesh with $n = 3$ layers of elements.

6.8.3 Uniformly Refined Square

The final example illustrates the behavior of the method on uniformly refined meshes in the case where the domain Ω is the unit square $(0, 1)^2$ with the data $\boldsymbol{f}$ and

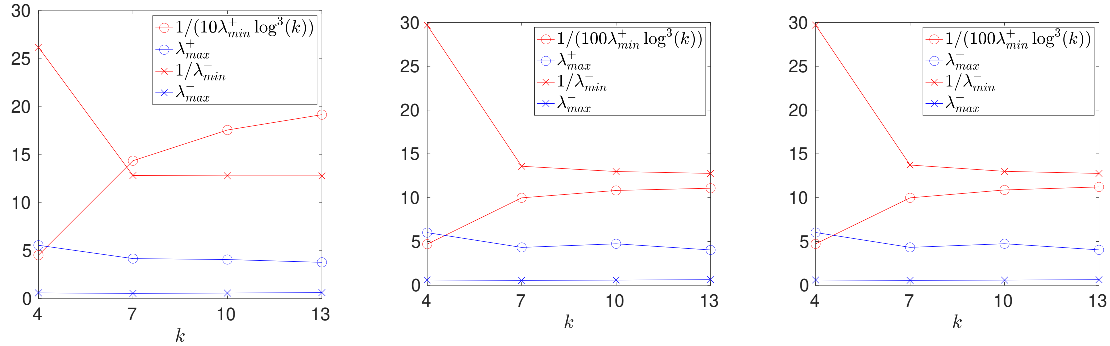

(a) (b) (c)

Figure 6.4: Extremal eigenvalues of $\boldsymbol{P}^{-1}\boldsymbol{S}$ for the T-shape problem with (a) $n = 1$, (b) $n = 2$, and (c) $n = 3$ layers of geometrically graded elements at the corners. All of the extreme eigenvalues are uniformly bounded in n for each fixed k. In addition, the introduction of small-angle "needle" elements for $n \geq 2$ greatly increases $1/\lambda^{+}_{min}$.

boundary conditions chosen so that the true solution is given by

$$\boldsymbol{u}(x, y) = \begin{bmatrix} -\cos(\pi x)\sin(\pi y) \\ \sin(\pi x)\cos(\pi y) \end{bmatrix} \quad \text{and} \quad p(x, y) = \cos(\pi x)\cos(\pi y).$$

The initial mesh is shown in Figure 6.6a which is progressively refined uniformly by subdividing each triangle into four congruent subtriangles, and we fix the polynomial degree to be $k = 10$.

According to Theorem 6.7.1, the extremal eigenvalues can be bounded independently of the number of times the mesh is refined. The numerical results displayed in Figure 6.6b confirm that the extremal eigenvalues remain virtually unchanged after two levels of refinement. The corresponding residual history for the preconditioned MINRES solver with stopping tolerance 10^{-8} are displayed in Figure 6.6c. Although

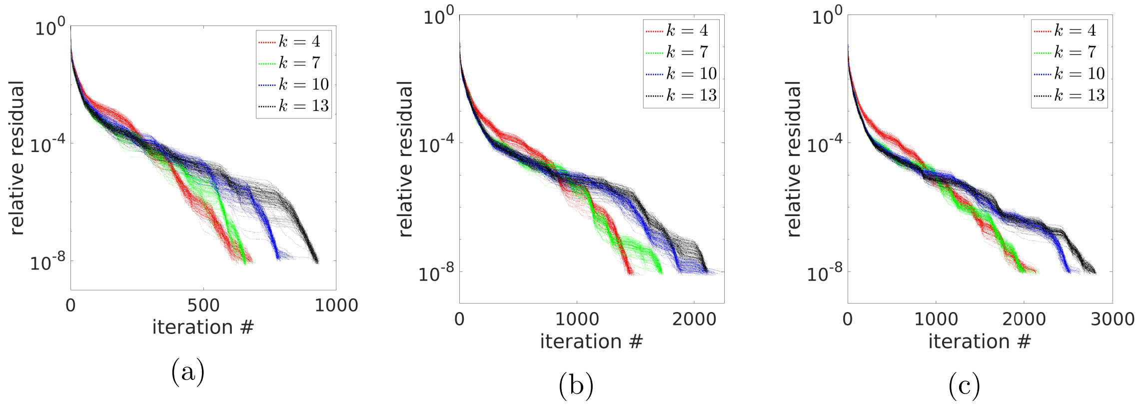

Figure 6.5: MINRES convergence history with $k \in \{4, 7, 10, 13\}$, stopping tolerance 10^{-8} for a sequence of random initial iterates for the T-shape problem with (a) $n = 1$, (b) $n = 2$, and (c) $n = 3$ layers of geometrically graded elements at the corners.

the iteration counts initially increase as the mesh is refined, the numbers of iteration counts approach an asymptotic limit. Interestingly, the iteration counts appear to require four levels of refinement to reach a steady state compared with the extremal eigenvalues which require just three levels of refinement.

6.9 Technical Lemmas

In this section, we establish a spectral equivalence of the ASM preconditioners given in Section 6.7 to the inner products appearing in the Stokes equations. The main result is the following theorem, which is an immediate consequence of Lemmas 6.9.4 to 6.9.6 and 6.9.9 proved later in this section:

Theorem 6.9.1. *There exists positive constants C_1 and C_2, independent of k and*

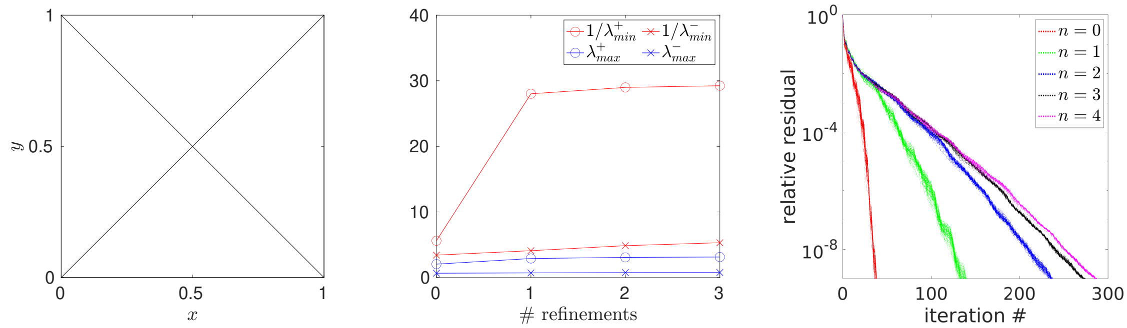

(a) (b) (c)

Figure 6.6: (a) Initial mesh, (b) extremal eigenvalues of $\boldsymbol{P}^{-1}\boldsymbol{S}$, and (c) MINRES convergence history with $n \in \{0, \ldots, 4\}$ levels of mesh refinement, $k = 10$, and stopping tolerance 10^{-8} for a sequence of random initial iterates for uniformly refined square problem. The extreme eigenvalues remain bounded as the mesh is refined.

h, such that

$$C_1^{-1}(p,p) \leq \bar{m}(p,p) \leq C_1(p,p) \qquad \forall p \in Q_I^{\perp}, \tag{6.9.1}$$

and

$$C_2^{-1}a(\boldsymbol{u},\boldsymbol{u}) \leq \bar{a}(\boldsymbol{u},\boldsymbol{u}) \leq C_2\beta^{-2}(1+\log^3 k)a(\boldsymbol{u},\boldsymbol{u}) \qquad \forall \boldsymbol{u} \in \tilde{\boldsymbol{V}}_E, \tag{6.9.2}$$

where $\bar{m}(\cdot,\cdot)$ is defined in (6.7.2), $\bar{a}(\cdot,\cdot)$ is defined in (6.7.6), and β is the inf-sup constant defined in (6.1.2).

6.9.1 Pressure ASM

We begin with the pressure ASM. The first lemma establishes a key estimate for the norm of the pressure vertex functions:

Lemma 6.9.2. *The pressure vertex functions $\tilde{\psi}^{\omega}_{\boldsymbol{a}}$, $\boldsymbol{a} \in \mathcal{V}$, $\omega \in \Omega_{\boldsymbol{a}}$, satisfy*

$$\|\tilde{\psi}^{\omega}_{\boldsymbol{a}}\|_{L^2(K)} \le C h_K k^{-2} \qquad \forall K \in \mathcal{T}, \tag{6.9.3}$$

with C independent of k, h_K, and $\boldsymbol{a}$.

Proof. Let $\boldsymbol{a} \in \mathcal{V}$, $\omega \in \Omega_{\boldsymbol{a}}$. Define the function $\chi \in Q$ by the rule $\chi = \chi_K$ on each element $K \in \mathcal{T}$ where χ_K is chosen as in Lemma 5.4.1. In particular, $\chi_K \in \mathcal{P}_{k-1}(K) \cap L^2_0(K)$ satisfies (i) $\chi_K \equiv 0$ if $K \not\subseteq \omega$, (ii) $\chi_K(\boldsymbol{b}) = \delta_{\boldsymbol{ab}}$ for $\boldsymbol{b} \in \mathcal{V}_K$, and (iii) $\|\chi_K\|_{L^2(K)} \le C h_K k^{-2}$ with C independent of h_K, k, and $\boldsymbol{a}$. By (6.4.2d), (6.4.2e), and Theorem 6.4.2, $\tilde{\psi}_{\boldsymbol{a}} = \tilde{\Pi}\chi$, and $\|\tilde{\psi}^{\omega}_{\boldsymbol{a}}\|_{L^2(K)} \le \|\chi\|_{L^2(K)} \le C h_K k^{-2}$, $\forall K \in \mathcal{T}$. □

We now show that the inner products on the subspaces are coercive:

Lemma 6.9.3. *There exists a positive constant C independent of k and h such that*

$$\begin{aligned} (p, p) &\le C m_{\boldsymbol{a},\omega}(p, p) \qquad && \forall p \in \tilde{Q}_{\boldsymbol{a},\omega},\ \forall \boldsymbol{a} \in \mathcal{V},\ \forall \omega \in \Omega_{\boldsymbol{a}}, \\ (p, p) &\le C m_K(p, p) \qquad && \forall p \in \tilde{Q}_K,\ \ \forall K \in \mathcal{T}. \end{aligned}$$

Proof. Let $p \in \tilde{Q}_{\boldsymbol{a},\omega}$, $\boldsymbol{a} \in \mathcal{V}$, $\omega \in \Omega_{\boldsymbol{a}}$. Then, $p = p(\boldsymbol{a})\tilde{\psi}^{\omega}_{\boldsymbol{a}}$, and by (6.9.3) and shape regularity (3.2.3), there holds

$$(p,p) \leq C \sum_{K\in\mathcal{T}:K\subseteq\omega} h_K^2 k^{-4} |p(\boldsymbol{a})|^2 \leq C|\omega|k^{-4} = m_{\boldsymbol{a},\omega}(p,p).$$

Now let $p \in Q_K$, $K \in \mathcal{T}$. Then, $p = (|K|^{-1}\int_K p\ d\boldsymbol{x})\tilde{\psi}_K$ and since $\tilde{\psi}_{\boldsymbol{a}}^{\omega} \in L_0^2(K)$,

$$\int_K \tilde{\psi}_K^2\ d\boldsymbol{x} = \int_K \left\{ 1 + \left(\sum_{\substack{\boldsymbol{a}\in\mathcal{V}_K \\ \omega\supseteq K}} \tilde{\psi}_{\boldsymbol{a}}^{\omega} \right)^2 \right\} d\boldsymbol{x} \leq |K| + Ch_K^2 k^{-4} \leq C|K|.$$

Thus, $(p,p) \leq Cm_K(p,p)$. $\square$

We are now able to establish the left-hand side of the equivalence (6.9.1):

Lemma 6.9.4. *There exists a constant C independent of k and h such that*

$$(p,p) \leq C\bar{m}(p,p) \qquad \forall p \in Q_I^{\perp}. \tag{6.9.4}$$

Proof. Let $p \in Q_I^{\perp}$. By Cauchy-Schwarz, there holds

$$(p,p)_K \leq 4 \left[\sum_{\substack{\boldsymbol{a}\in\mathcal{V}_K \\ \omega\supseteq K}} (p_{\boldsymbol{a},\omega}, p_{\boldsymbol{a},\omega})_K + (p_K, p_K)_K \right]$$

where $(p,q)_K := \int_K pq\ d\boldsymbol{x}$. (6.9.4) now follows from Lemma 6.9.3 and summing over the elements. $\square$

The right-hand side of the equivalence (6.9.1) is covered by the next result:

Lemma 6.9.5. *There exists a positive constant C independent of k and h such that*

$$\bar{m}(p,p) \leq C(p,p) \qquad \forall p \in Q_I^{\perp}. \tag{6.9.5}$$

Proof. By [6, Lemma 6.1], there holds

$$|p|_K(\boldsymbol{a})|^2 k^{-4} = |(p|_K \circ \boldsymbol{F}_K)(\hat{\boldsymbol{a}})|^2 k^{-4} \leq C\|p \circ \boldsymbol{F}_K\|_{L^2(\hat{T})}^2 \leq C h_K^2 \|p\|_{L^2(K)}^2$$

with $\hat{\boldsymbol{a}} = \boldsymbol{F}_K^{-1}(\boldsymbol{a})$, and by shape regularity,

$$m_{\boldsymbol{a},\omega}(p_{\boldsymbol{a},\omega}, p_{\boldsymbol{a},\omega}) = |\omega| k^{-4} |p|_\omega(\boldsymbol{a})|^2 \leq C \sum_{K \in \mathcal{T}: K \subseteq \omega} \|p\|_{L^2(K)}^2.$$

Summing over $\boldsymbol{a} \in \mathcal{V}$, $\omega \in \Omega_{\boldsymbol{a}}$ and again using shape regularity to bound the overlap $|\{\omega : \exists \boldsymbol{a} \in \mathcal{V} : K \subseteq \omega \in \Omega_{\boldsymbol{a}}\}|$ gives

$$\sum_{\substack{\boldsymbol{a} \in \mathcal{V} \\ \omega \in \Omega_{\boldsymbol{a}}}} m_{\boldsymbol{a},\omega}(p_{\boldsymbol{a},\omega}, p_{\boldsymbol{a},\omega}) \leq C \sum_{\substack{\boldsymbol{a} \in \mathcal{V} \\ \omega \in \Omega_{\boldsymbol{a}}}} \sum_{K \in \mathcal{T}: K \subseteq \omega} \|p\|_{L^2(K)}^2 \leq C\|p\|_{L^2(\Omega)}^2.$$

To bound the remaining $m_K(\cdot,\cdot)$ terms, we use Cauchy-Schwarz:

$$\sum_{K \in \mathcal{T}} m_K(p_K, p_K) = \sum_{K \in \mathcal{T}} \frac{1}{|K|} \left(\int_K p \, d\boldsymbol{x} \right)^2 \leq C \sum_{K \in \mathcal{T}} \|p\|_{L^2(K)}^2 \leq C\|p\|_{L^2(\Omega)}^2,$$

which completes the proof of (6.9.5). $\square$

6.9.2 Velocity ASM

We now turn to the velocity space, and start by extending the decomposition (6.7.5) as follows. For $\boldsymbol{u} \in \tilde{\boldsymbol{V}}_E$, we define $\boldsymbol{u}_\gamma \equiv \boldsymbol{0}$ for $\gamma \in \mathcal{E} \setminus \mathcal{E}_I$ and $\boldsymbol{u}_{\boldsymbol{a},\hat{\boldsymbol{\mu}}} \equiv \boldsymbol{0}$ for $\boldsymbol{a} \in \mathcal{V}$, $\hat{\boldsymbol{\mu}} \in D_{\boldsymbol{a}} \setminus \mathring{D}_{\boldsymbol{a}}$. Since the inner product on each of the subspace was taken to be $a(\cdot,\cdot)$, we immediately obtain the left-hand side of the equivalence (6.9.2):

Lemma 6.9.6. *For all $\boldsymbol{u} \in \tilde{\boldsymbol{V}}_E$, there holds*

$$a(\boldsymbol{u},\boldsymbol{u}) \leq 10\bar{a}(\boldsymbol{u},\boldsymbol{u}). \tag{6.9.6}$$

Proof. First recall that there are exactly 2 directional derivative degrees of freedom per velocity component per vertex on any given element, i.e. for $K \in \mathcal{T}$, $|\{\hat{\boldsymbol{\mu}} : K \subseteq \operatorname{supp} \phi_{\boldsymbol{a}}^{\hat{\boldsymbol{\mu}}}\}| = 2$. By Cauchy-Schwarz, there holds

$$|\boldsymbol{u}|^2_{\boldsymbol{H}^1(K)} \leq 10 \left\{ |\boldsymbol{u}_c|^2_{\boldsymbol{H}^1(K)} + \sum_{\substack{\boldsymbol{a}\in\mathcal{V}_K \\ \hat{\boldsymbol{\mu}}:K\in\operatorname{supp}\phi_{\boldsymbol{a}}^{\hat{\boldsymbol{\mu}}}}} |\boldsymbol{u}_{\boldsymbol{a},\hat{\boldsymbol{\mu}}}|^2_{\boldsymbol{H}^1(K)} + \sum_{\gamma\in\mathcal{E}_K} |\boldsymbol{u}_\gamma|^2_{\boldsymbol{H}^1(K)} \right\} \qquad \forall K \in \mathcal{T}.$$

Equation (6.9.6) now follows by summing over the elements and multiplying by ν. $\square$

To prove the right-hand side of (6.9.2), we need to establish some properties of the velocity vertex functions:

Lemma 6.9.7. *The C^0 velocity vertex functions satisfy the following: For $K \in \mathcal{T}$,*

$$\mathbb{R}^2 \ni \boldsymbol{c} = \sum_{\boldsymbol{a} \in \mathcal{V}_K} \sum_{i=1}^{2} (\boldsymbol{c} \cdot \hat{\boldsymbol{e}}_i) \boldsymbol{\Pi}_{\boldsymbol{V}} (\phi_{\boldsymbol{a}} \hat{\boldsymbol{e}}_i) \qquad \text{on } K \tag{6.9.7}$$

and

$$\|\boldsymbol{\Pi}_{\boldsymbol{V}}(\phi_{\boldsymbol{a}} \hat{\boldsymbol{e}}_i) \circ \boldsymbol{F}_K\|_{\boldsymbol{H}^1(\hat{T})} \leq C \qquad \forall \boldsymbol{a} \in \mathcal{V}, \ i = 1, 2, \tag{6.9.8}$$

where C depends only on the shape regularity parameter.

Moreover, the C^1 velocity vertex functions satisfy

$$\|\boldsymbol{\Pi}_{\boldsymbol{V}}(\phi_{\boldsymbol{a}}^{\hat{\boldsymbol{\mu}}} \hat{\boldsymbol{e}}_i) \circ \boldsymbol{F}_K\|_{\boldsymbol{H}^1(\hat{T})} \leq C \|D\boldsymbol{F}_K\|_{L^\infty(\hat{T})} k^{-2} \qquad \forall \boldsymbol{a} \in \mathcal{V}, \forall \hat{\boldsymbol{\mu}} \in D_{\boldsymbol{a}}, \ i = 1, 2, \tag{6.9.9}$$

where C depends only on the shape regularity parameter.

Proof. Let $K \in \mathcal{T}$. A simple computation reveals that $1 = (\lambda_1 + \lambda_2 + \lambda_3)^3 = \sum_{\boldsymbol{a} \in \mathcal{V}_K} \phi_{\boldsymbol{a}} + 6\lambda_1\lambda_2\lambda_3$ on K, where $\{\lambda_i : \ 1 \leq i \leq 3\}$ are the barycentric coordinates on K, and hence, for any $\boldsymbol{c} \in \mathbb{R}^2$,

$$\boldsymbol{c} = \sum_{\boldsymbol{a} \in \mathcal{V}} \sum_{i=1}^{2} (\boldsymbol{c} \cdot \hat{\boldsymbol{e}}_i)(\phi_{\boldsymbol{a}} \hat{\boldsymbol{e}}_i) + \underbrace{6\boldsymbol{c} \sum_{K \in \mathcal{T}} \lambda_1 \lambda_2 \lambda_3}_{\in \boldsymbol{V}_I} .$$

Applying $\boldsymbol{\Pi}_{\boldsymbol{V}}$ to both sides of this identity and noting that Theorem 6.4.1 gives

$\mathbf{\Pi}_{\boldsymbol{V}} : \boldsymbol{V}_I \to \{\mathbf{0}\}$, we obtain

$$\mathbf{\Pi}_{\boldsymbol{V}} \boldsymbol{c} = \sum_{\boldsymbol{a} \in \mathcal{V}} \sum_{i=1}^{2} (\boldsymbol{c} \cdot \hat{\boldsymbol{e}}_i) \mathbf{\Pi}_{\boldsymbol{V}} (\phi_{\boldsymbol{a}} \hat{\boldsymbol{e}}_i).$$

Finally, Theorem 6.4.1 implies that $\mathscr{E}(\boldsymbol{c}, 0) = (\boldsymbol{c}, 0)$ and (6.9.7) follows at once.

Now let $K \in \mathcal{T}$ and $i \in \{1, 2\}$. Clearly (6.9.8) holds if $\boldsymbol{a} \notin \mathcal{V}_K$ since $\phi_{\boldsymbol{a}} \hat{\boldsymbol{e}}_i = \mathbf{0}$. Otherwise, if $\boldsymbol{a} \in \mathcal{V}_K$, we apply a scaling argument in conjunction with (6.4.4) to arrive at

$$\frac{1}{|K|^2} \|\mathbf{\Pi}_{\boldsymbol{V}} (\phi_{\boldsymbol{a}} \hat{\boldsymbol{e}}_i)\|^2_{\boldsymbol{L}^2(K)} + |\mathbf{\Pi}_{\boldsymbol{V}} (\phi_{\boldsymbol{a}} \hat{\boldsymbol{e}}_i)|^2_{\boldsymbol{H}^1(K)} \leq C \left\{ |\phi_{\boldsymbol{a}}|^2_{H^{1/2}(\partial K)} + \frac{1}{|\partial K|} \|\phi_{\boldsymbol{a}}\|^2_{L^2(\partial K)} \right\},$$

where C is a positive constant independent of k and h_K. Thus,

$$\|\mathbf{\Pi}_{\boldsymbol{V}} (\phi_{\boldsymbol{a}} \hat{\boldsymbol{e}}_i) \circ \boldsymbol{F}_K\|_{\boldsymbol{H}^1(\hat{T})} \leq C \|\hat{\phi}_j\|_{H^{1/2}(\partial \hat{T})} \leq C \|\hat{\phi}_j\|_{H^1(\hat{T})} \leq C,$$

where j is the index such hat $\hat{\boldsymbol{a}}_j = \boldsymbol{F}_K^{-1}(\boldsymbol{a})$. For $K \subseteq \operatorname{supp} \phi_{\boldsymbol{a}}^{\hat{\boldsymbol{\mu}}}$, we argue similarly and use (6.6.10) to obtain

$$\|\mathbf{\Pi}_{\boldsymbol{V}} (\phi_{\boldsymbol{a}}^{\hat{\boldsymbol{\mu}}} \hat{\boldsymbol{e}}_i) \circ \boldsymbol{F}_K\|_{\boldsymbol{H}^1(\hat{T})} \leq C \left\| \begin{bmatrix} \hat{\boldsymbol{\mu}} & \hat{\boldsymbol{\xi}} \end{bmatrix}^{-1} \right\| \|D\boldsymbol{F}_K\|_{L^\infty(\hat{T})} \left\| \begin{bmatrix} \hat{\phi}_j^{(1,0)} \\ \hat{\phi}_j^{(0,1)} \end{bmatrix} \right\|_{\boldsymbol{H}^{1/2}(\partial \hat{T})},$$

where $\hat{\boldsymbol{\mu}} \neq \hat{\boldsymbol{\xi}} \in D_{\boldsymbol{a}}$ is chosen such that $\operatorname{supp} \phi_{\boldsymbol{a}}^{\xi} \supseteq K$, j is the index such that $\hat{\boldsymbol{a}}_j = \boldsymbol{F}_K^{-1}(\boldsymbol{a})$, and $\|\cdot\|$ is any matrix norm. By the definition of $D_{\boldsymbol{a}}$ (6.6.9) and shape regularity, $\left\|\begin{bmatrix}\hat{\boldsymbol{\mu}} & \hat{\boldsymbol{\xi}}\end{bmatrix}^{-1}\right\|$ is uniformly bounded by a constant depending only on κ (3.2.3). Since $\hat{\phi}_j^{(1,0)}(\hat{\boldsymbol{a}}) = \hat{\phi}_j^{(0,1)}(\hat{\boldsymbol{a}}) = 0$ for $\hat{\boldsymbol{a}} \in \mathcal{V}_{\hat{T}}$ by the construction (6.6.3), there holds

$$\|\boldsymbol{\Pi}_{\boldsymbol{V}}(\phi_{\boldsymbol{a}}^{\hat{\boldsymbol{\mu}}}\hat{\boldsymbol{e}}_i) \circ \boldsymbol{F}_K\|_{\boldsymbol{H}^1(\hat{T})} \leq C\|D\boldsymbol{F}_K\|_{L^\infty(\hat{T})}\|J\|_{H_{00}^{1/2}(I)}$$

where $I = (-1, 1)$ and

$$J(t) = \frac{1}{P_{k-3}^{(3,3)}(-1)}\left(\frac{1+t}{2}\right)\left(\frac{1-t}{2}\right)^2 P_{k-3}^{(3,3)}(t).$$

Thanks to Lemma 3.7.1, $\|J\|_{L^2(I)} \leq Ck^{-3}$ with C independent of k. Using interpolation, and the inverse estimate $\|J'\|_{L^2(I)} \leq Ck^2\|J\|_{L^2(I)}$ [25, Corollary 3.4], we obtain $\|J\|_{H_{00}^{1/2}(I)} \leq C\|J\|_{L^2(I)}^{1/2}\|J\|_{H^1(I)}^{1/2} \leq Ck^{-2}$, which completes the proof of (6.9.9). $\square$

We now use the properties of the vertex functions to prove element-wise stability of the subspace decomposition (6.7.5):

Lemma 6.9.8. *For $\boldsymbol{u} \in \tilde{\boldsymbol{V}}_E$ and $K \in \mathcal{T}$, there holds*

$$|\boldsymbol{u}_c|_{\boldsymbol{H}^1(K)}^2 + \sum_{\substack{\boldsymbol{a}\in\mathcal{V}_K \\ \hat{\boldsymbol{\mu}}: K \in \operatorname{supp}\phi_{\boldsymbol{a}}^{\hat{\boldsymbol{\mu}}}}} |\boldsymbol{u}_{\boldsymbol{a},\hat{\boldsymbol{\mu}}}|_{\boldsymbol{H}^1(K)}^2 + \sum_{\gamma\in\mathcal{E}_K} |\boldsymbol{u}_\gamma|_{\boldsymbol{H}^1(K)}^2 \leq C\beta^{-2}(1+\log^3 k)|\boldsymbol{u}|_{\boldsymbol{H}^1(K)}^2, \tag{6.9.10}$$

where C is independent of k, h_K, and $\boldsymbol{u}$.

Proof. Let $\boldsymbol{u} \in \tilde{\boldsymbol{V}}_E$ and $K \in \mathcal{T}$. For any $\boldsymbol{c} \in \mathbb{R}^2$, we have the decomposition

$$\boldsymbol{u} - \boldsymbol{c} = \boldsymbol{u}_c - \sum_{\boldsymbol{a}\in\mathcal{V}_K} \sum_{i=1}^{2} (\boldsymbol{c} \cdot \hat{\boldsymbol{e}}_i) \boldsymbol{\Pi}_{\boldsymbol{V}} (\phi_{\boldsymbol{a}} \hat{\boldsymbol{e}}_i) + \sum_{\substack{\boldsymbol{a}\in\mathcal{V}_K \\ \hat{\boldsymbol{\mu}}: K\in \operatorname{supp} \phi_{\boldsymbol{a}}^{\hat{\boldsymbol{\mu}}}}} \boldsymbol{u}_{\boldsymbol{a},\hat{\boldsymbol{\mu}}} + \sum_{\gamma\in\mathcal{E}_K} \boldsymbol{u}_\gamma \text{ on } K$$

thanks to (6.9.7). Thus,

$$\hat{\boldsymbol{u}} - \boldsymbol{c} = \hat{\boldsymbol{u}}_c - \sum_{\boldsymbol{a}\in\mathcal{V}_K} \sum_{i=1}^{2} (\boldsymbol{c} \cdot \hat{\boldsymbol{e}}_i) \boldsymbol{\Pi}_{\boldsymbol{V}} (\phi_{\boldsymbol{a}} \hat{\boldsymbol{e}}_i) \circ \boldsymbol{F}_K + \sum_{\substack{\boldsymbol{a}\in\mathcal{V}_K \\ \hat{\boldsymbol{\mu}}: K\in \operatorname{supp} \phi_{\boldsymbol{a}}^{\hat{\boldsymbol{\mu}}}}} \hat{\boldsymbol{u}}_{\boldsymbol{a},\hat{\boldsymbol{\mu}}} + \sum_{\gamma\in\mathcal{E}_K} \hat{\boldsymbol{u}}_\gamma \text{ on } \hat{T},$$

where $\hat{\boldsymbol{u}} = \boldsymbol{u} \circ \boldsymbol{F}_K$, $\hat{\boldsymbol{u}}_c = \boldsymbol{u}_c \circ \boldsymbol{F}_K$, etc. We first bound the energy of $\hat{\boldsymbol{u}}_c$. Since

$$\hat{\boldsymbol{u}}_c = \sum_{\boldsymbol{a}\in\mathcal{V}_K} \sum_{i=1}^{2} (\boldsymbol{u}(\boldsymbol{a}) \cdot \hat{\boldsymbol{e}}_i) \boldsymbol{\Pi}_{\boldsymbol{V}} (\phi_{\boldsymbol{a}} \hat{\boldsymbol{e}}_i) \circ \boldsymbol{F}_K = \sum_{\hat{\boldsymbol{a}}\in\mathcal{V}_{\hat{T}}} \sum_{i=1}^{2} (\hat{\boldsymbol{u}}(\hat{\boldsymbol{a}}) \cdot \hat{\boldsymbol{e}}_i) \boldsymbol{\Pi}_{\boldsymbol{V}} (\phi_{\boldsymbol{a}} \hat{\boldsymbol{e}}_i) \circ \boldsymbol{F}_K \qquad \text{on } \hat{T},$$

where $\boldsymbol{a} = \boldsymbol{F}_K(\hat{\boldsymbol{a}})$, we use [13, Corollary 6.3] and (6.9.8) to obtain

$$\begin{aligned} \|\hat{\boldsymbol{u}}_c - \boldsymbol{c}\|^2_{\boldsymbol{H}^1(\hat{T})} &\le \sum_{\hat{\boldsymbol{a}}\in\mathcal{V}_{\hat{T}}} |\hat{\boldsymbol{u}}(\hat{\boldsymbol{a}}) - \boldsymbol{c}|^2 \sum_{i=1}^{2} \|\boldsymbol{\Pi}_{\boldsymbol{V}} (\phi_{\boldsymbol{a}} \hat{\boldsymbol{e}}_i) \circ \boldsymbol{F}_K\|^2_{\boldsymbol{H}^1(\hat{T})} \\ &\le C(1 + \log k) \|\hat{\boldsymbol{u}} - \boldsymbol{c}\|^2_{\boldsymbol{H}^1(\hat{T})}. \end{aligned} \tag{6.9.11}$$

We now bound the vertex derivative contribution. For $\boldsymbol{a} \in \mathcal{V}_K$, we note that $\partial_{\hat{\boldsymbol{\mu}}}(\boldsymbol{u} \cdot \hat{\boldsymbol{e}}_i)(\boldsymbol{a}) = \hat{\boldsymbol{\mu}}^T D\boldsymbol{F}_K^{-T} \nabla(\boldsymbol{u} \cdot \hat{\boldsymbol{e}}_i \circ \boldsymbol{F}_K)(\hat{\boldsymbol{a}})$, $i = 1, 2$, where $\hat{\boldsymbol{a}} = \boldsymbol{F}_K^{-1}(\boldsymbol{a})$. Applying

[6, Lemma 6.1] to $\nabla(\boldsymbol{u} \circ \boldsymbol{F}_K)$, and using (6.9.9) and shape regularity gives

$$\|\hat{\boldsymbol{u}}_{\boldsymbol{a},\hat{\boldsymbol{\mu}}}\|^2_{\boldsymbol{H}^1(\hat{T})} \leq C\|D\boldsymbol{F}_K^{-T}\|^2_{L^\infty(K)} \cdot \|D\boldsymbol{F}_K\|^2_{L^\infty(\hat{T})} \cdot |\,\nabla\,\hat{\boldsymbol{u}}(\hat{\boldsymbol{a}})|^2 k^{-4} \leq C|\hat{\boldsymbol{u}}|^2_{\boldsymbol{H}^1(\hat{T})}. \tag{6.9.12}$$

Now, we define

$$\boldsymbol{u}^{\#} := (\boldsymbol{u} - \boldsymbol{c}) - (\boldsymbol{u}_c - \boldsymbol{c}) - \sum_{\substack{\boldsymbol{a}\in\mathcal{V}_K \\ \hat{\boldsymbol{\mu}}: K\in \operatorname{supp}\phi_{\boldsymbol{a}}^{\hat{\boldsymbol{\mu}}}}} \boldsymbol{u}_{\boldsymbol{a},\hat{\boldsymbol{\mu}}} \quad \text{on } K.$$

Then, $D^\alpha \boldsymbol{u}^{\#}(\boldsymbol{a}) = \boldsymbol{0}$ for $\boldsymbol{a} \in \mathcal{V}_K$, $|\alpha| \leq 1$, and thanks to (6.9.11) and (6.9.12), $\hat{\boldsymbol{u}}^{\#} := \boldsymbol{u}^{\#} \circ \boldsymbol{F}_K$ may be estimated as follows:

$$\|\hat{\boldsymbol{u}}^{\#}\|^2_{\boldsymbol{H}^1(\hat{T})} \leq C(1 + \log k)\|\hat{\boldsymbol{u}} - \boldsymbol{c}\|^2_{\boldsymbol{H}^1(\hat{T})} \tag{6.9.13}$$

Let $\gamma \in \mathcal{E}_K$. Equation (6.4.5), shape regularity (3.2.3), and the trace theorem give

$$|\hat{\boldsymbol{u}}_\gamma|_{\boldsymbol{H}^1(\hat{T})} \leq C\beta^{-1}|\boldsymbol{u}_\gamma|_{\boldsymbol{H}^{1/2}(\partial K)} \leq C\beta^{-1}|\hat{\boldsymbol{u}}_\gamma|_{\boldsymbol{H}^{1/2}(\partial\hat{T})} \leq C\beta^{-1}\|\hat{\boldsymbol{u}}^{\#}\|_{\boldsymbol{H}^{1/2}_{00}(\hat{\gamma})}, \tag{6.9.14}$$

where $\hat{\gamma} = \boldsymbol{F}_K^{-1}(\gamma)$. Thanks to [13, Theorem 6.5] and the trace theorem, we have the estimate

$$\|\hat{\boldsymbol{u}}^{\#}\|_{\boldsymbol{H}^{1/2}_{00}(\hat{\gamma})} \leq C(1 + \log k)\|\hat{\boldsymbol{u}}^{\#}\|_{\boldsymbol{H}^{1/2}(\hat{\gamma})} \leq C(1 + \log k)\|\hat{\boldsymbol{u}}^{\#}\|_{\boldsymbol{H}^1(\hat{T})}. \tag{6.9.15}$$

Using (6.9.13) to (6.9.15) gives

$$|\hat{\boldsymbol{u}}_\gamma|^2_{\boldsymbol{H}^1(\hat{T})} \leq C\beta^{-2}(1+\log^2 k)\|\hat{\boldsymbol{u}}^{\#}\|^2_{\boldsymbol{H}^1(\hat{T})} \leq C\beta^{-2}(1+\log^3 k)\|\hat{\boldsymbol{u}}-\boldsymbol{c}\|^2_{\boldsymbol{H}^1(\hat{T})}, \quad (6.9.16)$$

Combining (6.9.11), (6.9.12) and (6.9.16) leads to

$$|\hat{\boldsymbol{u}}_c|^2_{\boldsymbol{H}^1(\hat{T})} + \sum_{\substack{\boldsymbol{a}\in\mathcal{V}_K \\ \hat{\boldsymbol{\mu}}:K\in\operatorname{supp}\phi_{\boldsymbol{a}}^{\hat{\boldsymbol{\mu}}}}} |\hat{\boldsymbol{u}}_{\boldsymbol{a},\hat{\boldsymbol{\mu}}}|^2_{\boldsymbol{H}^1(\hat{T})} + \sum_{\gamma\in\mathcal{E}_K} |\hat{\boldsymbol{u}}_\gamma|^2_{\boldsymbol{H}^1(\hat{T})} \leq C\beta^{-2}(1+\log^3 k)\|\hat{\boldsymbol{u}}-\boldsymbol{c}\|^2_{\boldsymbol{H}^1(\hat{T})},$$

where we used that $|\hat{\boldsymbol{u}}_c|_{\boldsymbol{H}^1(\hat{T})} = |\hat{\boldsymbol{u}}_c - \boldsymbol{c}|_{\boldsymbol{H}^1(\hat{T})}$. Taking the infimum over all $\boldsymbol{c} \in \mathbb{R}^2$ and applying the quotient norm equivalence [86, Theorem 7.2] gives

$$|\hat{\boldsymbol{u}}_c|^2_{\boldsymbol{H}^1(\hat{T})} + \sum_{\substack{\boldsymbol{a}\in\mathcal{V}_K \\ \hat{\boldsymbol{\mu}}:K\in\operatorname{supp}\phi_{\boldsymbol{a}}^{\hat{\boldsymbol{\mu}}}}} |\hat{\boldsymbol{u}}_{\boldsymbol{a},\hat{\boldsymbol{\mu}}}|^2_{\boldsymbol{H}^1(\hat{T})} + \sum_{\gamma\in\mathcal{E}_K} |\hat{\boldsymbol{u}}_\gamma|^2_{\boldsymbol{H}^1(\hat{T})} \leq C\beta^{-2}(1+\log^3 k)|\hat{\boldsymbol{u}}|^2_{\boldsymbol{H}^1(\hat{T})}.$$

Equation (6.9.10) now follows from shape regularity (3.2.3). □

Summing (6.9.10) over the elements and multiplying by ν lead to the following:

Lemma 6.9.9. *There exists a constant C independent of k, h, and ν such that*

$$\bar{a}(\boldsymbol{u},\boldsymbol{u}) \leq C\beta^{-2}(1+\log^3 k)a(\boldsymbol{u},\boldsymbol{u}) \qquad \forall \boldsymbol{u} \in \tilde{\boldsymbol{V}}_E. \quad (6.9.17)$$

6.10 Extension to Variable Viscosity

The method and analysis readily extends to viscosities varying in space, provided that ν is a bounded measurable function satisfying

$$0 < \nu_{min} < \nu(\boldsymbol{x}) < \nu_{max} < \infty \qquad \forall \boldsymbol{x} \in \Omega.$$

In this case, the bilinear form $a(\cdot,\cdot)$, which we recall is given by

$$a(\boldsymbol{u},\boldsymbol{v}) = \int_\Omega \nu(\boldsymbol{x})\nabla \boldsymbol{u}(\boldsymbol{x}) : \nabla \boldsymbol{v}(\boldsymbol{x})\ d\boldsymbol{x},$$

is symmetric, bounded, and coercive on $\boldsymbol{V}_0$, so the discrete problem (6.1.1) is well-defined and has a unique solution. We outline the modifications to the preconditioner and analysis for the variable viscosity case.

Let $\bar{\nu}^{-1} := (\nu_{max}^{-1} + \nu_{min}^{-1})/2$. We now seek a block diagonal matrix of the form

$$\boldsymbol{P} = \begin{bmatrix} \bar{\boldsymbol{A}} & \boldsymbol{0} \\ \boldsymbol{0} & \bar{\nu}^{-1}\bar{\boldsymbol{M}} \end{bmatrix} \tag{6.10.1}$$

to precondition the Schur complement matrix $\boldsymbol{S}$ (6.2.3). Note that the only difference between (6.2.4) and the current block diagonal matrix is that ν^{-1} has been replaced by $\bar{\nu}^{-1}$. In particular, the factor ν in lines 10 and 13 of Algorithm 4 is replaced by

$\bar{\nu}$. The nonnegative constants δ, Δ, θ, and Θ are defined analogously as above:

$$\delta \leq \frac{\vec{u}_E^T \widetilde{\boldsymbol{A}} \vec{u}_E}{\vec{u}_E^T \bar{\boldsymbol{A}} \vec{u}_E} \leq \Delta \qquad \forall \boldsymbol{u} \in \boldsymbol{V}_0 \quad \text{and} \quad \theta \leq \frac{\vec{q}_e^T \widetilde{\boldsymbol{B}} \widetilde{\boldsymbol{A}}^{-1} \widetilde{\boldsymbol{B}}^T \vec{q}_e}{\bar{\nu}^{-1} \vec{q}_e^T \bar{\boldsymbol{M}} \vec{q}_e} \leq \Theta \qquad \forall q \in Q_0. \tag{6.10.2}$$

Then, exactly the same arguments as in the proof of of [48, Theorem 4.7] show that eigenvalues of $\boldsymbol{P}^{-1}\boldsymbol{S}$ satisfy (6.2.5).

The tilde spaces $\tilde{\Sigma}_E$, $\tilde{\boldsymbol{V}}_E$ and $\tilde{Q}_E$ are defined as in (6.3.8). All of the results of Section 6.3 hold without modification. The first difference is Theorem 6.4.1, which now reads as follows:

Theorem 6.10.1. *For all $\boldsymbol{u} \in \boldsymbol{V}$ and $K \in \mathcal{T}_h$, there holds*

$$\|\Pi_{\boldsymbol{V}} \boldsymbol{u}\|_{\boldsymbol{H}^1(K)} + \nu_{max}^{-1} \|\Pi_Q \boldsymbol{u}\|_{L^2(K)} \leq C \left(\frac{\nu_{max}}{\nu_{min}} \right) \|\boldsymbol{u}\|_{\boldsymbol{H}^{1/2}(\partial K)}, \tag{6.10.3}$$

where C is independent of h_K, k, ν_{min}, ν_{max}, and $\boldsymbol{u}$. In particular, if $\boldsymbol{u} \in \tilde{\boldsymbol{V}}_E$, then $\boldsymbol{\Pi}_{\boldsymbol{V}} \boldsymbol{u} = \boldsymbol{u}$. Moreover, the following equivalence of semi-norms holds:

$$C^{-1} |\boldsymbol{u}|_{\boldsymbol{H}^{1/2}(\partial K)} \leq |\boldsymbol{\Pi}_{\boldsymbol{V}} \boldsymbol{u}|_{\boldsymbol{H}^1(K)} \leq C \beta^{-1} \left(\frac{\nu_{max}}{\nu_{min}} \right) |\boldsymbol{u}|_{\boldsymbol{H}^{1/2}(\partial K)} \qquad \forall K \in \mathcal{T}, \tag{6.10.4}$$

where $C \geq 1$ is independent of k, h_K, β, ν_{min}, ν_{max}, and $\boldsymbol{u}$.

Proof Sketch. The two key differences are that (6.4.7) now reads

$$\nu_{min}|\boldsymbol{\Pi_V u}|^2_{\boldsymbol{H}^1(K)} \le \left(\nu_{max}|\boldsymbol{\Pi_V u}|_{\boldsymbol{H}^1(K)} + \sqrt{2}\|\Pi_Q \boldsymbol{u}\|_{L^2(K)}\right)|\boldsymbol{w}|_{\boldsymbol{H}^1(K)}$$

and (6.4.7) now reads

$$\beta\|\Pi_Q \boldsymbol{u}\|_{L^2(K)} \le \frac{b_K(\boldsymbol{v}, \Pi_Q \boldsymbol{u})}{|\boldsymbol{v}|_{\boldsymbol{H}^1(K)}} = \frac{a_K(\boldsymbol{\Pi_V u}, \boldsymbol{v})}{|\boldsymbol{v}|_{\boldsymbol{H}^1(K)}} \le \nu_{max}|\boldsymbol{\Pi_V u}|_{\boldsymbol{H}^1(K)}.$$

The remainder of the proof follows similar lines. □

Lemma 6.5.1 remains valid while the only modification to Theorem 6.5.2 is that the the nonzero eigenvalues of the generalized eigenvalue problem $\tilde{\boldsymbol{B}}\tilde{\boldsymbol{A}}^{-1}\tilde{\boldsymbol{B}}^T\vec{q}_e = \lambda\widetilde{\boldsymbol{M}}\vec{q}_e$ are contained in the interval $[\nu_{max}^{-1}\beta^2, \nu_{min}^{-1}]$. The definition of the ASMs is identical to the ones in Section 6.7. All of the results in Section 6.9.1 also remain valid, as does Lemma 6.9.6.

The next major change is that Theorem 6.10.1 impacts Lemma 6.9.7 by adding a factor of (ν_{max}/ν_{min}) to (6.9.8) and (6.9.9), which, in turn, means that (6.9.10) holds with an additional factor of $(\nu_{max}/\nu_{min})^2$. Collecting these results and applying the equivalences $\nu_{max}^{-1}a(\boldsymbol{u},\boldsymbol{u}) \le (\nabla\boldsymbol{u}, \nabla\boldsymbol{u}) \le \nu_{min}^{-1}a(\boldsymbol{u},\boldsymbol{u})$ leads to

$$\bar{a}(\boldsymbol{u},\boldsymbol{u}) \le C\beta^{-2}\left(\frac{\nu_{max}}{\nu_{min}}\right)^3(1+\log^3 k)a(\boldsymbol{u},\boldsymbol{u}).$$

As a result,

$$\beta^2 \left(\frac{\nu_{min}}{\nu_{max}}\right)^3 \left[C_2(1+\log^3 k)\right]^{-1} \bar{\boldsymbol{A}} \leq \widetilde{\boldsymbol{A}} \leq C_2 \bar{\boldsymbol{A}} \quad \text{and} \quad C_1^{-1}\bar{\boldsymbol{M}} \leq \widetilde{\boldsymbol{M}} \leq C_1 \bar{\boldsymbol{M}}.$$

Let $\tilde{\boldsymbol{A}}_1$ be the stiffness matrix corresponding to the bilinear form $(\nabla\cdot,\nabla\cdot)$ on $\tilde{\boldsymbol{V}}_0$. Then, the inf-sup condition (6.3.13) reads

$$\beta^2 \leq \frac{\vec{q}_e^{\,T}\widetilde{\boldsymbol{B}}\widetilde{\boldsymbol{A}}_1^{-1}\widetilde{\boldsymbol{B}}^T\vec{q}_e}{\vec{q}_e^{\,T}\widetilde{\boldsymbol{M}}\vec{q}_e} \leq 1 \qquad \forall \tilde{Q}_E \ni q = \vec{q}_e^{\,T}\vec{\psi}_e.$$

Using the equivalences $\nu_{min}\widetilde{\boldsymbol{A}}_1 \leq \widetilde{\boldsymbol{A}} \leq \nu_{max}\widetilde{\boldsymbol{A}}_1$ and $\nu_{min} \leq \bar{\nu} \leq \nu_{max}$, we obtain

$$\beta^2 \left(\frac{\nu_{min}}{\nu_{max}}\right) \leq \frac{\vec{q}_e^{\,T}\widetilde{\boldsymbol{B}}\widetilde{\boldsymbol{A}}^{-1}\widetilde{\boldsymbol{B}}^T\vec{q}_e}{\bar{\nu}^{-1}\vec{q}_e^{\,T}\widetilde{\boldsymbol{M}}\vec{q}_e} \leq \left(\frac{\nu_{max}}{\nu_{min}}\right) \qquad \forall \tilde{Q}_E \ni q = \vec{q}_e^{\,T}\vec{\psi}_e.$$

As a result, (6.2.5) holds with $\delta = \beta^2(\nu_{min}/\nu_{max})^3[C_2(1+\log^3 k)]^{-1}$, $\Delta = C_2$, $\theta = C_1^{-1}\beta^2(\nu_{min}/\nu_{max})$, and $\Theta = C_1(\nu_{max}/\nu_{min})$, and so we may argue as in the proof of Theorem 6.7.1 to conclude that the bound for $\sqrt{\sigma}$ in Theorem 6.7.1 now reads $C(\nu_{max}/\nu_{min})^4(1+\log^3 k)$.

6.11 Summary and Future Work

This chapter completes the discussion of a uniformly stable, pointwise mass conserving, high order mixed FEM for 2D Stokes flow. In Chapter 4, we showed that the finite element spaces Σ, $\boldsymbol{V}$, and Q, which have extra smoothness at noncorner vertices, satisfy an exact sequence property and that the pair $\boldsymbol{V} \times Q$ is uniformly inf-sup stable in both the mesh size h and polynomial degree k. We also showed how the finite element spaces can be modified to accommodate homogeneous Dirichlet conditions while maintaining an exact sequence property and uniform stability. In Chapter 5, we established optimal approximation properties of the spaces Σ_0 and Q_0, which led to optimal algebraic rates of convergence of the FEM with locally quasi-uniform meshes and exponential convergence rates of the FEM with geometrically graded meshes. Finally, in Chapter 6, we discussed implementation aspects of the method and provided a block diagonal preconditioner that controls the location of the eigenvalues of the preconditioned system in a reasonable way.

6.11.1 Generalizations

Taken as a whole, Chapters 4 to 6 are the first works to address the theory and implementation of the mixed method (6.1.1) in the context of high order methods. As such, there are many directions for future work related to this method. We generalized in [8] the stability results to the standard Scott-Vogelius elements, which are already implemented in standard finite element codes. Another direction is to improve the preconditioner presented in the current chapter by using overlapping subspace decompositions for the velocity space. Standard results such as [95] do not apply directly owing to the extra smoothness of $\boldsymbol{V}_0$ but offer a promising starting point. Additionally, other solution methods for the saddle point system (6.2.2) and preconditioners for those methods may be more efficient.

The most pressing generalizations of the current method are to nonlinear flows like Navier-Stokes and to 3D flows. Linearizations of nonlinear flows often introduce terms of the form $(\boldsymbol{w} \cdot \nabla \boldsymbol{u}, \boldsymbol{v})$ and $(\boldsymbol{u}, \boldsymbol{v})$ corresponding to convection and time discretization, respectively. The theoretical framework for preconditioning the latter term in the context of high order methods has recently received attention [6, 7], which may provide insight into the theory for the convective term. 3D flows also offer theoretical and computational complexities. While [85] proposes FEM spaces that satisfy an exact sequence property in 3D and that are uniformly stable with respect to the mesh size, the stability and approximation properties with respect to the polynomial degree and implementation aspects are underdeveloped. Additionally, the spaces in [85] have even more smoothness than the 2D counterparts presented here; e.g., the velocity space is C^2 at element vertices and the pressure space is C^1 at element vertices. Handling such smoothness complicates the analysis and requires generalizing the techniques developed here.

6.11.2 Comparison with Splitting Methods

One popular and computationally efficient way of solving the unsteady incompressible Navier-Stokes equations is high order splitting methods (see e.g. [67, §8.3]).

At each time step, the velocity and pressure for the next time step are computed through a sequence of three steps, two of which involve solving an elliptic system. Typically, high order/spectral elements are used for the spatial discretization and existing preconditioners for the methods are used to efficiently invert the elliptic systems. Certain splitting methods do not require discrete inf-sup stability for numerical stability or accuracy, and the resulting velocity field is pointwise divergence free.

For the (steady) Stokes or steady Navier-Stokes equations, splitting methods may be used with pseudo time stepping to find the steady-state solution. However, this technique inherently requires multiple time steps and thus multiple elliptic solves. Meanwhile, for the Stokes equations, the mixed method presented above only requires solving one saddle point system, for which we provided an effective preconditioner. In its current form and with additional work on improving the velocity subblock preconditioner to be uniform in the polynomial degree, solving the Stokes system will be computationally cheaper than the multiple elliptic solves in the splitting method. Thus, the mixed method stands to offer an attractive alternative with the same pointwise divergence free property and similar convergence properties, but better computational efficiency. For steady Navier-Stokes, additional work is required to properly precondition the linearizations resulting from Newton's method. Recent results in this direction for lower order elements [51] suggest that an augmented Lagrangian approach can be used to construct a solver that is robust in the Reynolds number. If this can be done, a proper comparison of directly solving the nonlinear equations with the mixed method and pseudo time stepping with a splitting method warrants further investigation.

For unsteady Stokes and Navier-Stokes, the comparison currently favors splitting methods due to the lack of existing research on preconditioners for the unsteady Stokes problem using the above mixed method. Once such preconditioners are constructed, the mixed method can be used in conjunction with an implicit/explicit (IMEX) scheme, such as the stiffly stable schemes in [67, §8.3.2] or more recently developed variable time-stepping schemes [40]. In these IMEX schemes, the nonlinear terms are treated explicitly and the remaining terms are treated implicitly. At each time step, the mixed method requires only one Stokes-like solve, compared to the two elliptic solves required by the splitting method. Whether the Stokes-like solve can be made more efficient than two elliptic solves is an interesting future direction.

6.11.3 Applications to Parametric PDEs

Neural networks (NNs) that solve nonlinear PDEs have recently received much attention (see e.g. [93, 76]). The generalization power of NNs, speed of forward propagation, and automatic differentiation make NNs very attractive for fast evaluation of the solution to linear or nonlinear PDEs with parameters. However, training these networks requires a vast amount of data comprising of the accurate solution to the PDE for a wide range of problem parameters, boundary conditions, initial data, domains, etc. In this context, high order methods are an attractive choice for generating this training data. In particular, we want to construct high order methods that have optimal convergence properties across the range of parameters and to construct preconditioners for these methods whose performance does not deteriorate as the parameters are changed. To illustrate this idea, we look at two simple examples. First, consider the Moffatt eddy problem in Section 5.7.1, where now the problem is parameterized by the apex angle of the wedge. By mapping the mesh for the particular wedge in Figure 5.3a, we can obtain a mesh for any other apex angle less than π. The convergence of the mixed method and the performance of preconditioner are unaffected by changes in the apex angle (so long as the angle does not approach 0). For the second example, we consider planar linear elasticity, which is parameterized by the Young's modulus E and Poisson ratio ν. Using similar techniques as in Chapter 4, we show in [8] that high order continuous finite elements give optimal convergence rates of the displacements and stresses for all physically relevant choices of the parameters. The construction of a preconditioner that is also effective for all parameter values is ongoing work.

Bibliography

[1] R. A. Adams and J. J. Fournier, *Sobolev Spaces*, Academic Press, Amsterdam, 2nd ed., 2003.

[2] M. Ainsworth, *A preconditioner based on domain decomposition for h-p finite-element approximation on quasi-uniform meshes*, SIAM J. Numer. Anal., 33 (1996), pp. 1358–1376.

[3] M. Ainsworth, *Discrete dispersion relation for hp-version finite element approximation at high wave number*, SIAM J. Numer. Anal., 42 (2004), pp. 553–575.

[4] M. Ainsworth and P. Coggins, *A uniformly stable family of mixed hp-finite elements with continuous pressures for incompressible flow*, IMA J. Numer. Anal., 22 (2002), pp. 307–327.

[5] M. Ainsworth and J. Coyle, *Conditioning of hierarchic p-version Nédélec elements on meshes of curvilinear quadrilaterals and hexahedra*, SIAM J. Numer. Anal., 41 (2003), pp. 731–750.

[6] M. Ainsworth and S. Jiang, *Preconditioning the mass matrix for high order finite element approximation on triangles*, SIAM J. Numer. Anal., 57 (2019), pp. 355–377.

[7] M. Ainsworth and S. Jiang, *Preconditioning the mass matrix for high order finite element approximation on tetrahedra*, SIAM J. Sci. Comput., 43 (2021), pp. A384–A414.

[8] M. Ainsworth and C. Parker, *Unlocking the secrets of locking: Finite element analysis in planar linear elasticity*, Comput. Methods Appl. Mech. Engrg., to appear (2022).

[9] M. Ainsworth and S. Sherwin, *Domain decomposition preconditioners for p and hp finite element approximations of Stokes equations*, Comput. Methods Appl. Mech. Engrg., 175 (1999), pp. 243–266.

[10] M. Ainsworth and H. A. Wajid, *Dispersive and dissipative behavior of the spectral element method*, SIAM J. Numer. Anal., 47 (2009), pp. 3910–3937.

[11] J. Argyris, I. Fried, and D. Scharpf, *The TUBA family of plate elements for the matrix displacement method*, Aero. J. Roy. Aero. Soc., 72 (1968), pp. 701–709.

[12] D. N. Arnold, R. L. Scott, and M. Vogelius, *Regular inversion of the divergence operator with dirichlet boundary conditions on a polygon*, Ann. Sc. Norm. Super. Pisa Cl. Sci., 15 (1988), pp. 169–192.

[13] I. Babuška, A. Craig, J. Mandel, and J. Pitkäranta, *Efficient preconditioning for the p-version finite element method in two dimensions*, SIAM J. Numer. Anal., 28 (1991), pp. 624–661.

[14] I. Babuška and B. Q. Guo, *The $h-p$ version of the finite element method for domains with curved boundaries*, SIAM J. Numer. Anal., 25 (1988), pp. 837–861.

[15] I. Babuška, R. B. Kellog, and J. Pitkäranta, *Direct and inverse error estimates for finite elements with mesh refinements*, Numer. Math., 33 (1979), pp. 447–471.

[16] I. Babuška and M. Suri, *The h-p version of the finite element method with quasiuniform meshes*, ESAIM Math. Model. Numer. Anal., 21 (1987), pp. 199–238.

[17] I. Babuška and M. Suri, *The optimal convergence rate of the p-version finite element method*, SIAM J. Numer. Anal., 24 (1987), pp. 750–776.

[18] I. Babuška and M. Suri, *Locking effects in the finite element approximation of elasticity problems*, Numer. Math., 62 (1992), pp. 439–463.

[19] I. Babuška and M. Suri, *On locking and robustness in the finite element method*, SIAM J. Numer. Anal., 29 (1992), pp. 1261–1293.

[20] I. Babuška and M. Suri, *The p and hp-versions of the finite element methods, basic principles and properties*, SIAM Rev., 36 (1994), pp. 578–632.

[21] S. Bartles, *Numerical Approximation of Partial Differential Equations*, Texts Appl. Math. 64, Springer International Publishing Switzerland, Cham, 2016.

[22] R. Becker, H. Kapp, and R. Rannacher, *Adaptive finite element methods for optimal control of partial differential equations: Basic concepts*, SIAM J. Control Optim., 39 (2000), pp. 113–132.

[23] F. B. Belgacem, *Polynomial extensions of compatible polynomial traces in three dimensions*, Comput. Methods Appl. Mech. Engrg., 116 (1994), pp. 235–241.

[24] M. Bernadou and J. Boisserie, *The Finite Element Method in Thin Shell Theory: Application to Arch Dam Simulations*, Progress in Scientific Computing, Birkhäuser, Boston, 1982.

[25] C. Bernardi, M. Dauge, and Y. Maday, *Polynomials in the Sobolev world*, Tech. Report 07-14, IRMAR, University of Rennes, 2007.

[26] C. Bernardi, M. Dauge, and Y. Maday, *The lifting of polynomial traces revisited*, Math. Comp., 79 (2010), pp. 47–69.

[27] C. Bernardi and Y. Maday, *Relevement polynomial de traces et applications*, ESAIM Math. Model. Numer. Anal., 24 (1990), pp. 557–611.

[28] C. Bernardi and Y. Maday, *Uniform inf–sup conditions for the spectral discretization of the Stokes problem*, Math. Models Methods Appl. Sci., 9 (1999), pp. 395–414.

[29] D. Boffi, F. Brezzi, and M. Fortin, *Mixed Finite Element Methods and Applications*, Springer Ser. Comput. Math., Springer, Berlin, 2013.

[30] E. Boillat, *On a right-inverse for the divergence operator in spaces of continuous piecewise polynomials*, Math. Models Methods Appl. Sci., 7 (1997), pp. 487–505.

[31] D. Braess, *Finite Elements: Theory, Fast Solvers, and Applications in Solid Mechanics*, Cambridge University Press, Cambridge, 3rd ed., 2007.

[32] H. Bramble and J. E. Pasciak, *A domain decomposition technique for Stokes problems*, Appl. Numer. Math., 6 (1990), pp. 251–261.

[33] J. Bramble, J. Pasciak, and A. Schatz, *The construction of preconditioners for elliptic problems by substructuring. I*, Math. Comp., 47 (1986), pp. 103–134.

[34] J. H. Bramble and R. S. Falk, *Two mixed finite element methods for the simply supported plate problem*, RAIRO Anal. Numér., 17 (1983), pp. 337–384.

[35] J. H. Bramble and X. Zhang, *Multigrid methods for the biharmonic problem discretized by conforming C^1 finite elements on nonnested meshes*, Numerical functional analysis and optimization, 16 (1995), pp. 835–846.

[36] J. W. Cahn and J. E. Hilliard, *Free energy of a nonuniform system. I. Interfacial free energy*, J. Chem. Phys., 29 (1958), pp. 258–267.

[37] T. Chan and T. Mathew, *Domain decomposition algorithms*, Acta Numer., 3 (1994), pp. 61–143.

[38] P. G. Ciarlet, *The Finite Element Method for Elliptic Problems*, Stud. Math. Appl. 4, North Holland, Amsterdam, 1978.

[39] M. Costabel and A. McIntosh, *On Bogovskiĭ and regularized Poincaré integral operators for de Rham complexes on Lipschitz domains*, Math. Z., 265 (2010), pp. 297–320.

[40] V. DeCaria and M. Schneier, *An embedded variable step IMEX scheme for the incompressible Navier–Stokes equations*, Comput. Methods Appl. Mech. Engrg., 376 (2021), p. 113661.

[41] L. Demcowicz, *Computing with hp-Adaptive Finite Elements. Vol 1. One and Two Dimensional Elliptic and Maxwell Problems*, Chapman & Hall/CRC Appl. Math. Nonlinear Sci. Ser., Chapman & Hall/CRC, Boca Raton, FL, 2007.

[42] L. Demcowicz and I. Babuška, *p interpolation error estimates for edge finite elements of variable order in two dimensions*, SIAM J. Numer. Anal., 41 (2003), pp. 1195–1208.

[43] L. Demcowicz, J. Kurtz, D. Pardo, M. Paszynski, W. Rachowicz, and A. Zdunek, *Computing with hp-Adaptive Finite Elements. Vol 2. Frontiers: Three Dimensional Elliptic and Maxwell Problems with Applications*, Chapman & Hall/CRC Appl. Math. Nonlinear Sci. Ser., Chapman & Hall/CRC, Boca Raton, FL, 2008.

[44] L. Demkowicz, J. Gopalakrishnan, and J. Schöberl, *Polynomial extension operators. Part I*, SIAM J. Numer. Anal., 46 (2008), pp. 3006–3031.

[45] L. Demkowicz, J. Gopalakrishnan, and J. Schöberl, *Polynomial extension operators. Part II*, SIAM J. Numer. Anal., 47 (2009), pp. 3293–3324.

[46] L. Demkowicz, J. Gopalakrishnan, and J. Schöberl, *Polynomial extension operators. Part I*, Math. Comp., 81 (2012), pp. 1289–1326.

[47] H. C. Elman, *Multigrid and Krylov subspace methods for the discrete Stokes equations*, Internat. J. Numer. Methods Fluids, 22 (1996), pp. 755–770.

[48] H. C. Elman, D. J. Silvester, and A. J. Wathen, *Finite Elements and Fast Iterative Solvers with Applications to Incompressible Fluid Dynamics*, Oxford University Press, Oxford, 2nd ed., 2014.

[49] A. Ern and J.-L. Guermond, *Theory and Practice of Finite Elements*, Springer Science+Business Media, New York, NY, 2004.

[50] R. S. Falk and M. Neilan, *Stokes complexes and the construction of stable finite elements with pointwise mass conservation*, SIAM J. Numer. Anal., 51 (2013), pp. 1308–1326.

[51] P. E. Farrell, L. Mitchell, L. R. Scott, and F. Wechsung, *A Reynolds-robust preconditioner for the Scott-Vogelius discretization of the stationary incompressible Navier-Stokes equations*, SMAI J. Comput. Math., 7 (2021), pp. 75–96.

[52] N. M. Ferraro, S. C. Jardin, and P. B. Snyder, *Ideal and resistive edge stability calculations with M3D-C1*, Phys. Plasmas, 17 (2010), pp. 102508–1 – 102508–10.

[53] G. B. Folland, *Real Analysis: Modern Techniques and their Applications*, John Wiley & Sons, New York, 2nd ed., 2013.

[54] G. Geymonat and F. Krasucki, *On the existence of the Airy function in Lipschitz domains. application to the traces of H^2*, C. R. Acad. Sci. Paris Sér I Math., 330 (2000), pp. 355–360.

[55] V. Girault and P. Raviart, *Finite Element Methods for Navier-Stokes Equations: Theory and Algorithms*, Spring-Verlag, Berlin, 1986.

[56] P. Grisvard, *Elliptic Problems in Nonsmooth Domains*, Pitman Advanced Publishing Program, Boston, 1985.

[57] B. Guo, *The $h-p$ version of the finite element method for elliptic equations of order $2m$*, Numer. Math., 53 (1988), pp. 199–224.

[58] B. Guo and I. Babuška, *Local Jacobi operators and applications to the p-version of finite element method in two dimensions*, SIAM J. Numer. Anal., 48 (2010), pp. 147–163.

[59] B. Guo and W. Cao, *A preconditioner for the h-p version of the finite element method in two dimensions*, Numer. Math., 75 (1996), pp. 59–77.

[60] B. Guo and C. Schwab, *Analytic regularity of Stokes flow on polygonal domains in countably weighted Sobolev spaces*, J. Comput. Appl. Math., 190 (2006), pp. 487–519.

[61] B. Guo and W. Sun, *The optimal convergence of the h-p version of the finite element method with quasi-uniform meshes*, SIAM J. Numer. Anal., 45 (2007), pp. 698–730.

[62] B. Guo and L. Yi, *Local Chebyshev projection-interpolation operator and applications to the h-p version of the finite element method in three dimensions*, Math. Models Methods Appl. Sci., 23 (2013), pp. 777–801.

[63] B. Guo and J. Zhang, *Stable and compatible polynomial extensions in three dimensions and applications to the p and h-p finite element method*, SIAM J. Numer. Anal., 47 (2009), pp. 1195–1225.

[64] B. Guo and J. Zhang, *Construction of polynomial extensions in two dimensions and application to the hp finite element method*, J. Comput. Appl. Math., 261 (2014), pp. 249–270.

[65] N. Heuer, *On the equivalence of fractional-order Sobolev semi-norms*, J. Math. Anal. Appl., 417 (2014), pp. 505–518.

[66] V. John, A. Linke, C. Merdon, M. Neilan, and L. G. Rebholz, *On the divergence constraint in mixed finite element methods for incompressible flows*, SIAM Rev., 59 (2017), pp. 492–544.

[67] G. Karniadakis and S. Sherwin, *Spectral/hp Element Methods for CFD*, Oxford University Press, Oxford, 1999.

[68] I. N. Katz and D. W. Wang, *The p-version of the finite element method for problems requiring C^1-continuity*, SIAM J. Numer. Anal., 22 (1985), pp. 1082–1106.

[69] A. Klawonn, *Block-triangular preconditioners for saddle point problems with a penalty term*, SIAM J. Sci. Comput., 19 (1998), pp. 172–184.

[70] A. Klawonn and L. F. Pavarino, *Overlapping Schwarz methods for mixed linear elasticity and Stokes problems*, Comput. Methods Appl. Mech. Engrg., 165 (1998), pp. 233–245.

[71] M. J. Lai and L. L. Schumaker, *Spline Functions on Triangulations*, Cambridge University Press, Cambridge, 2007.

[72] L. D. Landau and E. M. Lifshitz, *Theory of Elasticity*, Pergamon Press, Elmsford, NY, 3rd ed., 1986.

[73] P. L. Lederer and J. Schöberl, *Polynomial robust stability analysis for H(div)-conforming finite elements for the Stokes equations*, IMA J. Numer. Anal., 38 (2018), pp. 1832–1860.

[74] J. L. Lions and E. Magenes, *Non-Homogeneous Boundary Value Problems and Applications I*, Springer-Verlag, Berlin, 1972.

[75] L. Lliboutry, *General theory of subglacial cavitation and sliding of temperate glaciers*, J. Glaciol., 7 (1968), pp. 21–58.

[76] L. Lu, X. Meng, Z. Mao, and G. E. Karniadakis, *DeepXDE: A deep learning library for solving differential equations*, SIAM Rev., 63 (2021), pp. 208–228.

[77] Y. Maday, *Relèvements de traces polynomiales et interpolations hilbertiennes entre espaces de polynômes*, CR Acad. Sci. Paris, 309 (1989), pp. 463–468.

[78] Y. Mayday, D. Meiron, A. T. Patera, and E. M. Rønquist, *Analysis of iterative methods for the steady and unsteady Stokes problem: Applications to spectral element discretizations*, SIAM J.Sci. Comput., 14 (1993), pp. 310–337.

[79] V. Maz'ya and J. Rossmann, *Elliptic Equations in Polyhedral Domains*, vol. 162 of Mathematical Surveys and Monographs, American Mathematical Society, Providence, RI, 2010.

[80] D. P. McKenzie, J. M. Roberts, and N. O. Weiss, *Convection in the Earth's mantle: Towards a numerical simulation*, J. of Fluid Mech., 62 (1974), pp. 465–538.

[81] J. M. Melenk, *hp Finite Element Methods for Singular Perturbations*, Lecture Notes in Math. 1796, Springer, New York, NY, 2002.

[82] H. K. Moffatt, *Viscous and resistive eddies near a sharp corner*, J. Fluid Mech., 18 (1964), pp. 1–18.

[83] J. Morgan and R. Scott, *A nodal basis for C^1 piecewise polynomials of degree $n \geq 5$.*, Math. Comp., 29 (1975), pp. 736–740.

[84] R. Muñoz-Sola, *Polynomial liftings on a tetrahedron and applications to the hp version of the finite element method in three dimensions*, SIAM J. Numer. Anal., 34 (1997), pp. 282–314.

[85] M. Neilan, *Discrete and conforming smooth de rham complexes in three dimensions*, Math. Comp., 84 (2015), pp. 2059–2081.

[86] J. Nečas, *Direct Methods in the Theory of Elliptic Equations*, Springer Monographs in Mathematics, Springer, Heidelberg, 2012. Translated from the 1967 French original.

[87] N. Offermans, O. Marin, M. Schanen, J. Gong, P. Fischer, P. Schlatter, A. Obabko, P. Peplinski, M. Hutchinson, and E. Merzari, *On the strong scaling of the spectral element solver Nek5000 on petascale systems*, in Proceedings of the Exascale Applications and Software Conference, Stockholm, Sweden, 2016, ACM, pp. 1–10.

[88] E. T. Olsen and J. D. Olsen Jr, *Bounds on spectral condition numbers of matrices arising in the p-version of the finite element method*, Numer. Math., 69 (1995), pp. 333–352.

[89] C. C. Paige and M. A. Saunders, *Solution of sparse indefinite systems of linear equations*, SIAM J. Numer. Anal., 12 (1975), pp. 617–629.

[90] L. F. Pavarino, *Preconditioned mixed spectral element methods for elasticity and Stokes problems*, SIAM J. Sci. Comput., 19 (1998), pp. 1941–1957.

[91] L. F. Pavarino and O. B. Widlund, *Iterative substructuring methods for spectral element discretizations of elliptic systems. II: Mixed methods for linear elasticity and Stokes flow*, SIAM J. Numer. Anal., 37 (1999), pp. 375–402.

[92] J. Pestana, R. Muddle, M. Heil, F. Tisseur, and M. Mihajlovic, *Efficient block preconditioning for a C^1 finite element discretization of the Dirichlet biharmonic problem*, SIAM J. Sci. Comput., 38 (2016), pp. A325–A345.

[93] M. Raissi, P. Perdikaris, and G. E. Karniadakis, *Physics-informed neural networks: A deep learning framework for solving forward and inverse problems involving nonlinear partial differential equations*, J. Comp. Phys., 378 (2019), pp. 686–707.

[94] N. Salah, A. Soulaimani, and W. Habashi, *A finite element method for magnetohydrodynamics*, Comput. Methods Appl. Mech. Engrg., 190 (2001), pp. 5867–5892.

[95] J. Schöberl, J. M. Melenk, C. Pechstein, and S. Zaglmayr, *Addition Schwarz preconditioning for p-version triangular and tetrahedral finite elements*, IMA J. Numer. Anal., 28 (2008), pp. 1–24.

[96] D. Schötzau and T. P. Wihler, *Exponential convergence of mixed hp-DGFEM for Stokes flow in polygons*, Numer. Math., 96 (2003), pp. 339–361.

[97] G. Schubert, D. L. Turcotte, and P. Olson, *Mantle convection in the Earth and planets*, Cambridge University Press, Cambridge, 2001.

[98] C. Schwab, *p- and hp-Finite Element Methods. Theory and Applications in Solid and Fluid Mechanics*, Oxford University Press, Oxford, 1998.

[99] C. Schwab and M. Suri, *The p and hp versions of the finite element method for problems with boundary layers*, Math. Comp., 65 (2008), pp. 1403–1429.

[100] L. R. Scott and M. Vogelius, *Norm estimates for a maximal right inverse of the divergence operator in spaces of piecewise polynomials*, ESAIM Math. Model. Numer. Anal., 19 (1985), pp. 111–143.

[101] L. R. Scott and S. Zhang, *Finite element interpolation of nonsmooth functions satisfying boundary conditions*, Math. Comp., 54 (1990), pp. 483–493.

[102] D. Silvester and A. Wathen, *Fast iterative solution of stabilised Stokes systems Part II: Using general block preconditioners*, SIAM J. Numer. Anal., 31 (1994), pp. 1352–1367.

[103] B. Smith, P. Bjorstad, and W. Gropp, *Domain Decomposition: Parallel Multilevel Methods for Elliptic Partial Differential Equations*, Cambridge University Press, Cambridge, UK, 2004.

[104] R. Stenberg and M. Suri, *Mixed hp finite element methods for problems in elasticity and Stokes flow*, Numer. Math., 72 (1996), pp. 367–389.

[105] Y. Su, L. Chen, X. Li, and C. Xu, *On the inf-sup constant of a triangular spectral method for the Stokes equations*, Comput. Methods Appl. Math., 16 (2016), pp. 507–522.

[106] M. Suri, *The p-version of the finite element method for elliptic equations of order* $2l$., ESAIM Math. Model. Numer. Anal., 24 (1990), pp. 265–304.

[107] M. Suri, I. Babuška, and C. Schwab, *Locking effects in the finite element approximation of plate models*, Math. Comp., 64 (1995), pp. 461–482.

[108] G. Szegö, *Orthogonal Polynomials*, American Mathematical Society, Providence, RI, 1939.

[109] P. L. Tallec and A. Patra, *Non-overlapping domain decomposition methods for adaptive hp approximations of the Stokes problem with discontinuous pressure fields*, Comput. Methods Appl. Mech. Engrg., 145 (1997), pp. 361–379.

[110] S. Timoshenko and S. Woinowsky-Krieger, *Theory of Plates and Shells*, McGraw-Hill Book Company, Inc., New York, 2nd ed., 1987.

[111] A. Toselli and O. B. Widlund, *Domain Decomposition Methods: Algorithms and Theory*, vol. 34 of Springer Ser. Comput. Math., Springer, New York, 2005.

[112] F. Tröltzsch, *Optimal Control of Partial Differential Equations: Theory, Methods and Applications*, vol. 112 of Grad. Stud. Math., AMS, Providence, RI, 2010.

[113] M. Vogelius, *A right-inverse for the divergence operator in spaces of piecewise polynomials*, Numer. Math., 41 (1983), pp. 19–37.

[114] A. Wathen and D. Silvester, *Fast iterative solution of stabilised Stokes systems. Part i: Using simple diagonal preconditioners*, SIAM J. Numer. Anal., 30 (1993), pp. 630–649.

[115] J. Weertman, *Stability of the junction of an ice sheet and an ice shelf*, J. Glaciol., 13 (1974), pp. 3–11.

[116] L. C. Wilcox, G. Stadler, C. Burstedde, and O. Ghattas, *A high-order discontinuous Galerkin method for wave propagation through coupled elastic-acoustic media*, J. Comput. Phys., 229 (2010), pp. 9373–9396.

[117] X. Zhang, *Studies in Domain Decomposition: Multi-level Methods and the Biharmonic Dirichlet Problem*, PhD thesis, New York Univeristy: Courant Institute of Mathematical Sciences, 1991.

[118] X. Zhang, *Multilevel Schwarz methods for the biharmonic Dirichlet problem*, SIAM J. Sci. Comput., 15 (1994), pp. 621–644.

[119] X. Zhang, *Two-level Schwarz methods for the biharmonic problem discretized conforming C^1 elements*, SIAM J. Numer. Anal., 33 (1996), pp. 555–570.

[120] S. Zhong, M. T. Zuber, L. Moresi, and M. Gurnis, *Role of temperature-dependent viscosity and surface plates in spherical shell models of mantle convection*, J. Geophys. Res.: Solid Earth, 105 (2000), pp. 11063–11082.